ORNL-2480
Instruments cy 6
TID-4500 (13th ed., Rev.)
February 15, 1958

INSTRUMENTATION AND CONTROLS DIVISION

ANNUAL PROGRESS REPORT

FOR PERIOD ENDING JULY 1, 1957

OAK RIDGE NATIONAL LABORATORY, U.S. ATOMIC ENERGY COMMISSION

OAK RIDGE NATIONAL LABORATORY

operated by

UNION CARBIDE CORPORATION

for the

U.S. ATOMIC ENERGY COMMISSION

Printed in USA. Price $2.75 cents. Available from the
Office of Technical Services
U. S. Department of Commerce
Washington 25, D. C.

ORNL-2480
Instruments
TID-4500 (13th ed., Rev.)
February 15, 1958

Contract No. W-7405-eng-26

INSTRUMENTATION AND CONTROLS DIVISION

ANNUAL PROGRESS REPORT

For Period Ending July 1, 1957

C. J. Borkowski, Director
C. S. Harrill, Associate Director

DATE ISSUED

JUL 14 1958

OAK RIDGE NATIONAL LABORATORY
Oak Ridge, Tennessee
operated by
UNION CARBIDE CORPORATION
for the
U. S. ATOMIC ENERGY COMMISSION

CONTENTS

A PULSE CROSSOVER PICKOFF GATE FOR USE WITH A MEDIUM-SPEED COINCIDENCE CIRCUIT

E. Fairstein

Introduction

Coincidence measurements provide a powerful means of unraveling complex nuclear decay schemes. An instrumentation system frequently used for the purpose is shown in Fig. 1. The multichannel analyzer records a count only (1) if signals are simultaneously present in channels *A* and *B*, and (2) if the signal in channel *B* is in the energy range selected by the single-channel analyzer. While the gating criterion could be established entirely with the slow channel, the two-speed combination is used because the variations in the *B*-channel timing signal at the input terminal of the single-channel analyzer are less than at the output terminal, permitting a shorter over-all resolving time.

In the system just described, assuming that the multichannel analyzer is adjusted to cover the range of amplifier pulse amplitudes from noise to rated maximum output, and assuming that the threshold of the coincidence circuit is set at the edge of the noise level (approximately three times the rms noise level), the ultimate resolving time is one to three times greater than the amplifier rise time. The reason for this is shown in Fig. 2, in which (1) and (2) represent two double-line amplifier output pulses, v_1 represents the threshold level of the coincidence

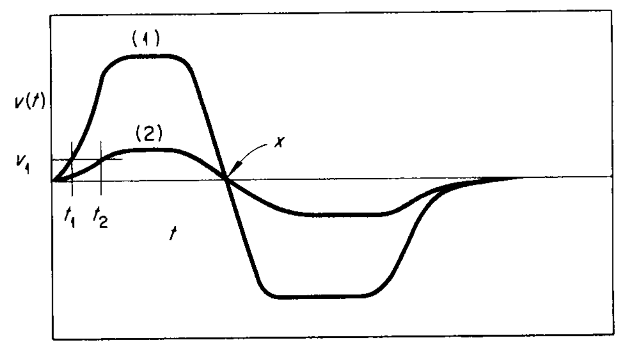

Fig. 2. Effect of Pulse Amplitude on Coincidence Gate Timing.

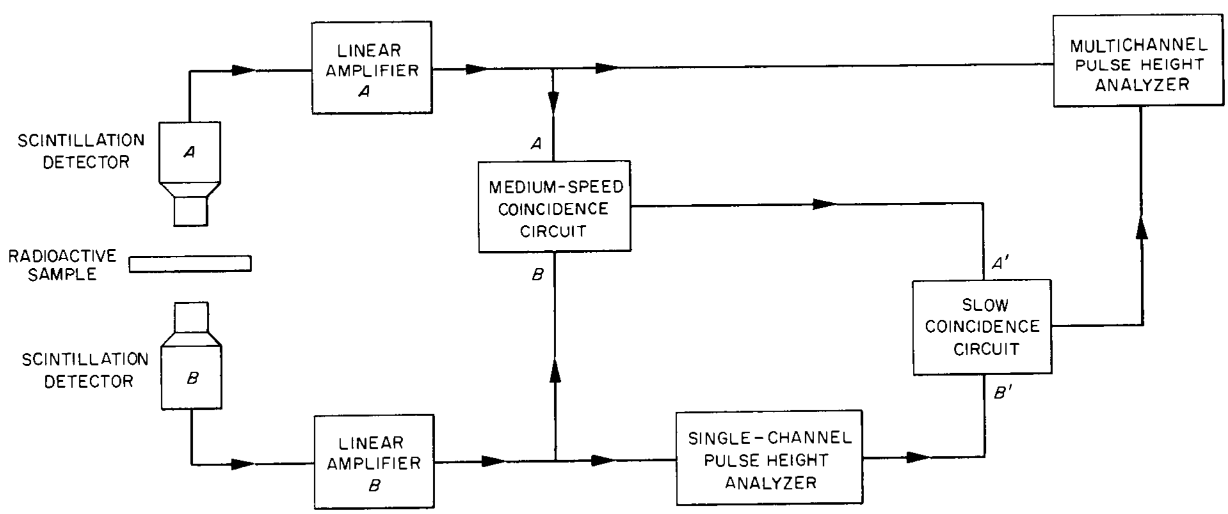

Fig. 1. Two-Speed Coincidence System.

circuit, and t_1 and t_2 represent the times of initiation of the coincidence gate signal. It should be obvious that the minimum resolving time must be at least as great as $t_2 - t_1$, and $t_2 - t_1$ will depend upon the range of amplitudes to which the multichannel analyzer is sensitive.

The effect of pulse amplitude on timing can be nearly eliminated by using the point *X* (the crossover point) to initiate the gating signal. Not only is the timing of this point relative to the initiation of the pulse independent of pulse height, but the rate of change of voltage at this point is greater than at any other. The hysteresis effect in a Schmitt trigger circuit[1] provides a practical means of establishing a gate level at the base line; the remainder of this section is devoted to a circuit which uses this technique. (The possibility of using the hysteresis in a Schmitt trigger circuit as a means of establishing a timing pulse coincident with the crossover point was first suggested by T. A. Love of the Bulk Shielding Group. In a separate report,[2] Peelle and Love describe several circuits of their own to accomplish the desired results.)

Theory and Operation of a Crossover Pickoff Gate

In any bi-stable device, the triggering threshold is greater in amplitude than the recovery threshold. The difference between these two levels is known as the hysteresis. In using a Schmitt trigger circuit to establish the desired timing signal, the triggering threshold is set just above the noise level and the hysteresis is adjusted to the value which causes the trigger circuit to be reset by the pulse just as it crosses the base line. The trailing edge of the output pulse from the Schmitt trigger circuit is then used to provide the necessary timing information. (Differentiating this output pulse produces two pips of opposite polarity, one at the leading edge and one at the trailing edge, providing a means of distinguishing between the two edges.)

Timing accuracy can be maintained only if the recovery level of the trigger circuit is accurately locked to the base line. To ensure this accuracy, the following conditions must be met:

1. Either the pulse amplitude must be limited to a low value or the dynamic range of the trigger circuit must be such that grid current never occurs. Otherwise, the charge on the input coupling capacitor will be altered by an amount proportional to the counting rate, with a corresponding shift in trigger threshold level.
2. Biasing for the trigger circuit must be accomplished in such a way that threshold shifts cannot occur with changes in duty cycle.
3. The trigger circuit and all circuits preceding it must be fast enough to follow the falling edge of the amplifier pulse. Otherwise, the timing signal will be later than the crossover point by an amount proportional to the amplitude of the input pulse.

The circuit shown in Fig. 3, designed to receive signals from a DD2 amplifier,[3] meets all three of the listed requirements. The output of the gate is of sufficient amplitude to drive a conventional coincidence circuit. A complete system requires two such gates, one for each of the medium-speed channels of the coincidence circuit.

Diode V_{1_a} is normally conducting, while V_{1_b} is nonconducting. If the input signal exceeds 10 v (positive), V_{1_b} conducts and limits the pulse at point *A* to 10 v. This not only prevents grid current in V_3 but relaxes the speed requirements of the Schmitt trigger circuit, V_3 and V_4, by limiting the range of signals which the trigger circuit must track.

At high counting rates, point *B* will shift in a positive direction because of the current flow through V_{1_b}. The circuit containing V_2 provides an equal and opposite shift at point *C*. The symmetry is such that point *D* does not shift with counting rate, except for the slight shift produced by the asymmetry of the amplifier output pulse under overload conditions. Because points *A* and *D* are connected by a path of low d-c resistance, any slight shift in voltage which may occur at *D* also appears at *A*. This common-mode shift has only a second-order effect on the sensitivity of the following trigger circuit.

The indicated resistance tolerances assure the required symmetry between the upper and lower parts of the circuit.

The tubes V_3 and V_4 are part of a conventional Schmitt trigger. The diode at the output of V_4

[1] W. C. Elmore and M. Sands, *Electronics: Experimental Techniques*, 1st ed., p 99–103, McGraw-Hill, New York, 1949.

[2] R. W. Peelle, T. A. Love, *Appl. Nuclear Phys. Prog. Rep. Sept. 1, 1957*, ORNL-2389, p 249–259.

[3] E. Fairstein, *Rev. Sci. Instr.* 27, 475 (1956).

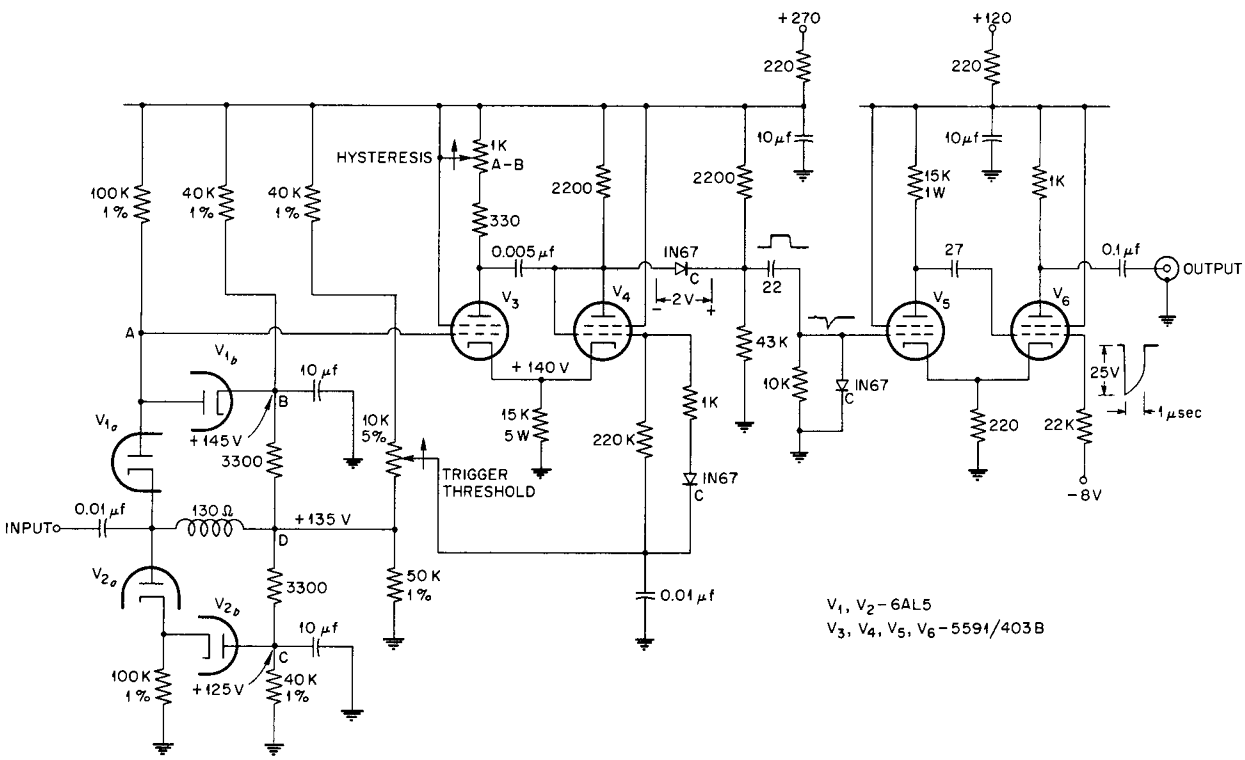

Fig. 3. Pulse Crossover Pickoff Gate.

blocks the precursor pulse which is caused by capacitive feed-through in V_3. The trigger output signal is differentiated by a clamped *R-C* circuit and applied to a one-shot univibrator, the leading edge of whose output pulse is in time coincidence with the crossover point of the amplifier output pulse.

Performance

Figure 4 is the block diagram of a setup used to test the circuit. The capacitor at the generator output terminal was used to smear the rise time to that of an NaI(Tl) scintillation pulse. The variable delay line was used to compensate for the delay in the signal channel. To prevent timing errors, the oscilloscope triggering level was held constant during the test, and the amplifier output was varied by the attenuator in the pulse generator.

The results of the test are shown in Fig. 5. The term "walk" is used to denote a shift in measured crossover point as a function of amplifier output, "jitter" to denote a random variation in the crossover point caused by amplifier noise. Measurements were made at several threshold settings to permit an estimate of the effect of bias drifts. Experience gained earlier with 5591/403B and 6AL5 tubes indicates that a year or more of steady operation would be required for a drift equal to the difference between two adjacent curves.

Two channels of the circuit shown in Fig. 2 were built for G. D. O'Kelley of the Chemistry Division. In three months of steady operation, no circuit readjustments were necessary, and it was found that the 0.68-μsec resolving time necessary with a conventional circuit could be reduced to 0.17 μsec with no loss in counting efficiency. It was estimated that an additional reduction of one-half was possible.

Limitations of the Method

The excited states produced in a scintillation phosphor by an incoming beta or gamma ray will

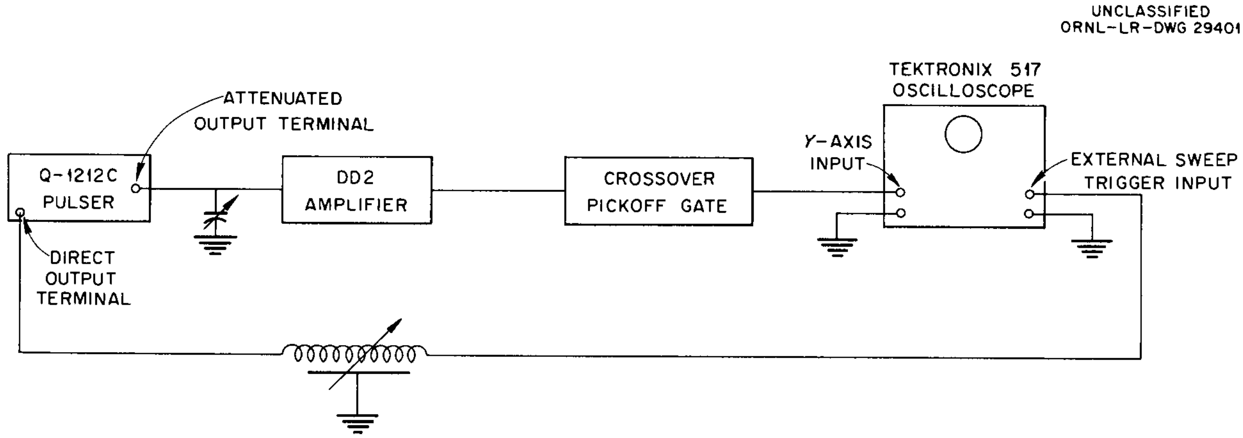

Fig. 4. Test Setup for Crossover Pickoff Gate.

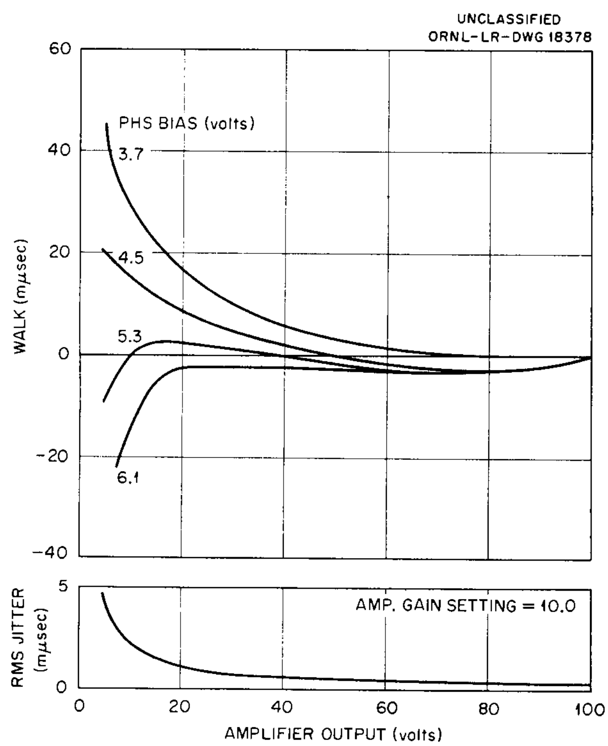

Fig. 5. "Walk" and "Jitter" of Crossover Point in DD2 Amplifier.

decay exponentially by photon emission. The emission time of any particular fraction of the total number of photons is subject to random fluctuations about a mean value, with the magnitude of the fluctuation being a function of both the total number of photons per burst and the fraction of the burst being observed. This fluctuation sets the limit of the coincidence circuit resolving time. Post and Schiff[4] showed that the least possible fluctuation exists for the emission of the first photon, the fluctuation increasing with the fraction of the total burst being observed.

Because of the reflective properties of the delay line pulse formers in the amplifier, the crossover point is the image of the half-maximum point on the leading edge of the output pulse, and therefore corresponds to the point in time at which half the emitted photons are observed. Figure 6 shows the approximate minimum resolving time as a function of the energy of the incoming gamma ray usable in a coincidence circuit (1) of the type which is the subject of this section and (2) of the type which detects the time of emission of the first photoelectron in a burst. Two identical NaI(Tl) detectors having decay constants of 0.25 μsec and resolutions of 8% at the Cs^{137} gamma-ray energy (661 kev) are assumed. It is also assumed that the coincidence counting efficiency is 90% and that the photomultiplier and amplifier add nothing to the required resolving times.

Computation of Resolving Times

If it is assumed that the resolution of a scintillation counter depends only upon the number

[4]R. F. Post and L. I. Schiff, *Phys. Rev.* 80, 1113 (1950).

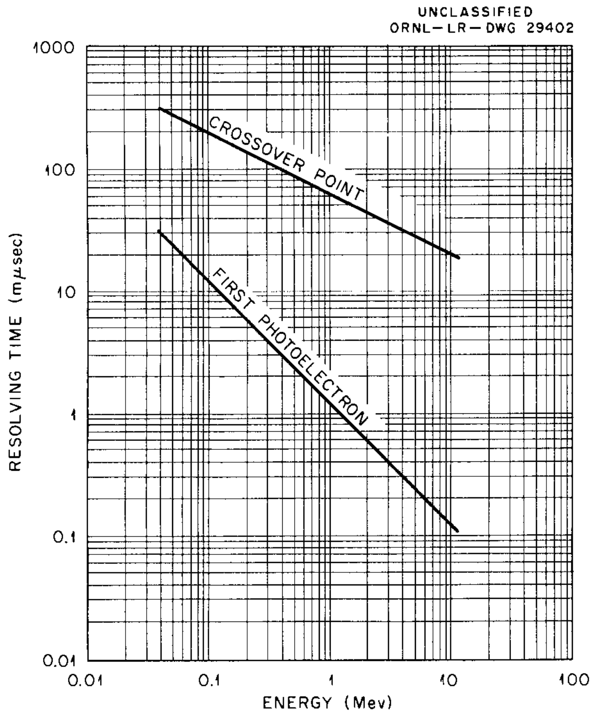

Fig. 6. Resolving Time for Two Types of Coincidence Circuit. Time, 2τ, required for 90% counting efficiency.

of electrons emitted by the photocathode under the influence of an incoming gamma ray, then

$$N = \frac{1}{E}\left(\frac{235}{\rho}\right)^2 , \qquad (1)$$

where

N = number of photoelectrons produced per Mev of energy loss in the phosphor,
ρ = the observed resolution (full width at half maximum) of a photopeak in per cent,
E = the energy of the photopeak in Mev.

In a scintillation counter exhibiting 8% resolution for a 0.661-Mev gamma ray, N is 1300 photoelectrons per Mev. The rate of emission of photons from a phosphor excited by a gamma ray decays exponentially with a time constant T. The mean time of emission of the first photoelectron can be computed from[3]

$$\bar{t} = \frac{T}{NE}\left(1 + \frac{1}{NE}\right), \qquad (2)$$

where T is the time constant of the phosphor in seconds. If the probability of observation of the first photoelectron is to be 0.95, the period of observation must be $3\bar{t}$. For the coincidence circuit to have 90% efficiency, the resolving time, 2τ, must be $6\bar{t}$ sec.

The mean time interval (measured from $t = 0$) corresponding to the emission of half the total number of photons is $0.69T$. The random variations about the mean value exhibited by this interval can be approximated by a Gaussian distribution having a standard deviation

$$\sigma = 0.69 \sqrt{\frac{2}{NE}}\, T = \frac{0.98T}{\sqrt{NE}} , \qquad (3)$$

where

σ = standard deviation in seconds,
NE = mean number of photoelectrons produced by a gamma ray of energy E Mev.

If the coincidence circuit is to have 90% efficiency, the resolving time must be

$$2\tau = 2 \times 2 \times 2.24 \times \frac{0.98T}{\sqrt{NE}} = \frac{8.8T}{\sqrt{NE}} \text{ sec} . \qquad (4)$$

The analyses given above are not to be considered rigorous and are presented only as a means of obtaining an approximate comparison of the ultimate resolving times of the two types of coincidence circuit described in this section.

DIGITAL COUNT-RATE METER

E. Fairstein J. L. Lovvorn

The conventional linear count-rate meter with analog output, when used to count nuclear events, produces an output voltage which exhibits random variations about a mean value. The magnitude of the variations is inversely proportional to the square root of the speed of response of the rate meter. It can be shown that, for a given magnitude of variation, a scaler has a shorter response time than a rate meter. (This is connected with the fact that the load resistor in the storage circuit of the rate meter is continuously draining charge, and therefore stored information, from the system, whereas in a scaler none of the stored information is lost prior to reading.) In measurements requiring a continuous record of counting rate, under low-counting-rate conditions, the difference in response time between the two instruments can be quite important. Since there are no commercially available instruments which combine in a single instrument the analog output characteristic of a rate meter with the counting mechanism of a scaler, a project was undertaken to develop such a device.

An experimental unit was built which contains a scaler, timer, reset mechanism, and a digital-to-analog converter. A correction circuit was incorporated which indicates on a panel meter the coincidence-loss correction[1] that occurs at high counting rates. The instrument can be used in conjunction with a 10-mv recorder to plot histograms, or it can be used as a conventional scaler, with or without a preset timing feature.

The electrical specifications are as follows:

Pulse Height. – Pulses from +4 to +100 v and –4 to –50 v are acceptable at the input.

Counting Rate. – The maximum counting rate is 100 kc/sec, a limit imposed by the commercially built decade scalers. The double-pulse resolving time is 5 μsec.

Scalers. – Six decades of Hewlett-Packard model AC-4A decade scalers are used. A seventh, partial-decade scaler in the most significant place gives a maximum full-scale capacity of 2,999,999 counts.

[1]E. Fairstein, *Instrumentation and Controls Semiann. Prog. Rep. Jan. 31, 1956*, ORNL-2067, p 1–4.

Analog Output. – Because strip-chart recorders have a resolution of approximately 0.5% of the full-scale reading, only the three most significant decades plus the partial-decade scaler have analog output. Stepped full-scale outputs of 200, 500, and 1000 counts are provided, plus a fine control which permits the step ranges to be multiplied by a factor which can be continuously varied from 1 to 2.5. The scale may be multiplied in steps of 10 by switching in additional decade scalers up to the full capacity of the system.

Counting Period. – The counting period is variable in a 1-2-5 sequence from 0.5 to 500 sec.

Recording Period. – The recording period is variable in a 1-2-5 sequence from 0.5 to 50 sec.

Test Signal. – A switch allows 60-cycle test voltage to be applied at the input.

Accuracy. – The accuracy, which depends on component-part tolerances, is ±1% of full scale on the 200-counts range setting. The drift for a 24-hr period is 3% on the 200-counts range setting, decreasing to less than 1% on the higher ranges.

The instrument is described in block diagram form in Fig. 7. The input pulse-height selector is a Schmitt trigger circuit employing two 6AU6 pentodes. The output drives the per-cent-true-rate circuit, which has a dead time of 5 μsec. (The panel meter shown in Fig. 8 indicates the correction on a linear scale calibrated from 0 to 100%.) The output of this circuit is used to drive the overflow gate after the gate is sensitized by the timing generator. The overflow gate is necessary to prevent an ambiguous reading which could result from a count which exceeded the capacity of the scaler.

The timing base controls allow for manual operation, single-period operation, or recurrent-period operation. The counting and recording periods can be varied as noted earlier. The operation of the timing circuits which control these periods depends on the charging rates of low-hysteresis capacitors.

In operation, a counting period is followed by a recording period (during which incoming signals are blocked by an input gate) which is then followed by a reset period. This cycle is repeated during recurrent operation. To prevent

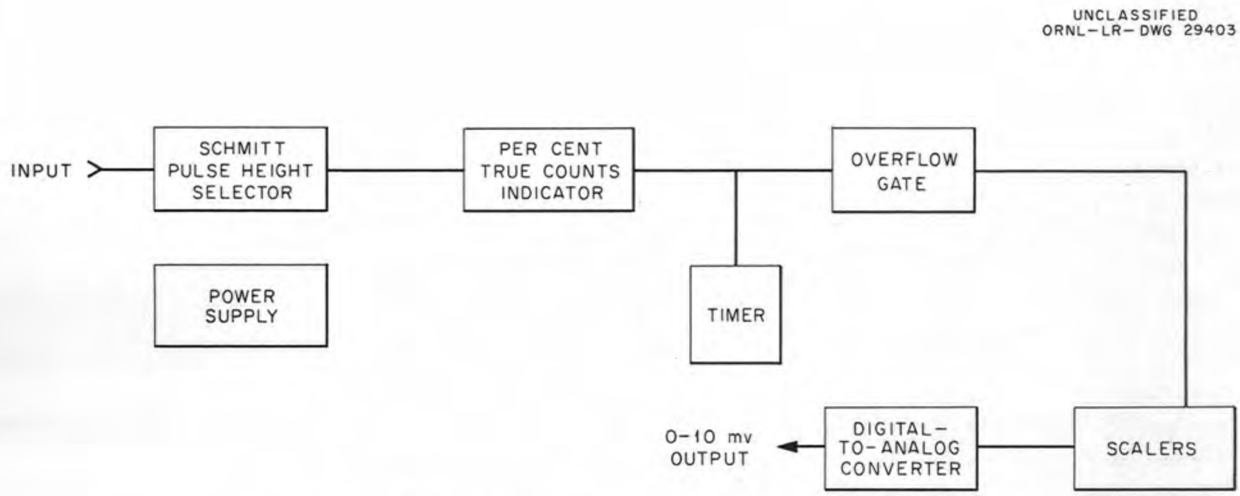

Fig. 7. Block Diagram of Digital Count-Rate Meter.

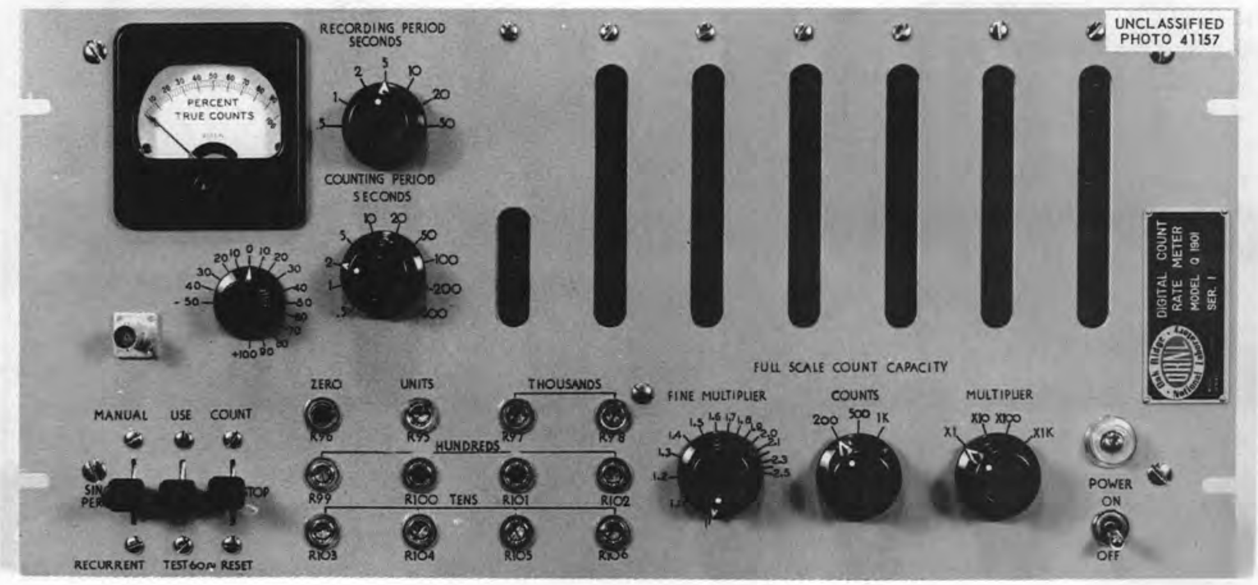

Fig. 8. Digital Count-Rate Meter.

the recorder pen from returning to zero between recording intervals, the pen drive motor is connected only during the recording period.

The Hewlett-Packard AC-4A decade scalers were selected because they have a staircase output. Small currents weighted in proper relation to the significance of the contributing scaler tube are added to give the analog output of 0–10 mv.

In selecting commercial scalers a calculated risk was taken in order to shorten the development time. This gamble did not pay off, partly because the drift was outside acceptable limits and partly because the calibration procedure was too complicated. Other portions of the digital count-rate meter easily meet the performance expectations.

A new digital-to-analog converter, which should improve accuracy and eliminate undesirable adjustments, is undergoing tests. Its accuracy is dependent only upon the stability of the B supply, precision resistors, and the forward-to-reverse current ratio of silicon junction diodes. Data taken thus far indicate that $\pm\frac{1}{2}\%$ drift for a 24-hr period is attainable.

GRID CURRENT IN RADIO RECEIVING TUBES

E. Fairstein

A study of grid current in low-power receiving and amplifying tubes was undertaken to determine what grid currents can reasonably be expected from present-day production. The results indicate that both the average grid current and the variation in grid current from tube to tube are much lower in today's tubes than in those manufactured several years ago.

Measurements were limited to grid currents exceeding 10^{-13} amp, to plate voltages in the range between 20 and 300 v, and to cathode currents in the range between 50 μa and 100 ma. Pentodes were triode-connected. It is emphasized that all statements made in the remainder of this section are known to be valid only within the bounds set forth above.

A typical graph of grid current vs grid bias in electron tubes[1] is shown in Fig. 9. To the left of point *A*, the grid current is mainly due to the emission of electrons by the grid, insulator leakage, and/or the collection of positive ions; to the right, to the collection of electrons. Point *A* is the floating-grid potential and is the point at which the positive and negative current components balance each other. In all circuits in which low grid current is of importance, the tubes are biased either at point *A* or to the left of it.

[1]A. B. Gillespie, *Signal, Noise, and Resolution in Nuclear Counter Amplifiers*, p 29–40, McGraw-Hill, New York, 1953.

UNCLASSIFIED
ORNL–LR–DWG 21732

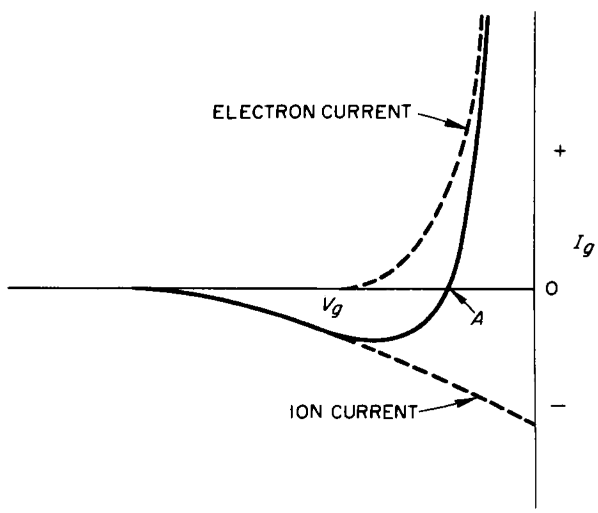

Fig. 9. Tube Grid Current vs Grid Bias.

The probable causes of electron emission from the grid are the following:

1. thermionic emission due to radiant heating of the grid by the cathode (as the tube ages, this effect becomes worse because of the cathode material which deposits on the grid),
2. photoelectric emission under the action of external light (because of the wavelength of the light emitted from the cathode, photoelectric emission from this source is probably negligible),
3. photoelectric emission under the action of soft x rays, ultraviolet radiation, and/or bremsstrahlung produced in the bombardment of screen grid and plate by the electron stream.

The first two sources of electron emission can always be made negligibly low by operating the cathode at a sufficiently low temperature and by shielding the tube from external light. In nearly all cases, the operating temperature necessary to attain low grid emission will still be high enough for adequate cathode emission. The third source of grid emission cannot be eliminated, if it exists, although it can be reduced by low-voltage and low-current operation of the tube.

The remaining sources of grid current are insulator leakage and the collection of positive ions.

Insulator leakage external to the tube can be eliminated as a source of trouble by surface cleaning and the correct choice of external hardware. Leakage due to support micas and getter splashes is not under the control of the user. Fortunately, less than one tube in ten in even the worst of the tube types gives trouble of this sort.

Positive ions arise from two sources: from the cathode and from ionized gas in the region between the control grid and the plate. (Ionization is produced by collisions between the electron stream and residual gas molecules.) As in the case of grid heating, positive-ion emission from the cathode can be made negligible by low-temperature operation.

It has long been assumed that ionized gas is the main source of grid current. Until quite recently, this was certainly the case, but improved evacuating techniques and better getters have resulted in much higher vacuums than those which existed in tubes several years ago. There is now some doubt as to whether the grid current is mainly due to ion current or to the emission of electrons caused by plate- (and screen-) emitted radiation under the action of the electron stream. The effects are difficult to separate in a particular tube because, in each case, the grid-current-causing processes are directly proportional to the space current and exponentially proportional to the applied voltage. Regardless of the cause, the experiments to be described show that it is now possible to predict the magnitude of the grid current in terms of the cathode current and plate voltage with an accuracy not possible several years ago.

An experiment was performed to determine the variation in grid current in tubes produced by several manufacturers. Seven manufacturers were represented, five American and two European. Each group of tubes was aged for 24 hr preceding the test at a plate potential of 150 v and a cathode current of 10 ma. Pentodes were triode-connected. The tubes were operated on the plateau of the curve of grid current vs heater voltage. Grid-current measurements were made at a grid-to-plate voltage of 100 and at a cathode current of 1 ma (except for the E180F, whose grid current was measured at 150 v and 1 ma and corrected to the 100-v value). The results, which were quite unexpected, are given in Fig. 10, which is a histogram of numbers of tubes exhibiting particular grid currents.

In a separate experiment, it was found that the grid current varies as the $\frac{3}{2}$ power of the grid-to-plate (screen) potential.

The results of both tests can be summarized by the statement that the grid current of at least 70% of a large batch of tubes selected without regard for manufacturer or type number, and subject to

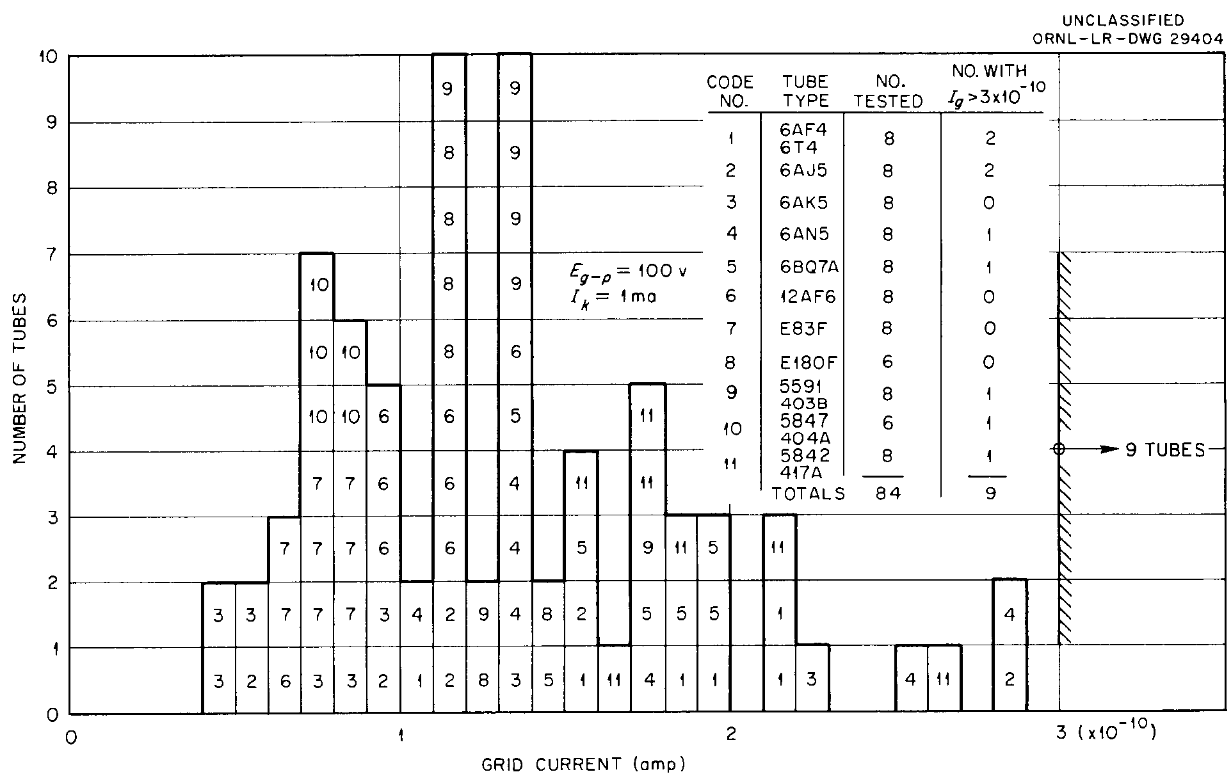

Fig. 10. Grid Current Spectrum of Eleven Tube Types.

the boundary conditions discussed earlier, will be within a factor of 2 of

$$I_g \approx E_{g\text{-}p}^{3/2} I_k \times 10^{-10} \text{ amp} ,$$

where $E_{g\text{-}p}$ is the grid-to-plate (screen) potential in volts and I_k is the cathode current in amperes.

It is well known that, in applications where low grid current is necessary, it is desirable to reduce the plate voltage and cathode current to the lowest possible value consistent with the necessity of keeping the grid bias more negative than the floating-grid potential and the transconductance at a usable level. Tubes with low-μ structures are particularly suitable in this regard, since they permit a lower plate (screen) voltage for a given cathode current and grid bias than high-μ tubes. This is demonstrated in Fig. 11, in which the plate voltage necessary to establish a grid bias 0.5 v more negative than the floating-grid potential, together with the resulting grid current, is plotted for the tubes listed in Fig. 10 at cathode currents of 1 ma and 10 ma. Each of the tubes was the best of the batch used in the test described earlier.

The author is indebted to C. J. Borkowski for pointing out that the grid current may be due primarily to the effects of electromagnetic radiation rather than to ion current.

UNCLASSIFIED
ORNL-LR-DWG 20815

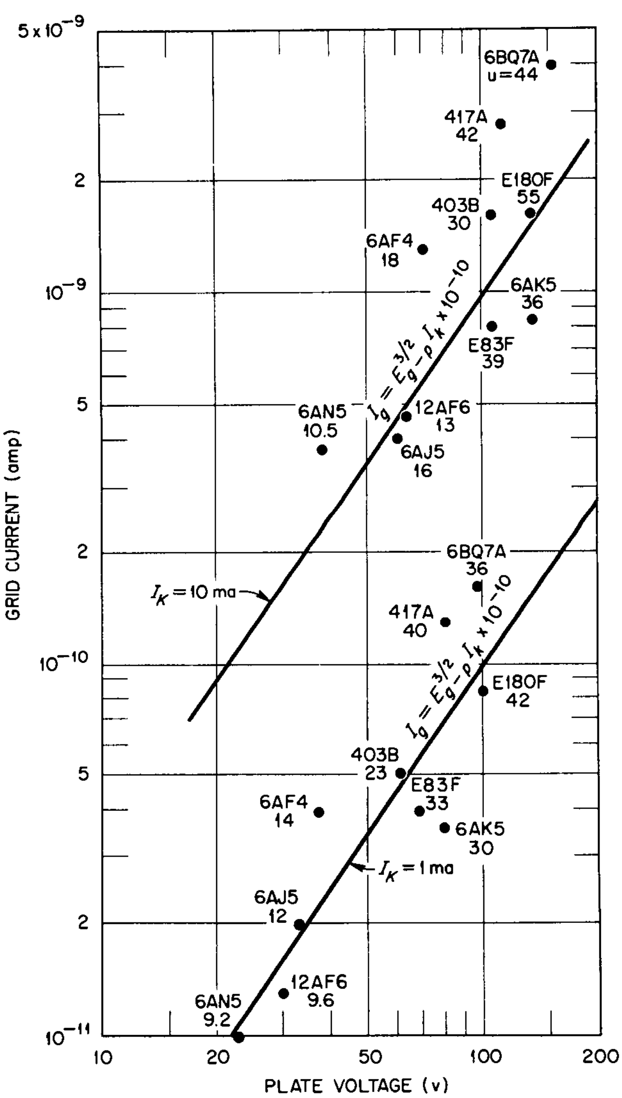

Fig. 11. Grid Current vs Plate Voltage of Ten Tube Types.

THE INTRINSIC STABILITY OF NEON-FILLED VR TUBES

E. Fairstein R. L. Livesey

Introduction

The use of VR tubes as voltage references in electronically regulated power supplies is very widespread. A knowledge of the intrinsic stability of the commonly used VR tubes is of considerable interest to equipment designers, and this section gives the results of a project undertaken to obtain the desired information.

Test Conditions

A fraction of the voltage drop across a particular tube was compared with a mercury battery reference by a strip-chart recorder having a full-scale sensitivity of 10 mv. The reference voltage was 5.2 or 50 v, depending on the desired sensitivity. The minimum detectable variations were 5 parts in 10^6 and 5 parts in 10^7, respectively. Tubes were tested in batches of five. A multipoint chart recorder was used, with two channels used for the temperature and supply-voltage monitoring. The supply voltage (285 v) was sufficiently well regulated so that at no time did supply-voltage fluctuations add any significant amount to the observed VR tube variations. All dividing networks were composed of low-temperature-coefficient wire-wound resistors. Dropping resistors for the VR tubes were ordinary wire-wound (Nichrome) units. The VR tubes, all resistors, reference batteries, and the input stage of the supply regulator were immersed in an oil bath containing approximately 3 gal of mineral oil. This tank, in turn, was immersed in a second tank of water. The liquids in both tanks were stirred continuously. The outer tank was heated and closely thermostatted. The inner tank was not heated internally, except by the power dissipated by tubes and resistors. The temperature of the inner tank was 36°C; variations were less than 0.01°C and less than the amount which gave any detectable cycling in the VR tube voltages. The 5651, 5651WA, 5783WB, and 85A2 tubes were run at approximately 2.5 ma. The remaining tubes were run at approximately 6 ma.

Results

The results of the stability test are given in Table 1.

Because of the time-consuming nature of the test, only two tubes of each type were tested, and the results must be considered in the light of this very small sample.

Drift rates are given from the viewpoint of an experimenter doing short-term experiments who wishes to know the expected voltage-reference drifts during his measurements.

The values given for the temperature coefficients are only approximate and only applicable at the tube envelope temperature of 36°C. In normal operation, the tubes will not be immersed in a liquid, and envelope temperatures will be different from that used in the test. It is generally the case that the temperature coefficient is a function of temperature.

The main conclusion to be drawn from the test is that, under ideal conditions, VR tubes having a gas filling which is predominantly neon exhibit jump-free drift rates of approximately 10 ppm/hr. In the case of the 5651, 5651WA, and 85A2, the peak-to-peak drift in a 75-hr period for well-aged tubes is less than 100 ppm.

Short-period (under 1 min) fluctuations for all the reference tubes tested (except the 5783WB, which may have been faulty) were less than 5 parts in 10^7.

Since internal impedance affects the choice of the tube type to be used in a particular design, some measurements were made on this parameter. The results are summed up in Table 2.

Recommendations for Application

As a result of this and earlier tests on many types of VR tubes, several generalizations can be made.

1. Only those VR tubes having a fill which is predominantly neon (characterized by an orange-red cathode glow) are useful as reference tubes. These include the VR75, 5651 series, 5783 series, 85A2, OB2WA (but not the OB2 or 6074), 6627, and the 5787 series. All known tubes having fillings other than neon exhibit random voltage jumps and high drift rates.

2. The double-liquid thermostatting arrangement used in the test, while ideal environmentally, is too expensive and bulky to be practical. A satisfactory arrangement for most applications is one in which the tube is completely enclosed in an unheated shield having good thermal conductivity and high "thermal mass." The shield container

Table 1. VR Tube Drift Rates

Envelope temperature: 36°C
Temperature held constant to <± 0.01°C
Current held constant to 200 ppm

Tube Type	Tube No.	Aging Period (weeks)	Drift (ppm) 1 hr	10 hr	75 hr	Temperature Coefficient (ppm/°C)
VR75	1	3	10	60	390	~90
	2	3	~5	15		
VR90	1	3	2000	>2000		
5651	1	3	~5	40	190	~55
	1	6	~5	20	50	
	1	10	6	20		
	2	3	12	25		
5651WA	1	3	~5	20	65	
	2	3	4	10		
5783WB	1	3	40	80	160	
85A2	1	3	~5	12	35	~185
	2	3	8	15		
5787WB	1	3	~5	30	220	
	2	3	10	50		
OB2WA }	1	3	~5	12		~320
6627 }	2	3	10	60	330	

Table 2. Internal Impedance of VR Tubes

Tube Type	Sample Size	Operating Current (ma)	Impedance at 60 cycles/sec (ohms)	Extremes of Impedance (ohms)
		Nominal Voltage 75 v		
VR75	6	5	135	122–170
		10	170	145–190
		20	120	102–140
		40	100	95–102

Table 2 (continued)

Tube Type	Sample Size	Operating Current (ma)	Impedance at 60 cycles/sec (ohms)	Extremes of Impedance (ohms)
		Nominal Voltage 83–87 v		
RCA 5651	6	1.5	760	360–480
		2.5	500	440–780
		3.5	610	560–700
Raytheon 5651	4	1.5	730	300–660
		2.5	900	780–960
		3.5	910	800–960
Raytheon 5651WA	6	1.5	430	224–520
		2.5	660	620–710
		3.5	770	750–810
5783WB	6	1.5	780	610–1020
		2.5	1100	1020–1180
		3.5	1100	990–1140
85A2	6	1	330	240–400
		3	270	200–300
		7	290	180–360
		Nominal Voltage 90 v		
VR90	6	5	280	200–430
		10	240	190–370
		20	250	170–300
		Nominal Voltage 98–105 v		
OB2WA, 6627	6	5	81	70–90
		10	74	43–105
		20	87	58–110
5787WB	6	5	19	11–29
		10	12	7–25
		25	53	33–63
		Nominal Voltage 150 v		
OA2WA	11	5	106	60–145
		10	57	49–98
		20	102	60–230

should be placed in a draft-free spot, or alternatively should be subjected to a constant-velocity, constant-temperature air stream. A constant-temperature oven of the type used for quartz crystals is not recommended; the temperature cycling will almost certainly appear as voltage cycling. With simple shielding of the type described, drift rates of 50 ppm/hr can be expected in the usual indoor laboratory, assuming that the current supply for the tube is held constant.

3. The voltage stability of a reference tube depends not only upon the combination of temperature coefficient and ambient temperature fluctuations but on the constancy of the current supply as well. For example, even though the 5651 has a lower temperature coefficient than the 85A2, the lower internal resistance of the 85A2 may lead to a steadier voltage reference if a composition type of load resistor is used, or if the current supply for the tube is obtained from an unregulated voltage source.

4. The most stable operating conditions result from the use of low-temperature-coefficient wire-wound load resistors.

5. In all but the most carefully designed regulated power supplies, noise and drift due to the first amplifier tube will usually exceed the noise and drift due to the reference tube, if the reference voltage consists of the potential drop across a single VR tube.

Special Characteristics of Particular Tubes

5651. – The 5651 has as low a temperature coefficient as any of the readily available VR tubes. At one temperature within the rated operating range, the temperature coefficient is zero.

The stabilizing time for a new tube is several days.

The voltage stability of premium versions of the 5651 is not significantly different from that of the 5651.

85A2. – The temperature coefficient of the 85A2 is much greater than that of the 5651, but in particular applications this may be compensated for by the lower internal impedance.

The stabilizing time for a new tube is several hours.

5783WB. – This is a subminiature version of the 5651, having a higher internal impedance.

5787WB. – This is a subminiature tube having characteristics approximately the same as those of an OB2WA. The internal impedance is exceptionally low.

OB2WA, 6627. – These tubes have an initial stabilizing time of about 1 hr but, unlike the 5651 and 85A2, exhibit a small but continuous drift in one direction throughout their useful life. They have a very low internal impedance.

NEUTRON CHOPPER SPEED CONTROL

B. C. Behr E. G. Manning

A neutron-chopper speed-control system is being developed for the Physics Division. It is to be used by J. A. Harvey in connection with the time-of-flight spectrometer. Preliminary specifications include adjustable controlled speed from 100 to 15,000 rpm, speed regulation of 0.1% or better at selected speed, and automatically controlled acceleration and deceleration.

The drive motor for the neutron chopper is rated at 48 v, 125 amp dc, and 15,000 rpm. Power is delivered from a 440-v 3-phase source through an induction regulator, a step-down transformer, and a 6-phase half-wave silicon rectifier. The 230-v d-c 400-ma motor field is supplied from a separate regulated source.

Figure 12 shows a block diagram of the power and speed control system.

Desired speed is set by rotating a series of five decade switches to the selected rpm. Actual rotor speed is measured by means of a magnetic pickup and digital counter with a conversion ratio of 60 pulses per revolution. During a normal 1-sec sampling period the count registered on the digital counter is the exact rotor speed in rpm.

Speed control is exercised through two independent feedback loops. Errors in the three most significant decades (that is, the ten-thousand, one-thousand, and hundred decades) are converted to voltage commands by means of a transistorized logic circuit and directly adjust the induction regulator so as to accelerate or decelerate the rotor. Upper and lower armature-current limits are superimposed upon this loop so as to limit maximum acceleration and deceleration rates.

When no error exists in the higher decades, the logic circuit transfers the speed-control function to the lower decade loop and inserts a bank of

UNCLASSIFIED
ORNL—LR—DWG 29405

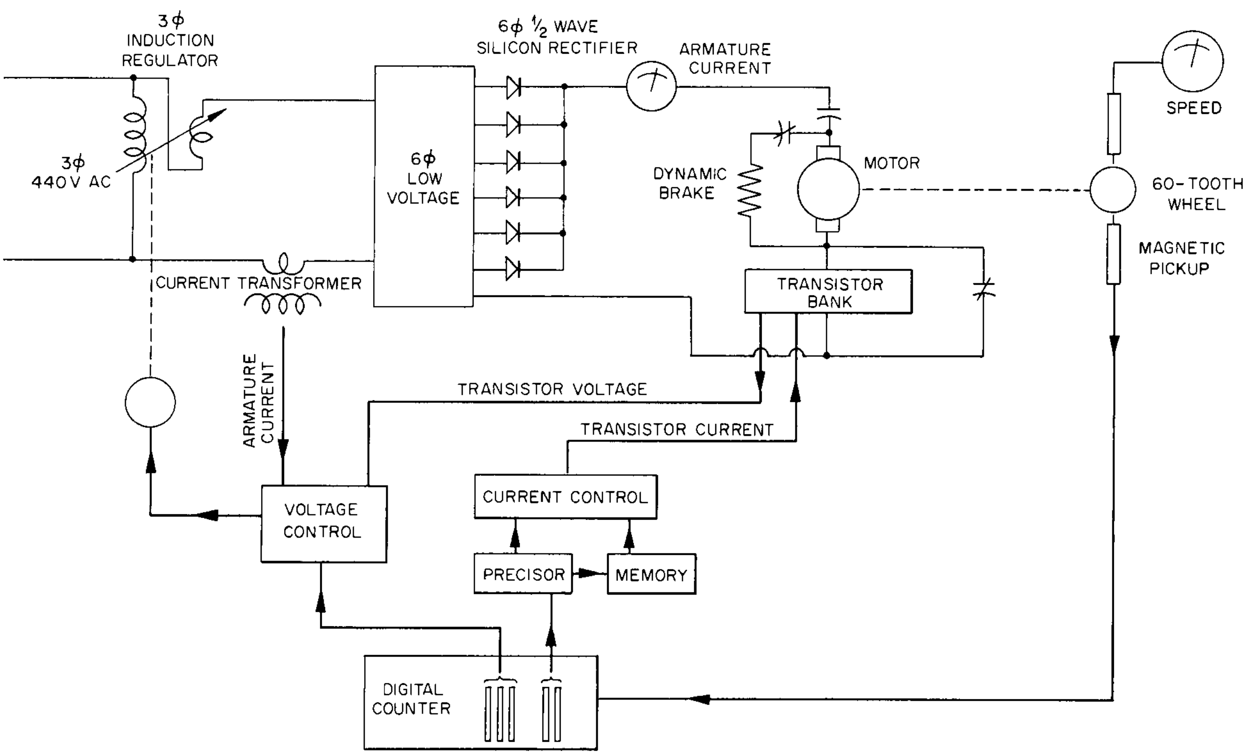

Fig. 12. Power and Speed Control System.

power transistors in the armature circuit. In this loop, digital information is converted to analog voltages. Voltages corresponding to actual speed, selected speed, and last previous speed are suitably combined to drive the bank of power transistors which in turn regulate the series armature current. The transistors are designed so as to pass a maximum of 40 amp.

Many safety features are included in the design. A totally independent analog speed-measuring device, with an overspeed trip, is used to measure the approximate rpm. Chopper vibration is continuously monitored, with safety trip above a preset displacement. Several critical operating temperatures are recorded, and the chopper vacuum system is monitored.

256-CHANNEL NEUTRON TIME-OF-FLIGHT SPECTROMETER

N. W. Hill T. L. Emmer J. B. Davidson

A 256-channel neutron time-of-flight spectrometer (Fig. 13) based on Schumann's[1] design has been installed at the Low Intensity Test Reactor and has been operating for a period of six months. The main features of the instrument, as previously described,[2] are the following:

1. a magnetic-core memory with 256 channels, each with a storage capacity of approximately 65,000 counts,
2. channel widths of 0.5, 1, 2, 4, and 8 μsec, selected by means of plug-in oscillator crystals,
3. an analyzing period of 0 to 1024T μsec, where T is the channel width (this period is divided

[1] R. W. Schumann, *Rev. Sci. Instr.* **27**, 686 (1956).

[2] T. L. Emmer and N. W. Hill, *Instrumentation and Controls Semiann. Prog. Rep. July 31, 1956*, ORNL-2234, p 17.

UNCLASSIFIED
ORNL LR DWG. 24028

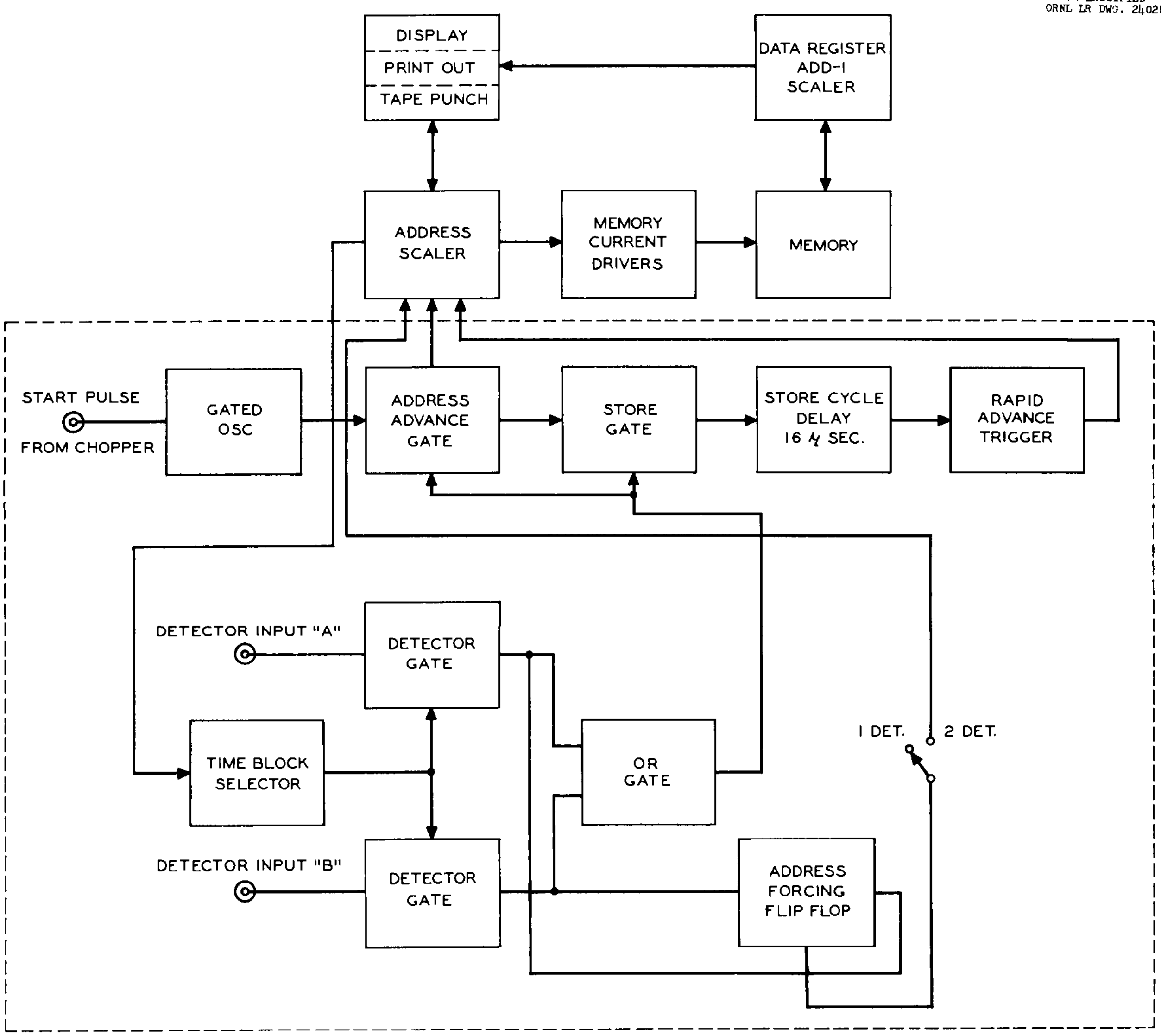

Fig. 13. 256-Channel Neutron Time-of-Flight Spectrometer.

into eight time blocks of $128T$ μsec each; any two of these time blocks may be selected for analysis),

4. two inputs which allow two detectors to be used simultaneously, with each detector being allotted 128 channels,
5. a linear oscilloscope display which allows the information in the memory to be monitored,
6. a strip-chart recorder print-out of the data,
7. a punched-tape output suitable for processing by the Oracle.

The magnetic-core memory, along with its control and its current-driving and power-supply circuits, was purchased from a commercial source and was used as received from the manufacturer with only minor modifications.

In order to be used as part of a neutron time-of-flight spectrometer, the memory address scaler must be supplied with suitably shaped, uniformly spaced pulses from a basic oscillator or "clock." The number of pulses presented to the memory is a measure of the time of flight of the neutron if the clock is turned on by a pulse signaling the opening of the neutron beam shutter and is turned off by a pulse from a neutron detector along the flight path. The number of the oscillator pulses, N, represents the time-of-flight interval NT, where T is the channel width. The number N is also the number of the channel in which the count representing the occurrence of a detected event is to be stored. The gating of the clock, the selection of the channel width, and the selection of the interval for analysis are functions of the control unit.

The time-block selector allows a predetermined time to elapse before analysis begins. It consists of a scale-of-eight counter which receives one count for every 128 counts from the gated oscillator. The states of the scale-of-eight binaries are used to control the detector gates and, thereby, the time interval to be analyzed. Using one detector, two separated intervals of $128T$ each may be selected out of the total time of $1024T$ by means of patch cords.

Two detectors may be used with one interval of $128T$ being selected. The counts from each detector are stored in separate halves of the memory. This is accomplished by means of an address-forcing flip-flop at the detector inputs. This flip-flop replaces the 2^7 stage in the address scaler of the memory. If a detector pulse is received at input A, the address-forcing flip-flop is set in the state which forces this count to be stored in channels 0 to 127. If a pulse is received at input B, the flip-flop is set to the opposite state (effectively adding 128 to the number in the address scaler), forcing this count to be stored in channels 128 to 255.

In order that more than one event per burst of neutrons may be analyzed, the address scaler is allowed to continue advancing after the storage of a count. However, it must be brought "up to date" since the oscillator was off during the storage time. This is accomplished by making the storage time an integral multiple of the channel width and rapidly advancing the address scaler by the appropriate integer at the end of a storage cycle.

The oscilloscope display of the counts stored in the memory versus the channel number is obtained from a binary-to-analog decoder, the voltages from which are displayed at a 5-kc rate. The analog voltages representing the counts are also applied to a Brown recorder, which prints the data at a rate of two channels per second. In order that the data might be processed by the Oracle, a punched-tape control unit was designed. This unit drives a standard Teletype high-speed tape punch. Eight rows of four holes each are required to specify the channel number and the count. One additional hole in each row is used for a parity check by the computer. The tape may be punched manually for coding the beginning and end of a tape.

The performance of the spectrometer has been checked by determining the known cross sections of several nuclides. Satisfactory agreement with published values has been obtained. The instrument has proved to be stable, reliable, and free from undue maintenance requirements. It is currently being used to study previously unmeasured cross sections.

PUMP SPEED MONITOR (Q-1724-11)

J. L. Blankenship

The design of the pump speed monitor has been evolved from a similarly named device (Q-1636), and both share ancestry with the linear count rate meter (Q-1511) reported by Glass.[1]

An instrument was needed which would indicate rotational speed with considerable accuracy, provide a failsafe indication if the speed should drop below a preset point, automatically reset if the underspeed condition should disappear, and undergo extended operation without maintenance. These requirements were approached by a conservative design philosophy which utilized 10,000-hr tube types such as the 5691, -2, and -3 series, oil or paper capacitors, all resistors generously derated in power, and a wide tolerance for tube characteristics.

The input signal must be greater than 10 mv peak-to-peak and may be any repetitive waveform, with 60 cycles per revolution to give the proper scale factor. The input signal waveform may be monitored with a self-contained 1-in. oscilloscope mounted on the front panel. Speed readout is provided by a 1% panel meter, external 100-μa meter, 10-mv recorder, external 100-v meter drawing up to 5 ma, and a panel-mounted 10-turn Helipot in a null-type comparison readout. A tuning-fork oscillator which is built into the device provides a calibration frequency of better than 0.03% accuracy. In addition, the Helipot may be set to a given speed, and the difference between the actual speed and the given speed set on the Helipot dial may be read on the dial of a meter face calibrated −500, 0, +500 rpm. Two ranges of speed indication are provided by a panel switch, 0 to 5000 and 0 to 500 rpm. The instrument accuracy and linearity is ±1% of full-scale for readout on the panel meter.

If a ¼% strip chart recorder, a digital voltmeter or the Helipot null balance comparison readout is used, and if the instrument is zeroed and calibrated from the internal calibration frequency, the reading will be accurate to ±¼% and linear to ±¼% referred to full-scale on the 5000-rpm range. After initial operation of 100 hr, and on a regulated line, zero drift will not exceed ±¼% per two months. Calibration drift will not exceed ±¼% per week or ½% per two months.

Three independent underspeed alarm levels with 5-amp dpdt contacts are provided. Alarm contacts actuate within 25 msec after the actual speed has fallen below the alarm level. Reclosure is within 20 msec after the speed has exceeded the alarm level. Hysteresis of the alarm circuit will not exceed 50 rpm. Operation of the range-change switch does not affect the alarm-level settings. Also, depressing the calibrate switch does not trip the alarm contacts, regardless of the level settings. The voltage output of +100 v for 5000 rpm is referenced to ground and will furnish up to 5 ma. This voltage output is suitable for an analog computer input.

[1]F. M. Glass, *Instrumentation and Controls Semiann. Prog. Rep. July 31, 1954*, ORNL-1768, p 14.

PULSE INTEGRAL ANALYZER (Q-1824)

J. L. Blankenship

The pile oscillator[1] is a device used to measure thermal neutron capture cross sections. Instrumentation for this installation, used at the ORNL Graphite Reactor for a period of ten years, has been redesigned for greater speed and accuracy. The new instrumentation takes only a fourth the time previously required for the same accuracy of measurement. In addition, the new instrumentation is much less sensitive to various sources of noise. Figure 14 is a front view of the electronic equipment assembled in a relay rack. Figure 15 is a block diagram of the pile oscillator system.

A sample is passed back and forth through the ionization chamber which is in a thermal neutron flux field. Small changes, or pulses, of current through the ionization chamber are produced by the absorption of neutrons as the sample passes through the chamber. The pulse amplitude is a measure of the capture cross section and mass of the sample. An integration of the current pulse will produce a voltage pulse that depends upon the capture cross section and not on the scattering cross section. The old instrumentation took the simple sum of the integral of a large number of current pulses. The pulse-integrator analyzer speeds up the measuring process by integrating each pulse, quantizing the integral value and storing the data in digital form. The pulse-integrator analyzer operation is shown in Fig. 16. Figure 17 shows the graphic display of the stored data which was accumulated for seven minutes for each of five samples of gold. Figure 18 shows a graph of the mass of the gold samples as a function of the channel number at which the peaks of Fig. 17 occurred.

[1]J. I. Hoover *et al.*, *Phys. Rev.* **74**, 864 (1948).

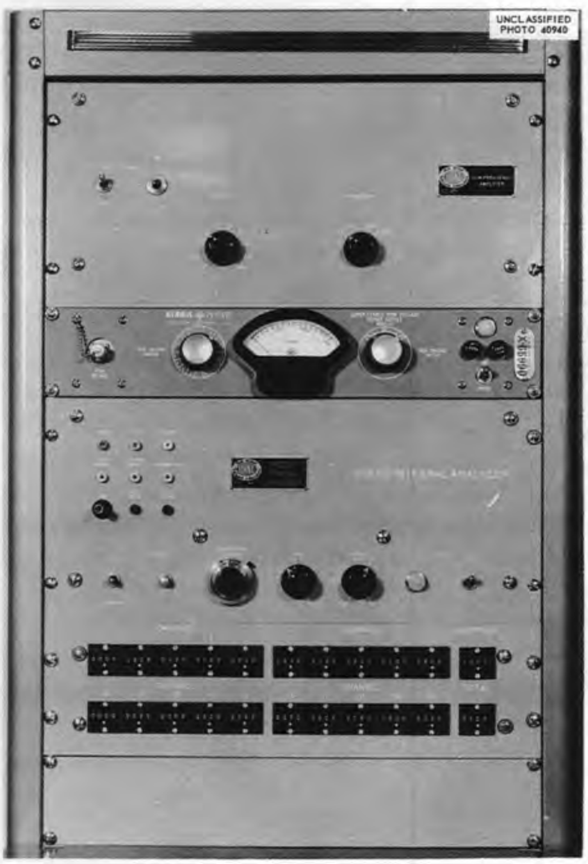

Fig. 14. Pulse Integral Analyzer.

UNCLASSIFIED
ORNL-LR-DWG 21271R

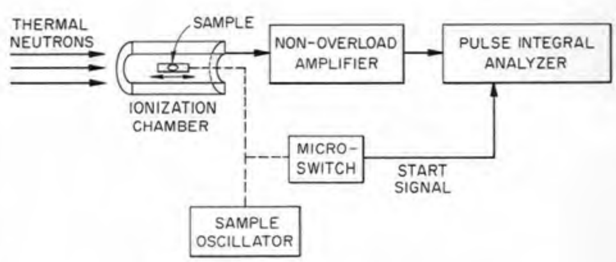

Fig. 15. Pile Oscillator System.

UNCLASSIFIED
ORNL-LR-DWG 21272

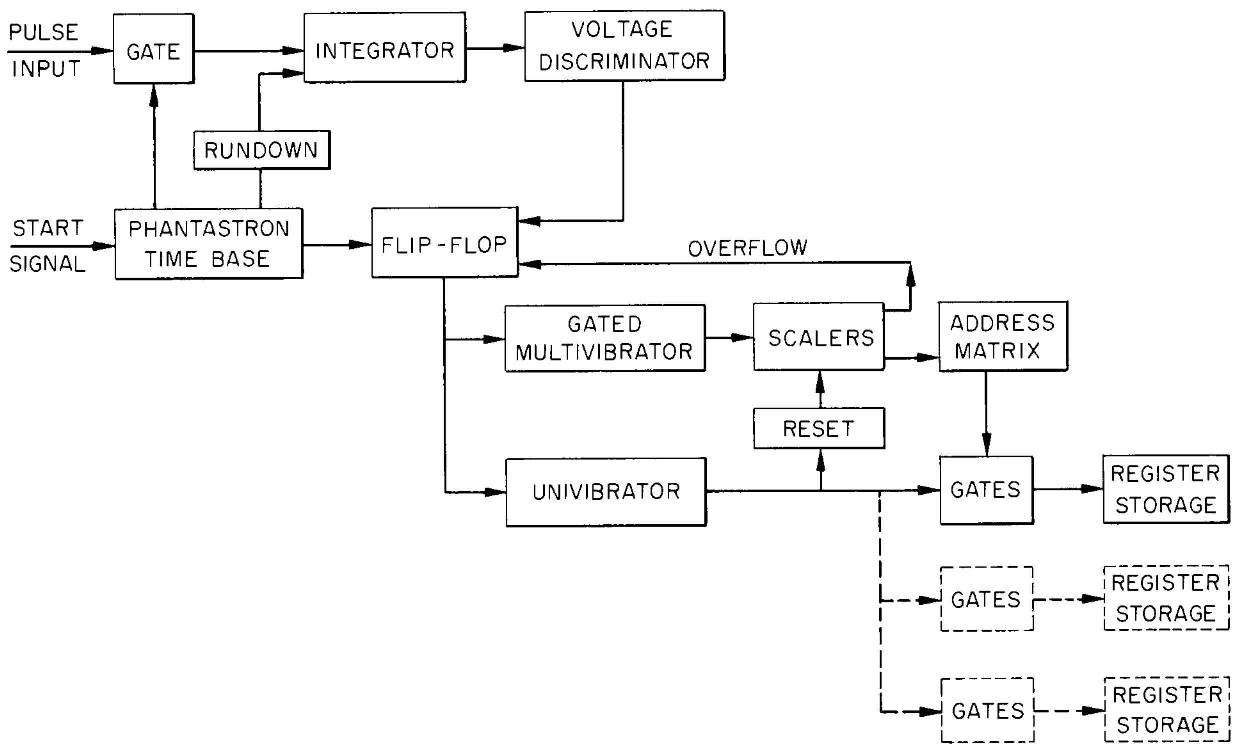

Fig. 16. Pulse Integral Analyzer.

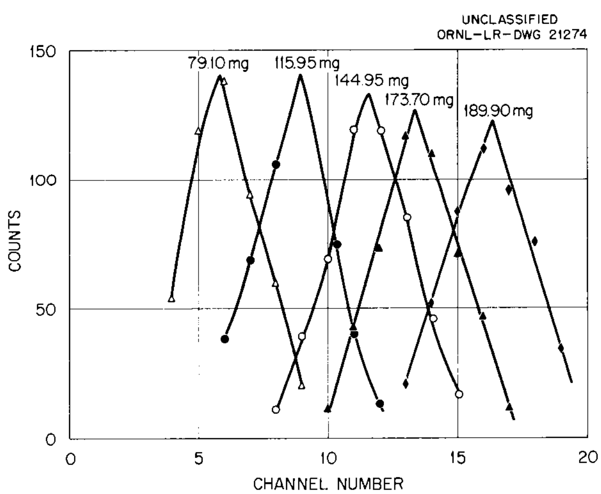

Fig. 17. Stored Data for Five Samples of Gold.

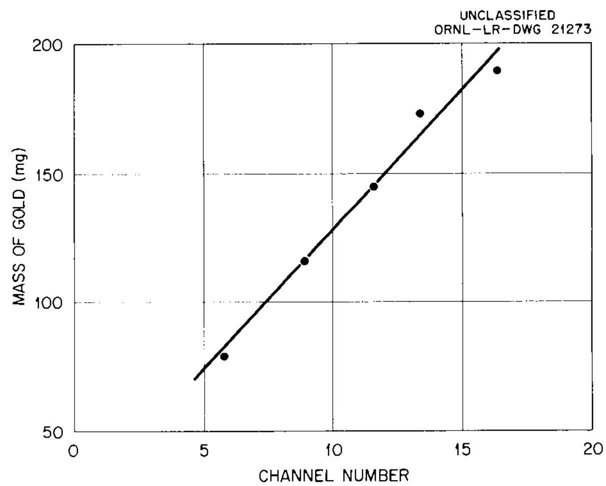

Fig. 18. Mass of Gold vs Channel Number for Peaks in Fig. 17.

18-CHANNEL TIME-BASE ANALYZER

F. M. Glass

An 18-channel time-base analyzer was developed for the Bulk Shielding group and has been used by G. DeSaussure and E. Silver. The purpose of the instrument is to determine the time-dependent neutron behavior of blocks of a moderator. The neutrons are produced in short bursts by deuteron-deuteron interaction. These bursts are controlled by the analyzer, which pulses the ion source in synchronization with the counting circuits. Since the ion source is located in the high voltage terminal of a high voltage accelerator, it is necessary to transmit the synchronizing pulses over a VHF radio link.

The complete time-base analyzer consists of 18 storage channels and their respective gates, one totals channel, a programmer, a VHF transmitter, a VHF receiver, and an ion deflector. Figure 19 is a block diagram of the equipment.

The complete operating cycle is divided into three intervals. The first interval is the time during which the sample is being bombarded. The second is a waiting period, and the third is

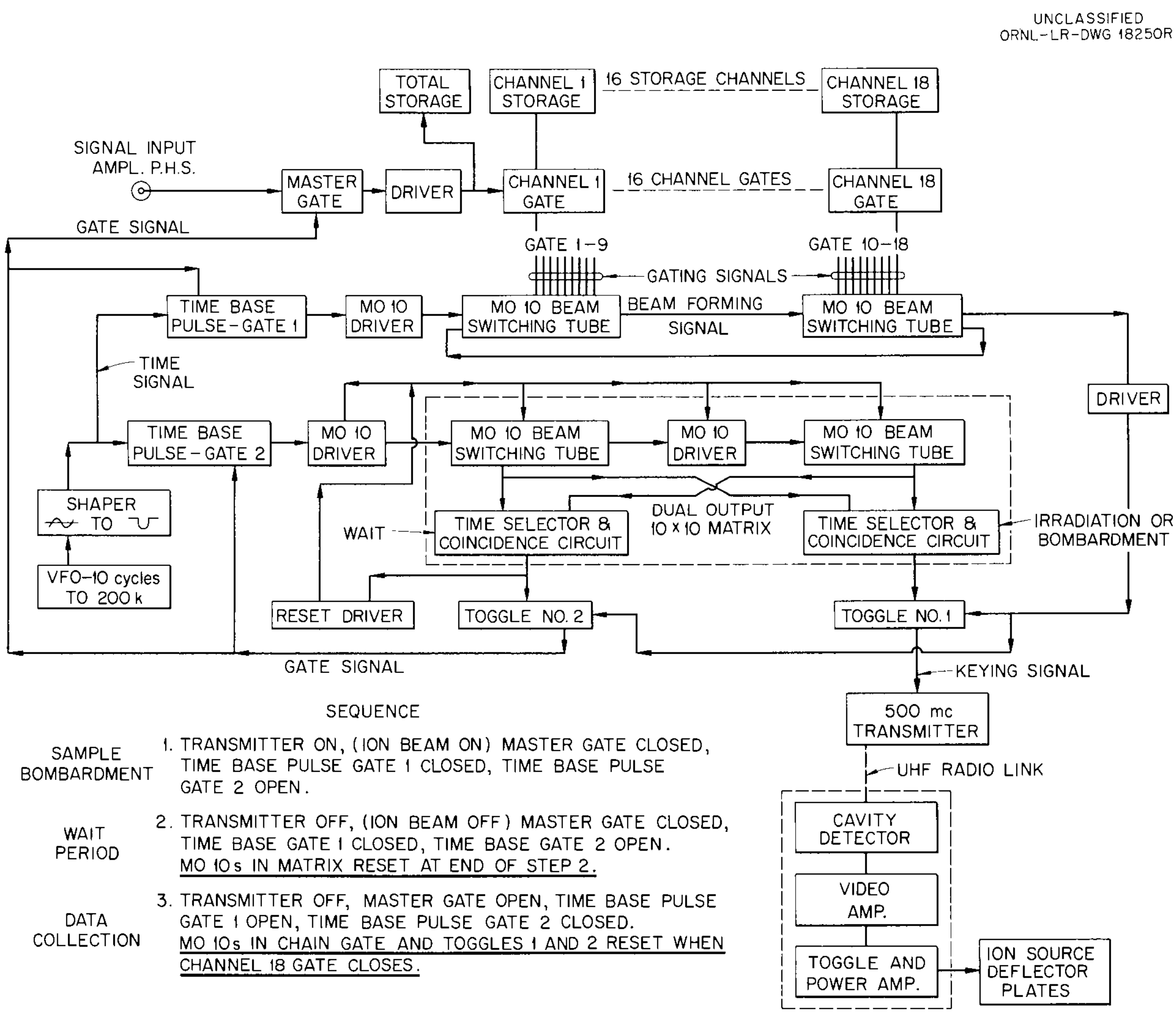

Fig. 19. 18-Channel Time-Base Analyzer.

the counting period during which the neutron pulses are being gated into the various storage scalers in a fixed time sequence. The basic timing signal is supplied by a variable-frequency oscillator. Therefore, the basic time interval is the reciprocal of frequency. The "sample bombardment time" and the "waiting time" are adjustable by means of selector switches in a 10×10 matrix and by the frequency of the oscillator from which the 10×10 matrix receives the basic time signal. The width of the storage gates is the same as the oscillator period. Since the gates open in sequence from 1 through 18, the counting or data collection period always consists of 18 periods of the oscillator. Two toggles, which receive their signals from the 10×10 matrix, perform all the gating and keying functions, excluding the chain gating. The printed sequence on the block diagram indicates the operating principle.

Figures 20 and 21 show the physical lay-out of the analyzer. A time intervalometer and a pulse amplifier have been included in the rack for convenient operation. These are shown in Fig. 20 and are located just above the desk top. Specifications of the time intervalometer are:

Beam switching time	1 μsec
Minimum channel gate width	5 μsec
Maximum channel gate width	0.1 sec
Gate opening time	0.2 μsec
Gate closing time	0.2 μsec

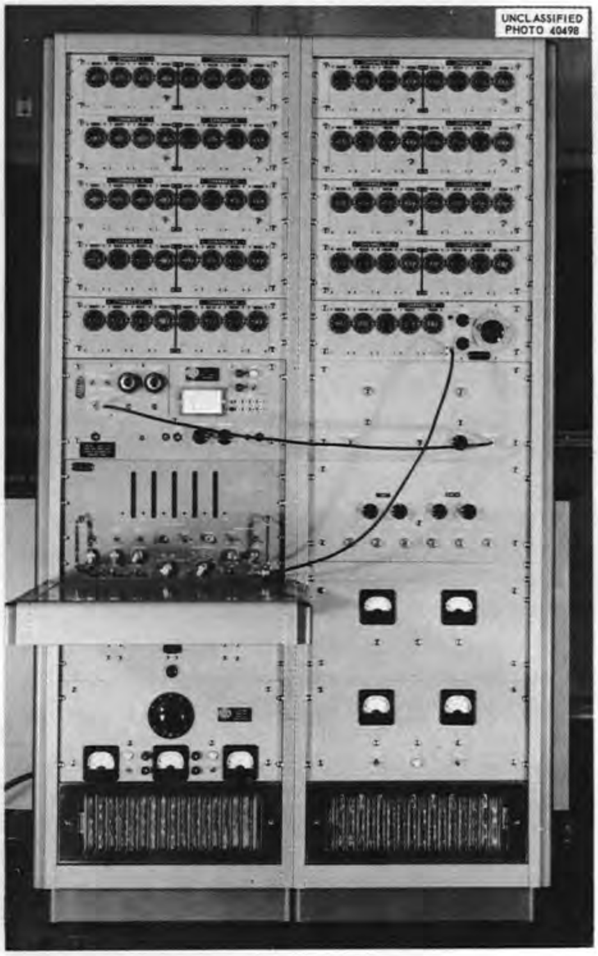

Fig. 20. 18-Channel Time-Base Analyzer, Front View.

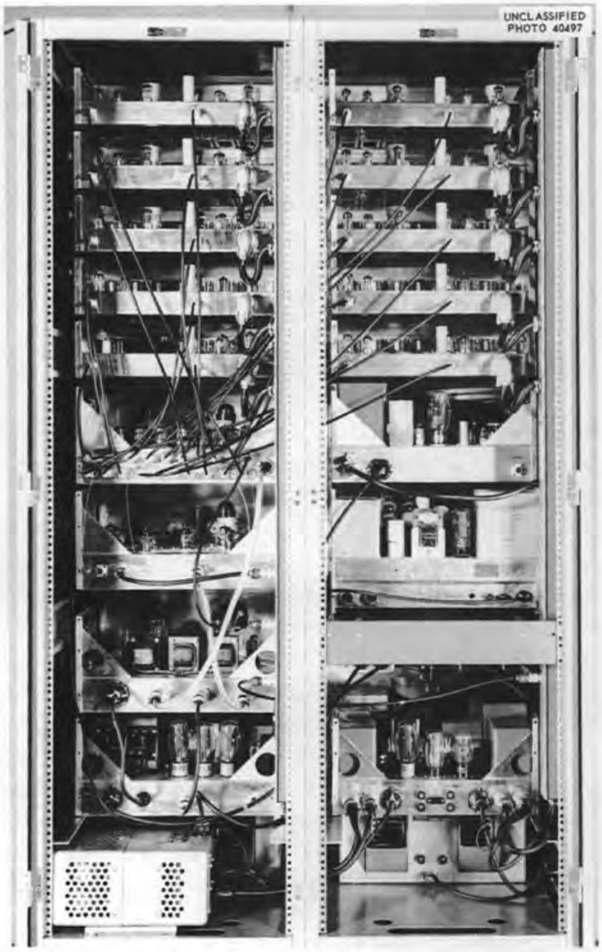

Fig. 21. 18-Channel Time-Base Analyzer, Rear View.

POSITION INDICATOR FOR BULK SHIELDING FACILITY SINGLE-CRYSTAL SPECTROMETER

D. J. Knowles

The Bulk Shielding Facility (BSF) is presently engaged in setting up additional test facilities consisting of a single crystal spectrometer, its shielding, a positioner for the shielding, and a position indicator for the shield. The spectrometer will utilize a 9-in.-dia NaI crystal in a massive cylindrical gamma shield which will operate both in and out of the pool at the BSF. This shielding, the weight of which is estimated at 15 tons, is being designed by the Mechanical Development Section of this division. A positioner for the shield, consisting of a bridge crane of suitable capacity with a modified vertical motion, has been purchased. A rigid member with a yoke end to cradle the shield will be added when the crane is installed. This modification to the crane is being designed by the Engineering and Mechanical Division, and the design is essentially complete. The yoke construction will allow the positioning of the shield in or out of the pool and, in addition, will make it possible to rotate the longitudinal axis approximately 300 deg in the horizontal plane and ±70 deg from the horizontal plane (see Figs. 22 and 23).

The data-taking point will be located at the end of a collimator on one end of the shield at approximately 5 ft from the axis of rotation of the shield. For efficiency in taking and in repeating data, the accuracy of locating this point in the water with respect to the center of the reactor is specified as $\pm \frac{1}{4}$ in. To utilize the convenience of the crane and save the time now used in determining the coordinates under water, a position indicator is now being designed.

A five-dial readout will continuously display the X, Y and Z coordinates of the data-taking point as well as the azimuth and tilt angles of the shield. Linear measurements of the position of the center of gravity of the shield will be made by rolling a wheel on the crane rails, and the vertical angle will be measured with respect to a pendulum. Horizontal angle is measured with respect to the bridge crane. All motions are transmitted to a computer by servo systems where the following equations are solved:

$$X = X_1 \pm X_2 \pm AB \cos V \sin H ,$$

$$Y = Y_1 \pm Y_2 \pm AB \sin V ,$$

$$Z = Z_1 \pm Z_2 \pm AB \cos V \cos H ,$$

where

X, Y, Z = coordinates of point A (end of collimator),

X_1, Y_1, Z_1 = coordinates of center of gravity of shield,

X_2, Y_2, Z_2 = possible corrections to X_1, Y_1, Z_1 for structural deflections, temperature effects, etc., of small but appreciable magnitude,

AB = distance from center of gravity of shield (point B) to point A,

V, H = angles of tilt and azimuth.

A schematic diagram of the computer is shown in Fig. 24. Additions are performed mechanically by differentials. Function generation and multiplication are done electrically by means of nonlinear potentiometers and a resolver. Criteria for the selection of parts and method of computation have been determined by the final accuracy specified.

The computed coordinates are also utilized to provide a limit-of-travel alarm for the protection of the equipment.

The preliminary design of the position indicator is essentially complete at this time and most of the equipment to be purchased is on hand. Fabrication of the position indicator is 80% complete, and installation and testing will follow the schedule of the other parts of the project.

UNCLASSIFIED
ORNL-LR-DWG 21206

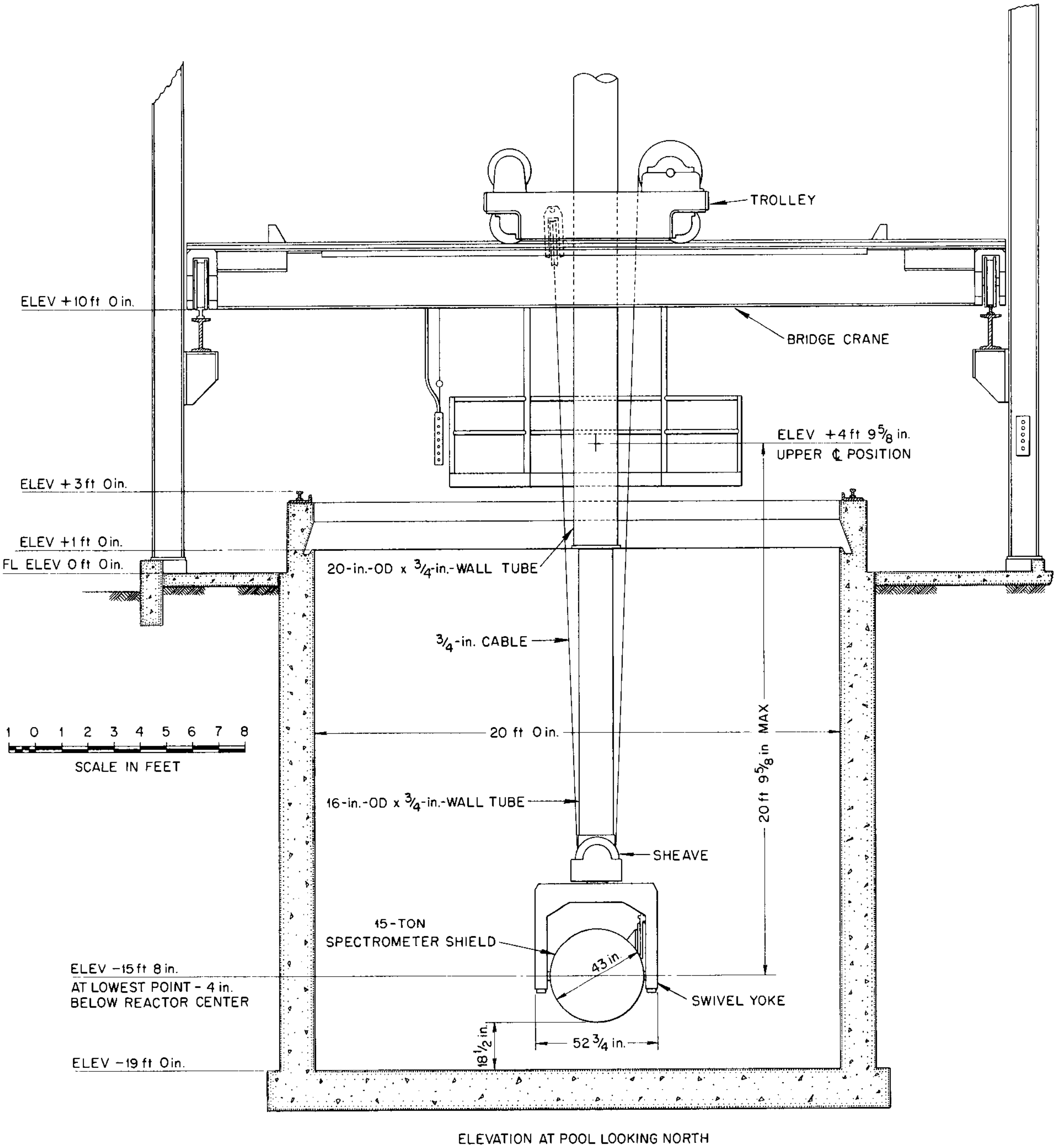

Fig. 22. Spectrometer-Positioning Device for BSF.

UNCLASSIFIED
ORNL-LR-DWG 21207

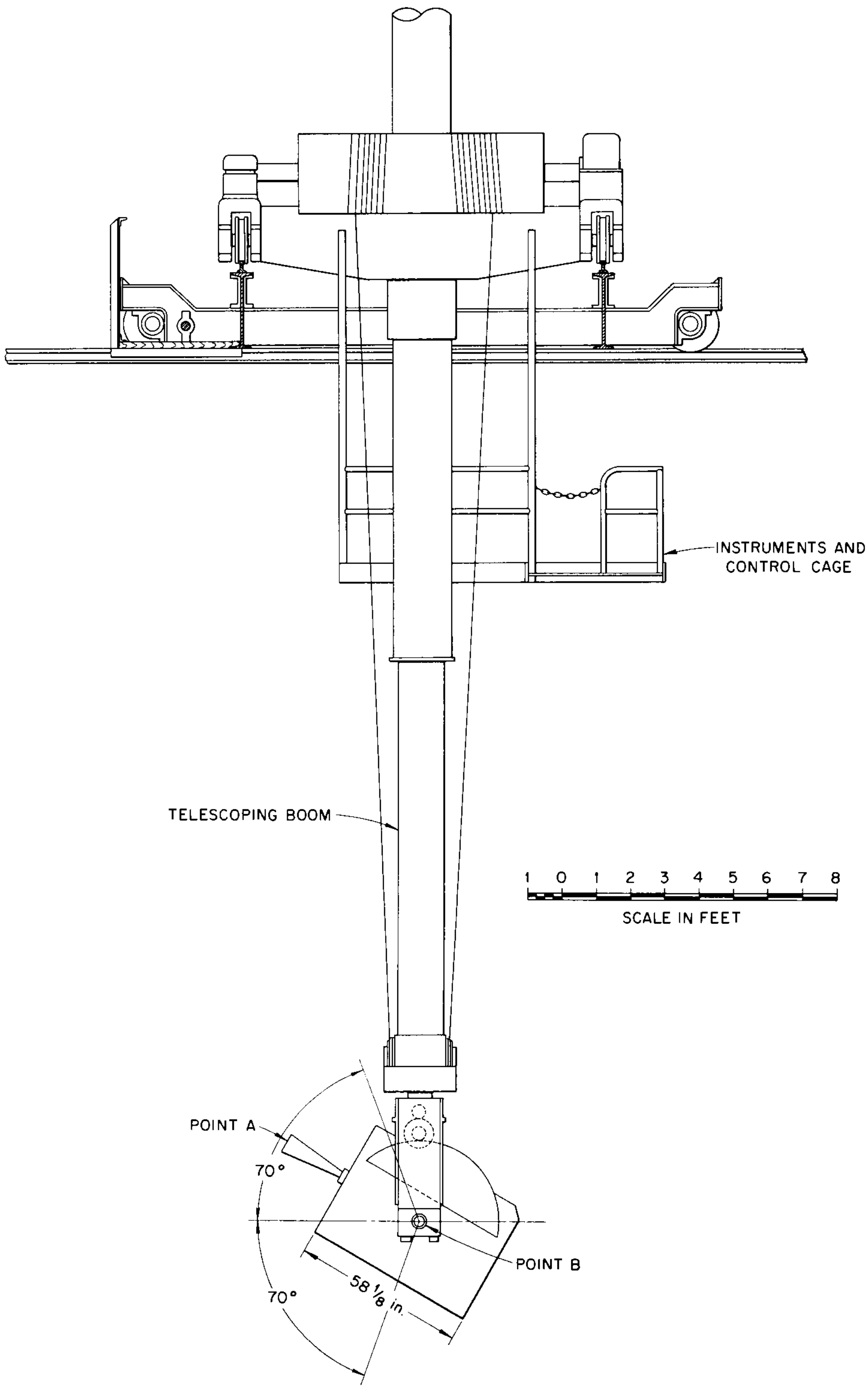

Fig. 23. Spectrometer-Positioning Device for BSF.

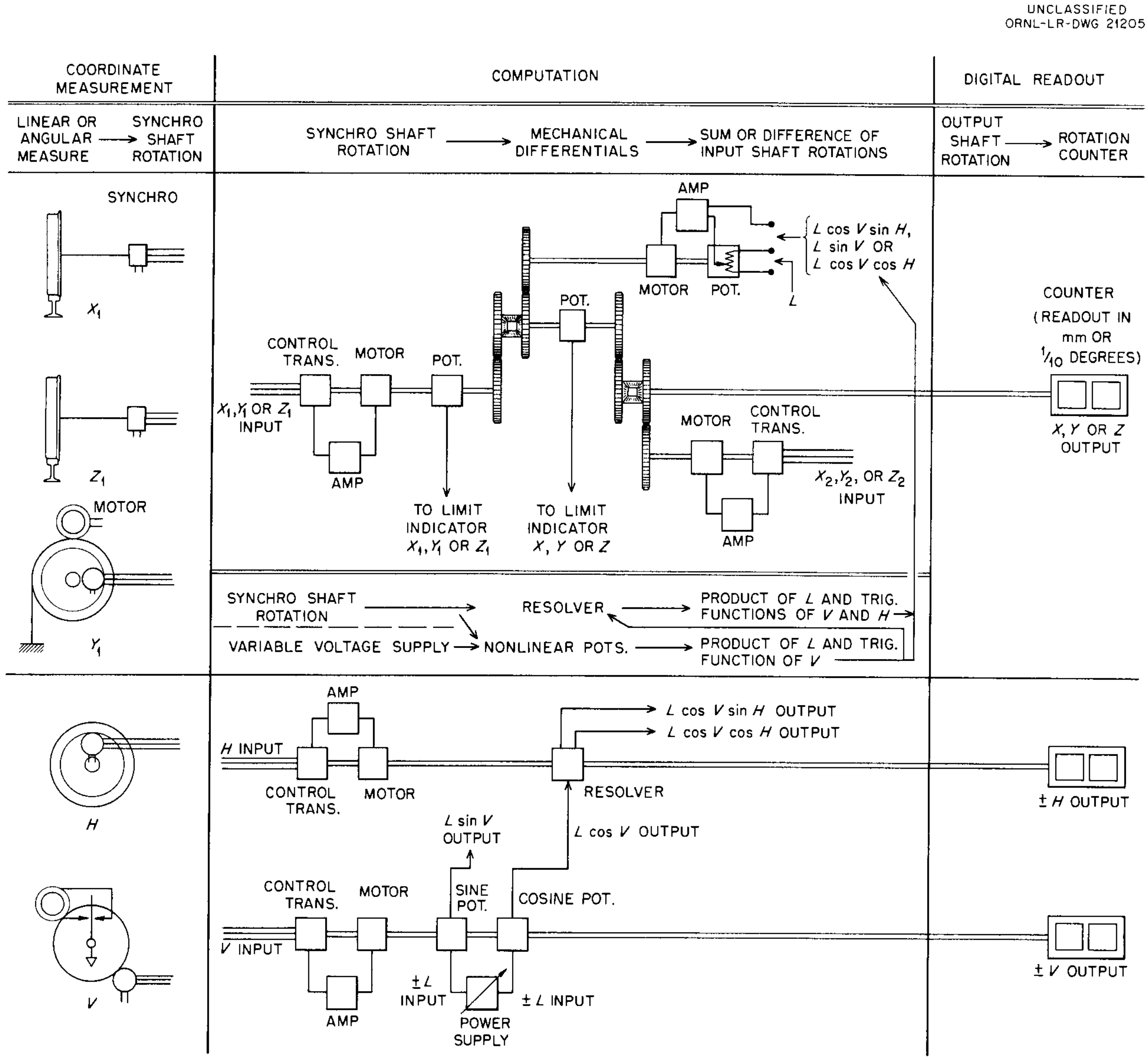

Fig. 24. Computer for Spectrometer-Positioning Device.

SUPERHETERODYNE ELECTRON-SPIN RESONANCE SPECTROMETER

J. L. Lovvorn

To improve the sensitivity and signal-to-noise ratio of an existing electron-spin resonance spectrometer, it was converted to a superheterodyne electron-spin resonance spectrometer. The major part of the conversion involved redesign and new design of the electronic chassis associated with the commercially built microwave components. A local-oscillator Klystron is used to generate the heterodyne frequency. The local oscillator incorporates automatic frequency control (AFC) for obtaining frequency stability. The frequency of the power oscillator is stabilized by employing the specimen cavity as a frequency reference; thus automatic compensation is provided for the effects of the paramagnetic dispersion.[1] The output of the spectrometer can be presented (1) as a pattern on an oscilloscope of paramagnetic resonance absorption vs magnetic field, (2) as a graph of absorption vs magnetic field on a strip chart recorder, or (3) as a continuous recorder trace of the derivative of the absorption vs magnetic field.

Frequency stabilization of the Power Klystron is obtained by a technique which is a modification of the 30-Mc/sec i-f system developed by Pound.[2] Figure 25 is a block diagram of the converted spectrometer. In this spectrometer the specimen cavity is used as the frequency-reference cavity, but instead of using a crystal modulator to supply the i-f, as was done by Pound, a local oscillator is employed. The signal for the lock-in mixer-detector is obtained from the limiter which is fed from the 30 Mc/sec i-f amplifier connected to the balanced mixer. The reference 30 Mc/sec signal required for the operation of the lock-in mixer is obtained from a second channel consisting of another 30 Mc/sec limiter fed from a 30 Mc/sec reference amplifier and mixer crystal. A small amount of the Power Klystron output is coupled out of the main line by a directional coupler and is transmitted through a load isolater and phase shifter (which enables proper phase adjustment of the reference signal) to the second crystal mixer in the reference-beat hybrid tee. Local-oscillator power for this beat hybrid tee is provided by the *H* arm of the dividing hybrid tee connected to the local oscillator. This 30 Mc/sec reference signal, which is independent of the reflection coefficient of the specimen cavity, is transmitted through a coaxial line to the 30 Mc/sec reference amplifier, and the output of the limiter on this amplifier is connected to the suppressor grid of the phase-sensitive lock-in mixer. A second output from the reference amplifier feeds three additional stages of amplification and a Foster-Seeley discriminator. The output of the discriminator is amplified by a two stage d-c amplifier and fed to the bottom end of a battery stack which furnishes the operating voltage for the reflector electrode of the local oscillator Klystron. The varying output of the d-c amplifier acts to provide AFC for the local oscillator. The output of the lock-in mixer acts on the reflector supply of the Power Klystron so as to correct for frequency changes, thus providing frequency stabilization for the Power Klystron.

The 30 Mc/sec i-f amplifier and AFC amplifier were made by LEL, Inc. The remaining parts of Q-1582-2 indicated on Fig. 25 were designed and constructed here. The lock-in mixer is a 6AS6 type tube. It is operating at a potential of approximately 1000 v and had to be well insulated. The reference amplifier limiter consists of two stages employing 6AK5 tubes, and the final stage uses a 6197 tube. The single stage of limiting following the output of the 30 Mc/sec i-f amplifier also employs a 6197 tube.

Because the gain of the control loop was insufficient as furnished by the slope of the commercially built AFC discriminator, it was necessary to add the two stage d-c amplifier. The 30 Mc/sec reference amplifier, though built for the formerly used system, required extensive revamping to provide additional gain and reduce its spurious signals. Because the lock-in mixer had to operate on the reflector supply for the

---

[1] J. M. Hirshon and G. K. Fraenkel, *Rev. Sci. Instr.* 26, 34 (1955).

[2] R. V. Pound, *Rev. Sci. Instr.* 17, 490 (1946).

UNCLASSIFIED
ORNL-LR-DWG 29406

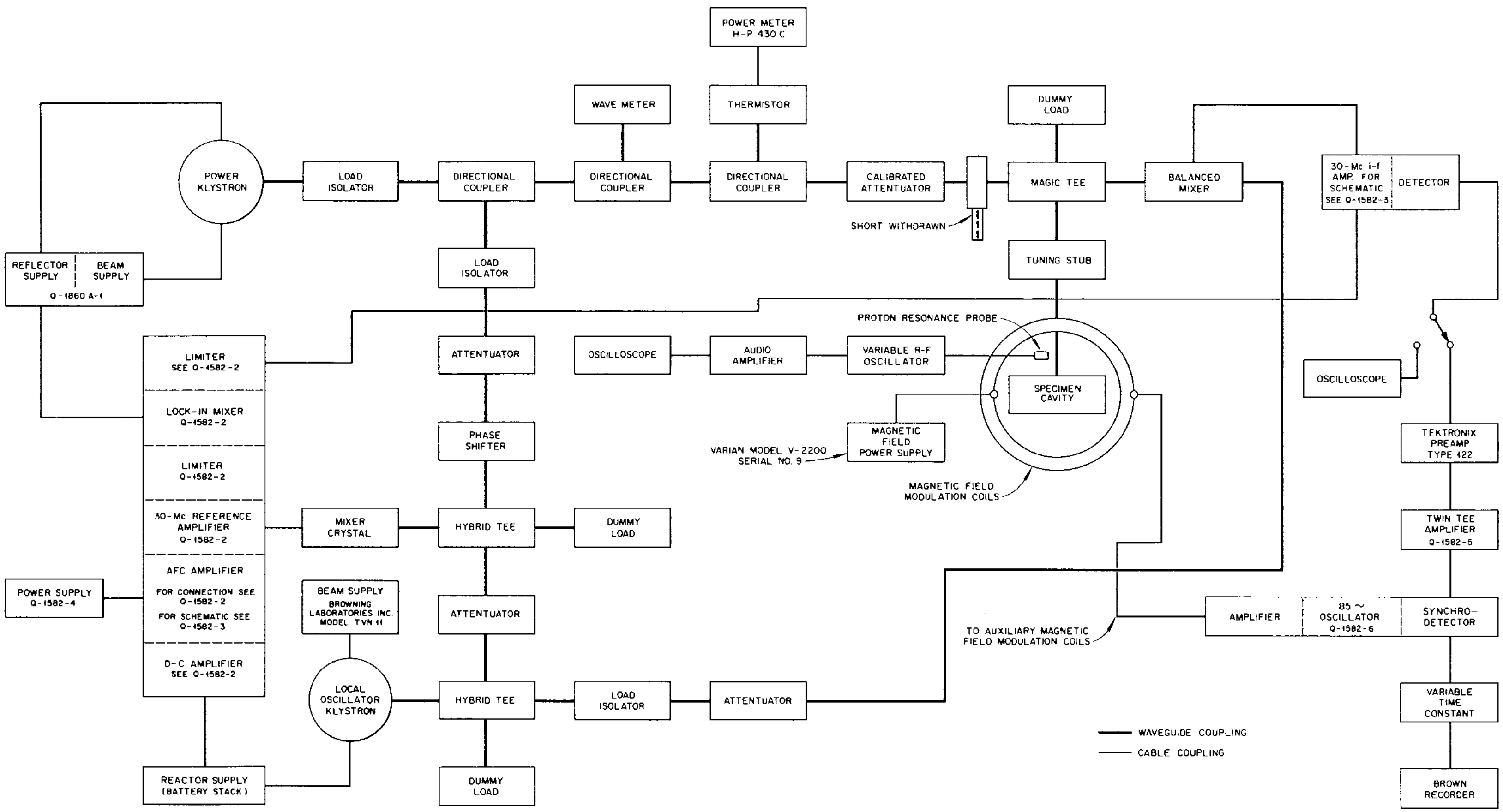

Fig. 25. Superheterodyne Electron-Spin-Resonance Spectrometer.

Power Klystron, it was necessary to modify Klystron Power Supply Q-1860 to Q-1860-A. Provision was made for switching control in and out on both the AFC and frequency stabilization loops. The gain for both loops was made variable. Careful layout shielding and decoupling were necessary to prevent signal leakage and consequent oscillation.

The superheterodyne electron-spin resonance spectrometer has an improvement factor of approximately 100 over the previously used simple bridge spectrometer. The work was performed for R. A. Weeks of the Solid State Division who performed the systems design and accepted the responsibility for the microwave portion of the system.

ADDITIONS AND IMPROVEMENTS TO ORACLE

J. W. Woody, Jr.

The New Oracle Input-Output System

A new input-output system (Fig. 26) has been installed and is superior to the old system in versatility, reliability, and speed. This has been accomplished by replacing some of the old equipment, by adding some new devices, and by adding circuitry which permits the Oracle to accept alphameric characters and which also allows more complete checking.

The console has been completely redesigned. Additional indicator lights have been added and all lights were regrouped to facilitate visual monitoring of the Oracle. The numerous toggle switches used in the old console to insert instructions and data manually (on a binary bit-by-bit basis) have been replaced with a compact keyboard. The keyboard, consisting of a control key panel and an information key panel, reduces by a factor of four the number of operator manipulations required to perform a specific operation. A console typewriter acts as a keyboard monitor by printing a character or symbol which is associated with each key each time that key is depressed. When used in this function the console typewriter produces a record of all information and instructions inserted into the Oracle by the operator.

While automatic input is still performed by a 200-character/sec Ferranti photo-electric reader, new output equipment has been added. The old 20-character/sec paper-tape punch has been

Fig. 26. Oracle Input-Output System.

replaced by a 60-character/sec unit, and high-speed output is now possible by means of a magnetic tape recorder which operates at a speed of approximately 900 characters/sec. In addition, the console typewriter can be used as an output device for small quantities of data.

The curve-plotter is the same as in the previous system with the exception of a few minor alterations. A cathode-ray tube designed for this specific function replaces the old, smaller tube, and a camera with greater film capacity is now used. Curve-plotter monitoring is accomplished by paralleling the display tube with a Hughes Memotron which has been installed in the console.

New off-line equipment has been added to complement the new input-output system. Paper-tape preparation units operating in either the hexadecimal or alphameric mode provide facilities for preparing, verifying, and reproducing tapes for Oracle input. Output from the Oracle can be printed on typewriters from either the paper tape or magnetic tape media (Fig. 27).

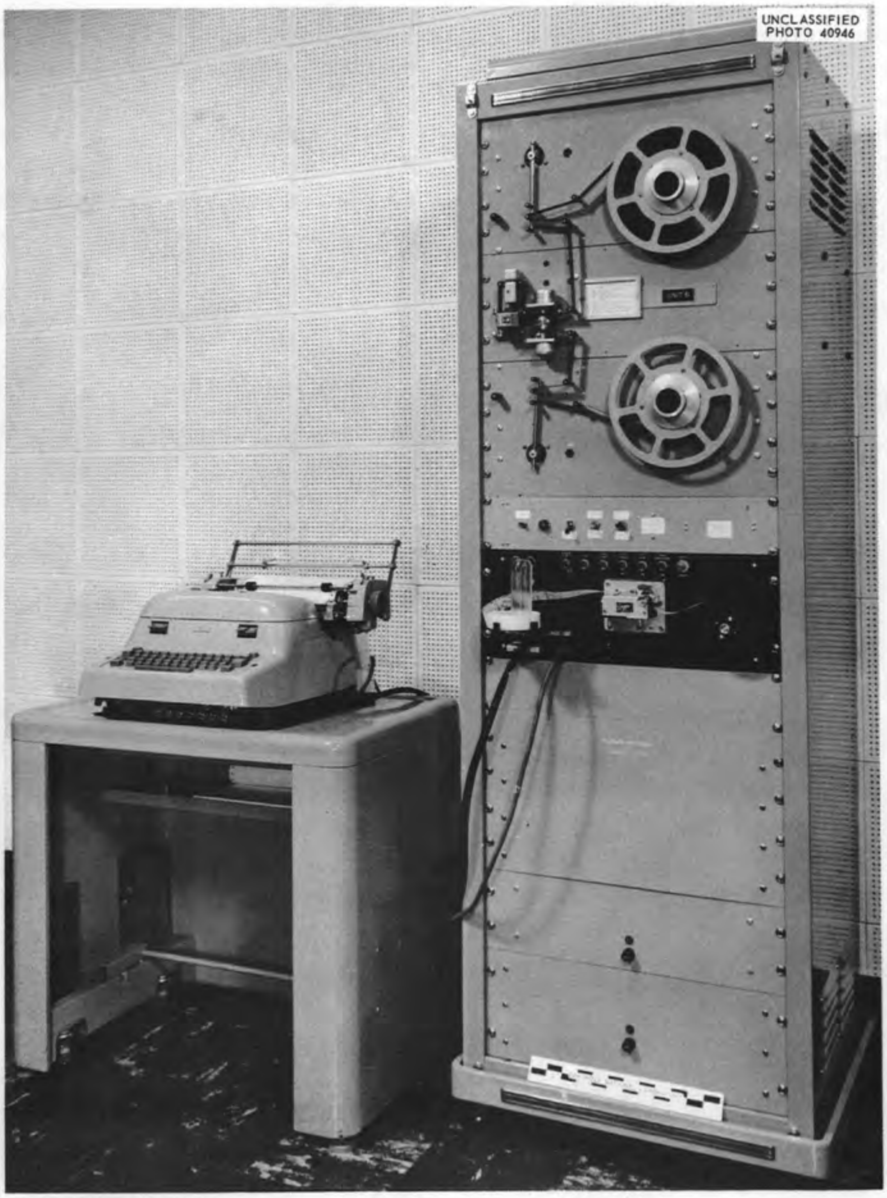

Fig. 27. Oracle Output Printing System.

The Oracle Magnetic Tape Auxiliary Memory

The reliability of the Oracle 2-in., 42-channel, magnetic-tape auxiliary memory has been improved by some recent electronic changes. "Drop-outs" have been virtually eliminated by the incorporation of a redundant recording scheme. Although this necessitated a reduction in word rate from 8.4 to 4.2 kc/s, the reduced error rate obtained was considered more important than the higher speed.

After incorporation of the above system, the remaining errors encountered were almost exclusively "pickups". These pickups have been dramatically reduced by substituting transistorized front ends in the playback amplifiers. Although only 12 of the 42 amplifiers have thus far been altered in this manner, the results show great promise.

Below is a breakdown of the error rate before and after the above modifications. The numbers represent the number of 42-digit words read per error for each of the four drives.

	Six-Month Average Before Modifications	Two-Month Average Since Modifications
Drive No. 0	4.3×10^6	12.2×10^6
Drive No. 1	4.5×10^6	13.0×10^6
Drive No. 2	11.6×10^6	13.7×10^6
Drive No. 3	4.6×10^6	32.5×10^6

Accurate error-data records were not kept before the above eight-month period. The average number of words read per month per drive was approximately 50×10^6.

Other improvements to the magnetic tape auxiliary memory are

1. plug-in add-subtract counters for the continuous monitoring of tape position by "blocks" of 128 words,
2. addition of automatic rewind facility by means of internal machine orders,
3. optional interlock to prevent accidental recording on tapes containing valuable data.

SCINTILLATION GEIGER COUNTER

R. E. Zedler

Some work has been done to develop a small gamma detector of good efficiency. The detector consists of a small scintillation crystal, ¾ in. dia × 1 in. long, and a small geiger counter whose cathode has been specially photosensitized to respond to the light emitted by the phosphor. The most photosensitive counters produced have a spectral response between 2200 to 3000 Å.

To date the phosphor that has worked most successfully with photosensitive geiger counters has been Ag-activated NaCl.[1] The principal emission spectra for this scintillator lie in the 2500 Å region.[2]

The major effort has been to produce a small, stable counter having a photocathode with high sensitivity in the 2500 Å region. Work has been done with the two types of counters illustrated in Figs. 28 and 29. Type 1 was made photosensitive by glow-discharge techniques at liquid-nitrogen temperature, as discovered by Scherb.[3] Some response to gamma radiation scintillations was achieved. The most sensitive and stable counter was produced by using an electromesh (nickel-copper) cathode with about 30% open area and a 10% ether-argon filling to 12 cm Hg pressure.

A more efficient and sensitive arrangement is shown as type 2. The most stable and sensitive cathode to date is made of electro-polished copper. It was activated at *room* temperature, in argon at 0.5 cm Hg pressure, by a glow discharge process. This gas was then removed and the counter was filled with 10% ether-argon at a pressure of 10 cm Hg. In a gamma flux radially entering the counter and crystal, the counting rate was increased a factor of 5 by detecting the crystal scintillations. The overall detection efficiency for this unit is about 4% for gamma energies in the 1 Mev range. For the size and type of phosphor used, calculations show that about 20% of the 1-Mev gamma photons interact with the crystal. This would be the maximum achievable efficiency.

Some work has been done with platinum cathodes. It was found that platinum may be made quite photosensitive without glow discharge techniques. This was done by "soaking" the cathode (which had previously been "fired" in a gas-oxygen flame) with hydrogen.

[1]C. E. Mandeville and H. O. Albrecht, *Phys. Rev.* 80, 299–300 (1950).

[2]H. O. Albrecht and C. E. Mandeville, *Rev. Sci. Instr.* 22, 855–56 (1951).

[3]M. V. Scherb, *Phys. Rev.* 73, 86 (1948).

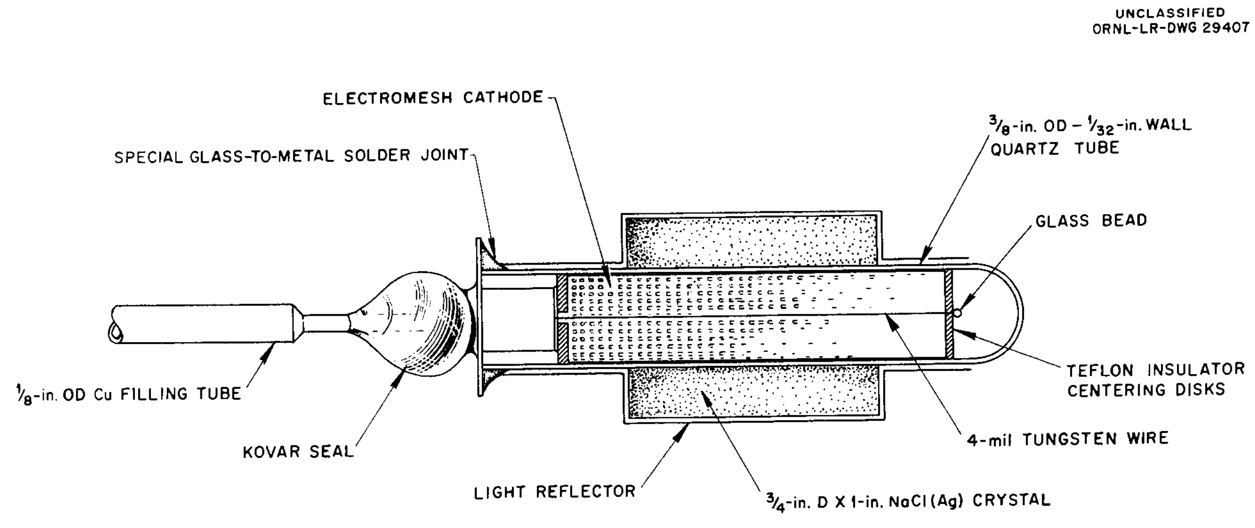

Fig. 28. Scintillation Geiger Counter, Type 1.

UNCLASSIFIED
ORNL-LR-DWG 29408

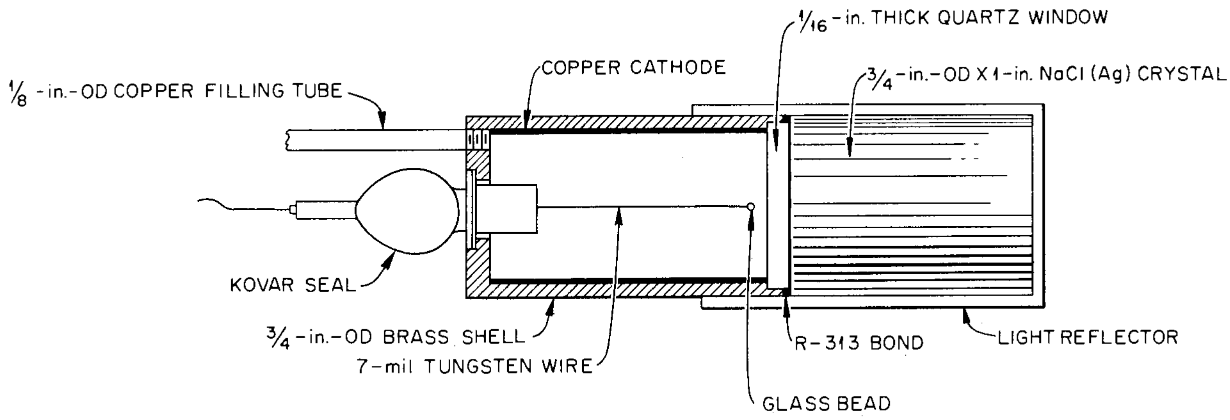

Fig. 29. Scintillation Geiger Counter, Type 2.

The nature of the Ag-activated NaCl imposes some limitations on its usefulness for quantitative flux measurements. The scintillations detected by the counter are fluorescent and phosphorescent events. When the crystal is first subjected to radiation the counting rate begins at some initial value and then increases at a decreasing rate. After 10 min the counting rate is constant. When the radiation is removed, the counting rate immediately drops to some initial value and then decays exponentially with time. The phosphorescent counts decrease by a factor of 2 in two to three min.

The production of stable, highly photosensitive geiger counters is still a trial and error proposition. Results indicate that photosensitive counters undergo a change in sensitivity with time. Improved techniques in conditioning the cathodes should result in more efficient and stable detectors.

METHODS OF ALPHA-SCINTILLATION PHOSPHOR FABRICATION

V. A. McKay

A recent request for the repair of the G-E poppy probe has induced a search for methods of preparing ZnS scintillation phosphors.

Three variations of a basic method have been investigated. The basic method employs a binder for the ZnS powder that will transmit the scintillation photons with high efficiency while offering only a slight absorber to the incident alpha particles. The phosphor is then covered with a light-tight reflector that does not excessively attenuate the incident alpha particles.

The first variation involved depositing ZnS, suspended in a liquid Lucite binder, onto a glass plate. Various thicknesses from 9 to 30 mg/cm^2 were tested. These phosphors all demonstrated approximately the same sensitivity or efficiency for a given alpha source – approximately 3200 counts/min from a 4000 counts/min alpha standard. The source was calibrated and counted in 2π geometry, and the counts were obtained with the source in contact with the phosphor. These data indicated that once a thickness equal to the range in ZnS had been deposited, the additional thicknesses provided good light-piping from the phosphor surface to the photomultiplier.

Some of these deposited phosphors were subsequently covered with thin films of aluminum by vacuum evaporation. The aluminum layer amounted to dark grey absorbers because the layer was broken up into very small and randomly oriented planes (areas and angles characteristic of the phosphor particles' random orientations). The pulse heights were attenuated as much as 50%, and the count rate was depressed as much as 20% by losses under the electronic bias rather than by absorption. Two particle sizes of ZnS were used, 3–5 μ and 25 μ. No particular difference was noted.

The second approach consisted of spraying a mixture of ZnS in liquid Lucite onto a glass disk. The 3- to 5-μ particle was used in this case. A strong, stable layer of the ZnS in Lucite was obtained. The sensitivity was better than that of the deposited phosphor (3600 counts/min from the 4000-counts/min source) but the surface was more irregular. The phosphor has some practical application, however. In counters involving the placement of samples in a light-tight container where the phosphor does not require light-tightness, the spray technique provides a very sensitive and very mechanically stable phosphor. The spray technique is especially useful when fabricating phosphors of irregular shapes, for example, conic sections.

The third approach involves depositing the layer on a Lucite disk. This deposited layer can be used in two ways: first, it may be employed as was the above phosphor with or without a foil reflector (an evaporate will not yield a good reflector); second, the ZnS surface may be molded so that the ZnS is embedded in the Lucite.

The molded phosphor can be machined to any reasonable extent. Usually the surface has an excess of Lucite after the first molding. In that case, the surface is machined off and the phosphor is remolded. This produces a very hard and smooth surface. This surface in turn can be coated with a very thin, highly reflective layer of aluminum. So far we have not obtained pinhole-free deposits of aluminum; however, the phosphor can be made light-tight by the addition of two layers of 180 μg/cm^2 aluminum foil bonded with approximately 100 μg/cm^2 of Krylon (acrylic) plastic spray. This gives approximately 600 μg/cm^2 of absorber over the phosphor surface. It is hoped that eventually the vacuum deposit can be made thick enough and pinhole-free enough to eliminate the foil; then reflector thicknesses as low as 300 μg/cm^2 may be obtained. The foil is quite stable however, and, for the present, provides a practical reflector.

The molded phosphor has about the same efficiency as the deposited phosphor described above. Its pulse height output is 30 to 50% higher than that obtained from any other method of preparation used.

Two inches is the largest diameter molded thus far. It is hoped that we may increase the diameters to as much as 5 in. This could be used on a 5-in. photocathode, allowing large-area monitoring. Molds are hard to fabricate, and a simple method of fabrication is being studied.

Sprayed phosphors through 5 in. have been fabricated. Their response is good, but it is difficult to bond foil to the sprayed phosphor because of the highly irregular surface.

We hope to perfect the molding, spraying, and aluminum evaporation techniques in the near future. We believe, as a consequence of the facility of use of these phosphors, that further development is warranted, and our studies of these techniques lead us to question an extension to glass embedding.

If ZnS can successfully be embedded in glass, it may be possible eventually to develop an in-solution alpha counter.

FUEL ELEMENT AND WIRE SCANNER

E. B. Johnson[1] T. F. Sliski
K. M. Henry[1] H. J. Stripling, Jr.

The fuel element and wire scanner (Fig. 30) is a device for obtaining the neutron flux distribution in a reactor by means of the activity induced in various materials. It does not replace the activated-foil mapping system, but rather is used to augment it. In general, the scanner will enable reactor-flux mapping time to be reduced by a large factor but at some sacrifice in accuracy. The absolute magnitude of flux will still be based on foil activations. Also, most of the constants necessary for scanner operation will be determined by foil measurements.

The fuel element and wire scanner consists of a mechanical positioning device and a spectrometer. The positioner is designed, as the name implies, for handling either wire or fuel elements (swimming pool type). It is the function of the positioner to locate wires and longitudinal elements of fuel element surfaces a fixed distance from the spectrometer collimator (Fig. 31) and then, while maintaining this fixed distance, to move the wires or fuel elements axially so that the entire active length of the wire or surface element is exposed to the collimator. Two views of the collimator and of a casting made in the collimator hole are shown in Fig. 32.

The collimator is a 4 in. dia × 4 in. long, high-density (about 16.6 gm/cc), sintered, tungsten-nickel-copper material with an axially centered hole. The hole is rectangular ($\frac{1}{2} \times 1$ cm) at the

[1]Applied Nuclear Phys. Division.

UNCLASSIFIED
ORNL-LR-DWG 29409

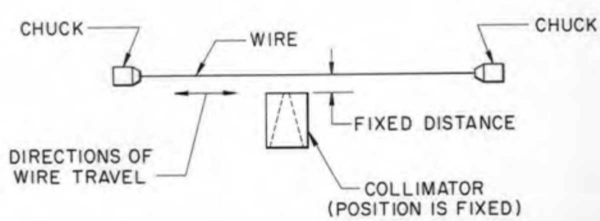

Fig. 31. Fuel-Element and Wire Scanner: Relative Positions of Wire and Collimator.

UNCLASSIFIED
PHOTO 17989

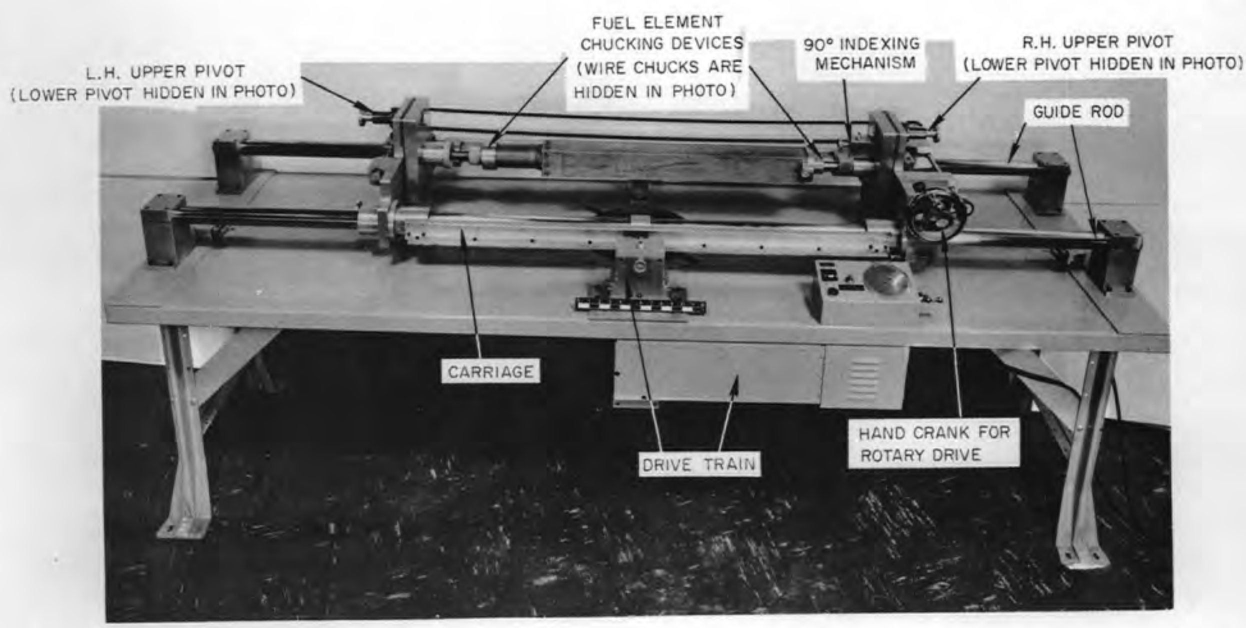

Fig. 30. Fuel-Element and Wire Scanner, Front View. Dummy fuel element in chucks, detector and shield omitted.

UNCLASSIFIED
PHOTO 17821

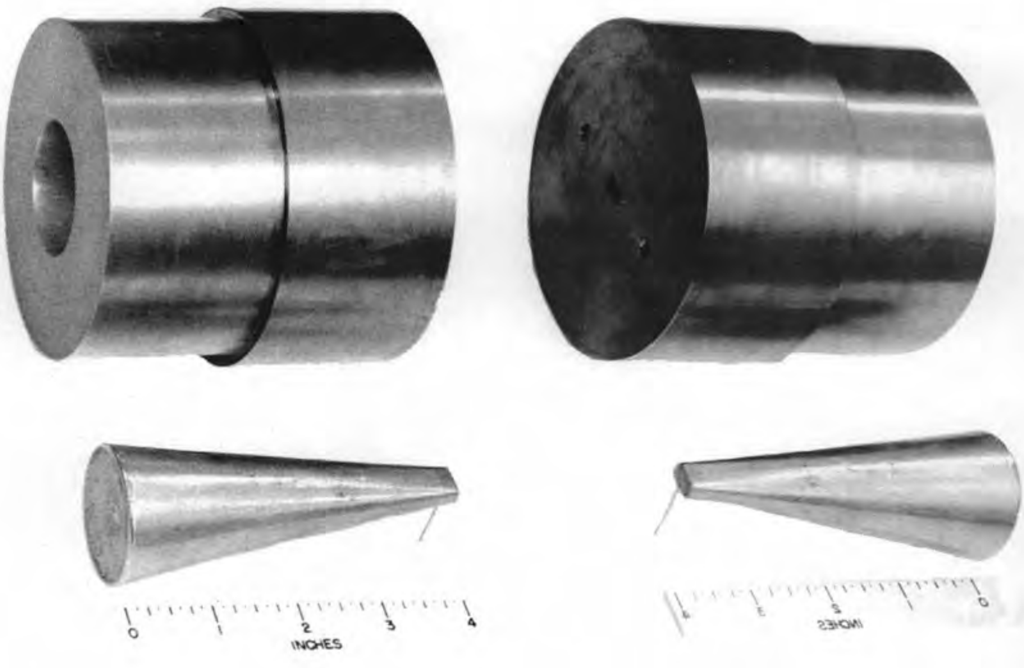

Fig. 32. Collimator for Wire Scanner and a Casting of the Hole in the Collimator.

upper end and circular ($1\frac{1}{2}$ in. dia) at the lower or crystal end. The surface connecting the rectangular and circular ends is generated by a straight line element. Either the long or short dimension of the rectangular end may be aligned with the direction of positioner travel. The spectrometer crystal, photomultiplier tube, and preamplifier are housed in a cylindrical, lead-lined steel can (Fig. 33) which rests on an angle-iron table. In the top of the lead-lined can is a cylindrical hole which receives the collimator. When the collimator is installed, its top surface is flush with the top surface of the can.

The positioner is mounted on a steel table which has a hole cut in its center to receive the lead-lined can. Primary elements of the positioner are the carriage, guide rods and drive train. The guide rods, which are fastened to the table, support the carriage and guide its motion in a straight line. In the drive train an electric motor drives a variable-speed reducer which in turn drives a fixed-gear train. Finally, the fixed-gear reducer is coupled to a rack on the carriage by means of a pinion, thus providing carriage motion. A synchro transmitter, tied into the fixed-gear train and electrically coupled to a receiver synchro which replaces the drive motor in a strip chart recorder, provides synchronization between carriage and chart paper travel. The carriage incorporates chucking devices for holding wires and fuel elements, a 90-deg indexing mechanism for orienting the four sides of a fuel element relative to the collimator, and a pivot and hand-operated rotary drive arrangement for locating any longitudinal element of the concave or convex surfaces of the fuel element directly over the collimator. Thus the positioner allows continuous scanning of wires, of the center element of each of the flat fuel element sides, and of all the elements of the concave and convex fuel element sides.

UNCLASSIFIED
PHOTO 17988

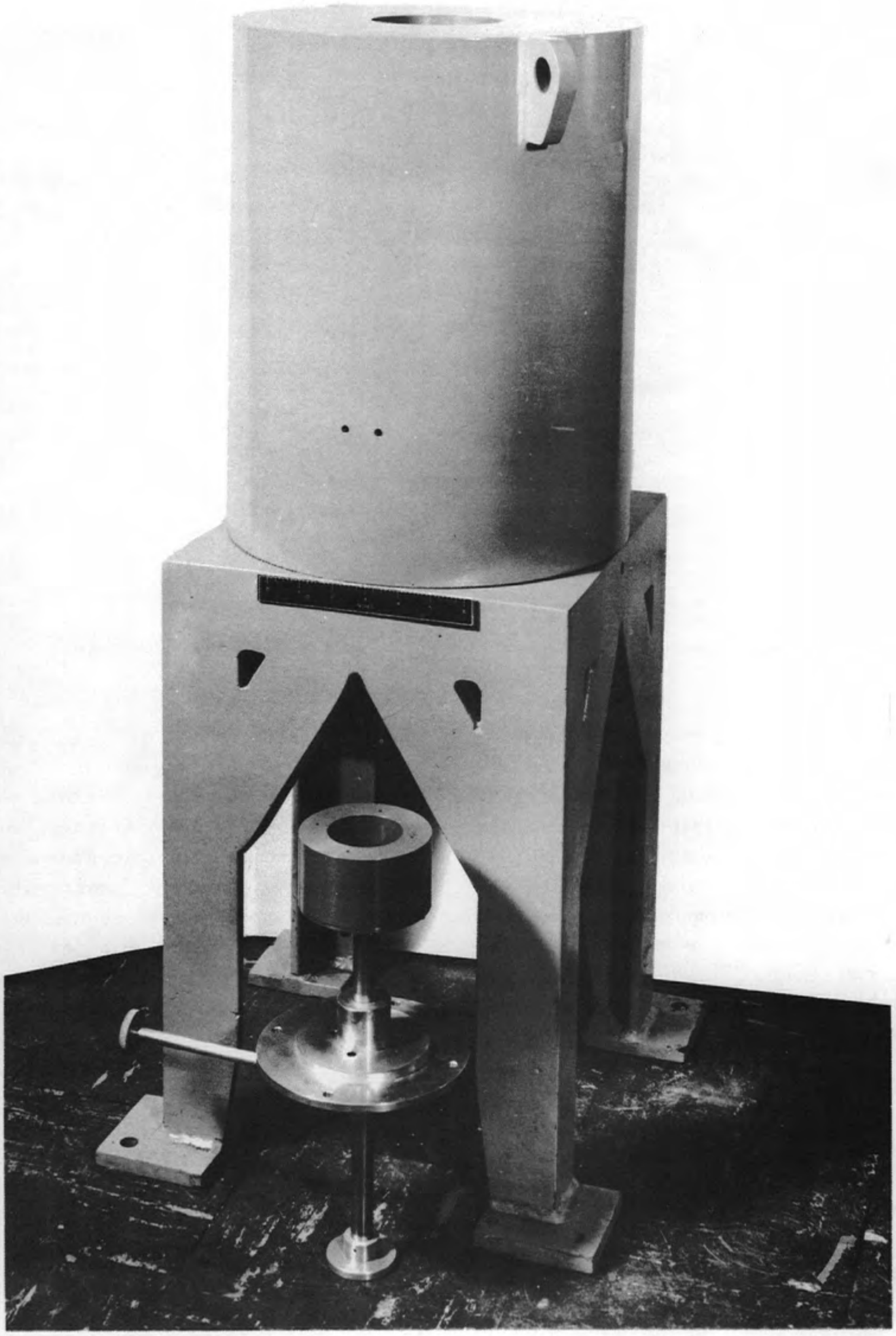

Fig. 33. Detector Shield.

In the wire method of mapping neutron fluxes in a reactor, wires are positioned in and around the reactor and irradiated at nominal power for a known time. The activity measured by the scanner is proportional to the neutron flux. The proportionality constant contains startup, operating, and shutdown power-time factors, nuclear cross sections and half life, counter efficiencies and geometrical constants. Advantages of the wire method are speed and continuity of measurements.

The use of fuel or reflector elements for flux mapping is restricted to cold or essentially unirradiated elements. The reflectors, unless they contain fissile material, are treated as wires. The emissions from fission products in the low-level irradiated fuel are used to determine flux distributions only. Absolute flux levels are exceedingly difficult to calculate. The use of fuel and reflector elements as sources of emissions offers an advantage in that the reactor flux is not perturbed by the introduction of extraneous materials. The disadvantages arise from three factors. (1) The decay scheme and half life are not accurately known. (2) Background counts must be taken before reuse of elements (wires and foils can either be disposed of or set aside to decay). (3) Reactor operations are restricted to low power levels (the choice of wire material can permit simultaneous operation for wire activations and other experiments).

LID TANK DETECTOR CARRIAGE

J. L. Blankenship T. F. Sliski H. J. Stripling, Jr.

The lid tank is a structural steel tank approximately 6 ft deep × 7 ft wide × 11 ft long (long dimension parallel to reactor face), located on the west face of the ORNL Graphite Reactor. The location is directly in front of a beam hole which provides the radiation for shielding experiments.

The mechanical design of the lid tank detector carriage (Fig. 34) is basically the same as that of the Tower Shielding Facility detector carriage. The lid tank device differs from the TSF unit mainly in that it is larger, the "θ" drive has been omitted, and the horizontal-travel limit-switch arrangement has been changed. Due to the increased size, two additional Z-axis load-carrying members were placed under the Z-axis guide and load-carrying shafts. In the new horizontal limit-switch arrangement a spring-loaded flexible coupling device, between the X-axis drive shaft and the detector, triggers a snap-acting switch when the detector encounters an obstruction while traveling in a horizontal plane. This switch has been found to be sufficiently accurate for such locating purposes.

Carriage position is sensed by two selsyns connected by gears to the drive trains of each of the three directions of travel. The two selsyns are part of two separate readout systems, one providing a coarse indication of position, and the other a readout of position accurate to within ± 1 mm. The fine readout is provided by an in-line digital presentation which minimizes human errors in readout.

The carriage motion is manually controlled by toggle switches which supply power to servo-type two-phase motors. This drive system was designed for conversion to automatic positioning at a later date. A system of relay logic had to be devised to provide travel-limit protection for motion in either of the two directions in the horizontal plane. The limit overtravel information is provided by only one microswitch.

The lid tank detector carriage was designed for an over-all positioning accuracy of ± 1 mm. An accuracy test made on the carriage assembly in the machine shop (before installation in the lid tank) showed the actual error to be less than ± $\frac{1}{2}$ mm. A great part of the credit for this success is due the Central Machine and Mechanical Shops who fabricated and installed the machine.

UNCLASSIFIED
ORNL-LR-DWG 21379

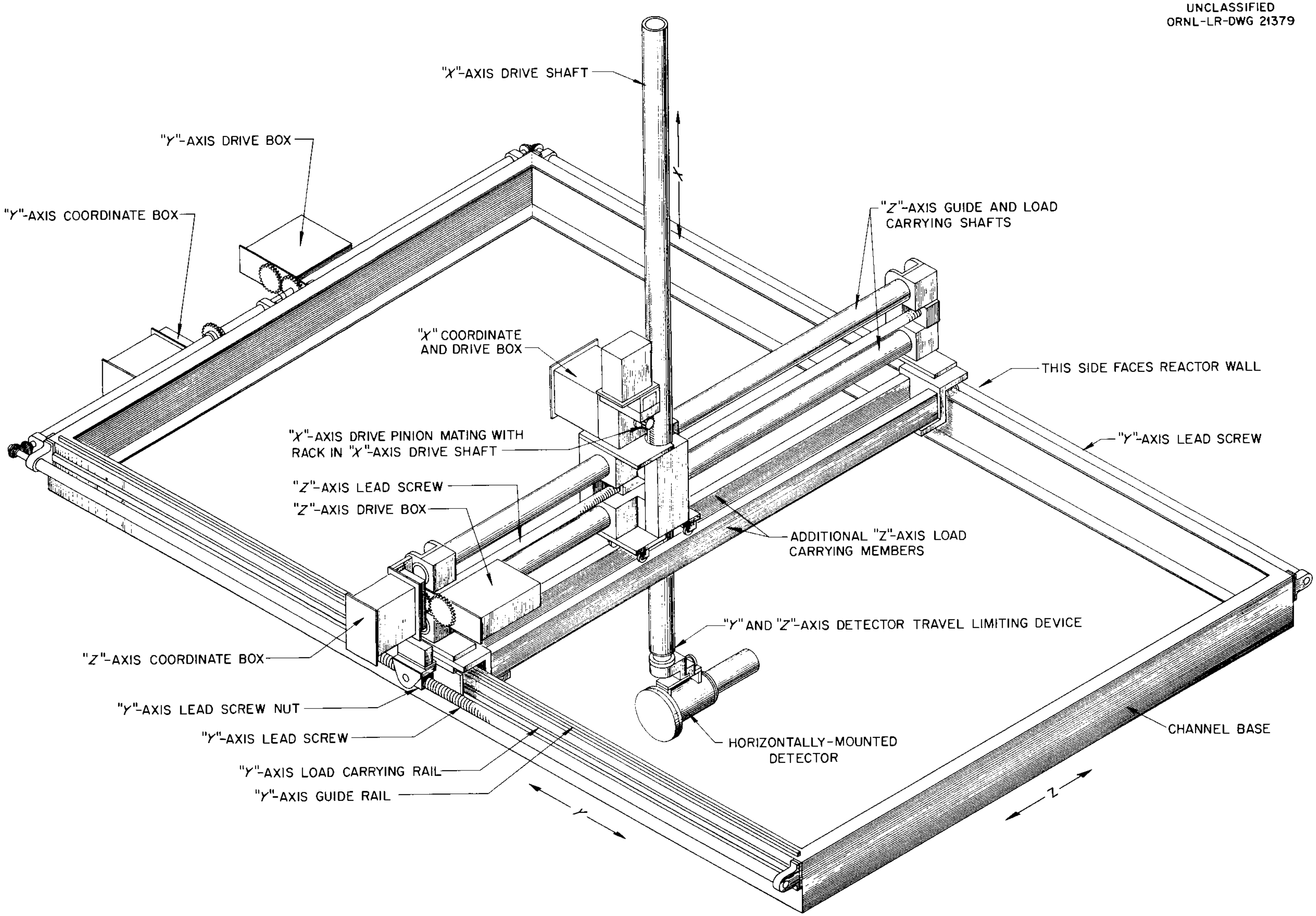

Fig. 34. Lid Tank Detector Carriage.

FREQUENCY-RESPONSE TESTING OF PNEUMATIC PROCESS CONTROLLERS

R. K. Adams

The physical and chemical processes encountered at ORNL are usually small systems, which, by virtue of their size and consequent comparatively short response times, restrict the use of some commercially available instruments which would be satisfactory for a full-sized plant.

In an effort to evaluate pneumatic process controllers in the light of these restrictions, and also the further requirement of flexibility for use on any process which may be investigated at ORNL, a test and evaluation program was begun.

Approximately 100 tests have been made on 14 pneumatic controllers, manufactured by five companies. The tests ranged from complete frequency-response investigations, to adjustment-knob calibrations and process startup capabilities.

The test apparatus is shown in Fig. 35. Conclusions which can be drawn from the tests are:

1. The manufacturer's calibration of the needle valves used to adjust pneumatic controller gain, reset and derivative time constants, in general

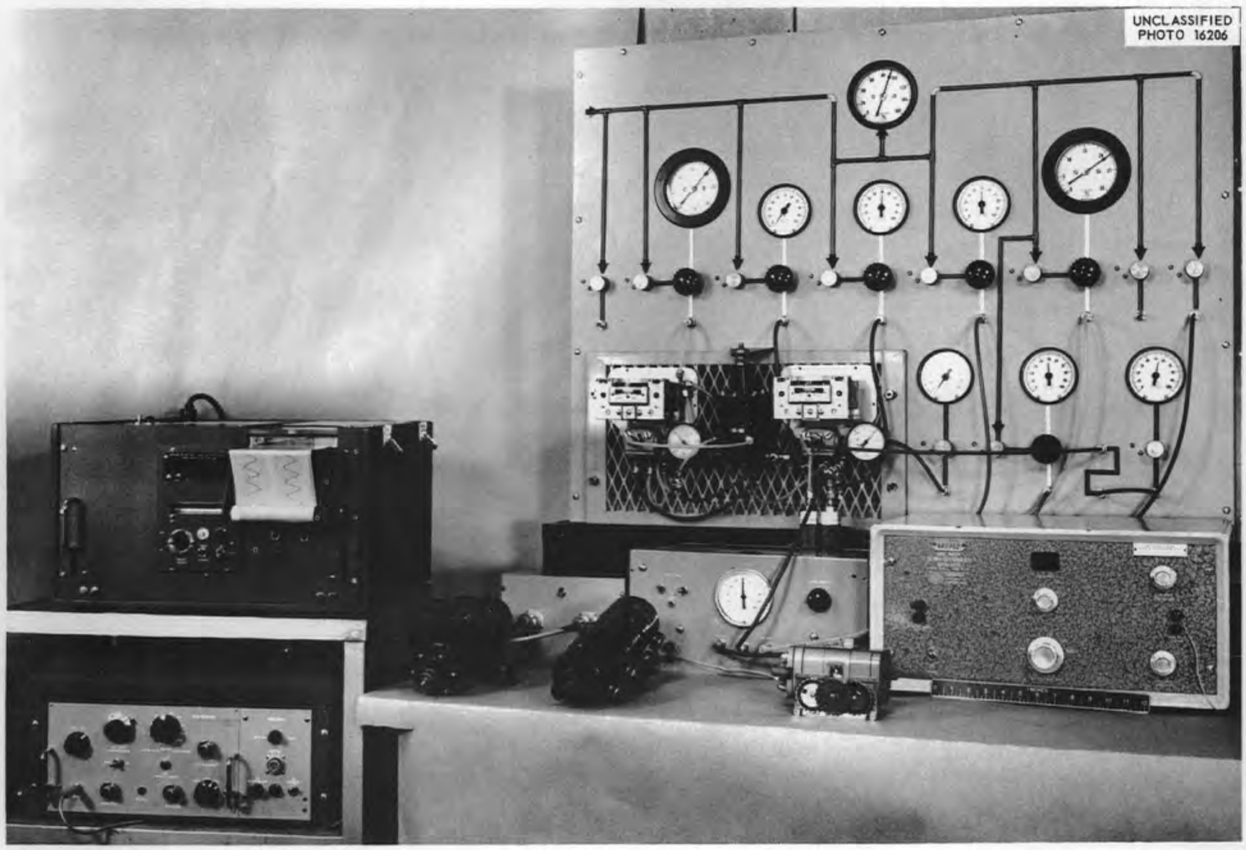

Fig. 35. Frequency-Response Test Equipment.

cannot be relied upon to closer than a factor of 2.

2. The magnitude-ratio and phase-shift characteristics of the controllers tested showed wide differences between various manufacturers' products. The most significant factors observed were in the high-frequency response and maximum available derivative phase shift.

3. The significant results of the process startup tests are shown in Fig. 36. These show the controllers whose startup characteristics most nearly meet the requirements of "no-overshoot", "minimum time to set point."

Based on the test results, a specification to ensure the procurement of the pneumatic process controller which best meets the needs of ORNL has been written.

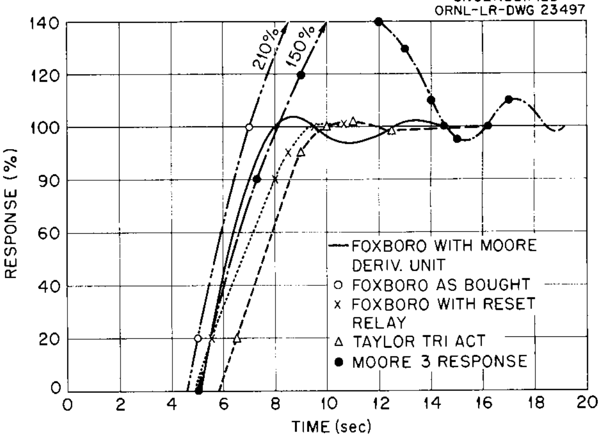

Fig. 36. Comparative Controller Startup Responses (Best Startup Settings).

DISPLACEMENT METER FOR AN ION EXCHANGE RESIN BED

T. Gayle P. D. Koster

This meter was developed primarily to satisfy the need of the Chemical Technology Division for a unit that would sense the linear displacement of a packed resin bed in a continuous Higgins-type ion exchange column. The basic requirements for the sensing element are: that it be readily installed in existing columns, that it be resistant to dilute sulphuric and nitric acid, that it give an output signal only upon movement of the resin bed and be unaffected by the movement of the liquid carrier.

The meter developed (see Fig. 37) consists essentially of a propeller-type sensing element driving a General Electric Mark 14 Telsyn Transmitter through a magnetic coupling. After some study, a propeller shape that would not respond to the movement of the water carrier and would give approximately 40 deg of angular rotation per in. of resin travel was developed. It was further decided that the most satisfactory way to ensure a dependable seal for the selsyn was to completely can it and drive it through a magnetic coupling through one end of the can. Indox I ceramic-ring magnets with eight poles on the face were used for the coupling.

Readout on the device is effected by a receiver selsyn and indicating dial. Control of the resin pulse-distance is accomplished by means of a wiper, commutator, and an Eagle Signal Corp. microflex reset counter.

UNCLASSIFIED
ORNL-LR-DWG 29411

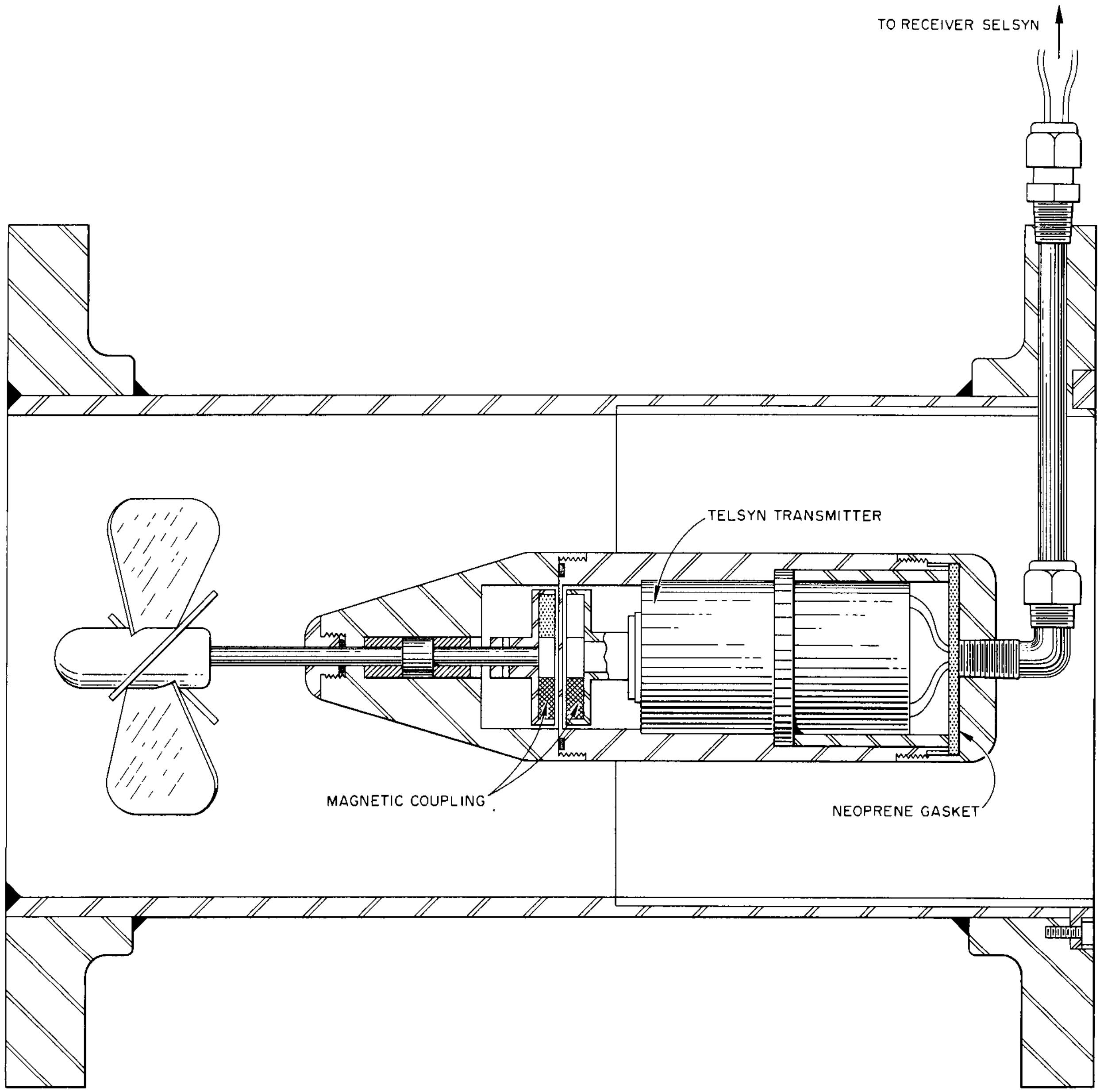

Fig. 37. Ion Exchange Resin Bed Displacement Meter.

INSTRUMENTATION FOR MULTICURIE FISSION PRODUCT PILOT PLANT

B. Lieberman L. A. Scott[1]

The Multicurie Fission Product Pilot Plant was designed to fulfill two functions:

1. to separate and refine the isotopes present in the ORNL chemical plant wastes which are now marketable,
2. to study the feasibility of removing all fission products from the waste streams to such an extent that the remaining waste may be dumped in nearby streams.

The instrumentation for this plant is one of the larger instrument installations at ORNL, having 36 ft of operating panel board, containing 900 major instrument components, and having cost $160,000 (not including the engineering design costs).

The instrument design, including detail drawings, was done by the Instrument Department and then offered, as a complete job, for bid. The best price for the job was obtained by awarding the supplying of all instruments and instrument accessories to the Foxboro Company and the complete installation to the Panellit Service Company, which specializes in this type of work.

The instrumentation for this plant is similar in general to the techniques and equipment used in the Thorex Pilot Plant. Since this instrumentation has been previously reported, no further explanation of this equipment will be given. There are, however, a certain number of innovations which are worthy of note.

Previous applications of graphic panels at ORNL have been for continuous or semicontinuous processes. However, at the request of the Operations Division, the panel board was designed as a wholly graphic panel (see Figs. 38 and 39).

[1]Summer participant, University of Florida.

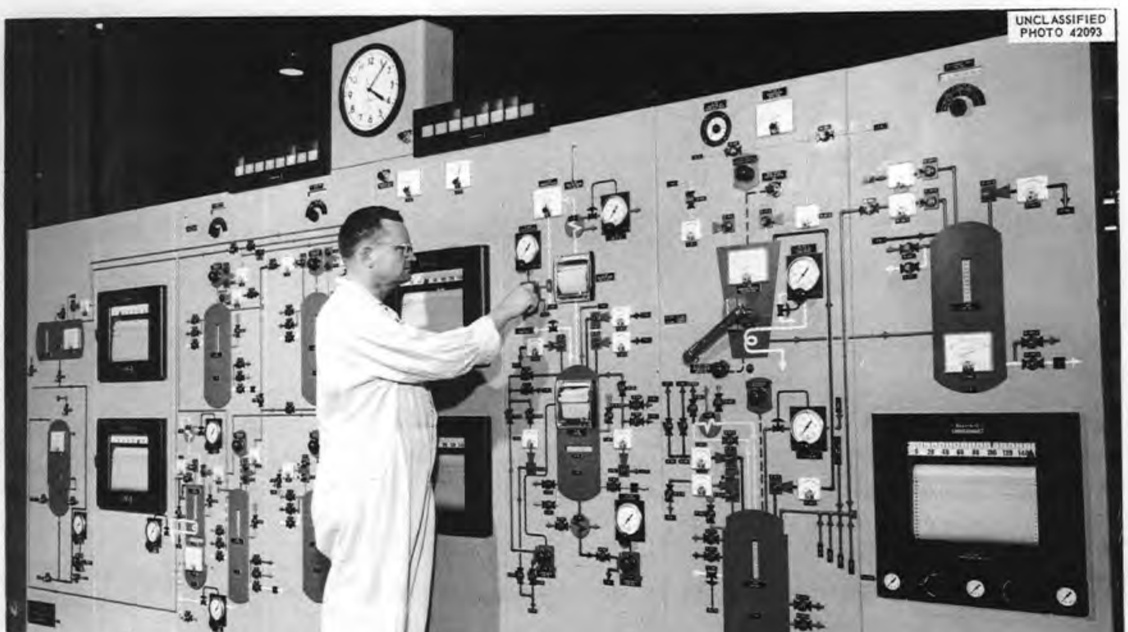

Fig. 38. Panel Board for Multicurie Fission Products Pilot Plant.

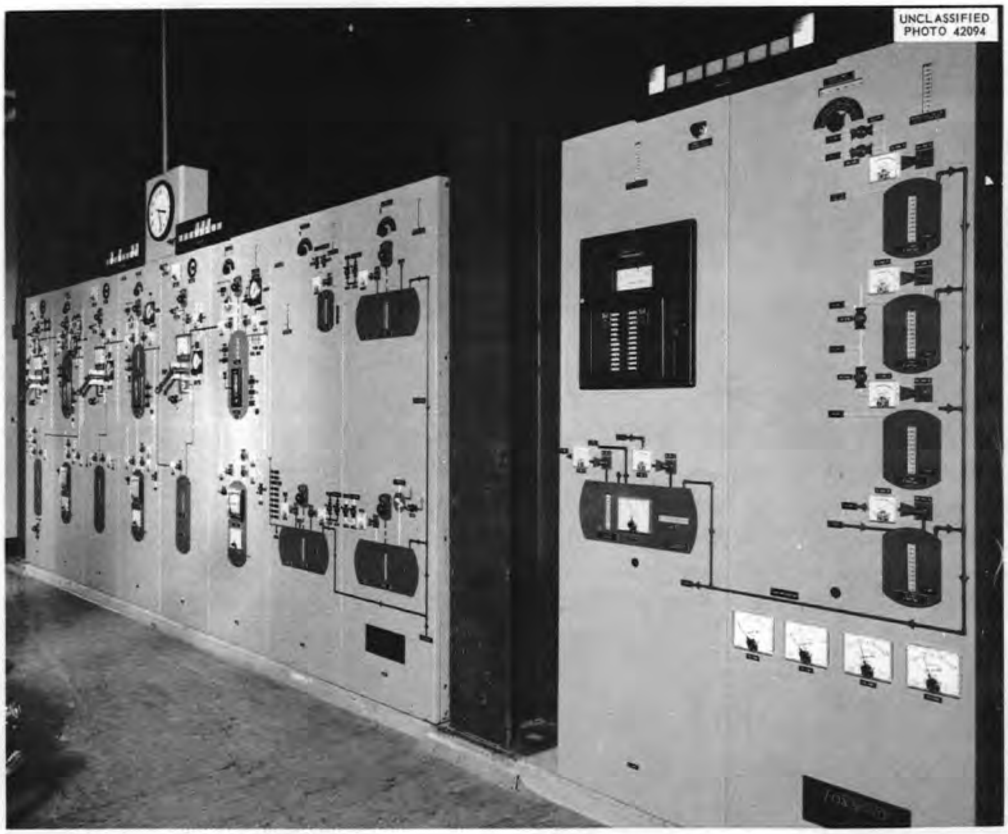

Fig. 39. Panel Board for Multicurie Fission Products Pilot Plant.

Previous operating experience had shown that one of the major problems for a plant of this type had been that of operator errors; that is, the operator would open or close the wrong valve, fill the wrong tank, etc. It is hoped that, by the use of a graphic panel with its complete pictorial representation, these operational errors will be reduced, thereby effecting a considerable saving in time and money.

It has long been the practice at ORNL to use steam jets to transfer liquids from vessel to vessel in chemical plants of this type. Since jets are erratic in their operation, a system has been designed which will aid the operating group in determining whether a jet transfer is being made successfully. The operation of the system is such that when a pneumatic toggle switch on the board is depressed a remote valve is opened, admitting steam to a jet. A thermocouple, welded to the outside of the pipe 12 in. downstream from the outlet of the jet and connected to a small board-mounted $2\frac{1}{2}$-in. millivoltmeter, indicates the temperature in the pipe. The meter scale is segmented and is colored as follows: 0 to 40°C, white; 40 to 80°C, green; 80 to 100°C, red. The operator now has an immediate indication of the operation: white – no steam through the jet; green – successful operation; red – steam flowing but no liquid being transferred.

Another innovation being tried in this plant in behalf of economy is the use of a single transmitter for the density measurements in each cell, the various differential pressures being switched to a common transmitter. Previous practice has been to provide a separate transmitter for each measurement point, even though only periodic measurements were needed. The new system uses an electrical switch to open and close appropriate solenoid valves in the purge lines from the various vessels. In this way the density (differential pressure) may be read in the various vessels with a single measurement system. The use of this system reduced by 24 the number of density systems (at $400 each) in the plant.

INSTRUMENTATION FOR THIRD URANIUM CYCLE ADDITION TO THOREX PILOT PLANT

J. Marks B. Lieberman W. Greter

The third uranium cycle was added to the Thorex Pilot Plant to facilitate a more satisfactory recovery of uranium and thorium with the processing of the new short-cooled (30 days vs 180 days) fuel elements.

The total cost of the instrumentation for this addition was $45,000. The instruments used were selected to match the existing Thorex Pilot Plant instrumentation.

A significant design innovation is being used in this addition. As part of a general program in the Instrument Department to standardize the design in as many areas of instrumentation as possible, the transmitter rack on this project has been designed as a standard for this and future jobs. On previous jobs, each transmitter rack was especially designed and field-constructed for the particular combination of transmitters required. The new standard design uses as a frame the standard 24 × 24 × 78-in. angle-iron frames used on control boards (see Figs. 40 and 41). The individual transmitters are mounted on 13 × 24-in. plates which are predrilled to take any combination of piping hookups required by the ten or more different types of transmitters commonly used at ORNL. Stainless steel panels are used, since the transmitter racks are normally located in or near process areas where corrosive vapors are present. Panel finish or the extra holes were not considered objectionable since the transmitter rack

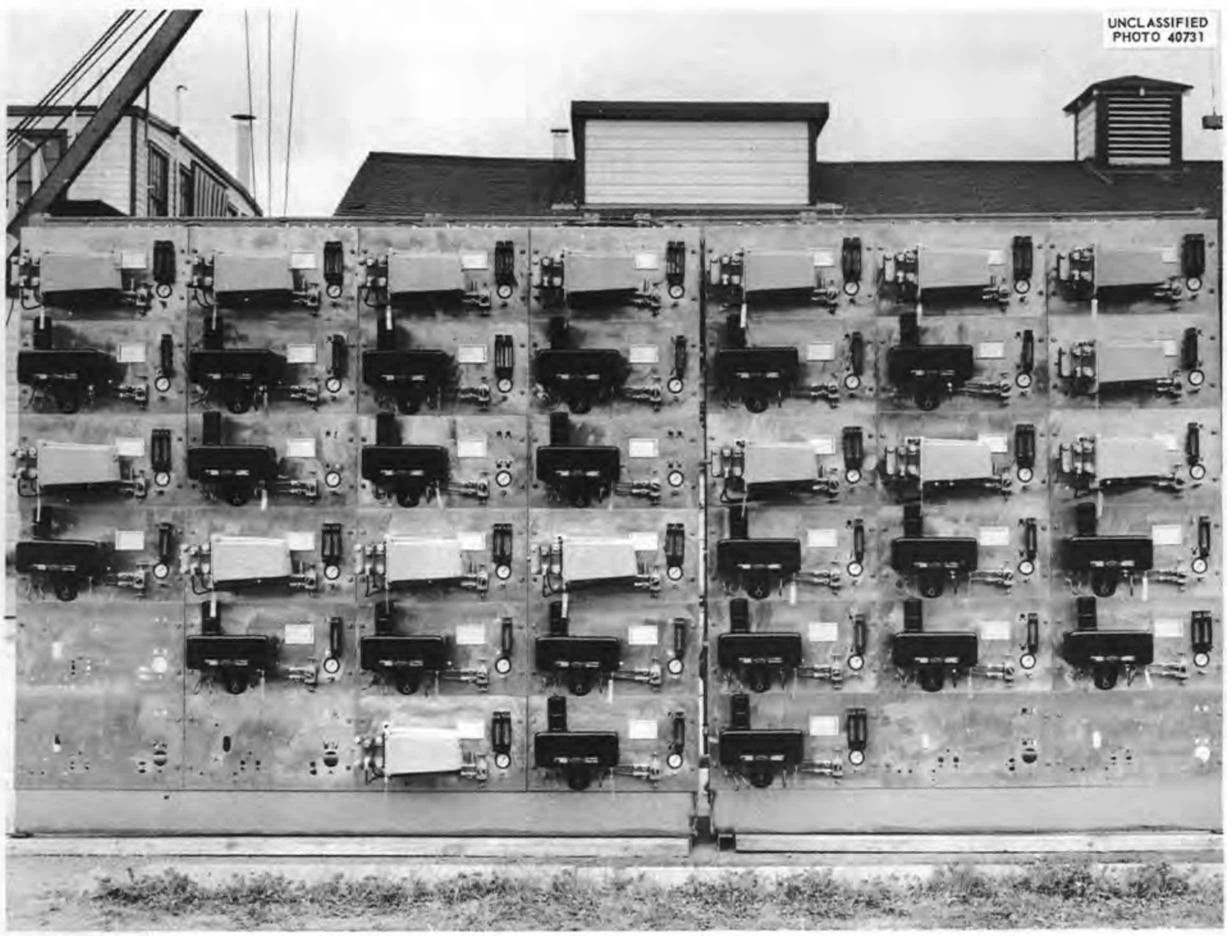

Fig. 40. Thorex Pilot Plant Transmitter Rack, Front View.

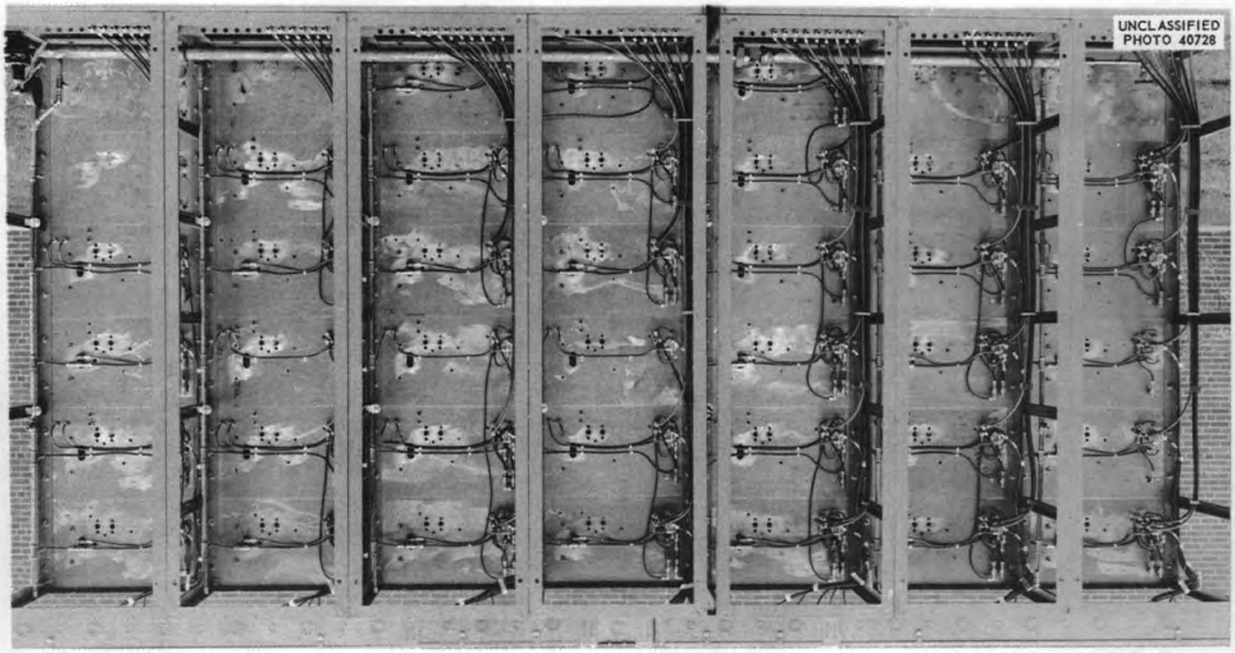

Fig. 41. Thorex Pilot Plant Transmitter Rack, Rear View.

is not located in an area where appearance is important. Complete drawings have been made for each type of application, including a bill of materials. The advantages of this design are:

1. Panels are precut and drilled and are stocked in stores.
2. Panels may be prepiped in the shop.
3. The complete bill of materials is shown on each drawing.
4. The engineer may design by specifying the appropriate drawing numbers.
5. Quick-disconnects are provided on all lines to facilitate checking and calibration.
6. Stainless steel panels eliminate the corrosion problem previously encountered on painted panels.

INSTRUMENTATION FOR POWDER METALLURGY LABORATORY

R. K. Adams

Powder metallurgy is becoming an increasingly important method for the study and manufacture of many of the unusual metallic alloys and cermets used by ORNL. The Metallurgy Division has recently completed construction of an improved and expanded facility for such work in Building 2000-A.

Shown in Fig. 42 is the control panel for eighteen high-temperature furnaces used for alloy development, characteristics determination, and various other powder metallurgical techniques. The right-hand rack assembly provides mounting space for eight furnaces within the rack.

Nine furnaces are controlled by Wheelco on-off controllers, five by Wheelco time-proportioning units, two by Speedomax model H DAT controllers, and two by Micromax model C DAT units (salvaged from a previous job). Temperatures are monitored by the two strip-chart recorders.

Figure 43 is a close-up view of the variable transformer power panel which has found wide use in this type of job. It is designed to facilitate plug-in application of the controller, the power source, and the furnace or other load. These units are currently being supplied by an outside vendor at a fraction of the cost of assembling the individual components for each job at ORNL.

The use of the standard power control unit, modular frames, and precut panels allowed considerable saving in electrical wiring and instrument installation costs. Total job costs for instrumentation were $17,800, of which approximately $2,500 was due to craft labor and overhead.

Fig. 42. Furnace Control Panel, Metallurgy Laboratory.

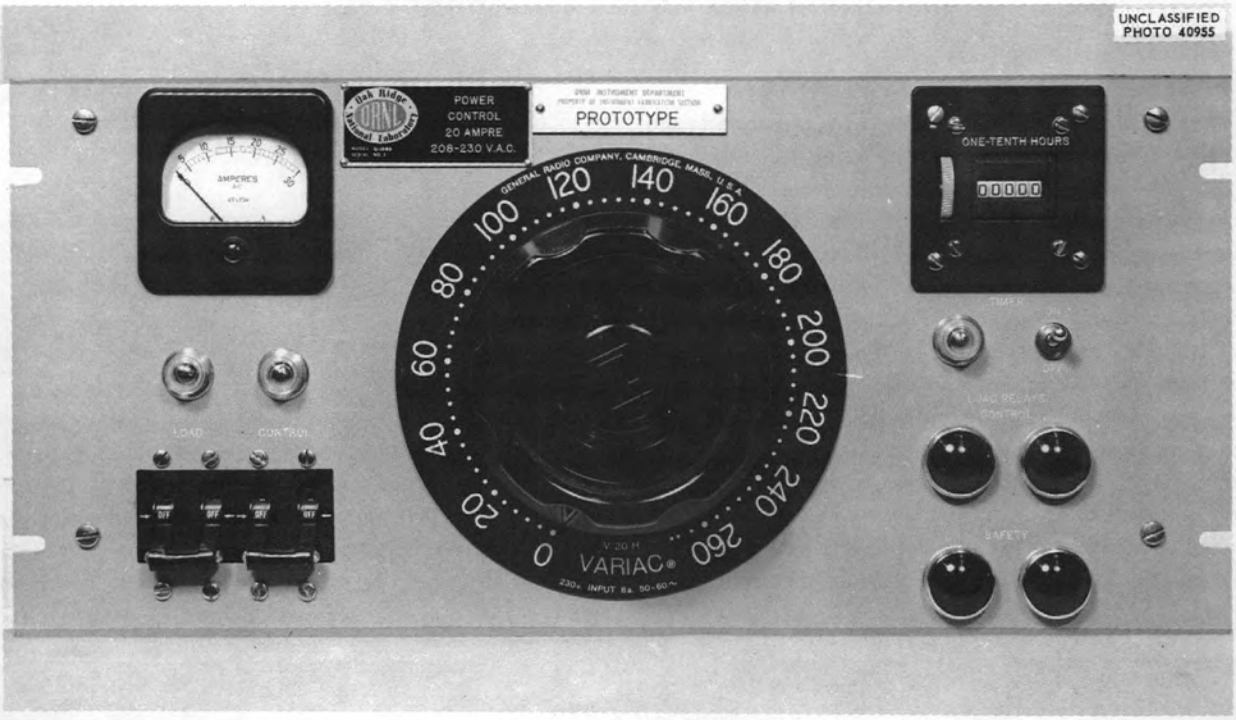

Fig. 43. Variable Transformer Power Panel.

INSTRUMENTATION FOR VOLATILITY PILOT PLANT

L. H. Chase W. J. Greter B. Lieberman

The Volatility Pilot Plant was designed and built to recover uranium from fused-fluoride-salt-type fuels, and at a later date from zirconium-uranium-type fuels such as that used in the submarine Nautilus. Recovery from fused salt is accomplished by bubbling fluorine gas into the fused salt and converting liquid UF_4 to gaseous UF_6. The gas is conducted through traps for the removal of zirconium fluoride, through absorbers for the removal of fission products, and through cold traps for the collection of UF_6. The process equipment is located in two concrete-enclosed cells in Building 3019.

Total plant cost to July 31, 1956, was $478,989, of which $116,422 or 24.3% was for instrumentation.

The cost of instrumentation to April 30, 1957, was:

Design	$ 19,419
Material	76,922
Labor	29,683
Overhead	17,809
Total	$143,833

The control panel board (Fig. 44) is 38 ft long, including 8 ft of blank panels provided for expansion, a 10-ft graphic section at the center, a 12-ft section of standard panel at the left end, and an 8-ft section of standard panel at the right end. The panel board was constructed by Taylor

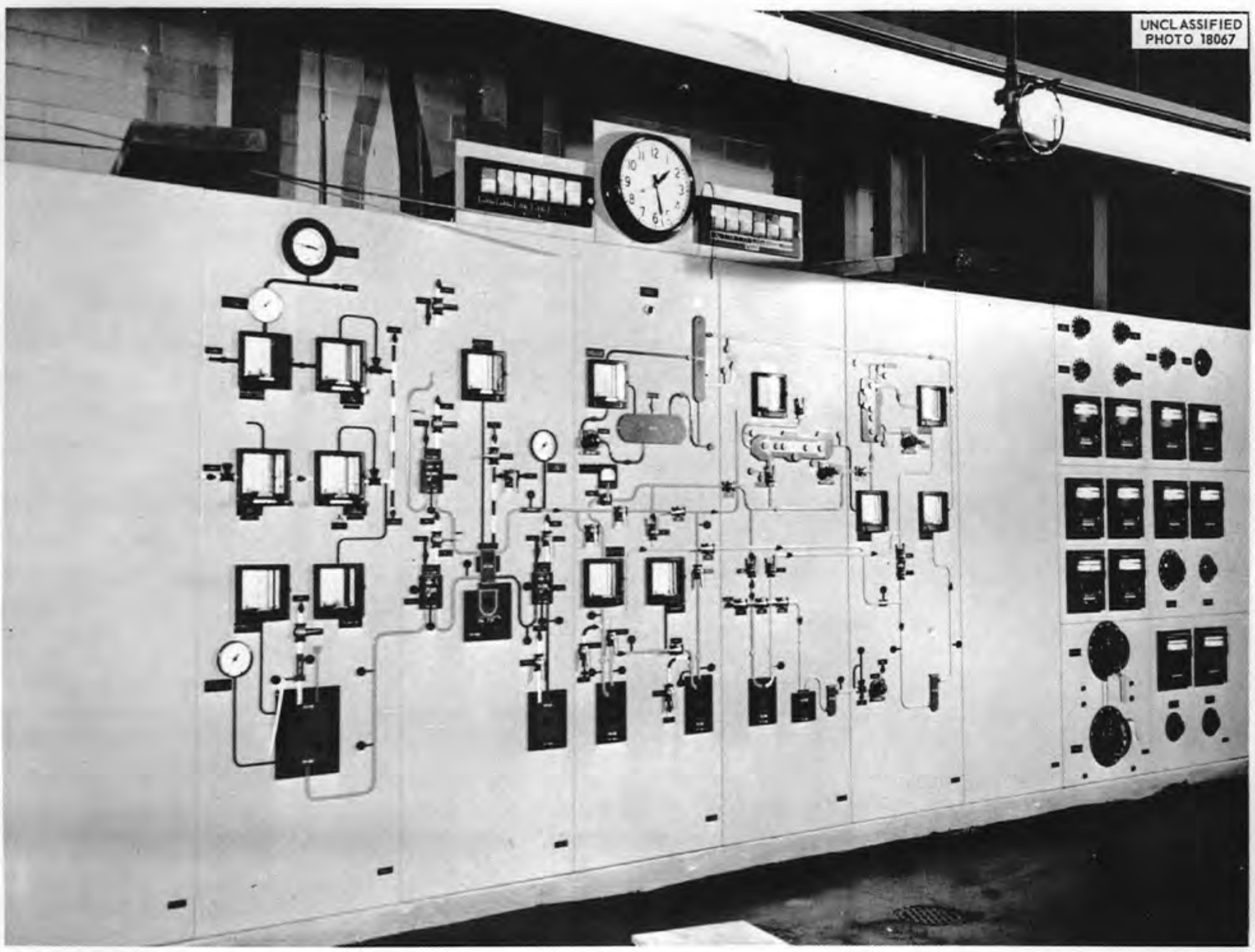

Fig. 44. Volatility Pilot Plant Control Panel Board.

Instrument Companies of Rochester, New York, from drawings provided by the Instrument Department. All panel-board instruments were purchased by the Instrument Department and shipped to Taylor for assembly on the panel.

The standard panel sections contain instruments for recording, indicating, and controlling temperature. The graphic section was designed to simulate the process flowsheet and contains the instruments for recording, indicating, and controlling flow, pressure, and liquid level and, in addition, pneumatic switches for opening and closing remote valves.

Temperature measurements are made with thermocouples. Remote valves are of Monel construction. Flow, liquid level, and pressure measurements are made with pneumatic transmitters which are located above and outside the cells. Backup of radioactive and corrosive gases from the process to the transmitters is prevented by purging each connecting line with nitrogen.

Automatic controls are limited to temperature and flow of feed gas.

Considerable difficulty has been caused by the deposit of solid material in the remote valves during the early runs with unirradiated material. The material interfered with tight shutoff and in many cases scored the seat or plug of the valve, so that relapping was necessary. For the last four runs with unirradiated material, some of the Monel plugs were replaced with fluorothene plugs. These plugs suffered from the same difficulty, but by cycling at least 100 times tight shutoff was re-established. For runs with ARE fuel more than half the valves downstream from the chemical reaction vessel will be equipped with fluorothene plugs.

INSTRUMENTATION FOR SLURRY STUDIES

T. M. Gayle

An aqueous thoria slurry offers many advantages for use as a blanket in a homogeneous-type breeder reactor. Lack of knowledge of the behavior of aqueous slurries at high temperature and pressure has prompted extensive studies in the field.[1] Two irradiation facilities at the LITR involving extensive instrumentation have been completed and placed in operation. A number of individual devices for measuring the physical properties of thorium oxide slurries have been developed.

PUMP FOR THORIUM OXIDE SLURRIES

A pump suitable for low-head pumping at high static pressure has been developed in colloboration with V. D. Allred of the Chemical Technology Division.

The pump consists essentially of a free piston operating in a heavy-walled cylinder (Fig. 45). The piston has a hole bored through its vertical axis and a floating-ball check valve in its top. The piston is made of magnetic stainless steel (type 416) and is oscillated vertically by means of two coils on the outside of the cylinder. The coils are alternately energized approximately two to three times per second. The resulting vertical movement of the piston and action of the check valve cause flow to take place. A second check valve or "foot valve" has been added for increased efficiency in loop operation.

Two pumps have been built, with an accumulated out-of-pile operating time of about 200 hr at 200 to 250°C. Flow rate was approximately 1 liter/min against a 10-ft head.

The most logical use of the pump appears to be for in-pile loop service, although larger scale models may find other uses where high static pressures are involved. The gross efficiency of the pump is quite low, due primarily to the high-reluctance magnetic circuit.

FALLING-BALL VISCOMETER INSTRUMENTS

A falling-ball type of viscometer suitable for in-pile use on thorium oxide slurry has been designed, constructed, and extensively tested

UNCLASSIFIED
ORNL-LR-DWG 22275

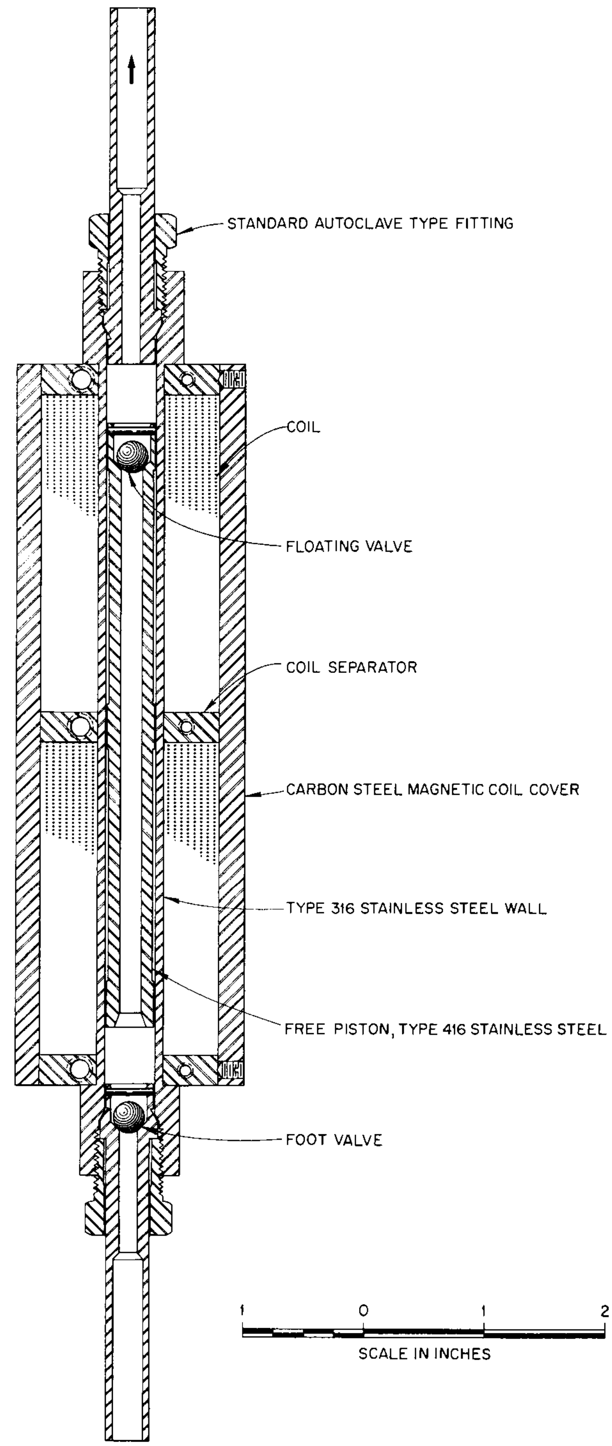

Fig. 45. Thorium Oxide Slurry Pump.

[1] J. P. McBride *et al.*, *Mass Subsidence of Thoria Slurries at High Temperatures and Pressures*, paper presented at the American Nuclear Society Meeting, June 10–12, 1957, Pittsburgh, Pa.

out-of-pile by the Chemical Technology Slurry Group. Careful study revealed that the design parameters of the classical falling-ball method could be scaled down to a size suitable for in-pile use.

The pump in the loop is similar to the pump previously described except that the unit is inverted and the check valves are of such design as to pass a solid ball. The exit line from the pump, rising vertically and forming the loop itself, is of a reduced diameter, and the ball is raised by the velocity of the slurry. A small electromagnet holds the ball in the top portion until it is ready to be dropped through the straight vertical test section. This section is approximately 1 ft long. Detection of the ball is made by coils at each end of the test section. The coils are connected in a bridge circuit (Fig. 46) which feeds a high-gain carrier amplifier (2500 cycle) and drives a conventional recording galvanometer. As the ball passes through the coil, the change in coil impedance causes a bridge unbalance and resulting deflection on the recorder chart. With a chart speed of 100 mm/sec, accurate determination of the time of falling is easily accomplished.

UNCLASSIFIED
ORNL-LR-DWG 22274

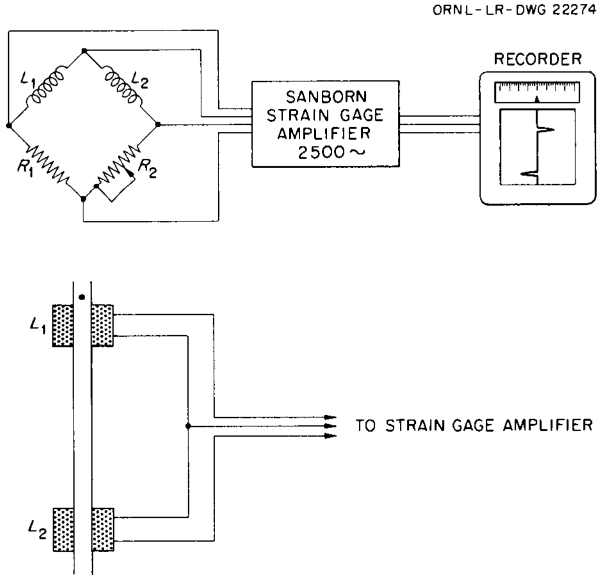

Fig. 46. Falling-Ball Viscometer Instruments.

The balanced-bridge method of measurement has the advantage that shifts in temperature and radiation effects on the coils are inherently compensating, since any coil changes tend to cancel each other. Remote balancing of the bridge is simple and presents no problem for in-pile service. The use of 2500 cycles is helpful in avoiding interferences from the usual heavy 60-cycle fields caused by the pump and other equipment in the vicinity.

Balls used to date have been 0.047 and 0.054 in. in diameter, of magnetic stainless steel. Testing to date indicates close conformity with theoretical data.

CAPILLARY VISCOMETER INSTRUMENTATION

Measurement of the viscosity of a fluid with a capillary viscometer utilizes the fact that, for laminar flow, Poiseuille's equation gives the relation between the capillary dimensions, the volumetric rate of flow, the pressure drop, and the fluid viscosity.[2] Thus, the fundamental requirement that must be met in the design and operation of a capillary viscometer is that flow always be in the laminar region, so that Poiseuille's equation will be applicable. For Newtonian fluids this requirement is fulfilled if the Reynolds number is less than 2100. These equations define the limits on the capillary length and diameter. In addition, the ratio of capillary length to diameter should be greater than 50 in order to minimize kinetic and end effects.[2]

Design requirements for the viscometer included extended operation at 300°C and 2000 psi. The basic design of a viscometer being used by F. Kertesz of the Chemistry Division on molten salts appeared to offer a number of merits. Design modifications by Thomas[2] adapted the basic unit for aqueous thoria slurry. As shown in Fig. 47, the device consists of two concentric cylindrical reservoirs with the capillary located between them. Pumping through the capillary is afforded by manipulation of the differential pressure between the reservoirs.

The major departure in instrument design from previous devices involves the detection of reservoir level (flow rate times time) by pneumatic

[2]D. G. Thomas and T. M. Gayle, *The Rheology of Thorium Oxide Slurries*, ORNL CF-55-10-73 (Oct. 17, 1955).

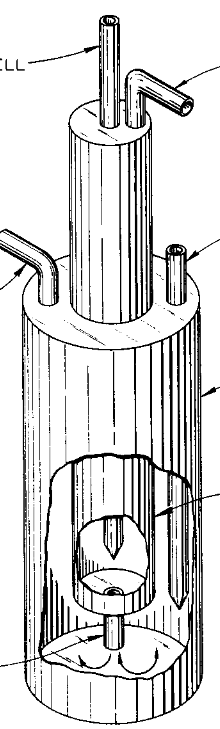

Fig. 47. Capillary Viscometer.

rather than electrical means. Level detection with the fused salts was accomplished by electrical contact of the salt with an insulated probe. The difficulty of making a pressure seal for the electrical leads out of the bomb at 2000 psi and in the presence of steam, together with the desirability of making measurements on rather pure slurries of low electrolytic conductivity, ruled out the use of electrical probes.

The change in differential pressure across the capillary as the last of the fluid passed through was used as the signal indicating the completion of the pump cycle. Preliminary test in a glass mockup showed that at the end of the cycle the pressure drop across the capillary was reduced by 50% in about 5 sec. With long cycle periods, this drop is sufficiently short to keep timing errors within acceptable limits. The differential pressure is measured by a differential pressure cell, and the equalization of pressure across the capillary indicates the end of the cycle.

The final instrumentation included recording of the differential pressure and of various temperatures and semiautomatic operation of valving for pressure manipulation.

HRT CHEMICAL PLANT INSTRUMENTATION

R. K. Adams C. S. Lisser

The Homogeneous Reactor Test Chemical Plant was designed to extract, on a continuous basis, the fission and corrosion products manufactured by the HRT (see flow diagram, Fig. 48). The chemical plant (HRT-CP) is housed in a pit-type cell 12 ft wide, 24 ft long, and 21 ft deep, adjoining the reactor cell. The instrumentation consists of some 600 instruments, 14 ft of control board (see Fig. 49), 16 ft of transducer rack, and 6 ft of miscellaneous panels. Procurement and installation costs were $126,133, not including engineering. The cost for development and engineering design was $61,183; 90 drawings, 38 sketches, and 140 specification sheets were used.

Process Conditions

The parameters and conditions of the process which dictated the selection and application of instruments are as follows:

1. an operating temperature of up to 350°C and an operating pressure of up to 2000 psig (with required over-range protection to 4000 psig),
2. a gamma radiation intensity of up to 300 r/sec,
3. the requirements of an absolutely leak-tight system,
4. inaccessibility of instruments under operating conditions,
5. an expected corrosion rate in excess of 2 mils/year in 300-series stainless steel,
6. an installation compatible with underwater maintenance and with an acid wash for in-cell decontamination.

With the exception of several developmental items, the instruments chosen are commercially available. However, most primary elements are specifically adapted for service under homogeneous reactor process conditions.

UNCLASSIFIED
ORNL-LR-DWG 17742A

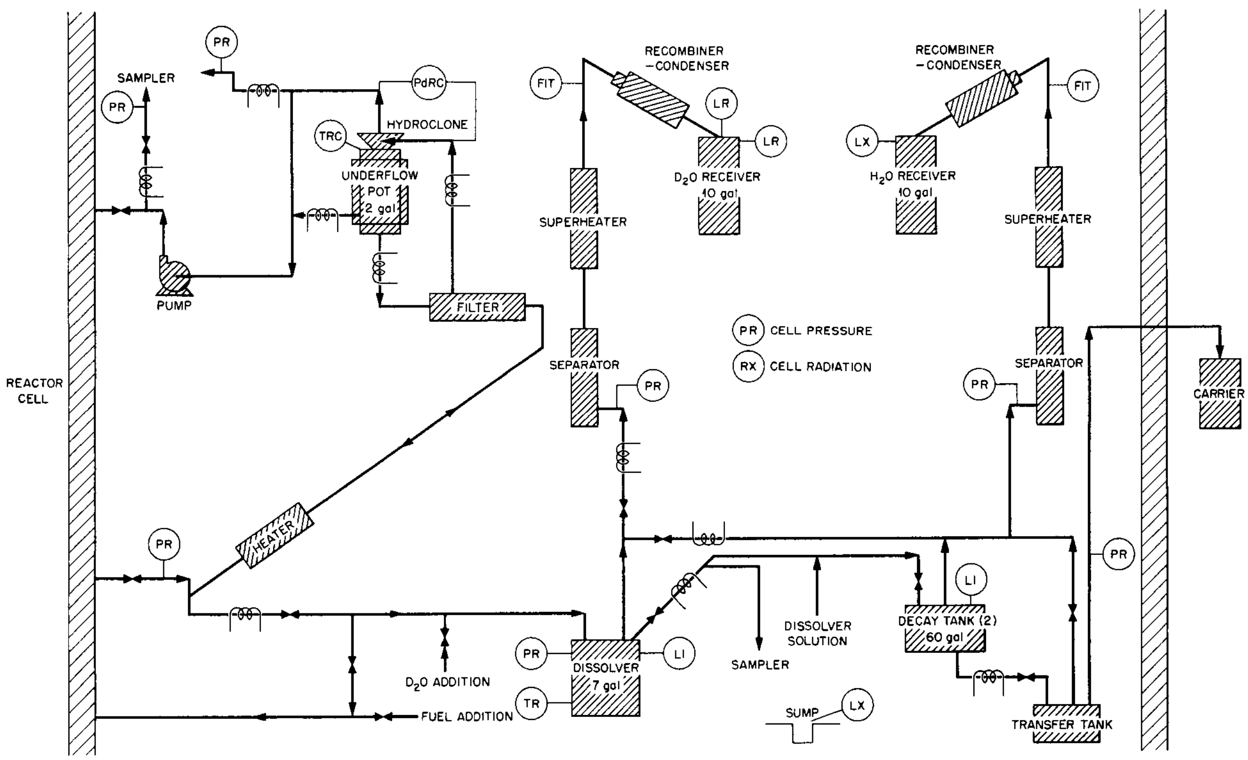

Fig. 48. Flow Diagram of HRT Chemical Plant.

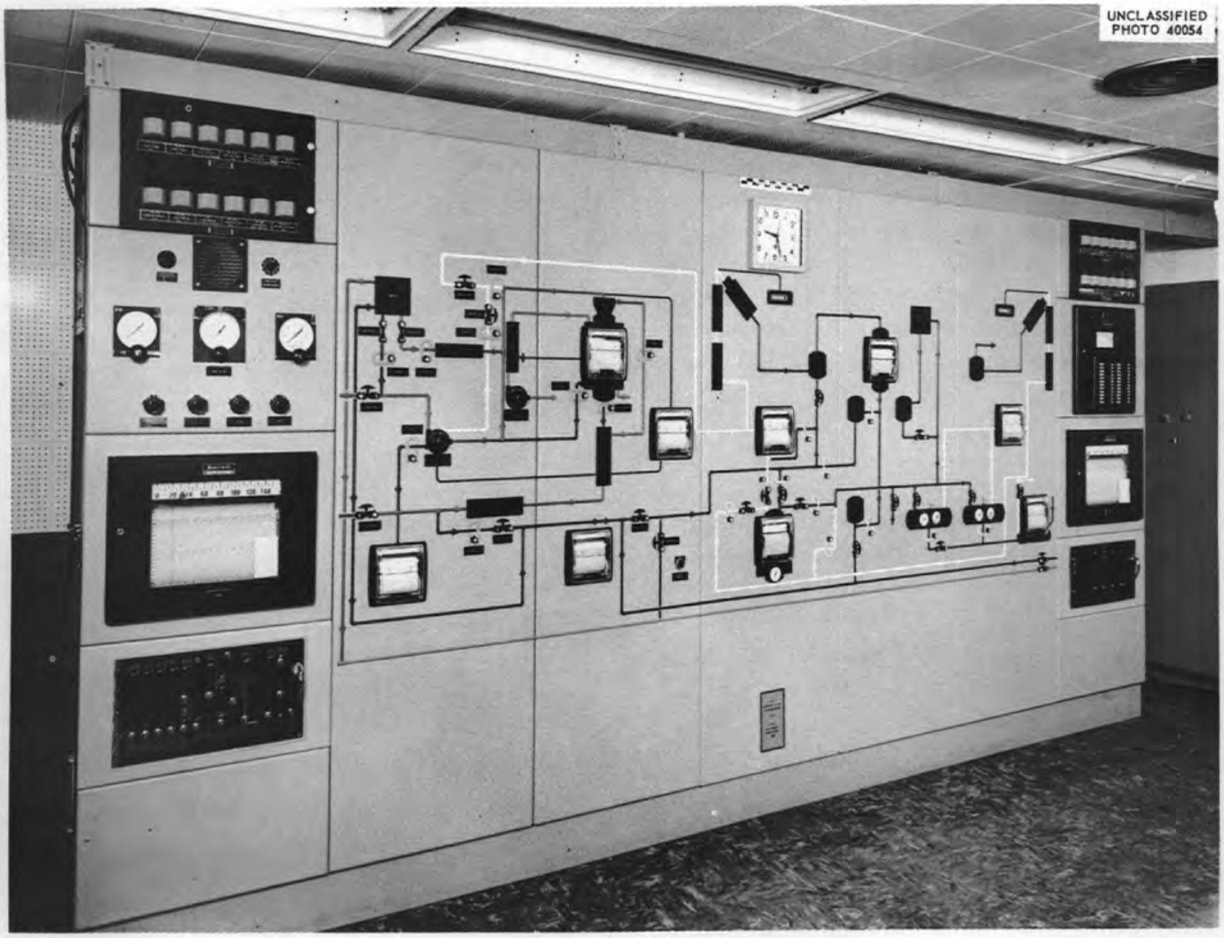

Fig. 49. Control Board of HRT Chemical Plant.

Design Philosophy

The following were salient points in over-all instrumentation design considerations:

1. Primary elements would be provided with subshielding and mounted inside the process cell (see Fig. 50).
2. Primary elements of the electrically transmitting type would be used for in-cell applications wherever possible to avoid open cell shield penetrations.
3. Heavy-water buffers would be interposed between the process tap point and the primary elements.
4. Primary elements of the a-c electrically transmitting type would use a 1000-cps carrier to minimize 60 cps pickup problems.
5. A graphic panel with miniature instruments would be provided.
6. Miniature recorders and controllers of the pneumatic type would be utilized in order to provide adequate limit switches and the correct signals for final control elements. Electrical signals would be converted to their pneumatic analog.
7. Patch panels would be mounted in the control board to facilitate the jumpering of interlock circuits (see Fig. 51). By locating all process patches in the face of the control board, it is thought that the operator cannot fail to be aware of interference with normal circuitry.

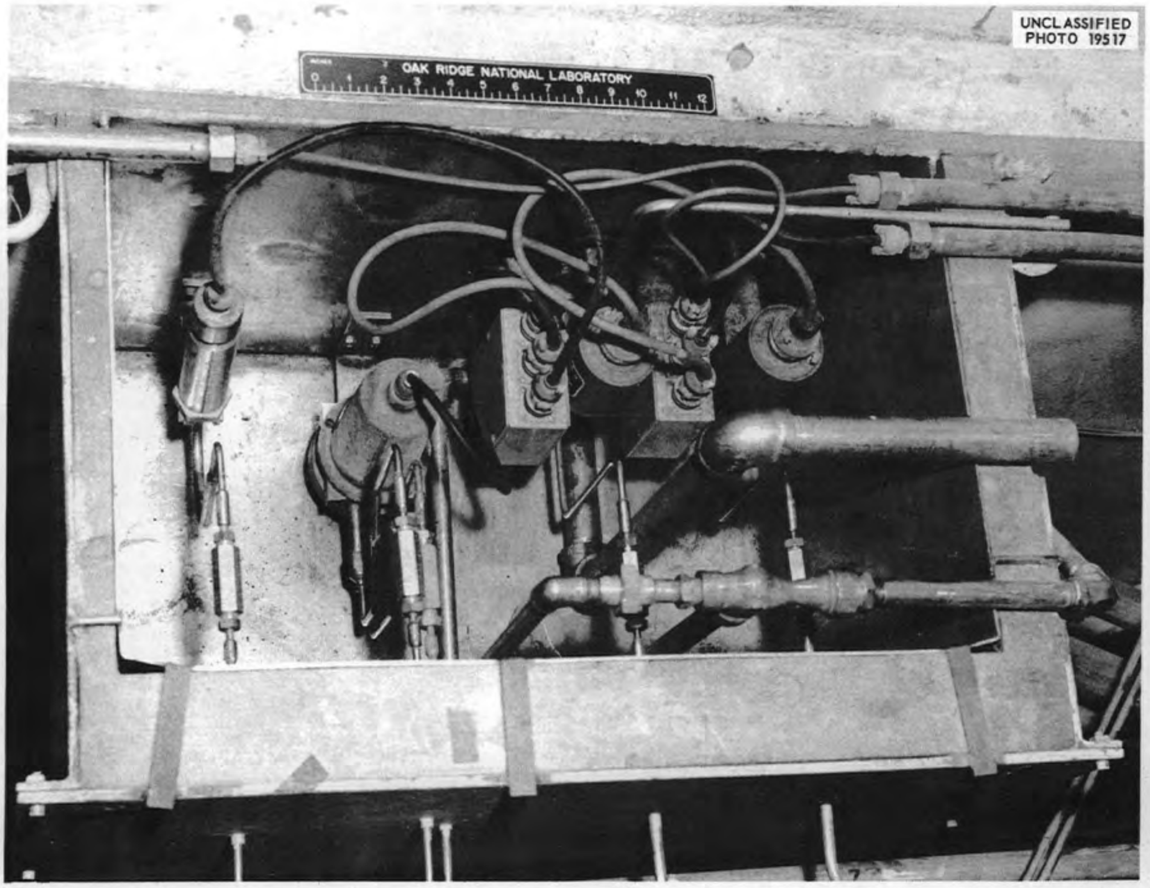

Fig. 50. Instrument Box No. 1 of HRT Chemical Plant.

UNCLASSIFIED
PHOTO 19514

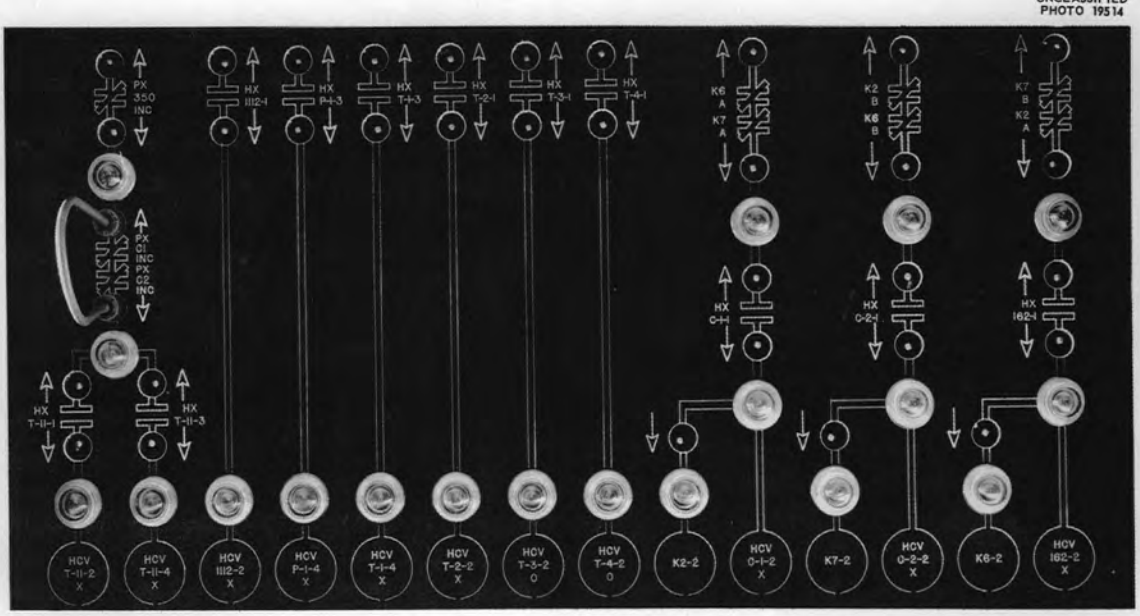

Fig. 51. Face of Patch Panel, HRT Chemical Plant.

Components

The following standard instruments were used in the plant:

Temperature	Potentiometers of the recording, indicating, and controlling types, for Chromel-Alumel thermocouples
Pressure	Baldwin strain-gage pressure cells and Foxboro special all-welded differential pressure cells
Level	Baldwin strain-gage load cells and differential pressure cells with purged dip tubes
Radiation	Mobile air monitors (Q-1740), a remote monitron (Q-1154), and a ten-channel Victoreen process monitor

Special Instruments and Controls

The following are special instruments and controls used in the plant:

1. A thermal level probe was developed at ORNL which utilizes the difference in heat transfer coefficients of vapor vs liquid phases as a principle of operation. In this instrument, thermocouples surround a heater wire inside a tube. This assembly is inserted into a well, mounted vertically in a tank. Two types of these probes have found application. A single-point or "spot" level probe (Fig. 52) merely indicates a liquid–no-liquid condition. The other type, a calibrated "proportional" level probe, senses level change continuously, having thermocouples embedded at 1-in. increments along its length (Fig. 53).

2. All thermocouples in the plant are of the Chromel-Alumel type, insulated with glass fiber. In-cell lengths of the couples are protected with $\frac{1}{8}$-in.-OD type 304 stainless steel tubing. Both a "live" and a spare thermocouple are installed at all in-cell applications.

3. Turbine-type flowmeters are employed to measure the low boilup rates in the chemical plant.

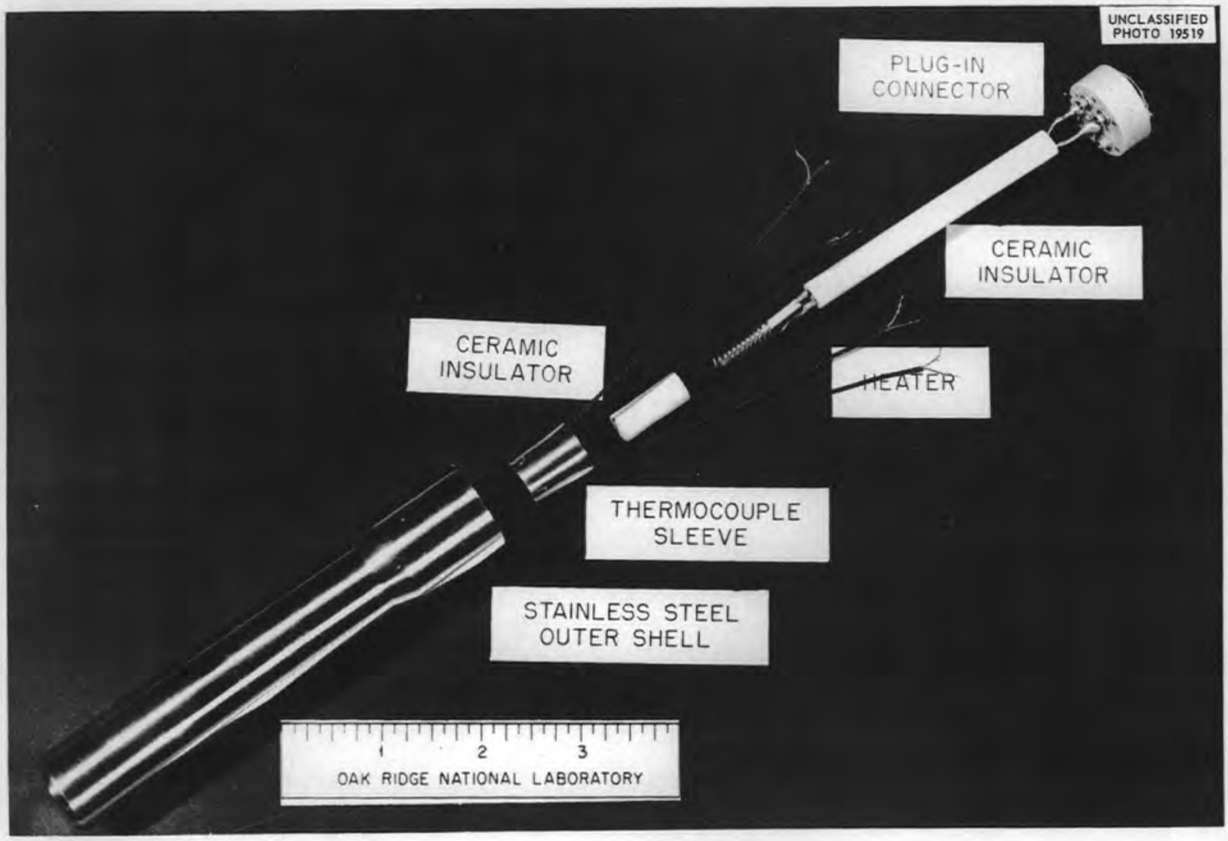

Fig. 52. Spot Level Probe.

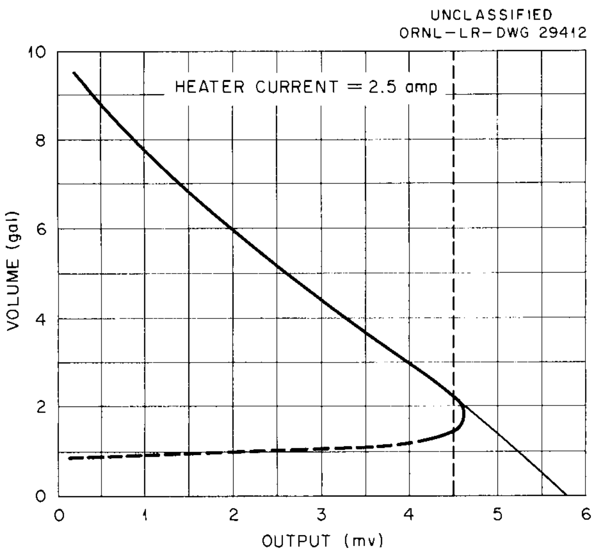

Fig. 53. Calibration of Continuous Level Probe.

The use of such instruments in superheated steam is unusual and required considerable redesign of the bearings.

4. An ORNL-developed instrument obviated the need for individual controllers for 16 freeze plugs. These process plugs freeze or thaw slowly enough to permit two automatic thermocouple scanners (Q-1671-37) to sample each point for 10 sec and take the appropriate control action. The period of rotation for the two scanners is 4 min.

5. The patch panels make use of an auxiliary set of contacts for all field interlock contacts represented in the electric schematic on the face of the patch panel. Each of these auxiliary contacts has patch plug receptacles on either side and continuity lights below it. The insertion of a plug (without cord) into any socket will break the control circuit at this point. Use of a complete patch cord (one plug inserted above, the other below any contact) will establish continuity between the two points in the control circuit.

Control Centers

Aside from field-mounted components, the following are areas of instrument concentration: the main control board, the transducer rack, the two sampler panels, and the bubbler rack.

All panels were constructed of standard ORNL modules. These are angle-iron frames, 2 ft square and 6½ ft high, and preformed panels 24 in. wide by 6½, 13, 19½, 26, or 78 in. high. The adaptability of these modules was reconfirmed when design revisions to the HRT-CP required the addition or revamping of some 14 ft of both the control board and the transducer rack. These changes were made with an expenditure of less than 35 man-days, including mounting and connecting of instruments. Neither of the two panels was effectively out of commission for longer than 24 hr during the period of rework.

The control board is located in the control room and consists of seven 2-ft sections of panels (Nos. 1–7). Panels No. 2–6, in the center of the control board, constitute a graphic panel of the process. Panels No. 1 and No. 7, at either end of the control board, are laid out in standard fashion and contain instrumentation common to more than one part of the process, that is, the temperature recorders and indicators, the annunciators, the patch panels, and the noise-pickup loudspeakers. Otherwise, recording and controlling instruments, as well as valve and freeze-plug actuators, are located according to their process functions in the graphic panel sections.

The transducer rack, located in cell D, consists of eight 2-ft sections of panel board (panels No. 11–18) and is used to mount electric-to-pneumatic transducers, solenoid valves, pressure switches, radiation monitors, temperature scanners, and other equipment.

There are two sampler panels, panel No. 21 (for the overflow and underflow sampler) and panel No. 31 (for the dissolver sampler). Both are installed on the main floor. All sampler instrumentation is displayed on these panels with the exception of the primary elements and their transducers.

The level and density panel (No. 41), installed in cell A, contains the differential pressure cells used in connection with the dissolver and decay tanks.

HRP INSTRUMENTATION AND CONTROL

D. S. Toomb

S. J. Ball
E. H. Bell
A. M. Billings
J. R. Brown
D. G. Davis
G. W. Greene
J. D. Grimes[1]
J. C. Gundlach
P. G. Herndon
R. L. Moore
R. M. Pierce[1]
J. A. Russell

H. D. Wills

The testing and improvement of instruments and control valves that were developed for the Homogeneous Reactor Test have continued in the engineering test mockup facility and in specially designed test stands. Specific experience with these components is described below.

LIQUID-LEVEL TRANSMITTERS

The pressurizer level transmitter developed for the HRT has operated for approximately 8000 hr on the mockup without being touched. This transmitter, shown in Figs. 54 and 55, consists of a 5-in.-long float displacer suspended by two helical springs. An extension rod above the springs positions a magnetic piston in the center of a differential transformer. Vibration of the float is damped by the action of the field from permanent magnets on a one-turn copper ring. The only nonwelded closure is the 2500-psi ring-joint flange, which makes the unit amenable to remote replacement. The transmitter is also self-draining – a very desirable feature in systems containing radioactive fluids. A systematic study of pressure and temperature effects on the span and zero of this level transmitter has been made.[2] The shift of level signal with pressure was found to be linear and amounted to 1% of the full-scale reading (5 in. of water) per 500 psi change in pressure. Temperature effects on the level indication are greater and are due to density changes in the vapor and liquid, differential expansions, changes in the modulus of elasticity of the spring material, and electrical resistance changes in the motion-sensing differential transformer windings. These effects are most serious when temporary local temperature differences occur in the transmitter during periods of heating or cooling of the reactor system.

The HRT outer-storage-tank liquid-level transmitter, illustrated in Fig. 56, has a range of 0 to 47 in. of water and is hydraulically damped by the interaction of two moving vanes attached to the displacer and a baffle fastened to the housing. This transmitter has a design pressure rating of 500 psi and is also designed for remote adjustment or replacement.

The original Iso-elastic alloy helical suspension springs utilized in the pressurizer and storage-tank level transmitters have been replaced with gold-plated springs of the same alloy in order to achieve corrosion resistance. Elgiloy springs, which have superior corrosion resistance, have shown a susceptibility to stress-corrosion cracking in the heat-treated states tested to date.

Prototype linear differential transformers suitable for sensing displacer (float) motion in the above transmitters have been received from the G. L. Collins Company and the Crescent Engineering & Research Company. The transformers are designed to be radiation resistant by incorporating no organic materials and are suitable for operation at pressurizer temperatures. The Collins transformer, shown at the far right of Fig. 57, is wound with copper wire insulated with ceramic, and the leads are brought through the stainless steel housing by ceramic-to-metal seals. The Crescent unit, shown at the center of Fig. 57, is wound with silver wire insulated with ceramic, and the leads are brought through the stainless steel housing by compression-type seals. The transformers presently in use, shown at the left of Fig. 57, were fabricated at ORNL and are wound with Sprague Electric Company Ceroc T wire on American Lava Corporation Lava forms. The new

[1]On loan from TVA.

[2]D. A. Cameron and J. C. Bolger, *HRT Pressurizer Level Instrument, Range and Zero Shifts*, KT-242 (Nov. 27, 1956).

UNCLASSIFIED
ORNL-LR-DWG 14045R

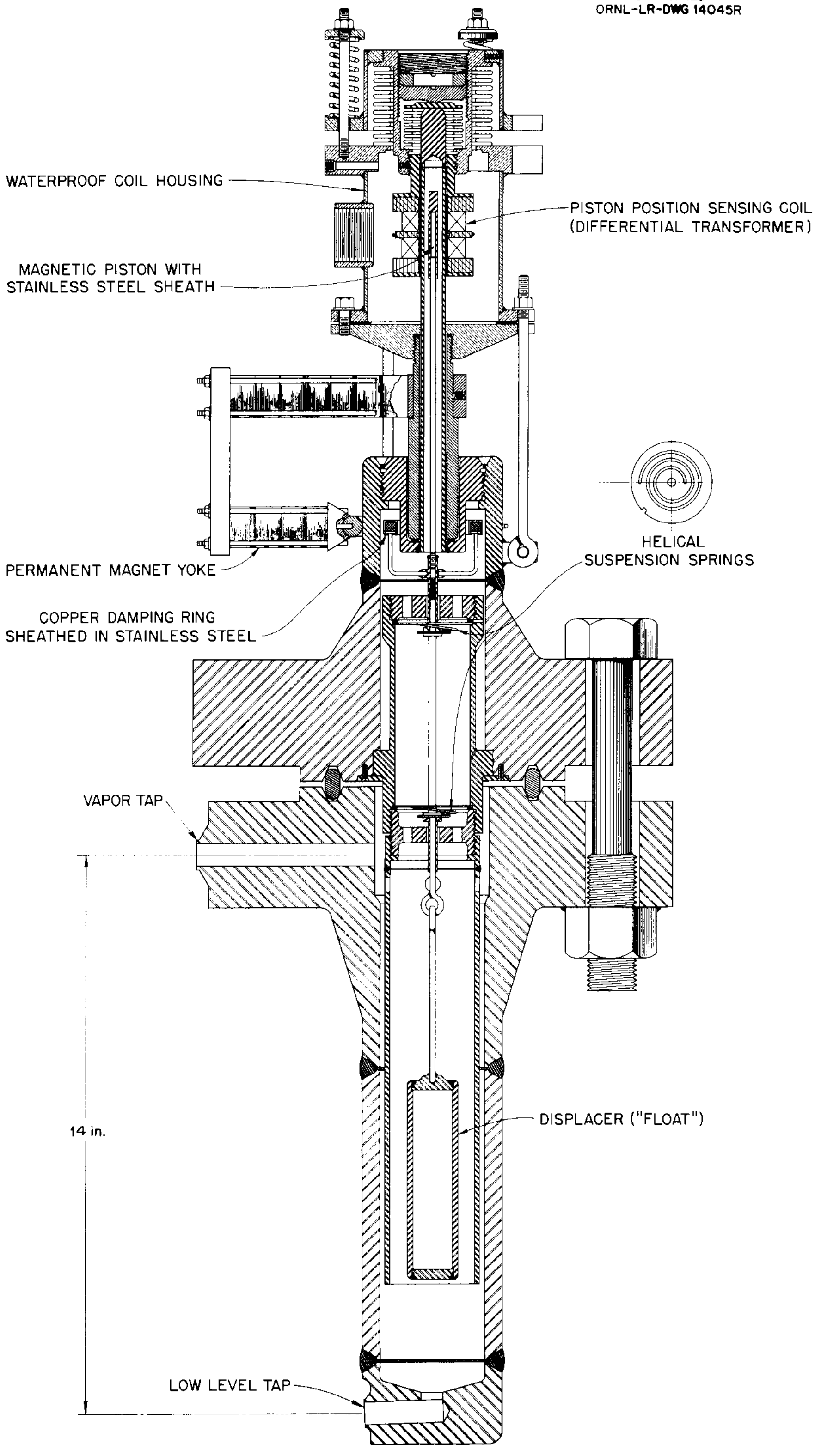

Fig. 54. HRT Pressurizer Liquid-Level Transmitter Assembly.

UNCLASSIFIED
PHOTO 25285

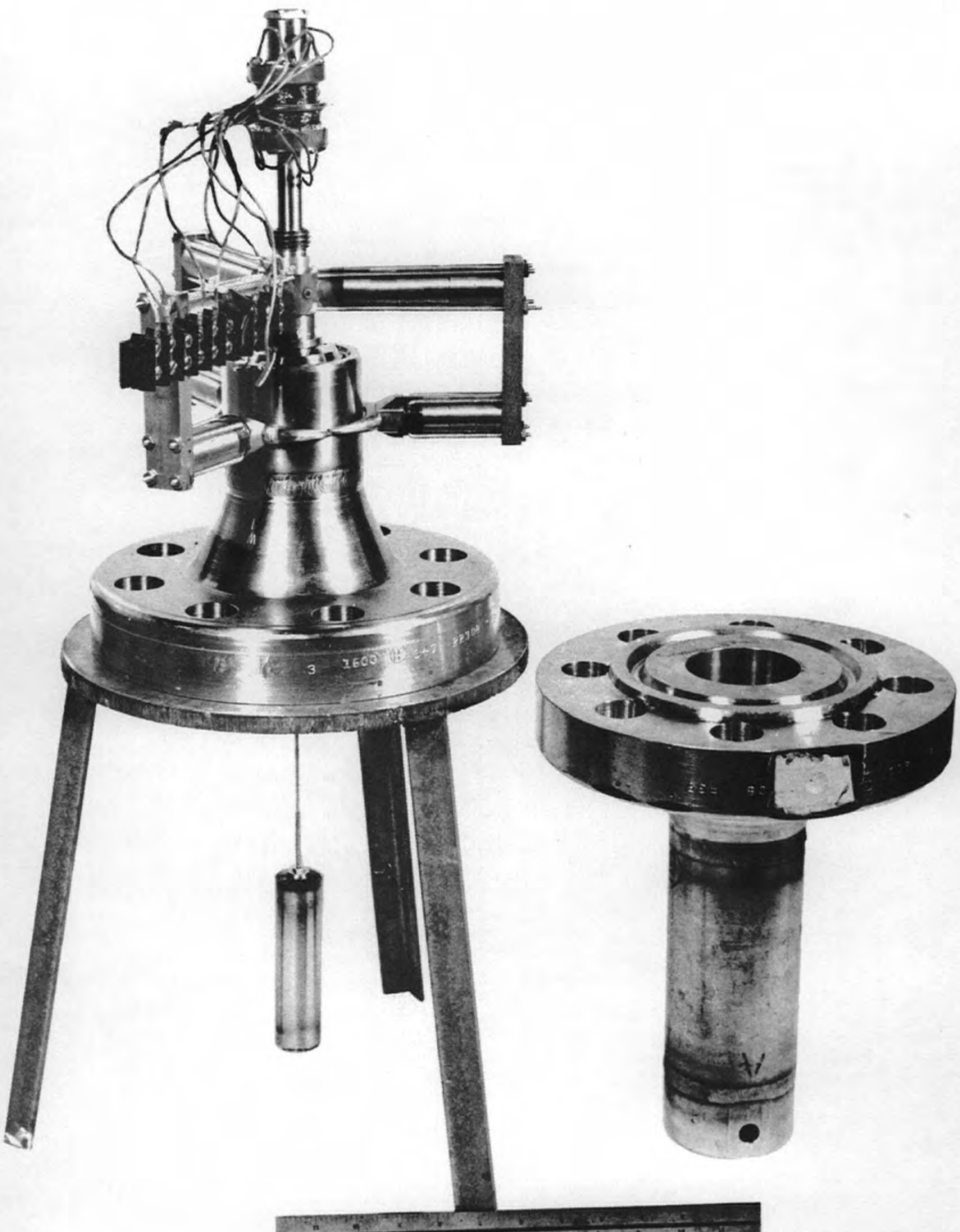

Fig. 55. Prototype of HRT Pressurizer Liquid-Level Transmitter.

UNCLASSIFIED
ORNL-LR-DWG 14046

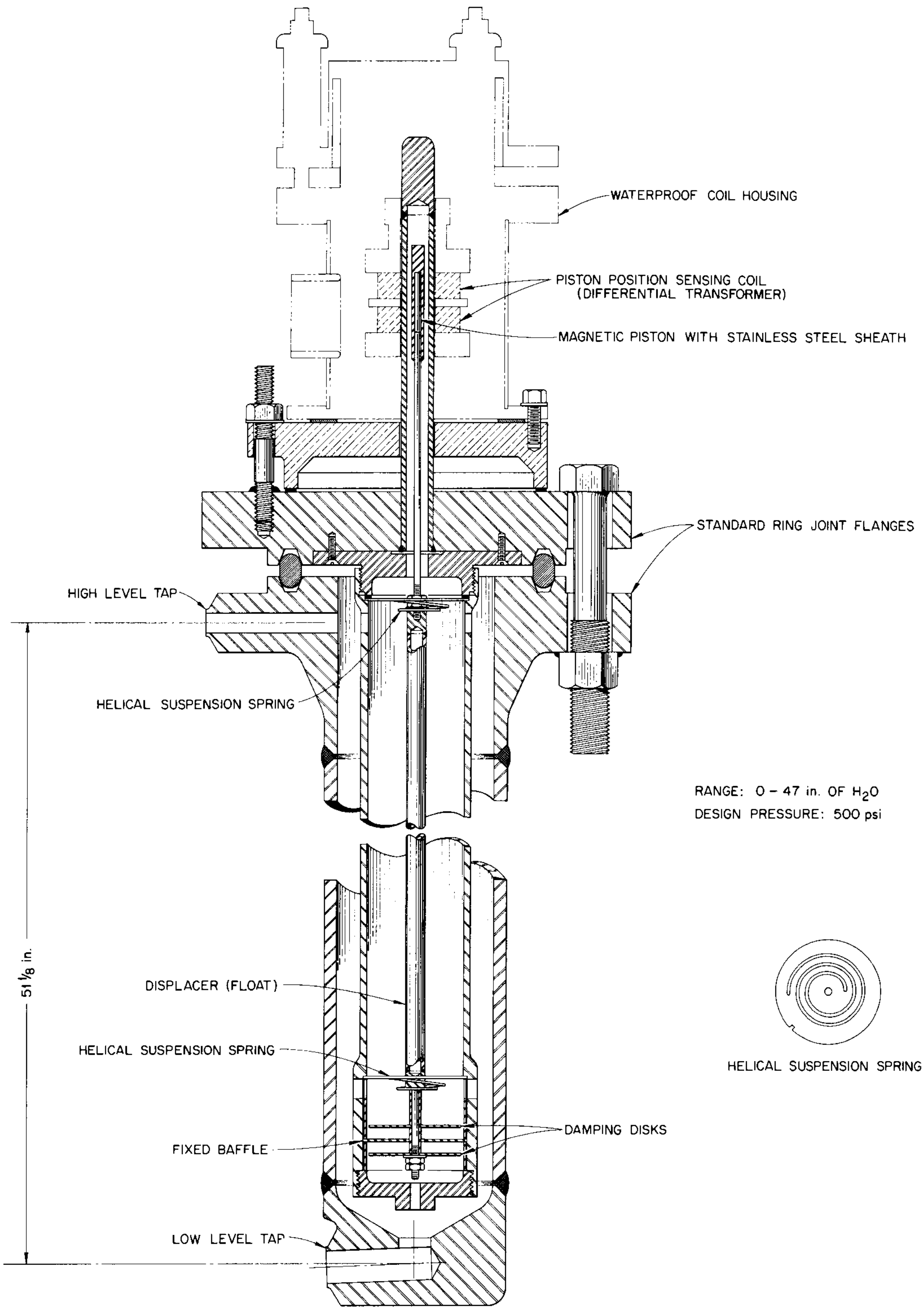

Fig. 56. HRT Outer Storage Tank Liquid-Level Transmitter Assembly.

Fig. 57. Prototype Differential Transformers for HRT Liquid-Level Transmitters.

units, which should be more radiation resistant than those presently installed, will be thoroughly tested before the existing units are replaced.

A completely weld-sealed liquid-level alarm-control manufactured to Homogeneous Reactor Project specifications by Magnetrol, Inc., is shown in Fig. 58. A spherical stainless steel float actuates a mercury-contact switch through the housing extension by magnetic attraction. The unit is used for high- and low-liquid-level alarm in vessels used in systems designed for a maximum pressure of 500 psi.

PRESSURE TRANSMITTERS

The pressure transmitter shown in Fig. 59 was manufactured by the Callery Chemical Company and is being evaluated as to suitability for use in HRP systems. The transmitter is designed for operation at temperatures to 640°F, and therefore can be directly connected to process lines. Presently used Bourdon-tube-element transmitters are not suitable above 200°F and must be connected through long, uninsulated lines to reduce the operating temperature. The new transmitter was found to have a natural frequency of 375 cps and an accuracy of 2%. It should be useful in reactor kinetic experiments where long connecting lines limit the response of Bourdon-tube-element transmitters. It is expected that this transmitter will be used in studies to determine the effectiveness of the HRT fuel system pressurizer in damping reactivity excursions.

UNCLASSIFIED
ORNL-LR-DWG 14062

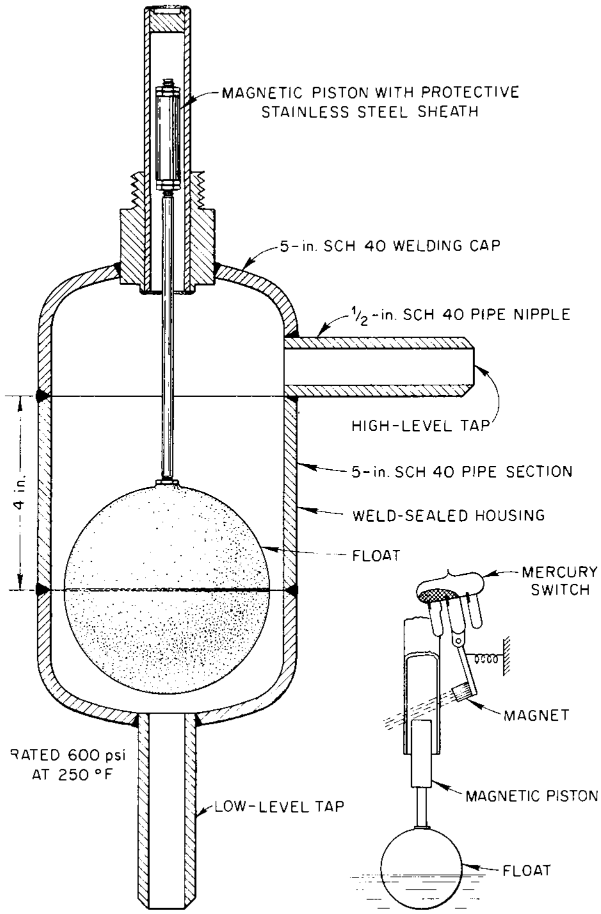

Fig. 58. Liquid-Level Alarm Transmitter.

DIFFERENTIAL PRESSURE TRANSMITTERS

An improvement on the design of the electric-signal differential pressure transmitters used in the HRT has been made for new units to be employed in the component development programs. The new design by the Foxboro Company, shown in Fig. 60, eliminates the threaded joint which was subject to galling and the difficult weld which joins the pressure taps to the body block. Different ranges of differential from 50 in. of water to 50 psi may be had by changing range springs. Without the spring, the range is approximately 50 in. of water, which may be reduced to 25 in. if a $\frac{1}{2}$-mv/v-sensitivity receiver is used.

FUEL-BLANKET DIFFERENTIAL PRESSURE TRANSMITTERS

Tests after preliminary system operation were performed on the two installed differential pressure transmitters which produce pneumatic signals proportional to the difference in pressure between the HRT fuel and blanket systems. The results indicate that one cell shifts zero 11% linearly with applied static pressure to 2000 psi, and the other 2% over the same range.

The transmitters shown in Fig. 61 exhibited excellent stability with cycling. They are supplied by the Foxboro Company. Errors of less than 1% in range and $1\frac{1}{4}$% in zero were observed after 500 cycles with a ±75-psi differential signal.

To indicate zero stability with time, the transmitters were adjusted at 2000 psi and held at this pressure. No change in output signal was observed in 12 hr.

As a result of these tests, the transmitters will be zero-adjusted at operating pressure. The more stable instrument will be used for control, with the other on standby.

INVENTORY SYSTEM

The dump- and condensate-tank pneumatic weighing systems have proved to have less than 1% error. These are difficult applications, as the ratio of tare to inventory load is about 2.5:1 for the dump tanks, and continuous piping connections are made to the tanks. This installation is shown in Fig. 62. The dump tanks are about 16 ft long and are suspended by hangers from a pivoted beam which actuates the pneumatic transmitter shown at the top of the illustration. The pneumatic schematic of this system is shown in Fig. 63.

FLOW TRANSMITTERS

A variable-area-type flowmeter with an induction coil pickup has been installed on the feed-pump test loop and appears to be a solution to the difficult problem of measuring reactor feed- and purge-pump flows. Flowmeters for this service must be installed on the discharge side of these pumps to avoid pressure drops in the suction line. As these flows are pulsing from the action of the diaphragm pumping heads, a meter with linear

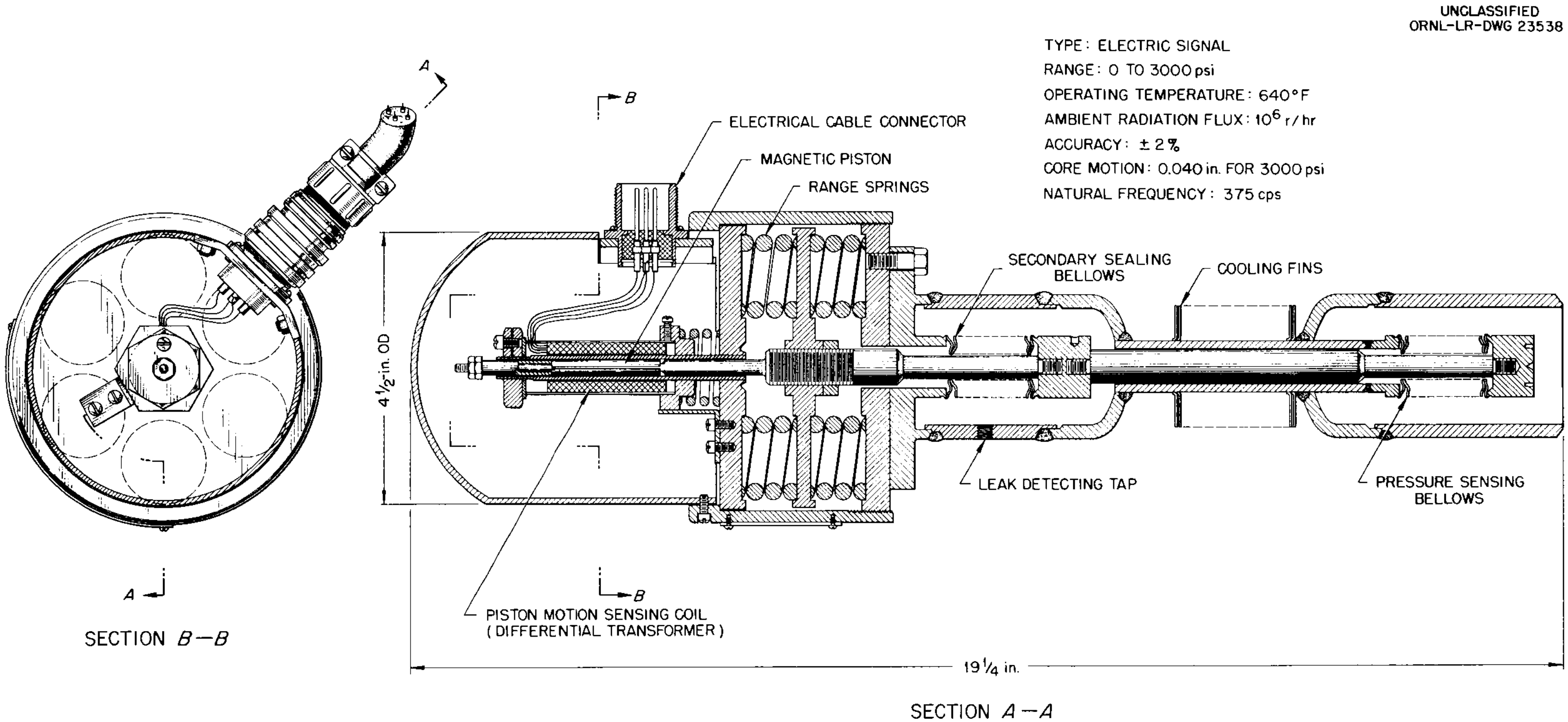

Fig. 59. High-Temperature Differential Pressure Transmitter.

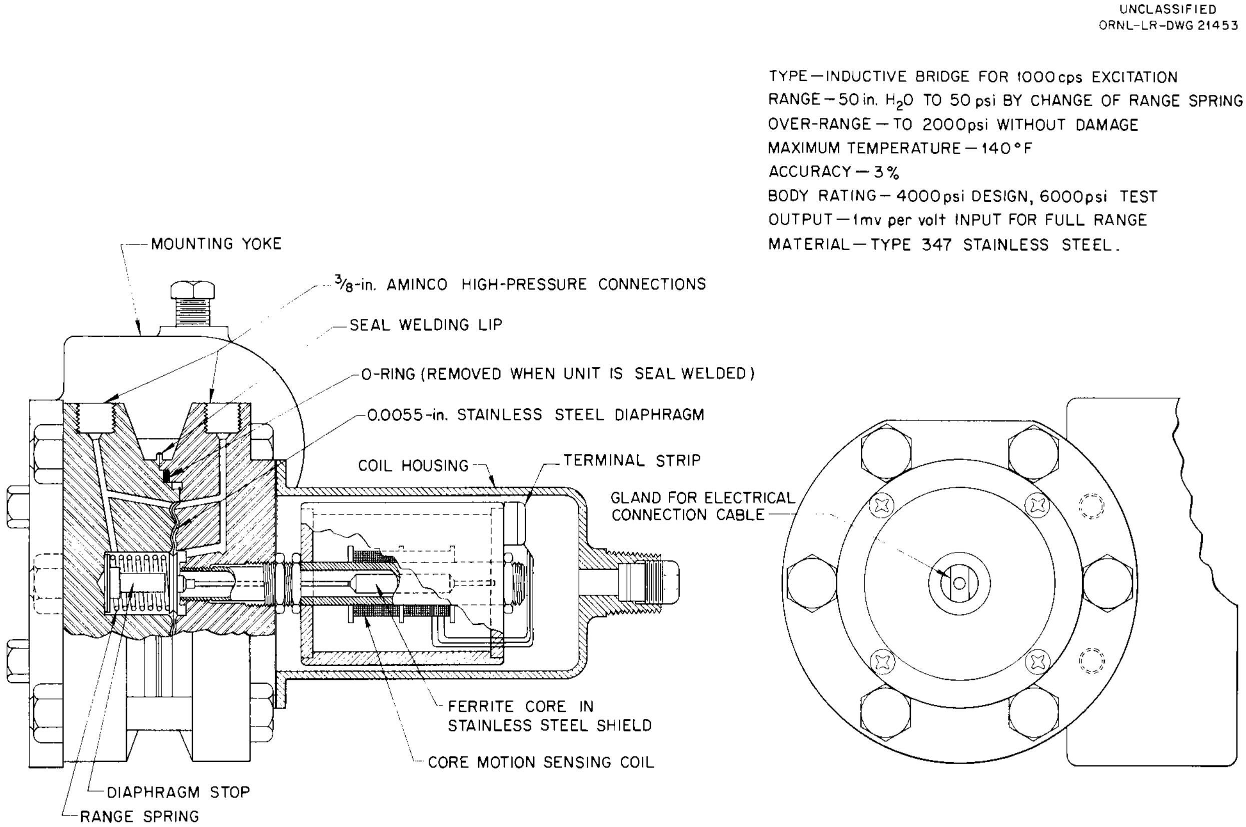

Fig. 60. Differential Pressure Transmitter, Electric Signal Type.

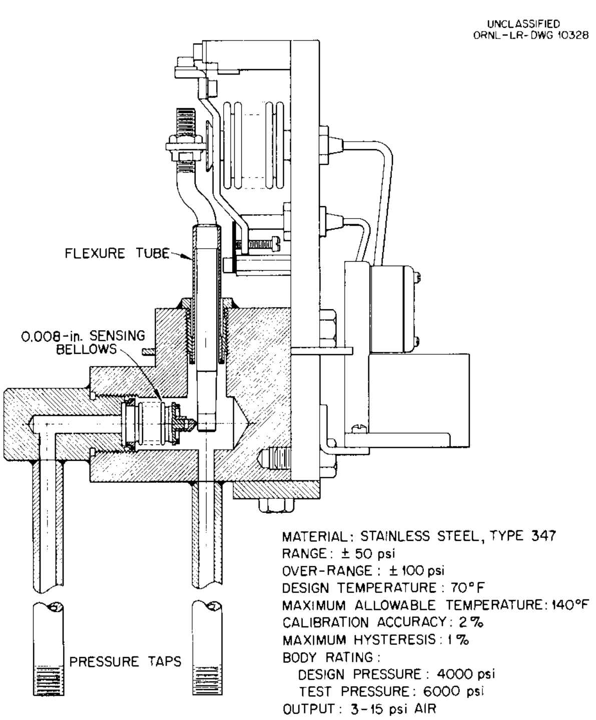

Fig. 61. Differential Pressure Transmitter, Pneumatic Signal Type.

output must be used so that the damped record will be an accurate indication of the average flow. The flow transmitter supplied by the Schutte & Koerting Company and shown in Fig. 64 has been used to date.

HIGH-LEVEL GAMMA IONIZATION CHAMBER

A high-level gamma ionization chamber has been developed to measure radiation levels inside the HRT containment cell. This chamber is shown in Fig. 65. Information on the radiation level is needed to evaluate the effectiveness of shielding, to assess the rate of radiation damage to reactor components, to measure radiation levels during maintenance operations, and to provide data for future reactor designs. Preliminary tests indicate that the chamber will measure levels to 10^7 r/hr and that it is sensitive down to background radiation levels.

REMOTE-AREA RADIATION MONITORING SYSTEM

In the HRT, service lines from the reactor are monitored for activity by remote radiation detection

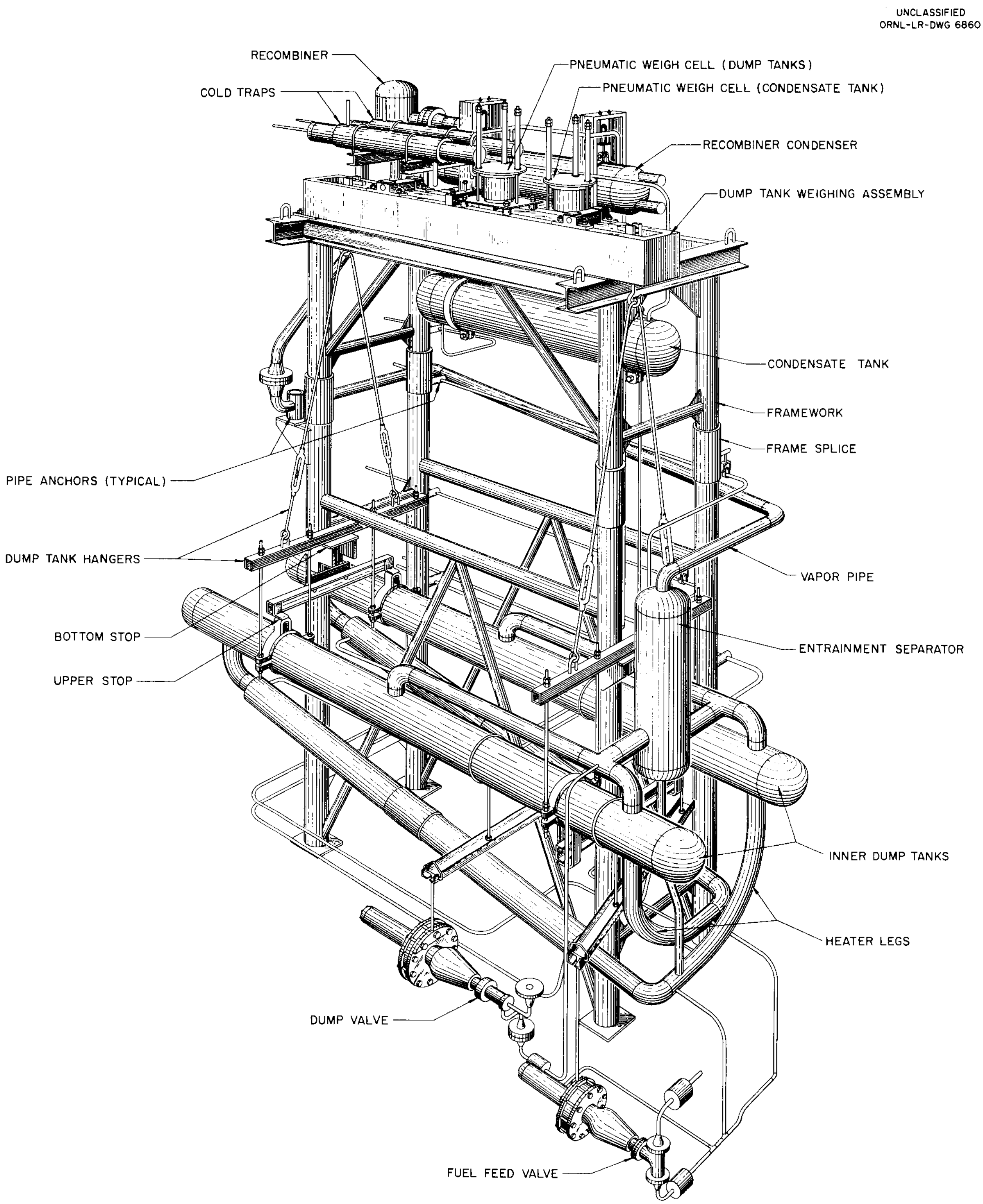

Fig. 62. Weighing System for HRT Dump and Condensate Tanks.

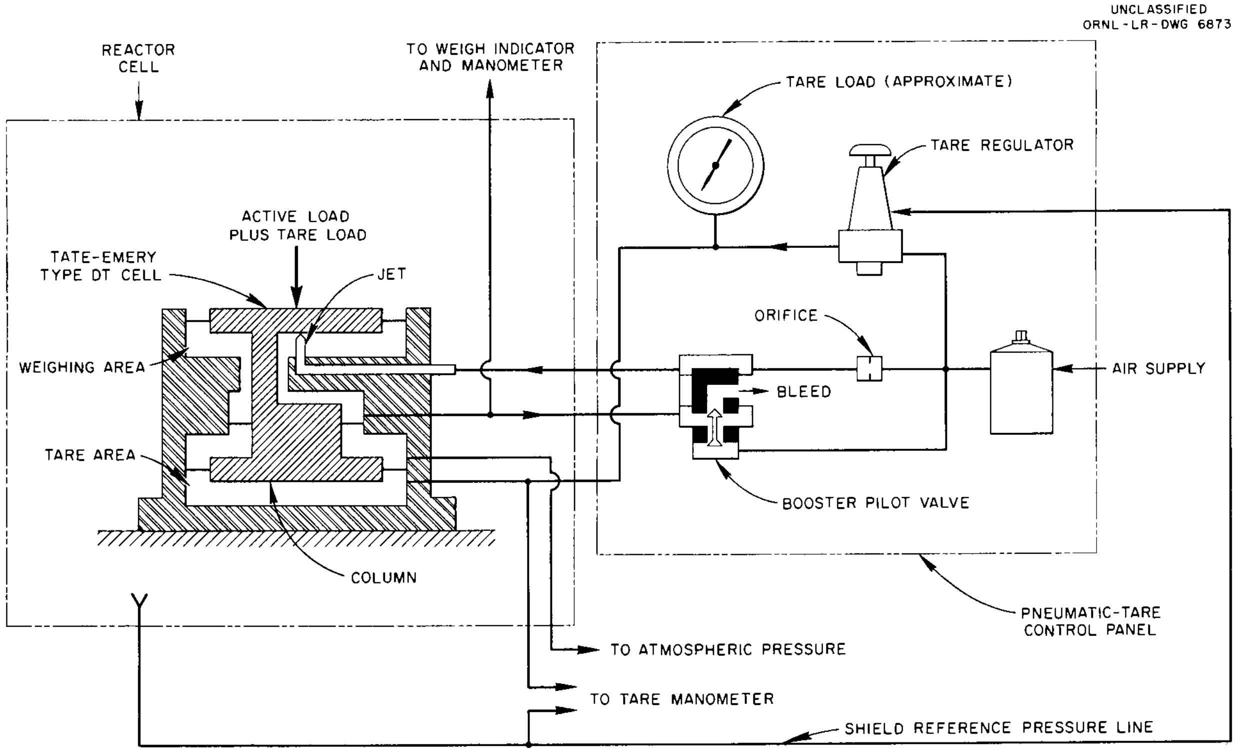

Fig. 63. Tank Pneumatic Weighing System.

elements which are small gamma ionization chambers. A simple one-tube three-decade logarithmic amplifier is sealed within the chamber head and drives a remote contact-making meter and a multipoint recorder. This system is shown schematically in Fig. 66. These detectors can be remotely calibrated by exposure to a radioactive source upon actuation of a solenoid-operated shielding shutter. All channels are duplicated, and control action is initiated only upon a simultaneous signal from both channels, in order to minimize false scrams. However, a signal from either channel is annunciated. These assemblies were fabricated by the Victoreen Instrument Company to ORNL specifications and were accepted after performance testing at the ORNL Health Physics Division calibration facility.

OXYGEN INJECTION SYSTEMS

The addition of oxygen to the HRT circulating system is necessary to prevent the reduction of uranyl ions within the solution and to inhibit corrosion. The system, shown in Fig. 67, meters the gas flow from a high-pressure oxygen source to the reactor high-pressure system. The gas flow is first restricted by the snubbing capillary to prevent the damaging of the differential pressure cell by the sudden application of pressure. The transmitter provides an electrical signal proportional to flow by sensing the differential pressure produced by the gas flow through the metering capillary. The electric flow signal is recorded in the control room and provides a means of actuating the differential-expansion-type flow-control valve shown in Fig. 68. This valve consists of a cylinder and a plug made of two materials with different coefficients of thermal expansion. The plug is made of the low-coefficient material and at ambient temperature has a shrink fit in the cylinder of 0.0005 in. As the temperature of the valve is raised by the heater windings, the clearance between the plug and cylinder increases and, as a result, there is an increase in flow.

An air-operated block valve to prevent the backflow of liquid from the reactor high-pressure

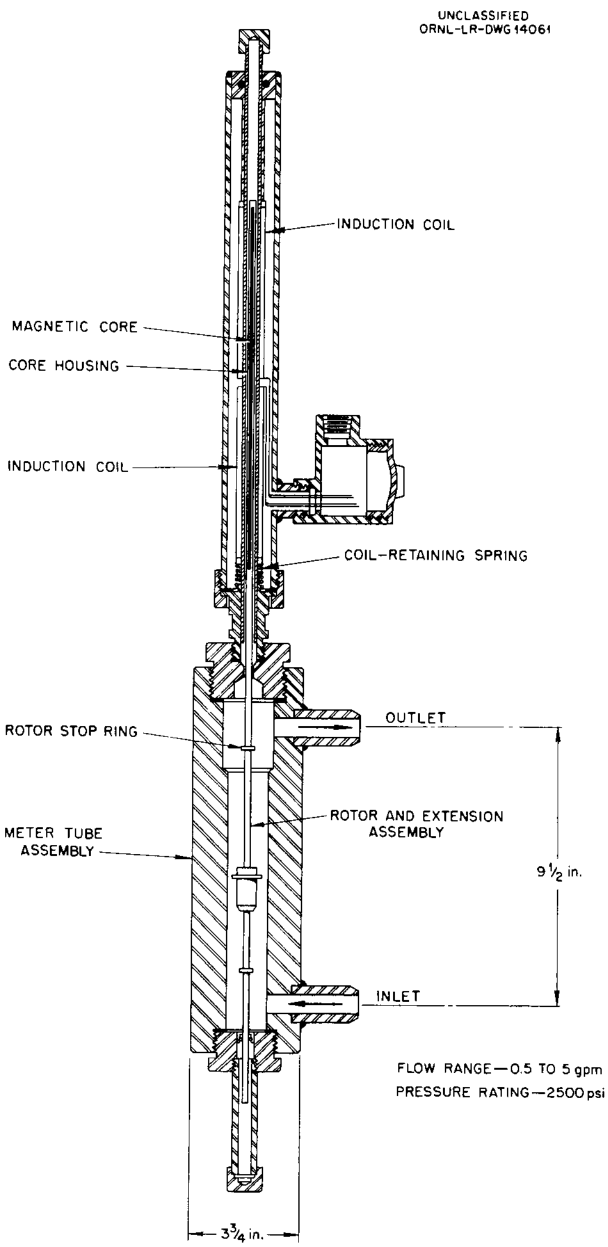

Fig. 64. Prototype Flow Transmitter for Small Pulsing Flows.

system in case oxygen-system pressure is lost is shown in Fig. 69. This valve incorporates a novel gold sealing-gasket ring to provide a resilient seat for positive shutoff.

CONTROL VALVES

The HRT-model letdown valve installed on the HRT mockup was taken out of service after 6500 hr of operation. Of this time, 10 hr was with 5% HNO_3, about 400 hr with water, 5500 hr with HRT fuel solution, and the last 576 hr with 300 g/liter uranyl sulfate. The valve, which was mounted vertically with the operator down, was in excellent condition after this service period. However, Stellite No. 6 plugs have been eroded in oxygenated water service, and the Stellite No. 6 plugs in the reactor letdown valves have been replaced with Armco 17-4 PH stainless steel. Details of this valve and actuator design are shown in Figs. 70–72. The valve was supplied by the Fulton Sylphon Division, Robertshaw-Fulton Controls Company, and the actuator by the Annin Company.

The blanket dump valve shown in Fig. 73 was tested for 400 cycles in the HRP valve test loop with no appreciable change in leak rate being noted. The leak rate, after testing, was less than that called for by HRP valve specification No. 303, which is 500 std cc/day of nitrogen gas applied to the valve inlet at 2000 psi. The dump valves and their associated pneumatic actuators were supplied by the Fulton Sylphon Division, Robertshaw-Fulton Controls Company.

Chloride-induced pitting on the leak detector side of the bellows heads of the HRT low-pressure valves (500 psi design) has necessitated the replacement of the bellows assemblies in these valves. The valve design and bellows-plug assembly are illustrated in Figs. 74 and 75. The bellows plug illustrated in Fig. 75 has been threaded for use on a hand valve. However, most of these valves installed in the reactor are pneumatically actuated, and the drive stem is internally threaded to be fastened to the actuator.

UNCLASSIFIED
ORNL-LR-DWG 18860AR

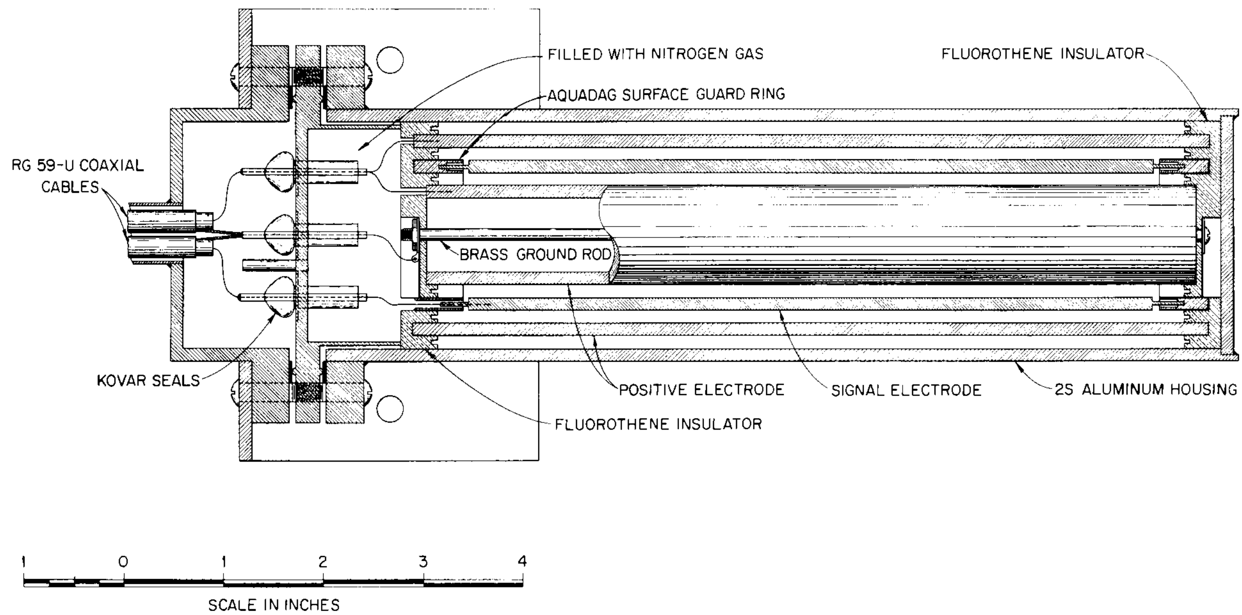

Fig. 65. **HRT High-Level Gamma Ionization Chamber.**

UNCLASSIFIED
ORNL-LR-DWG 5256

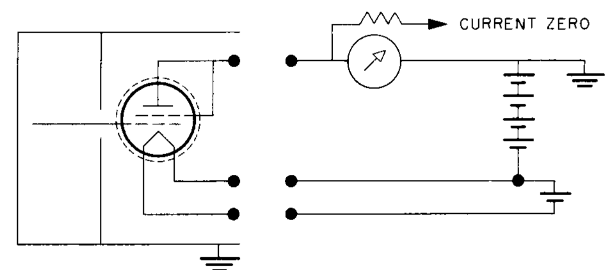

Fig. 66. HRT Remote-Area Radiation Monitoring System.

The valve-stem sealing bellows of the type illustrated in Fig. 75 have been life-tested in uranyl sulfate at 2000 psi and 300°C in the test stand shown in Fig. 76. The average life for single bellows assemblies stroked $\frac{1}{8}$ in. has been 35,000 cycles.

A Fulton Sylphon Division stainless steel bellows of the type used in the HRT for sealing valve stems was gold-plated at ORNL in an attempt to increase its corrosion resistance. These bellows, because of their thinness, are subject to short-term failure if subjected to

UNCLASSIFIED
ORNL-LR-DWG 17190R

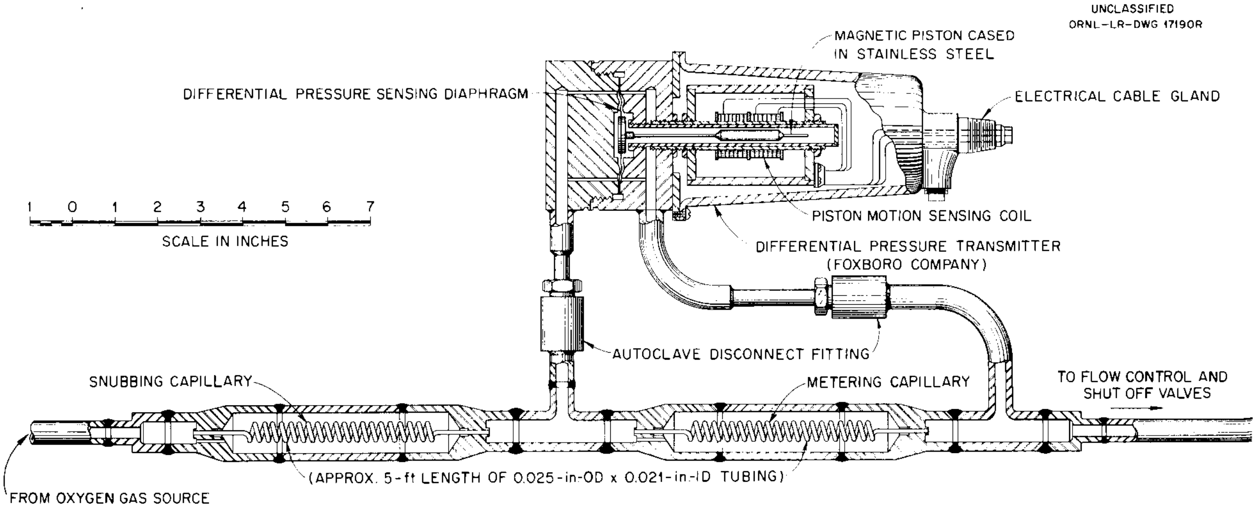

Fig. 67. HRT Oxygen Injection System.

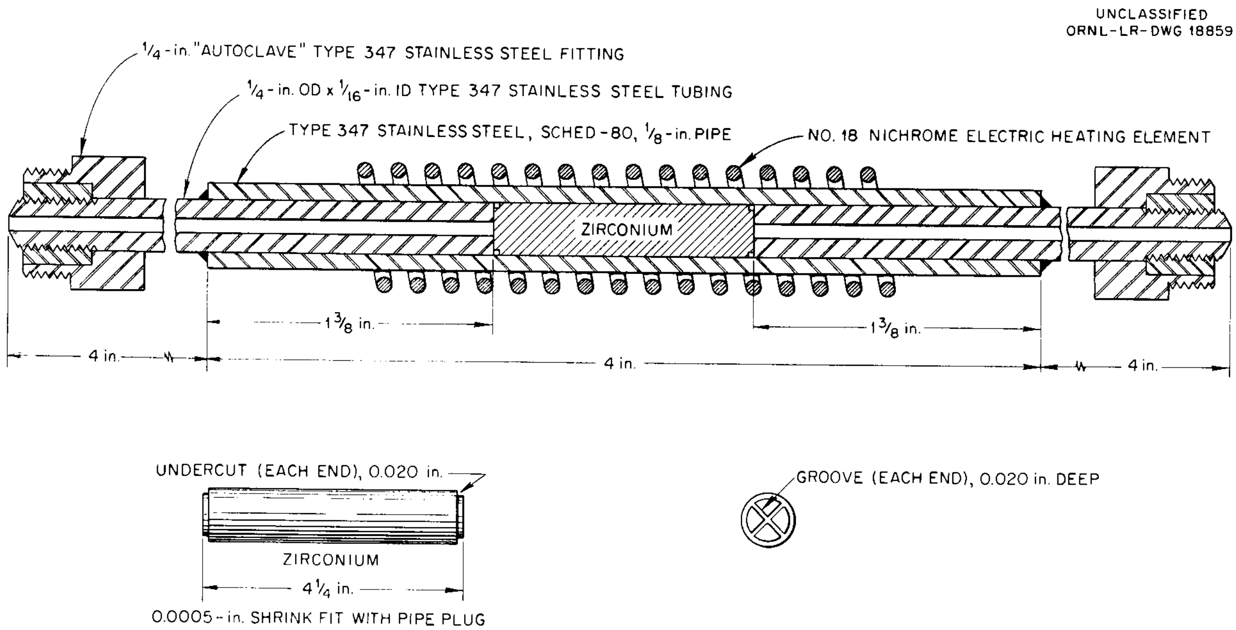

Fig. 68. HRT Oxygen Flow Control Valve, Differential Expansion Type.

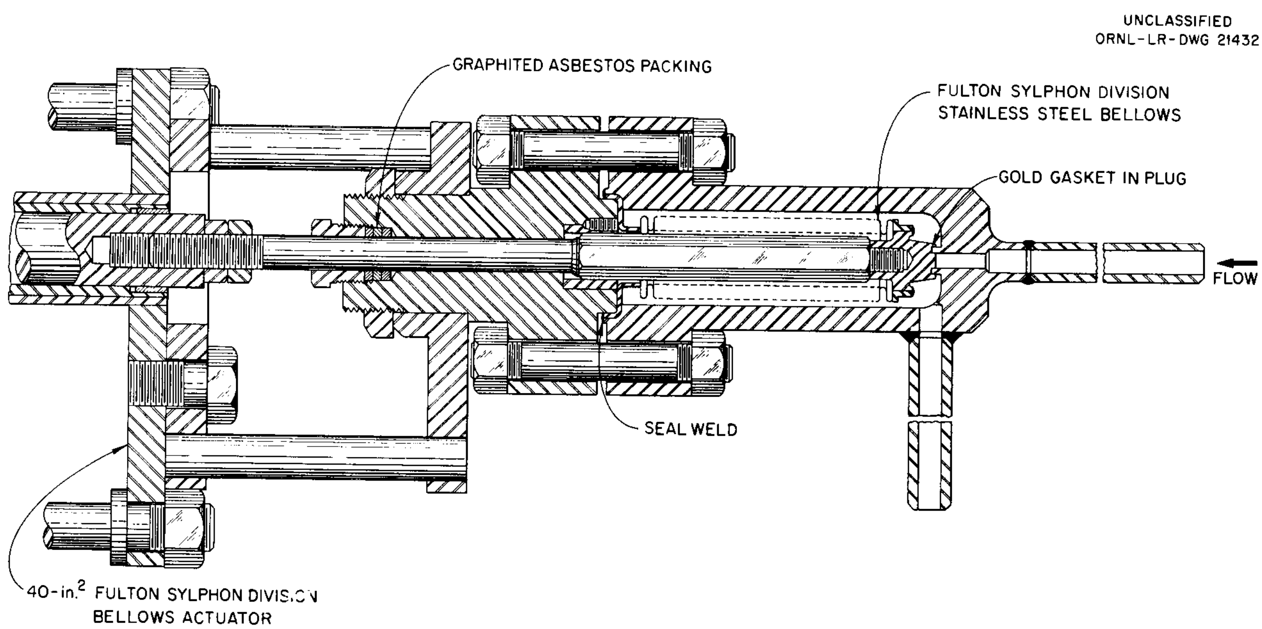

Fig. 69. HRT Oxygen Flaw Block Valve.

UNCLASSIFIED
ORNL-LR-DWG 14047R

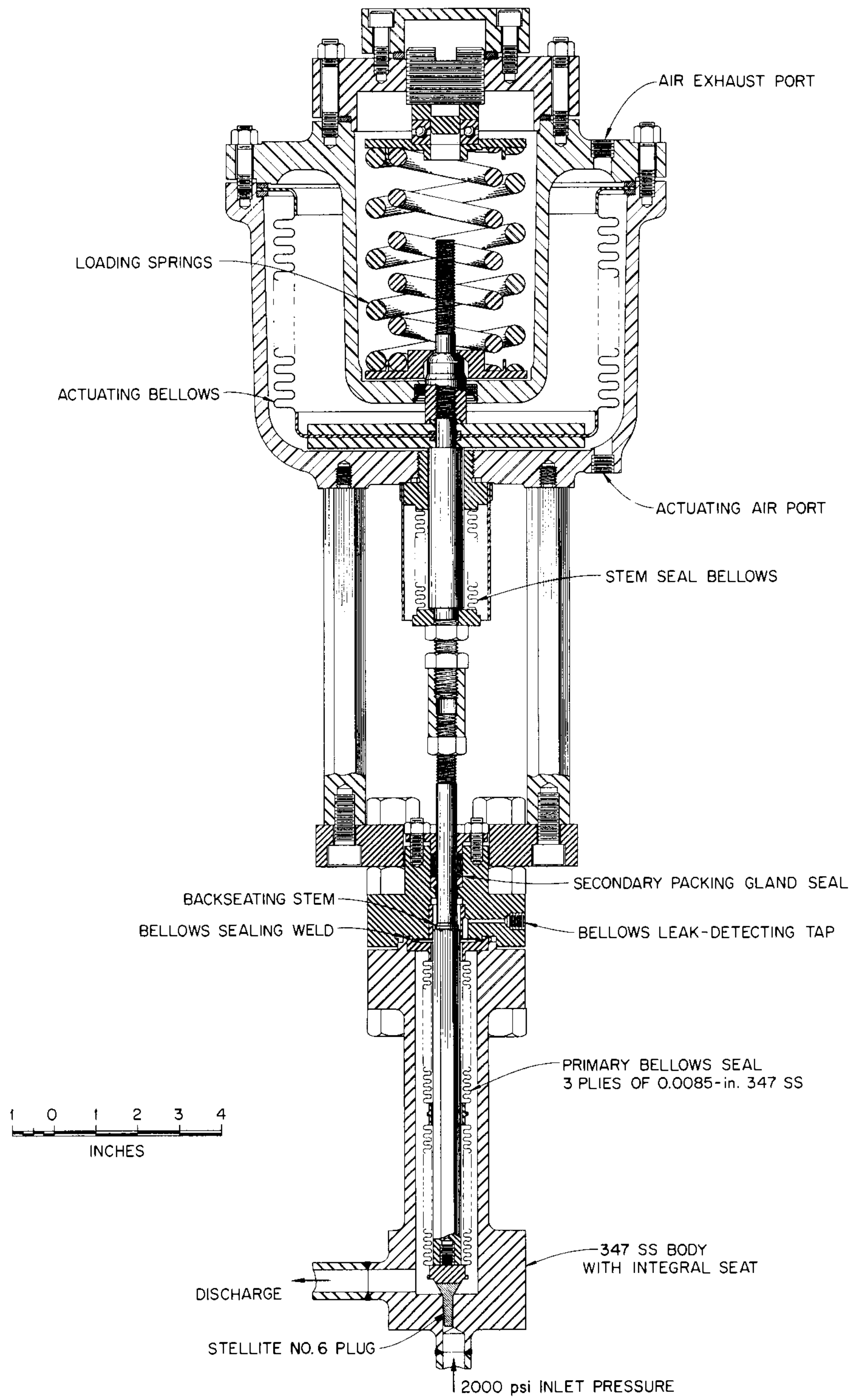

(a)

Fig. 70. HRT Letdown Valve Assembly.

UNCLASSIFIED
PHOTO 25837

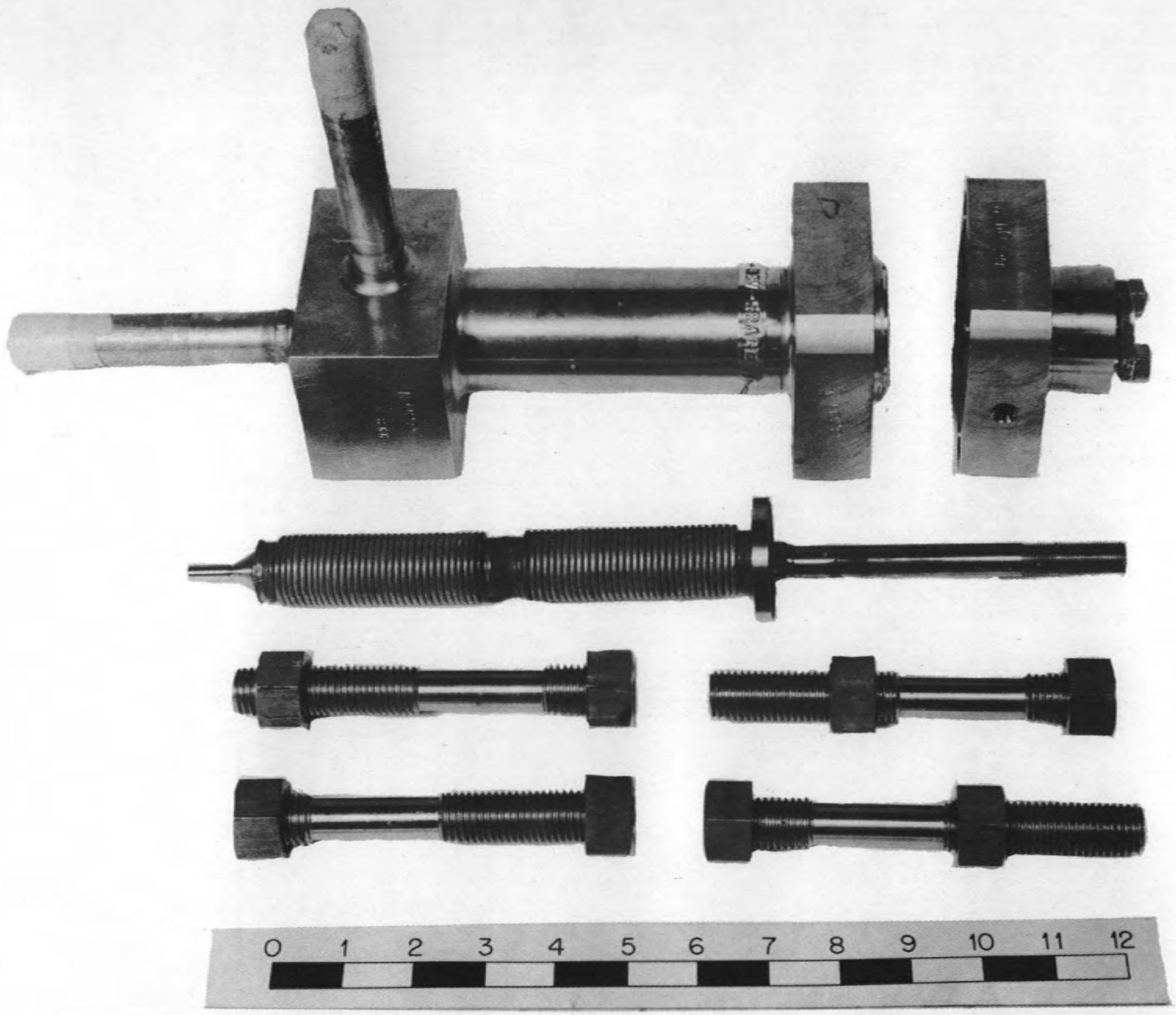

Fig. 71. HRT Letdown Valve Parts.

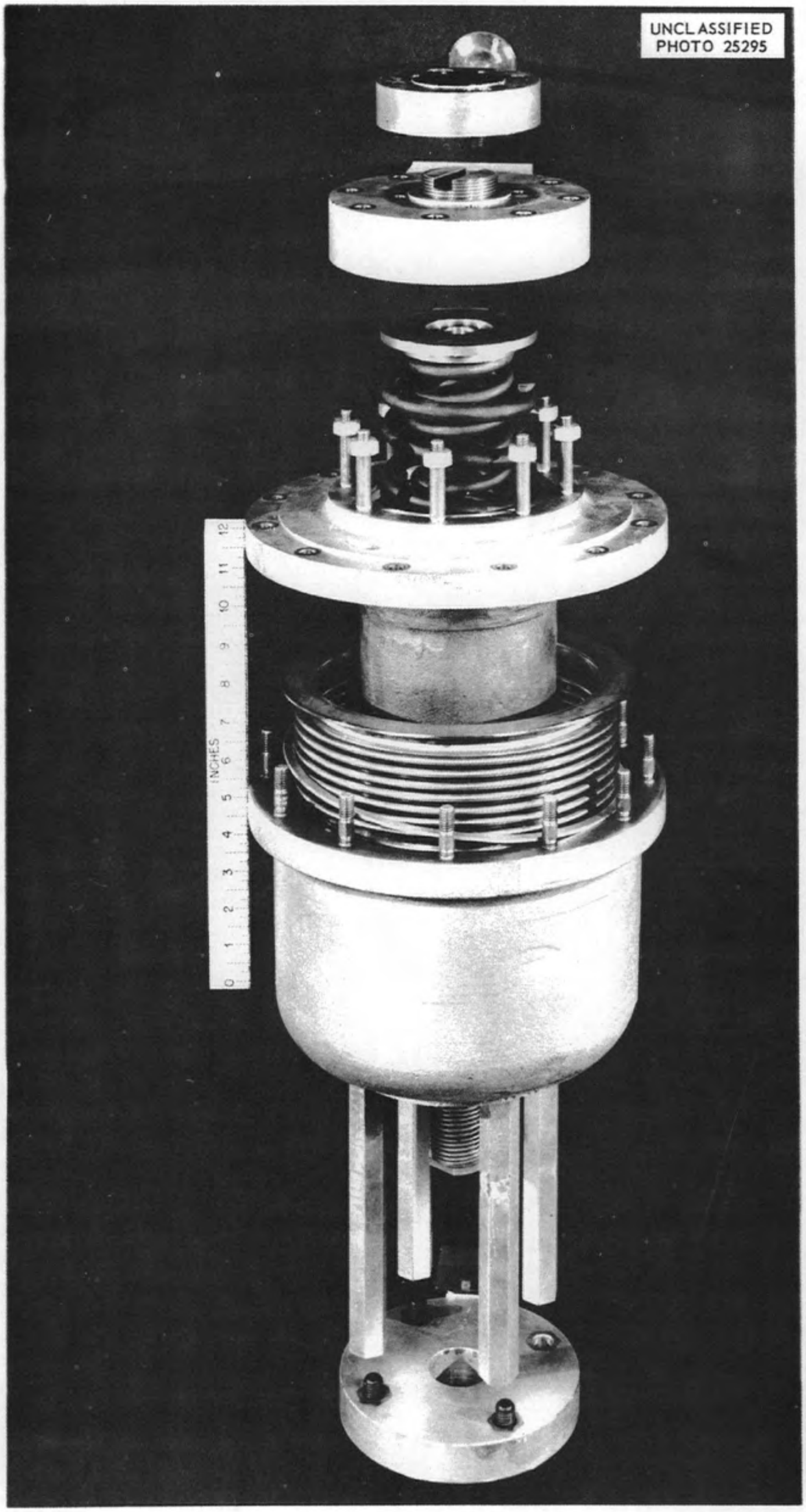

Fig. 72. HRT Letdown Valve Actuator.

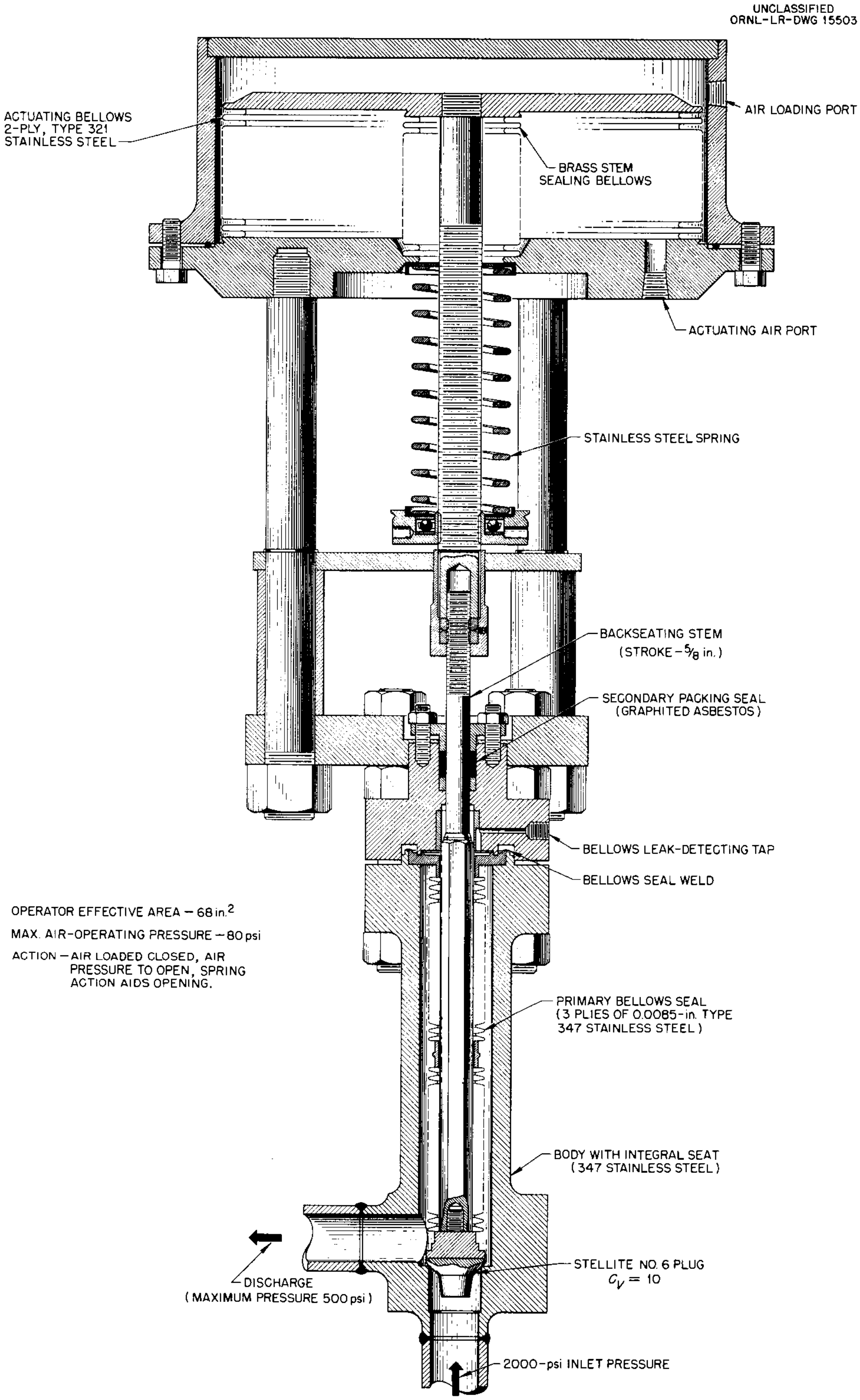

Fig. 73. HRT Blanket Dump-Valve Assembly.

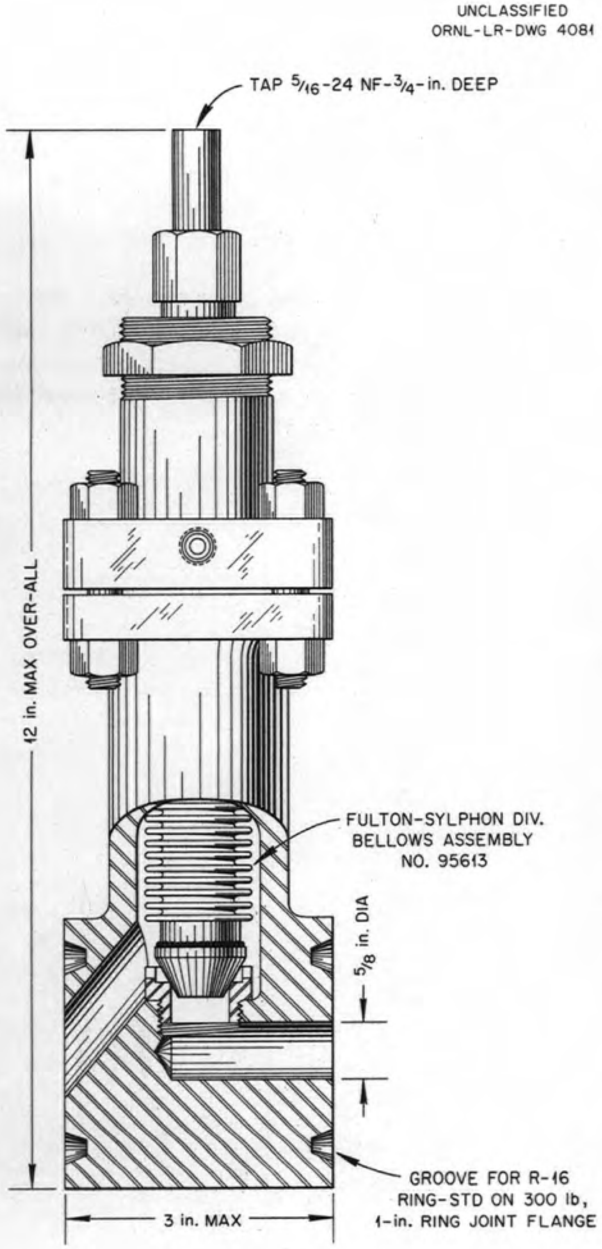

Fig. 74. HRT Low-Pressure Control Valve Assembly.

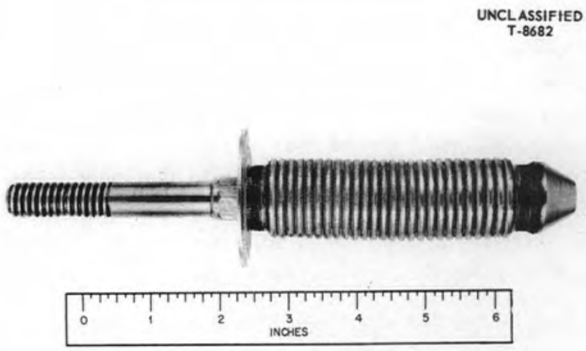

Fig. 75. HRT Low-Pressure Control Valve Bellows, Plug, and Stem Assembly.

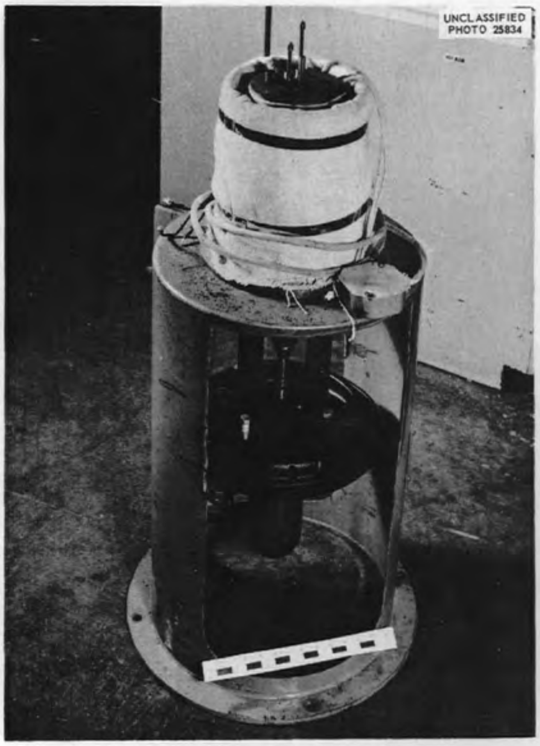

Fig. 76. Test Stand for Low-Pressure Control Valve Assembly.

oxygen-deficient uranyl sulfate solutions at elevated temperatures. Upon testing in uranyl sulfate at 2000 psi and 300°C, the bellows failed after 3500 cycles through a stroke of $\frac{1}{8}$ in. However, it had been overstressed in the shop before plating by stretching to spread the convolutions and permit the plating solution to penetrate to the inner folds. Another test is planned in which the bellows will be plated before the final mechanical forming operation which compresses the bellows.

Smaller and larger valve actuators than those installed in the HRT are being life-tested. The new actuators, also supplied by Fulton Sylphon Division, are pneumatically powered by a metallic bellows and are radiation resistant. The smallest unit, shown in Fig. 77, failed after 1300 cycles of a $\frac{3}{4}$-in. stroke with a pressure of 45 psi applied. No units have as yet been tested at the manufacturer's recommended operating conditions of 30 psi and $\frac{1}{2}$-in. stroke.

Intermediate-sized actuators are shown in Figs. 78 and 79.

The larger valve actuator, shown in Fig. 80, is capable of developing thrusts to 12,000 lb and has not failed in 90,000 test cycles consisting in a $\frac{1}{2}$-in. stroke and an applied pressure of 80 psi.

UNCLASSIFIED
ORNL-LR-DWG 17247

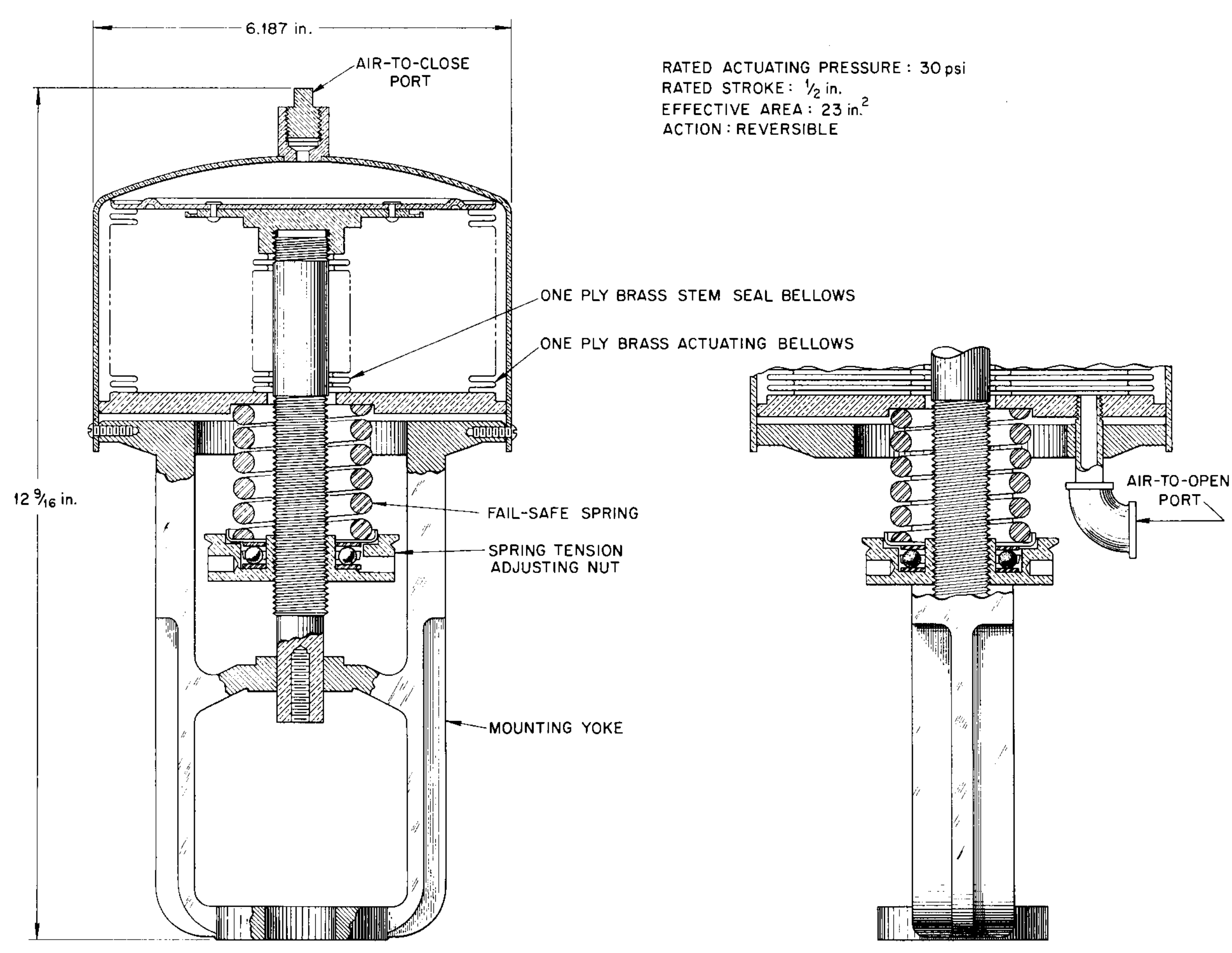

Fig. 77. Valve Actuator. Metallic bellows type, small area.

UNCLASSIFIED
ORNL-LR-DWG 17187R

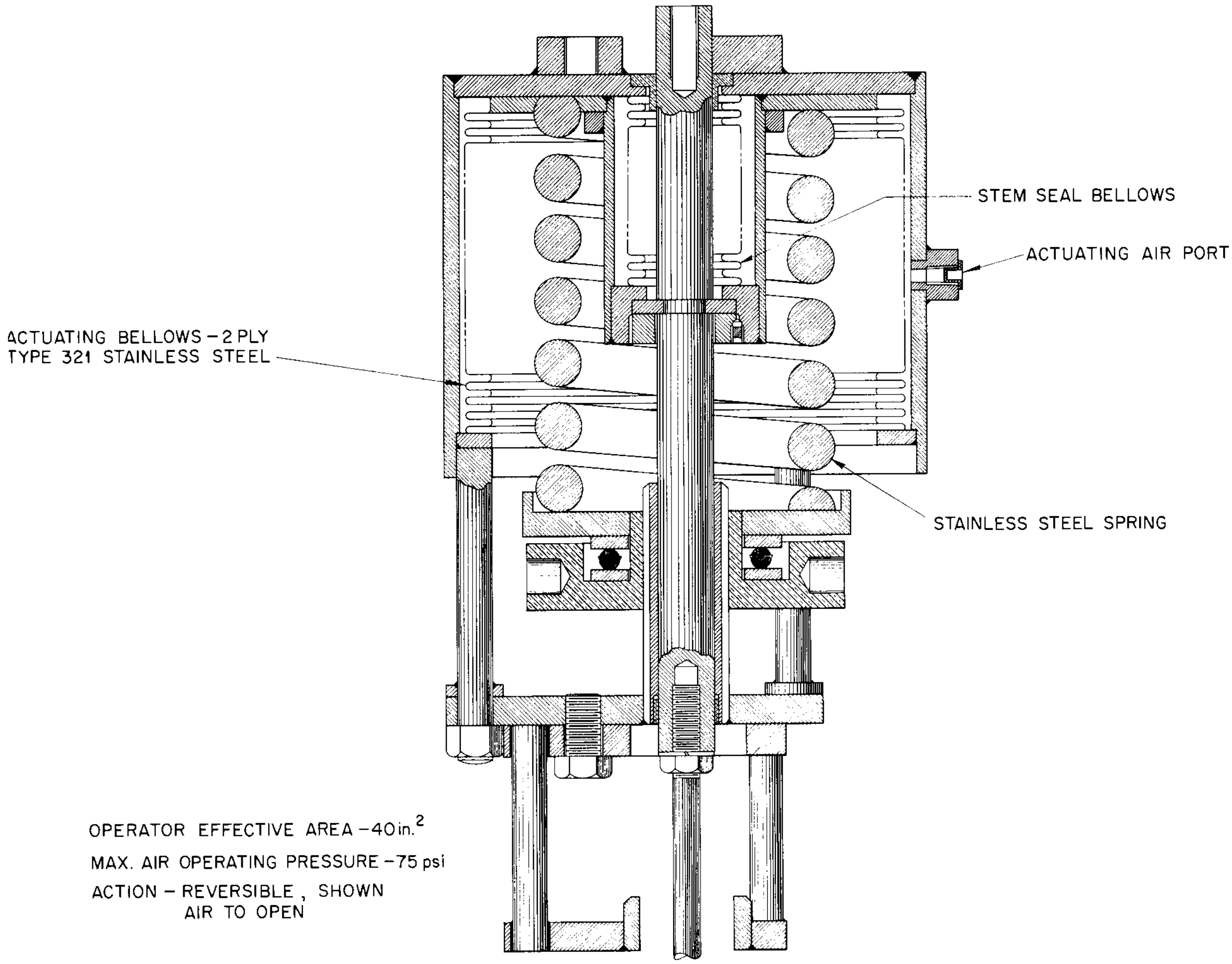

Fig. 78. Valve Actuator. Intermediate-sized area.

A valve-trim materials evaluation test program is being carried on in a valve test loop. About 8 gal of HRT uranyl sulfate is periodically flowed from a high-pressure tank at 1200 psi and 220°C through a valve containing the test trim to a receiver tank at atmospheric pressure. The materials to be tested are fabricated in the geometry shown in Fig. 81. The order of leak-tightness after this test is shown in Table 3.

UNCLASSIFIED
ORNL-LR-DWG 12044

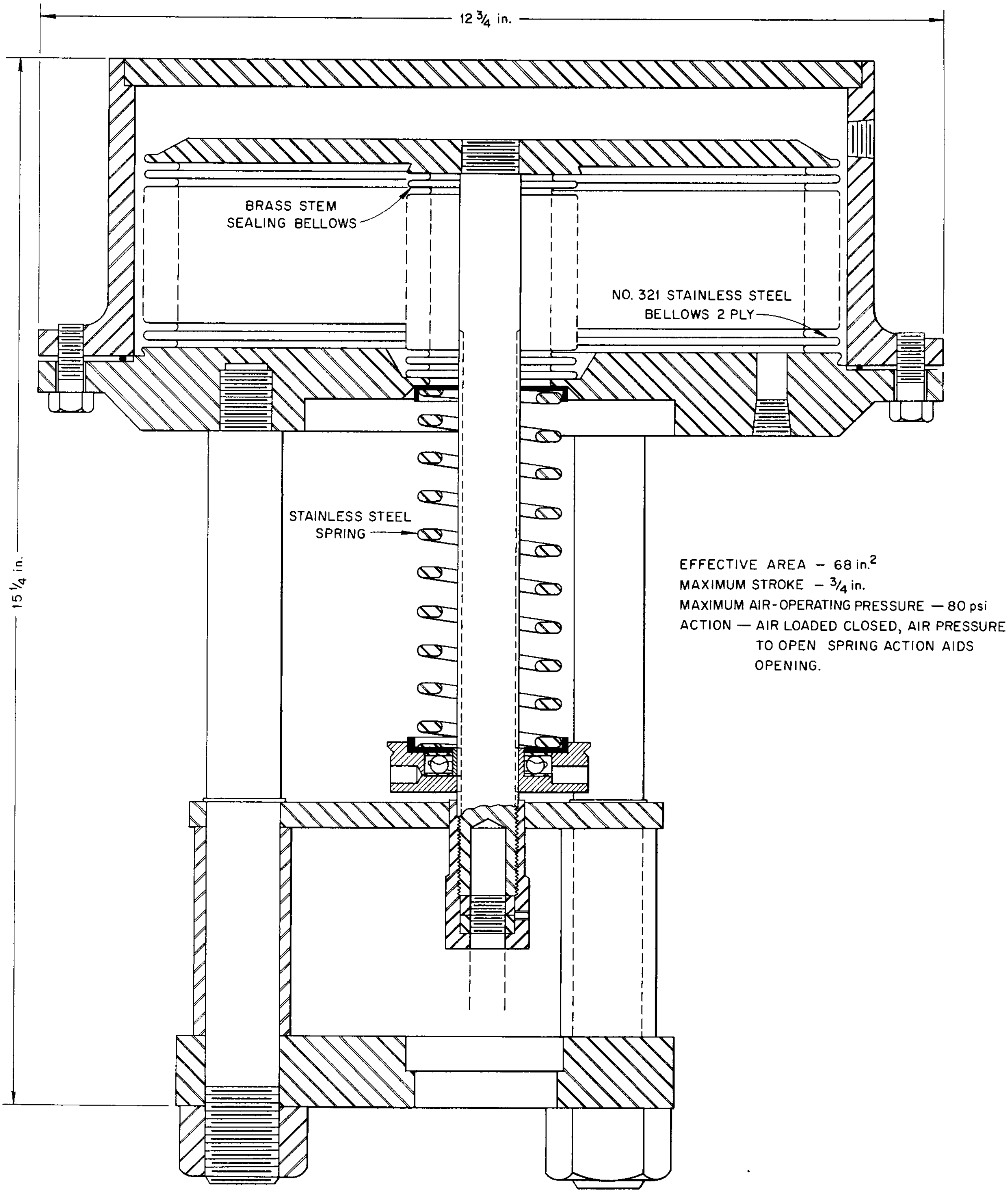

Fig. 79. Valve Actuator.

UNCLASSIFIED
ORNL-LR-DWG 23539

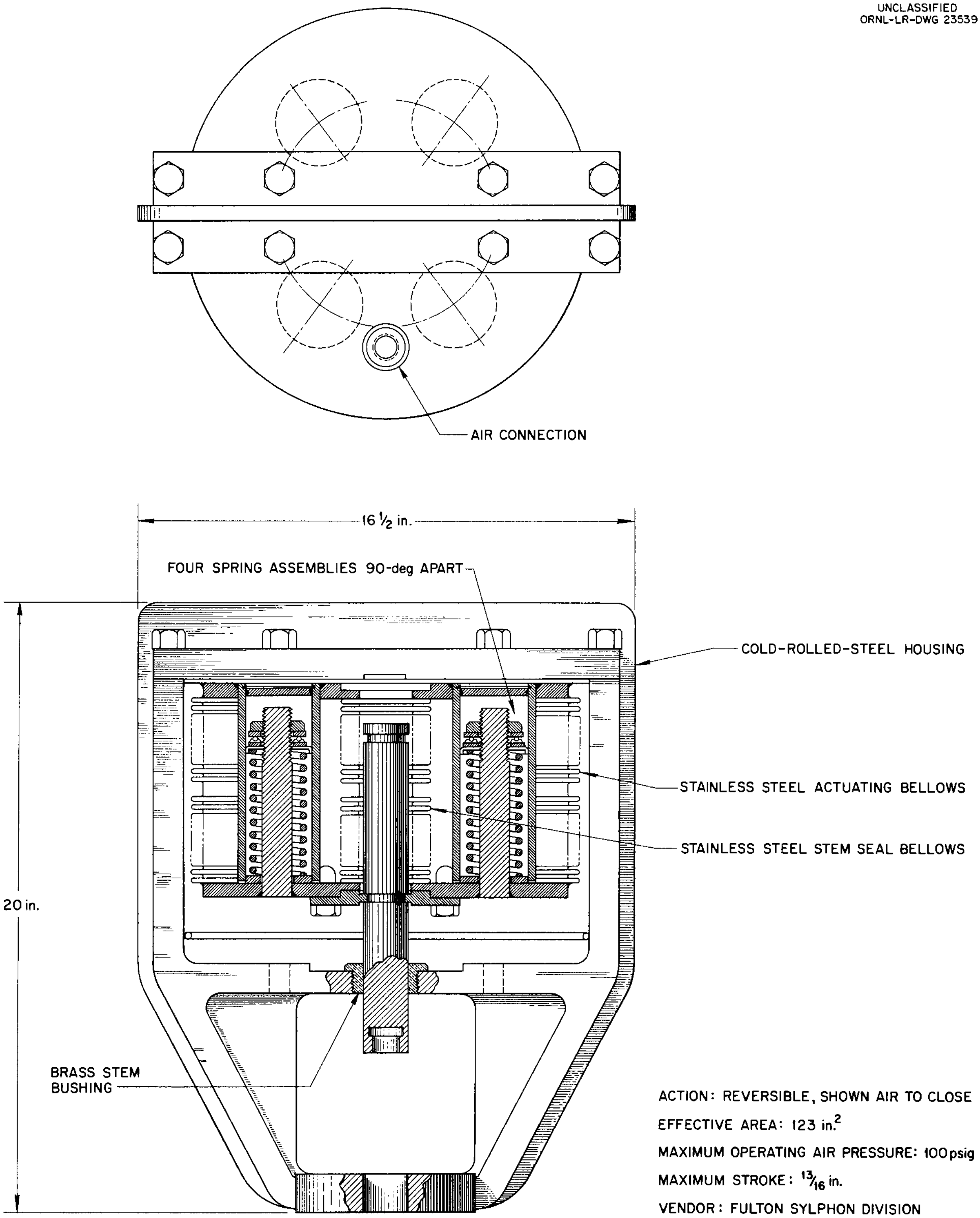

Fig. 80. Valve Actuator. Large effective area.

UNCLASSIFIED
T-9004

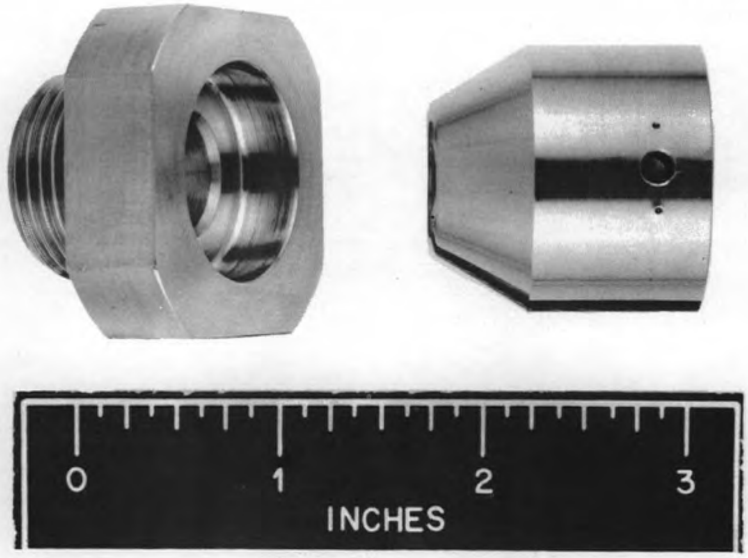

Fig. 81. Valve Trim Materials Evaluation Test Plug and Seat Set.

Table 3. Evaluation of Valve-Trim Materials

Material*	Remarks
Armco 17-4 PH	Hardened to 39 Rockwell C
347 SS capped with Baker alloy (80% Pt, 20% Ir)	Hardened to 25 Rockwell C; some difficulty keeping caps on
347 SS capped with Baker alloy No. E-130 (70% Pt, 20% Au, 10% Pd)	Hardened to 29 Rockwell C; some difficulty keeping caps on
347 SS capped with Baker alloy No. 872 (80% Pt, 10% Au, 10% Pd)	Hardened to 20 Rockwell C; some difficulty keeping caps on
347 SS flame-plated with tungsten carbide by Linde	
347 SS	
Stellite No. 6	
347 SS hard-faced with Stellite No. 6	Cleveland Hard Facing, Inc. torch applied
347 SS flame-plated with aluminum oxide by Linde	Chipped
Kennametal K501 (cemented tungsten carbide composition employing a platinum binder)	Shattered
Kennametal K96 (similar to above except cobalt binder)	Shattered
MST 6Al-4V titanium	Failed by ignition
Rem-Cru Ti-130AM	Failed by ignition

*In order of leak-tightness.

CALIBRATION AND TESTING OF MAGNETIC FLOWMETERS

G. H. Burger C. L. Pearce, Jr.

The magnetic flowmeter program was undertaken to provide high-accuracy flow measurements of NaK under the high temperature conditions required for a reactor development project. Twenty-four complete magnetic flowmeter assemblies were purchased from General Electric Company in 2- and $3\frac{1}{2}$-in. pipe sizes. These units were designed and built for ORNL by General Electric Company to ORNL specifications. The units are shown in Figs. 82 and 83. An exploded view of the 2-in. unit is shown in Fig. 84.

The specifications for the $3\frac{1}{2}$-in. units required an accuracy within 3.5% for 3000 hr over a flow range of 45 to 1400 gpm at NaK temperatures from 750 to 1600°F. The 2-in. units were required to have an accuracy within 1% for 3000 hr over a flow range of 45 to 200 gpm, and within 5% over a flow range from 200 to 800 gpm at NaK temperatures of 750 to 1600°F. The specified ambient magnet-temperature range for both units was from 100 to 560°F. The signal output was specified to be not less than 35 gpm/mv for the $3\frac{1}{2}$-in. units and 15 gpm/mv for the 2-in. units. The specified medium was NaK, 56% Na and 44% K by weight.

The operation of the magnetic flowmeter is based on Faraday's principle that a conductor moving through a magnetic field will induce a voltage perpendicular to both the magnetic field and the direction of motion of the conductor. In the magnetic flowmeter, a permanent magnet is used to

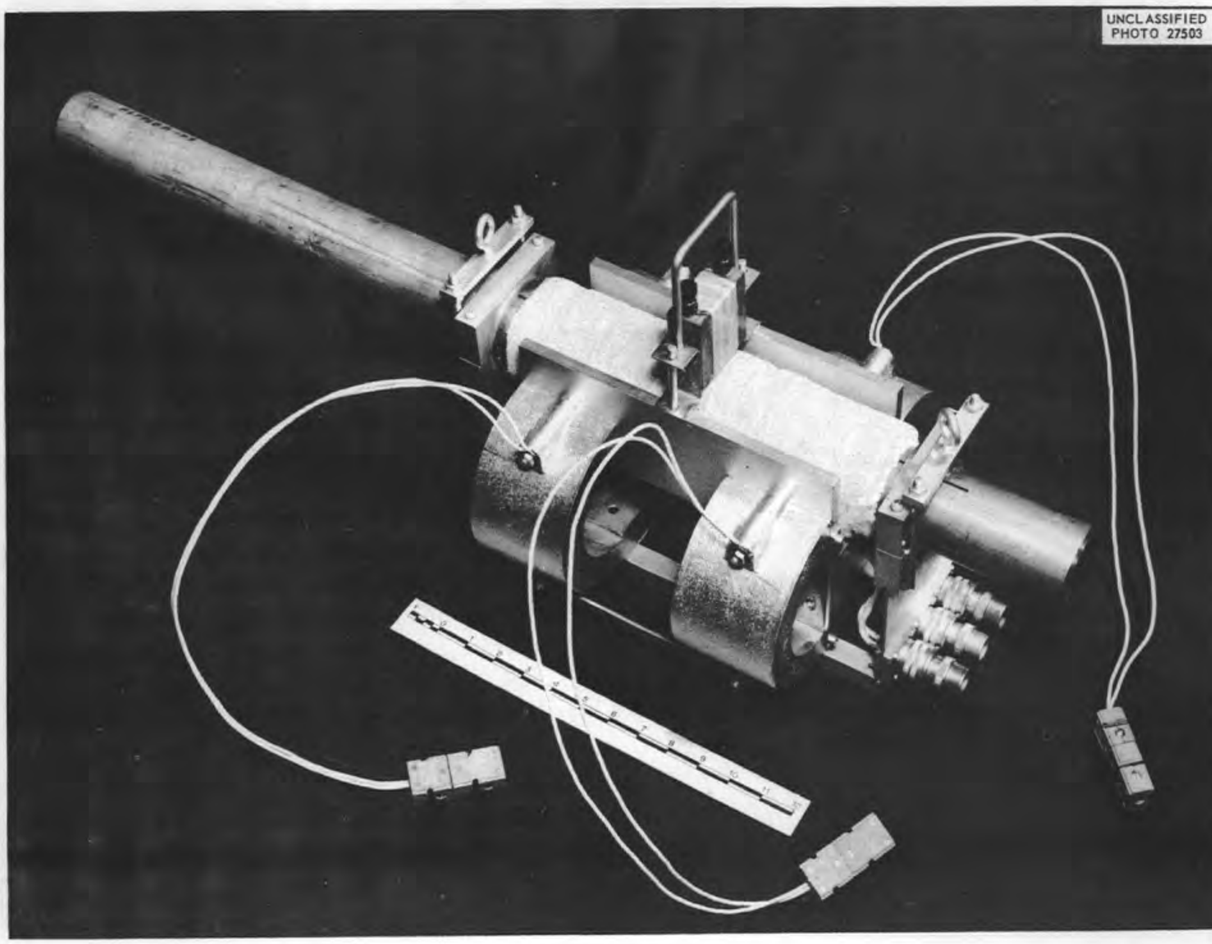

Fig. 82. The 2-in. Magnetic Flowmeter with Flux Coils.

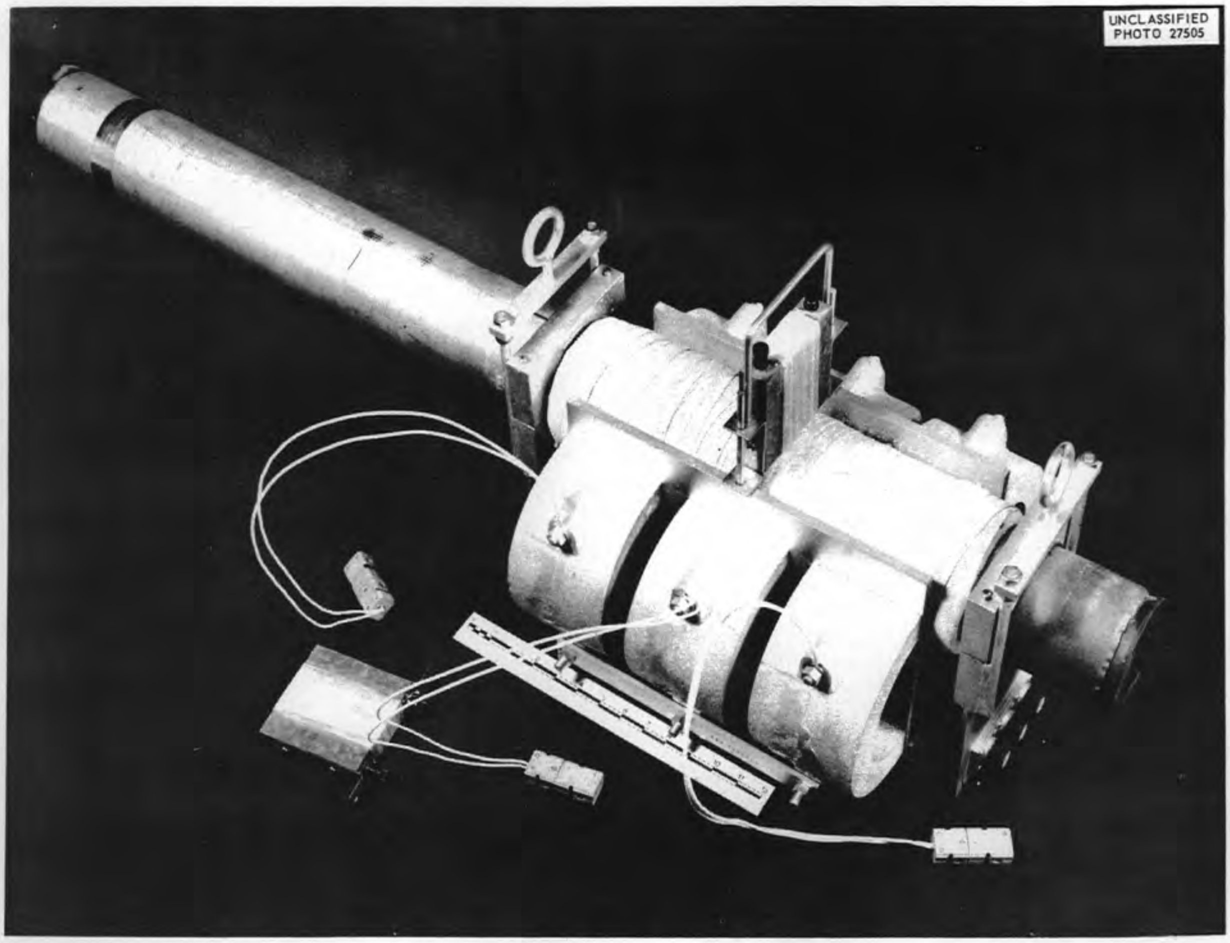

Fig. 83. The $3\frac{1}{2}$-in. Magnetic Flowmeter with Flux Coils.

produce an accurately known uniform flux across the pipe. Voltage pickup leads are welded at diametrically opposite points on the pipe, on the diameter that is at right angles to the field. The flow of the conducting fluid through the pipe will produce a voltage between the pickup leads which is proportional to the rate of flow.

The flowmeter equation used to predict output takes into consideration the variables in the application of the fluid as a moving conductor. The output voltage, E, in mv, depends upon the flow rate, Q, in gpm, the air-gap flux density, B_a, in gauss, and a fluid temperature factor, Y, in gpm·gauss/mv. The relation between these variables is theoretically

$$E = \frac{B_a}{Y} Q \ .$$

Then B_a/Y is the sensitivity of the magnetic flowmeter in mv/gpm.

The Y factor in the equation takes into account fluid temperature and pole-face length effects upon flowmeter sensitivity and is found in practice to amount to approximately 5% for a change of fluid temperature from 750 to 1600°F. These effects are due to changes in resistivity of the NaK and the Inconel pipe and the changes in dimensions of the pipe wall due to fluid temperature changes. Expanded, this factor is theoretically

$$Y = \frac{1581[1 + \alpha(T_f - 77)]}{Dk} \left[D^2 + d^2 + \frac{\rho_f}{\rho_w} (D^2 - d^2) \right] ,$$

where

α = thermal coefficient of expansion for Inconel at T_f in in./in./°F,

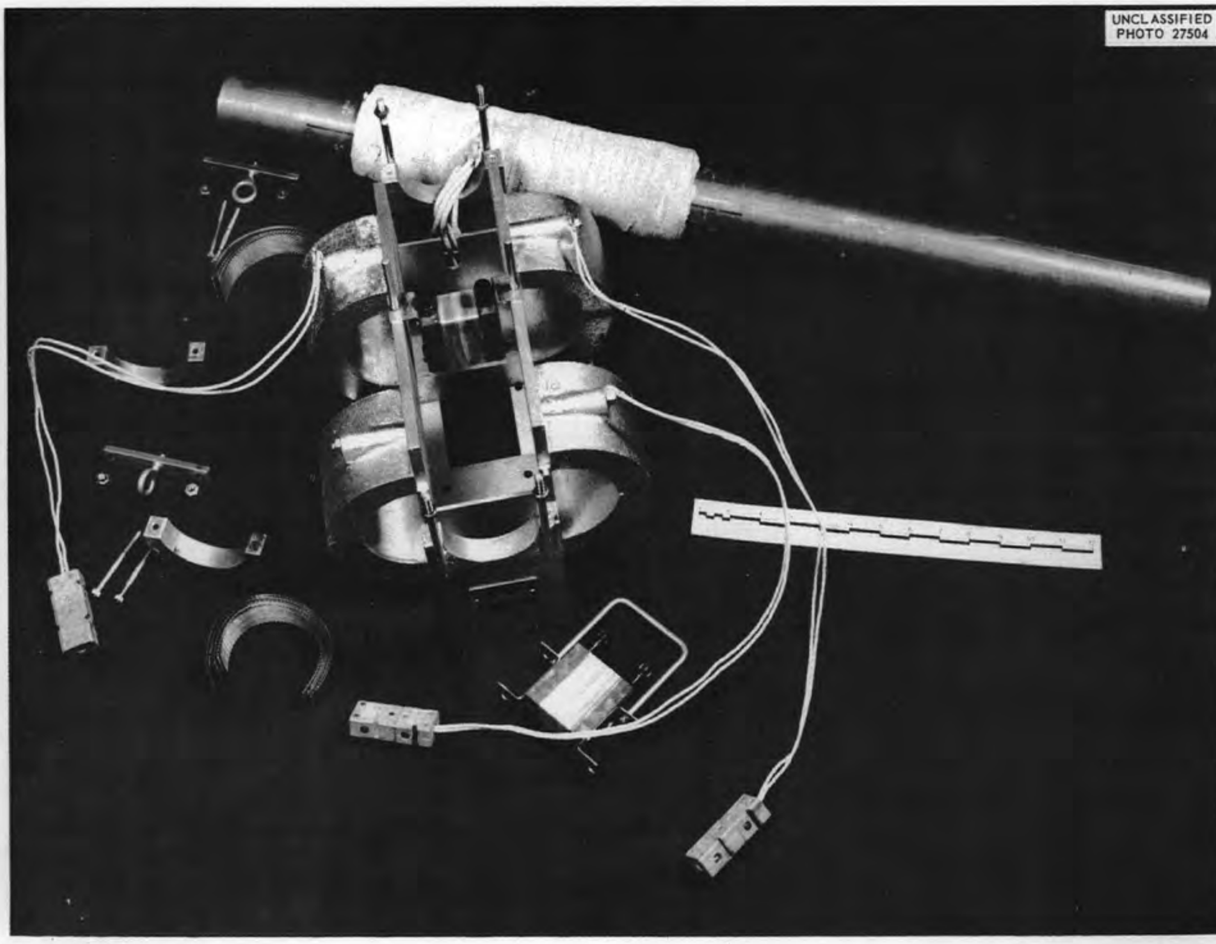

Fig. 84. The 2-in. Magnetic Flowmeter with Flux Coils, Exploded View.

ρ_f = resistivity of NaK at T_f,

ρ_w = resistivity of Inconel at T_f,

T_f = fluid temperature in °F,

k = an experimentally determined pole-length factor which is 0.98 for the $3\frac{1}{2}$- and 2-in. units,

D = outside diameter of pipe in inches,

d = inside diameter of pipe in inches,

1581 = a unit factor.

In applying the flow-output equation, direct measurement of B_a and Y may be replaced by the simpler measurements of magnet temperature T_m and fluid temperature T_f, if B_a can be related to T_m and Y can be related to T_f. The flowmeter is supplied with three thermocouples to measure magnet temperature continuously during operation. A means of measuring flux directly is provided by search coils which may be positioned on two posts mounted on the pole face in the vicinity of the signal pickup leads. The pipe may be removed to permit a search coil to be positioned to measure air gap flux density. In Fig. 83 the air-gap search coil may be seen to the left of the flowmeter, and it is shown in place in the exploded view in Fig. 84. Since in operation it is impractical to remove the pipe, a leakage-flux coil is provided to measure the leakage-flux density in the vicinity of the signal pickup leads. The leakage-flux density may be multiplied by a constant air-gap-to-leakage-flux factor to give air-gap flux density B_a. Leakage-flux coils may be seen in place on the coil posts in Figs. 82 and 83. By use of these coils it is possible to monitor the magnets for possible changes in air-gap flux density B_a due to factors such as handling. Leakage-flux coils may be used to determine B_a at various magnet temperatures T_m in order to plot B_a versus T_m for determining sensitivity in actual operation.

The Y factor may be theoretically related to the fluid temperature T_f by inserting individual flowmeter dimensions into the equation and plotting a Y-factor-vs-T_f curve. The Y factor may be experimentally determined by actual calibration. The fluid temperature may be easily measured continuously by insertion of a sheath-type thermocouple into a well in the pipe.

The sensitivity of the flowmeters may be continuously monitored during operation by measuring magnet temperature, T_m, and fluid temperature, T_f. This temperature-dependent sensitivity may be applied to flowmeter output voltage E to indicate the flow, Q, in gpm.

The magnetic flowmeters are under test and calibration in the NaK-pump test loops. The objectives of these tests are: (1) to calibrate the magnetic flowmeters against a water-calibrated venturi flow standard of 0.25% accuracy, (2) to test the theoretical calculations as to flow output and accuracy, (3) to investigate the effects of temperature and handling, (4) to determine long-term reliability, and (5) to provide general operating data for use in the operational system.

A pump test loop in which Lot No. 1 of six 3½-in. flowmeters was installed was put into operation on February 12, 1957. Another pump test loop in which Lot No. 1 of six 2-in. flowmeters was installed was put into operation May 23, 1957. The two loops were identical in general construction and operation. The 2-in. loop was a scaled-down version of the 3½-in. loop. A photograph of the interior of the 2-in. loop is shown in Fig. 85. Each flowmeter was suspended by a counterbalance system to allow for thermal expansion of the pipe.

The instrumentation of this loop is shown in Fig. 86. In the Nos. 1 and 2 racks from the left are six 0.25%-accuracy Brown Electronik single-point 0–100 mv strip-chart recorders (0–60 mv for 2-in. loop), one for each flowmeter. Since each flowmeter has 3 flow-signal pickup elements, a Lewis switch is provided to select each of the 3 flow output signals. The No. 3 output on each flowmeter may also be selected by a Lewis switch on the Brown Electronik dual-pen strip-chart recorder in the center of the No. 3 rack. The second pen on this recorder measures all the magnet temperatures and the inlet, center, and outlet fluid temperature, as selected by a Lewis switch. These temperatures are also continuously monitored on a sixteen-point Brown Electronik recorder at the bottom of rack No. 3. At the top of rack No. 3 is a Foxboro square-root differential pressure recorder which continuously records the loop flow as measured by the 0.25% venturi standard. The bottom instrument panel on rack No. 4 and the dolly to the right contain the Weston integrating fluxmeter and its flux standard which is tied into the system so that periodic flux readings of magnets in the loop may be displayed on the dual-pen recorder in the center of rack No. 3. The two top instruments in rack No. 4 are not used in this test.

The six 3½-in. magnetic flowmeters in Lot No. 1 were operated for 770 hr, and the six 2-in. magnetic flowmeters in Lot No. 1 were operated for 1038 hr. At the end of the runs on Lot No. 1, four flowmeters were removed from each loop and replaced by four uncalibrated flowmeters to form Lot No. 2. Two flowmeters from Lot No. 1 remained in the loop for continuing tests and to provide reference to data from Lot No. 1. To date (9/3/57), Lot No. 2 of 3½-in. units has operated 1408 hr and Lot No. 2 of 2-in. units, 431 hr. The two reference 3½-in. units have operated 2178 hr and the two reference 2-in. units, 1469 hr. The units were operated under widely varying conditions of ambient temperature, fluid temperature, magnet temperature, flow rate, and NaK oxide contents. These variables were continuously monitored by the instrumentation just described and were recorded on data sheets at 2-hr intervals throughout the run. Additional data were recorded during controlled runs in order to observe the effect of each of the variables on flow output as measured by the units. In addition to these measurements, the air-gap flux density of the magnets was determined at frequent intervals by measuring leakage-flux density in order to determine the effects of temperature, aging, vibration, and flow on the magnetic circuit, and to observe the effect of flux change on the flow output. Flux-density measurements were made during operation at magnet temperatures over the range of 77 to 600°F. These measurements are used to

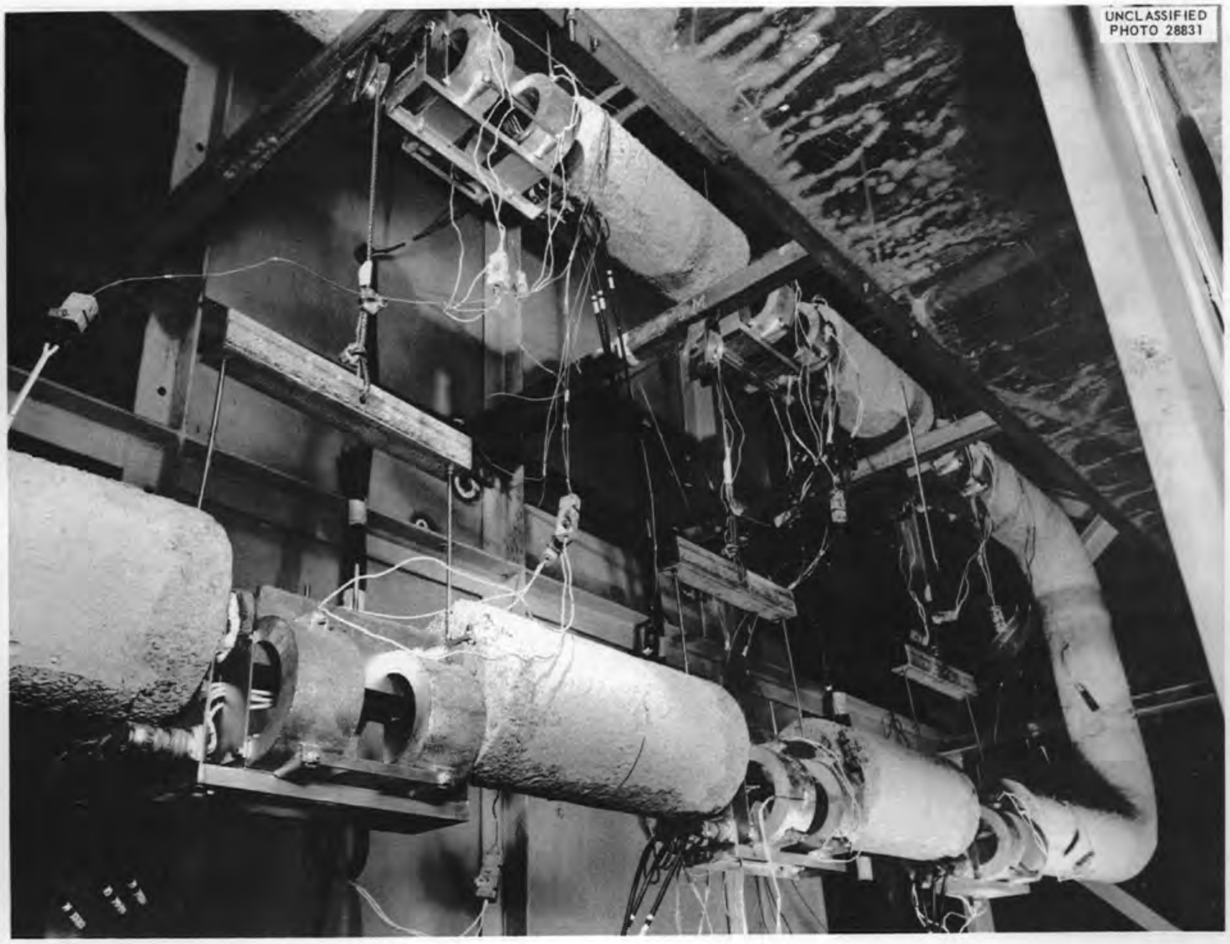

Fig. 85. Interior View of 2-in. Test Loop.

relate the air-gap flux density to the magnet temperature so that flux measurements will be unnecessary in actual operation.

Three types of runs were made on the flowmeters:

1. Constant-Temperature Runs. – The fluid temperature was held constant and the flow was varied in 100-gpm steps from 600 to 1600 gpm. Constant-temperature runs were made, in 100°F steps, from 400 to 1500°F.

2. Constant-Flow Runs. – The flow was held constant and the fluid temperature was varied from 400 to 1500°F in 100°F steps. Constant-flow runs were made in 100-gpm steps from 600 to 1600 gpm.

3. Magnet-Temperature Runs. – Each flowmeter was enclosed with the pipe by wrapping with insulating blankets and was allowed to heat toward the pipe temperature. When the magnet temperature reached 600°F, the blankets were removed and the air-gap flux densities of the magnets were measured while cooling to the ambient temperature of the loop enclosure.

A survey of the data which has been processed indicates that the units may be expected to give satisfactory service if calibrated.

Each flowmeter incorporates three separate flow elements to provide for spares and auxiliary outputs. No difference in the outputs from the three elements could be read in comparing the outputs on the 0.25% accuracy Brown recorders. It was also found that three separate recorders may be connected to the three flow elements without interaction. In practice, satisfactory operation is obtained by connecting two recorders to the same flow element. The speed of response of the magnetic flowmeter system is limited by the speed

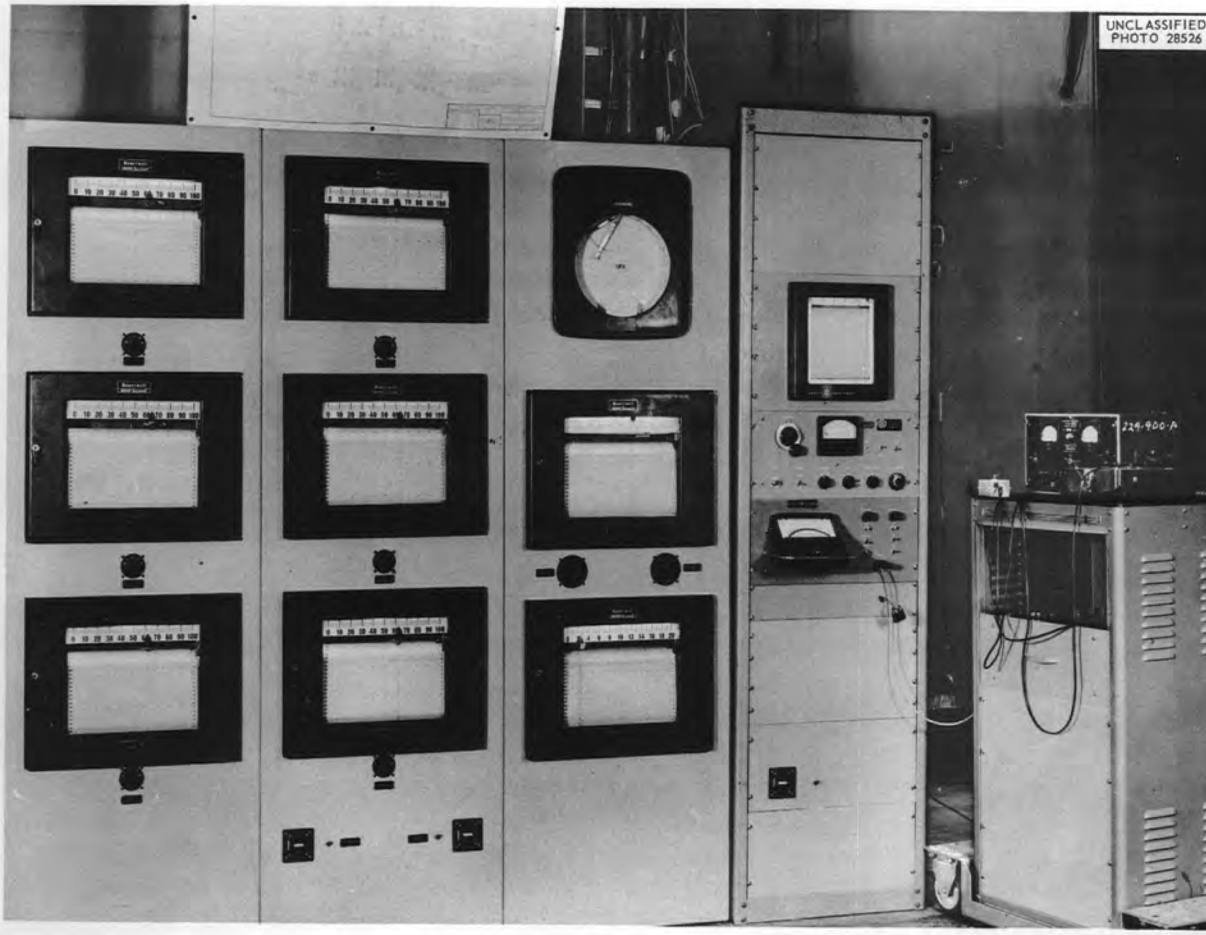

Fig. 86. Instrument Panel for Magnetic Flowmeter Calibration.

of response of the Brown recorder used. The flowmeter appears to follow minute variations of flow faithfully and responds well to abrupt changes in flow. As had been anticipated, noise pickup proved to be no problem, since the impedance of the flow element (Inconel flow pipe filled with NaK) is very low.

The linearity of the $3\frac{1}{2}$-in. units was better than 1% over the flow range of the test. For those units, an experimental sensitivity may be derived which fits all the data on Lot No. 1 to better than 1%. The short-term accuracy of the units after calibration with sufficiently close flux-monitoring appears better than 2%. The reproducibility of the measurements was better than 1% over the range of the test.

The aging and handling effect on the flux density of the magnets over a seven-month period is from 0.6% to 3.6%. The drop appears to be due mainly to handling of the units. No permanent drop in air-gap flux density was observed during operation of the units. Further monitoring as well as completion of the reduction of present data should give additional information about flux stability.

The experimentally derived sensitivity at 1500°F is as much as 8.5% higher than the theoretical sensitivity given by the flow equations. The experimentally derived sensitivity decreases linearly with fluid temperature, with approximately the same slope for all the 3½-in. units. The sensitivity of the units drops 6% with a fluid-temperature change from 400 to 1600°F, or with a magnet temperature change from 100 to 500°F. The change in flowmeter output with fluid temperature for one of the units is shown in Fig. 87.

The characteristics of the 2-in. units are very similar to those of the 3½-in. units. Note that the magnetic flowmeter, though simple in basic theory and operation, is quite complex when the unit is required to maintain high accuracies over long periods of time. The units require continuous monitoring, at the present time, in order to ascertain that they are measuring the flow at the required accuracies as indicated by the output signal. The objective of the tests now in progress is not only to calibrate the units but to provide information on their behavior and characteristics so that future units may be used with reasonable accuracy without the necessity of individual unit calibration.

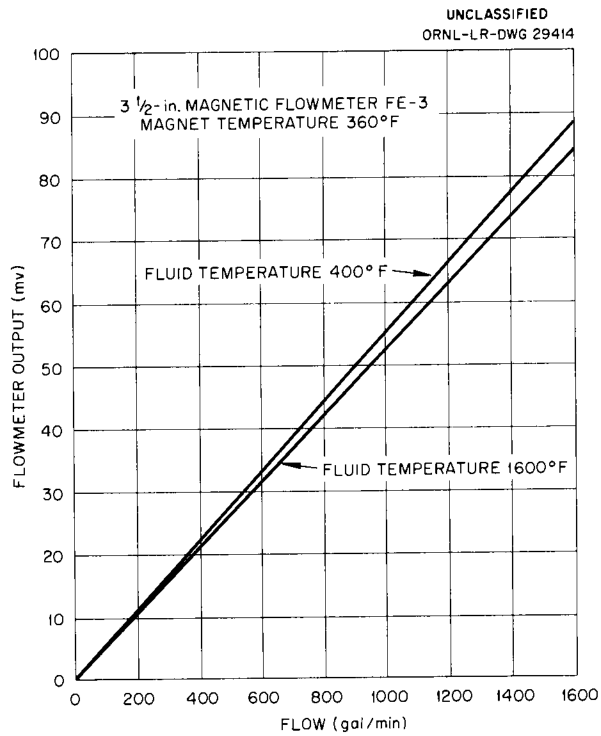

Fig. 87. Flowmeter Output vs Flow.

PRESSURE TRANSMITTERS

W. R. Miller

Requirements for high-temperature pressure transmitters with unique corrosion resistance qualities have been responsible for an industry-wide survey and the initiation of a test-and-evaluation program. In the past, pressure transmitters were not available which would operate in the temperature range from ambient to 1400°F and measure corrosive fluids from 0 to 200 psig with accuracies of 1% or less.

Of 36 manufacturers contacted, 12 submitted design proposals worthy of consideration, and seven were authorized to supply prototype models. While the prototype models were being manufactured, a test facility (Fig. 88) was constructed to evaluate the units in operating environments.

Prototype transmitters employed single and multiple diaphragms as well as formed and prefabricated bellows as sensors. To maintain corrosion resistance, a sensor thickness of no less than 0.025 in. could be tolerated. At the above temperatures and pressures transmitter-housing thicknesses assumed 1-in. proportions. For these reasons, special weld-joint designs and special welding techniques had to be devised.

Because process fluids within the transmitter had to be kept at an elevated temperature, the addition of Calrod heaters to the transmitter housing was necessary. Thus, transmitters employing differential transformers and induction coils as sensor-position detectors were subject

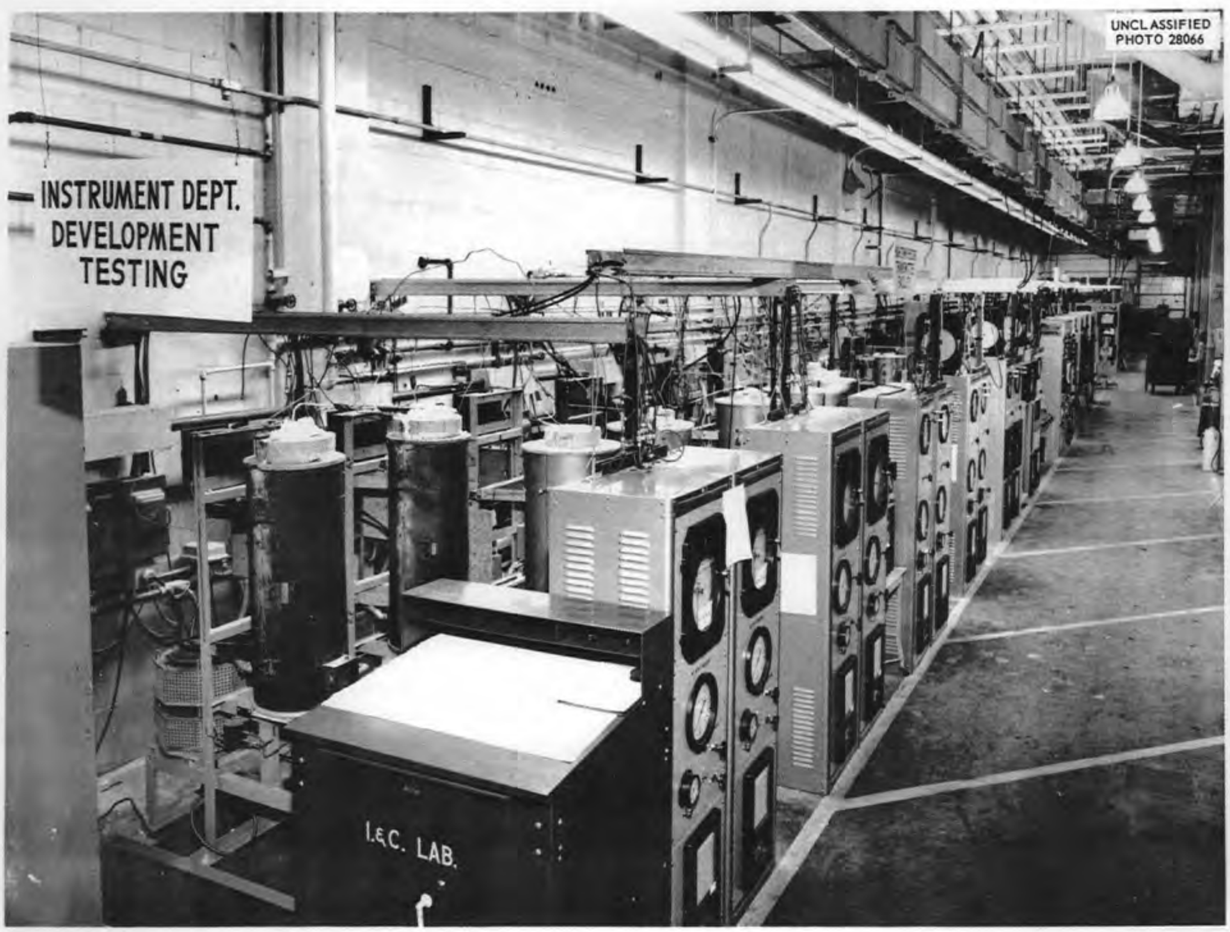

Fig. 88. Test Facility for Pressure Transmitters.

to a-c pickup from the heaters. Those units which employed the tube-system principle to transmit sensor motion out of the hot zone were most successful since they were unaffected by the heaters.

Once the sensor motion is available outside the hot zone, the method of transmission employed depends solely on its state of development and not on the temperature or pressure of the application. Our experience indicated that the d-c excited strain gage produced the best accuracy.

Figure 89 is a graph of average characteristics of each type of transmitter tested. These curves illustrate the extreme variations produced by different approaches to the same problem. Table 4 is a compilation of test results on units of each model tested. Incomplete data (blanks) means that the units were discarded for inherent design defects early in the testing, or that delivery delays prevented test completions.

Figures 90 and 91 show the most successful unit employing pneumatic transmission, with its performance curves.

Figures 92 and 93 show the most successful unit employing electrical transmission, with its performance curves.

UNCLASSIFIED
ORNL-LR-DWG 29415

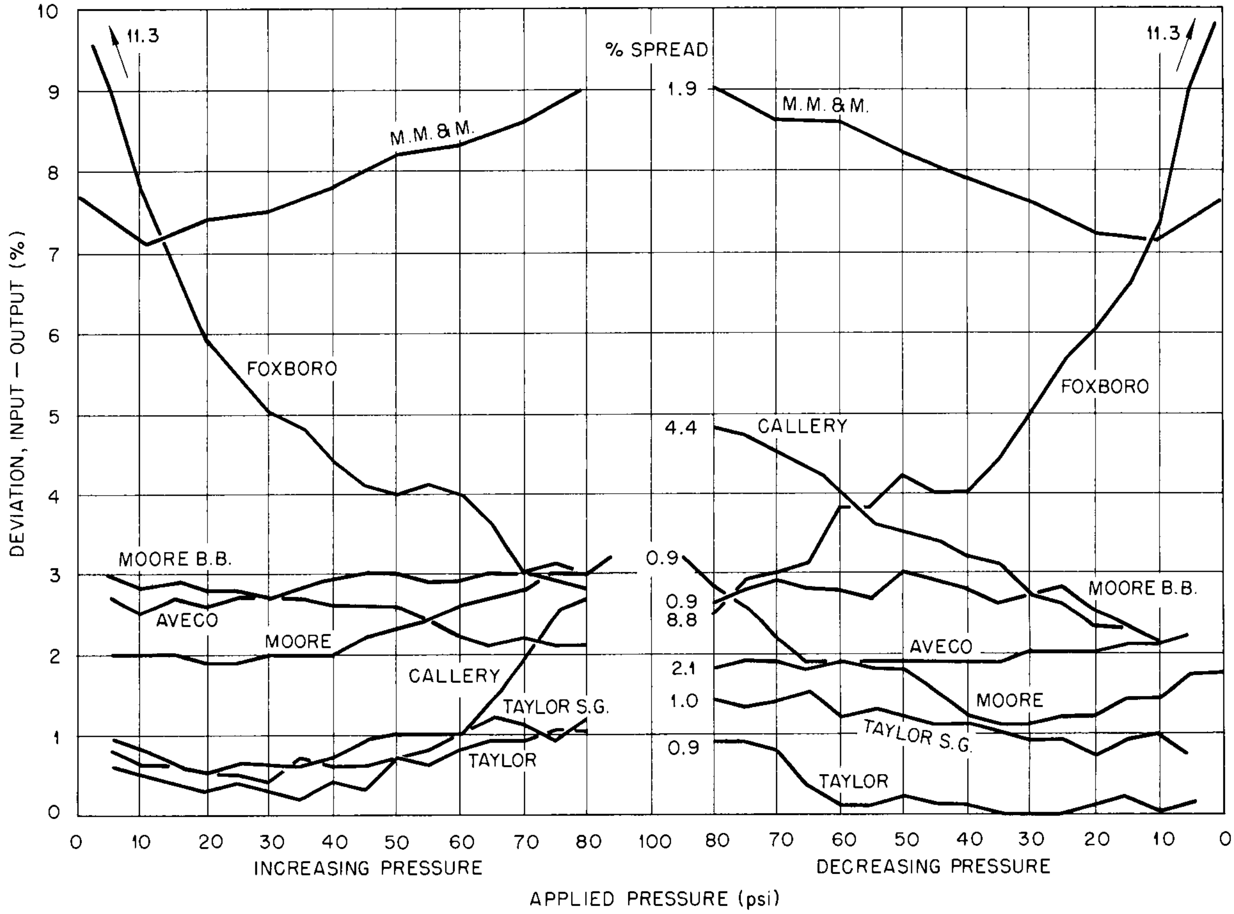

Fig. 89. Average Transmitter Characteristics.

Table 4. Tabulation of Data for All Units Tested

Unit No.	Temperature (°F)	Taylor Instrument Companies				Moore Products Co.		Associated Valve and Eng. Co.	Foxboro Co.	Manning, Maxwell & Moore, Inc.	Callery Chemical Co.	Crescent Eng. and Research Co.
		6 Units Special Pneumatic Transmitter	6 Units 226 RN Pneumatic	6 Units Strain Gage	6 Units 706 TN Strain Gage	6 Units Formed Bellows	6 Units Breeze Bellows	6 Units Pneumatic	6 Units Pneumatic	6 Units Electrical	6 Units Electrical	1 Unit Electrical
		Input-Output Deviation (% full scale)										
1	Ambient	0.7	2.0	0.4	0.3	1.3	0.4		2.4	1.4	2.7	Unsatisfactory
2		1.4	1.6	0.5	0.4	2.7	0.4			1.5	1.4	performance
3		0.3	2.4	0.3	0.4	0.7	1.4			1.6	1.6	
4		1.1	0.5	0.3	0.6	1.4	1.4			1.5	1.2	
5		1.5	0.5	0.2	0.2	1.9	0.7	0.3			1.8	
6		0.4	0.4	0.5	0.2	1.7	0.2				1.4	
		Av 0.9	1.2	0.36	0.42	1.61	0.75			1.50	1.68	
1	500	0.9	2.0	0.5	0.4	1.3	0.9		11.1	1.7	3.7	
2		1.5	1.4	0.6	0.6	2.7	0.7			1.1	1.1	
3		0.9	2.0	0.2	0.3	1.0	1.1			1.5	1.5	
4		1.2	0.8	0.8	0.7	1.3	1.7			1.9	1.4	
5		1.5	0.3	0.4	0.4	1.5	0.5	0.5			2.9	
6		0.8	0.35	0.7	0.2	2.1	0.7				1.1	
		Av 1.13	1.1	0.53	0.52	1.71	0.93			1.55	1.95	
1	1000	0.9	2.8	0.4	0.3	1.5	0.3		9.0	1.2	3.8	
2		2.0	1.0	0.3	0.6	2.4	0.4			0.9	1.4	
3		0.5	2.2	0.2	0.4	1.8	1.1			1.7	1.6	
4		1.2	0.8	0.5	0.6	1.5	1.7			1.9	2.2	
5		1.3	0.2	0.6	0.4	1.4	0.5	0.9			3.3	
6		0.3	0.45	0.5	0.1	2.3	0.2				1.4	
		Av 1.03	1.2	0.41	0.48	1.85	0.70			1.42	2.28	
1	1200	1.3	2.6	0.3	0.3	0.9	0.3		8.8	1.2	4.0	
2		1.8	1.2	0.4	0.6	2.5	0.9			1.6	1.3	
3		0.8	1.8	0.5	0.4	1.9	1.2			1.7	1.2	
4		1.2	0.9	0.5	0.7	1.7	1.6			2.1	2.8	
5		1.3	0.2	0.9	0.2	1.9	0.7	0.9			3.6	
6		0.9	0.45	0.5	0.2	2.1	0.2				1.7	
		Av 1.21	1.2	0.51	0.48	1.83	0.81			1.65	2.43	
1	1400	0.8	2.0	0.4	0.3	1.3	0.4			1.2	5.2	
2		1.9	1.8	0.5	0.6	2.8	0.5			1.1	2.1	
3		1.1	2.0	0.3	0.4	1.4	1.3			1.5	2.5	
4		2.0	0.9	0.5	0.7	1.8	1.6			1.7	3.6	
5		1.2	0.3	1.0	0.3	1.6	0.6	1.2			4.6	
6		0.8	0.4	0.6	0.1	2.0	0.7				2.5	
		Av 1.30	1.2	0.55	0.48	1.81	0.85			1.37	3.41	
	All Temperature Av	1.11	1.18	0.47	0.47	1.74	0.80	0.76	7.82	1.45	2.35	

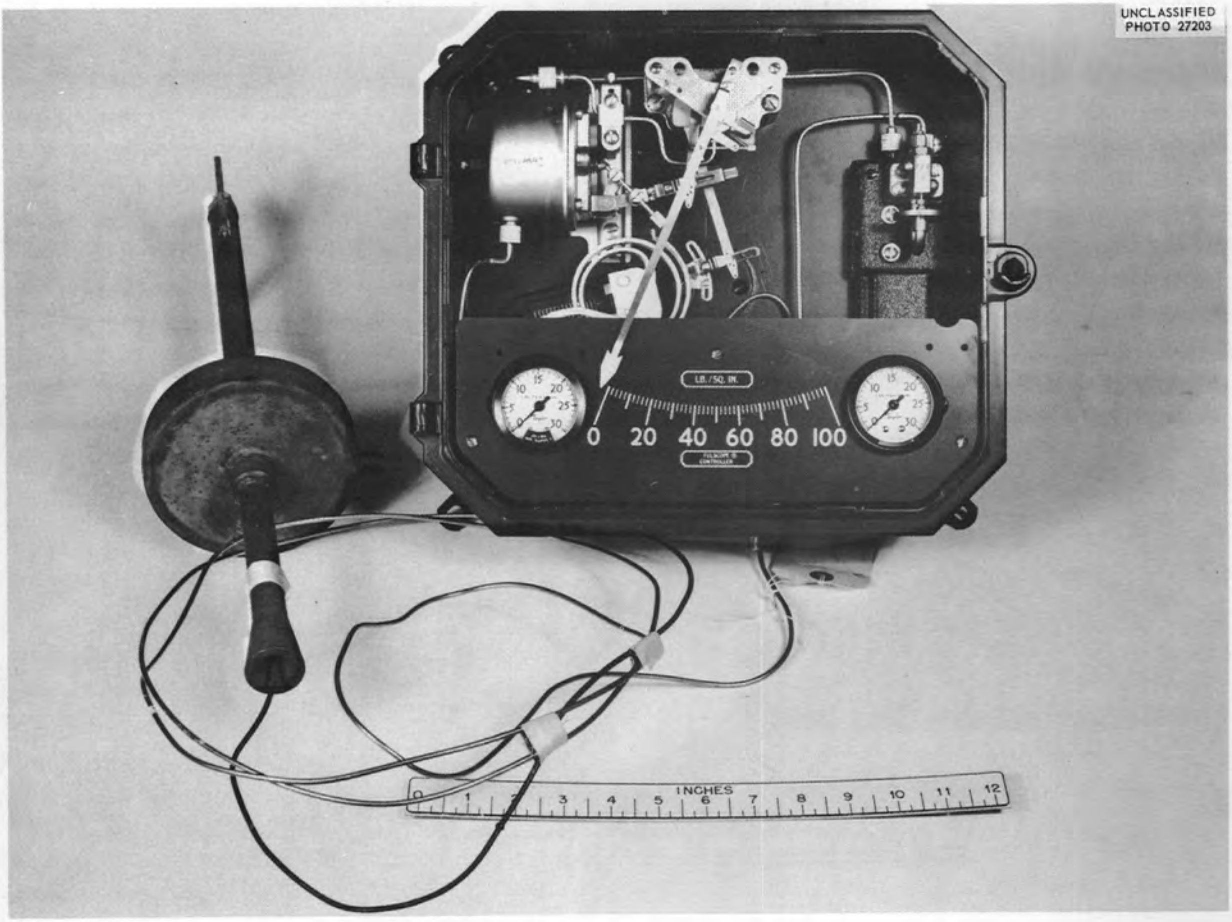

Fig. 90. Taylor 226R Transmitter.

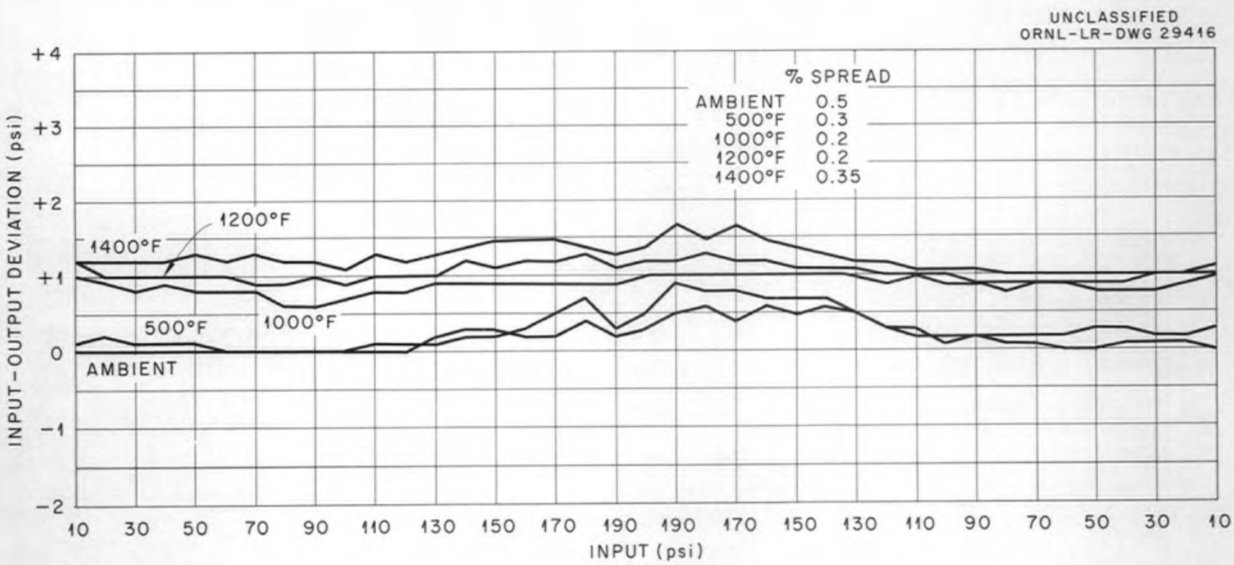

Fig. 91. Taylor 226R Transmitter Data.

UNCLASSIFIED
PHOTO 28160

Fig. 92. Taylor 706TN Transmitter.

UNCLASSIFIED
ORNL-LR-DWG 29417

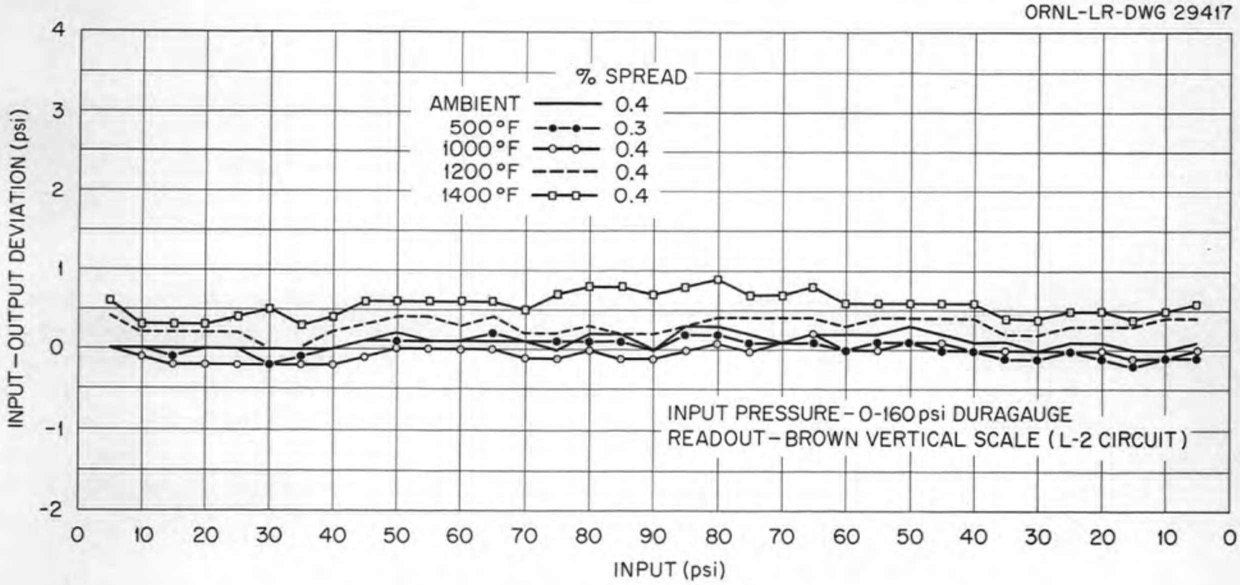

Fig. 93. Taylor 706TN Transmitter Data.

HIGH-TEMPERATURE TURBINE-TYPE MAGNETIC FLOWMETER

G. H. Burger

The turbine-type flowmeter development and testing program was initiated in an attempt to provide an accurate flow-measuring device for liquid metal and fused salt at high temperatures. The use of a turbine-type sensor for flow measurement of these fluids was an attempt to eliminate or reduce the varied and numerous problems encountered by the use of conventional flow-measuring devices for reactor service. Pressure-type systems using venturis or orifices are not completely acceptable for extended service because of erosion and corrosion of the units, which reduce accuracy, and because of the always-present danger of leaks in those systems which penetrate the process lines with pipes or tubes. In addition to those disadvantages there are also the effects of fluid temperature, viscosity, and density upon the accuracy of the system, as well as the difficult task of calibrating the system under operating conditions. All this limits the final accuracy of a venturi- or orifice-type measuring system.

Some of the disadvantages of the pressure-type flow-measuring systems exist also in systems using magnetic flowmeters; further, magnetic flowmeters are limited in use to the measurement of highly conducting fluids. This then almost precludes the use of this type of unit with fused-salt systems. In addition, the accuracy of the units is largely dependent upon temperature and the exact measurement of the magnetic flux, and even then, the accuracy is poor at high flow rates. For high accuracies at all times, the magnet flux and fluid temperature must be accurately known at any instant. The temperature-dependence of the units, the inaccuracy of large units, as well as the complexity and cost of a calibrating system, make the use of magnetic flowmeters a very difficult and costly method of flow measurement at high accuracies. While it does eliminate the use of penetrating lines into the process piping and is then as safe, or solid, as the whole system, the unstable and presently unknown nature of the magnetic flowmeter properties makes calibration of the unit mandatory, at the present time, when high accuracy is required.

As a result of the difficulties encountered in these systems, the turbine-type magnetic flowmeter was placed under development and test. Basically, the unit is a very simple device requiring little maintenance, is an integral part of the process system in which it is placed, and is but slightly dependent upon temperature over its usable range, or upon fluid properties within the limitations of the physical properties of the unit's bearings. These qualities give the flowmeter system higher accuracy with less system complexity by eliminating the need for external piping to the process fluid and eliminating the need for monitoring process-fluid or flowmeter temperatures for flowmeter signal corrections. In addition, the unit should be capable of long-term operation with little or no change in its operating characteristics and accuracy.

The unit (shown in Fig. 94) consists of an Inconel turbine or rotor, supported by titanium carbide bearings, and flow-straightening vanes of Inconel which in turn support the turbine bearings. The fluid enters the vanes and then impinges on the turbine blades, causing the turbine to rotate at a speed determined by the fluid velocity and designed flowmeter conditions, such as bearing friction and blade angle. A magnet is located outside the piping to establish a uniform magnetic field perpendicular to the axis of rotation of the turbine and its contained cobalt vane. A pickup coil (Fig. 95) is mounted so that it intercepts the magnetic lines of flux of the magnet. When the turbine is rotated by the fluid and the cobalt vane cuts the magnet flux lines, a voltage is generated in the pickup coil. This voltage is in the form of sine-wave pulses of which the number per unit interval of time is dependent upon the turbine rotational speed, which is a linear measure of the flow rate. The speed of the turbine (in pulses or counts per second) can be measured quite readily by conventional electronic counting equipment such as a count-rate meter or scaler. Since the turbine speed is a linear function of flow, the flow rate in gpm can be plotted against counts (pulses) per second. The device appears to be only slightly dependent upon temperature over the normal range up to 1500°F and not at all upon pressure. Nor is the viscosity effect appreciable at viscosities below 6 centipoises. A typical water-calibration curve is presented in Fig. 96. Water calibrations with this type of flowmeter appear to be valid for fused

UNCLASSIFIED
PHOTO 27499

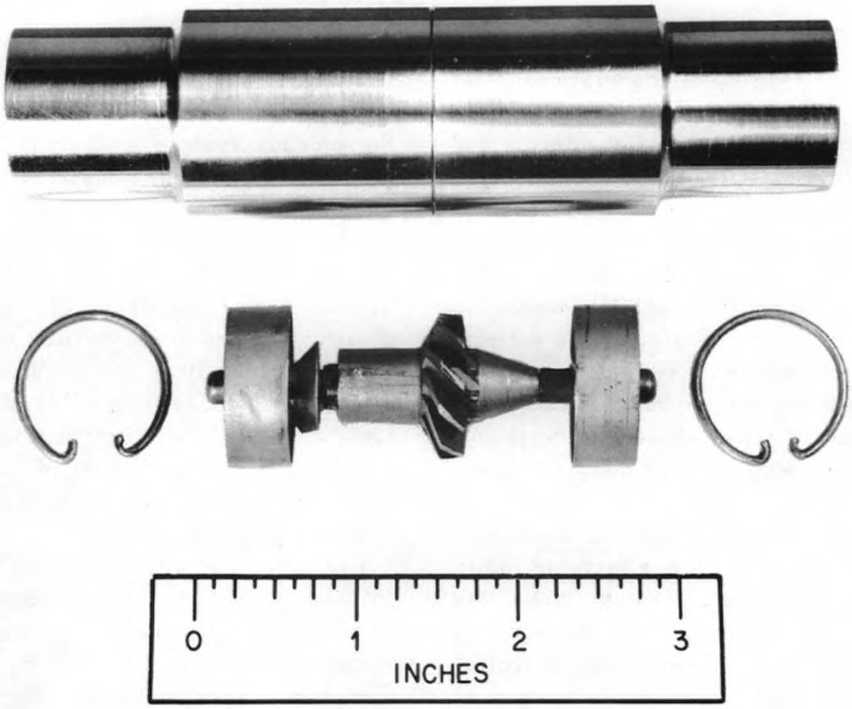

Fig. 94. Turbine-Type Magnetic Flowmeter, Exploded View.

UNCLASSIFIED
PHOTO 29727

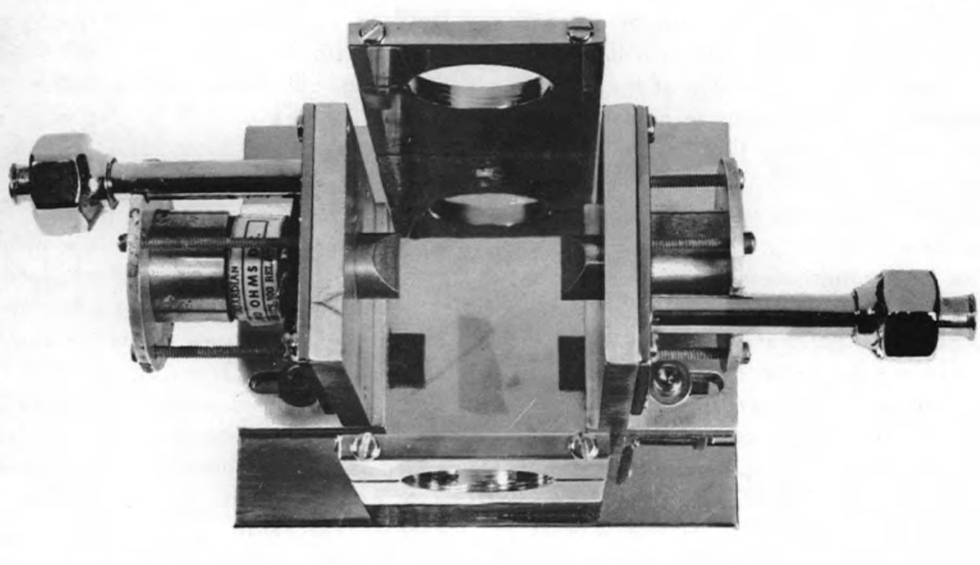

Fig. 95. Pickup Coil for Turbine-Type Magnetic Flowmeter.

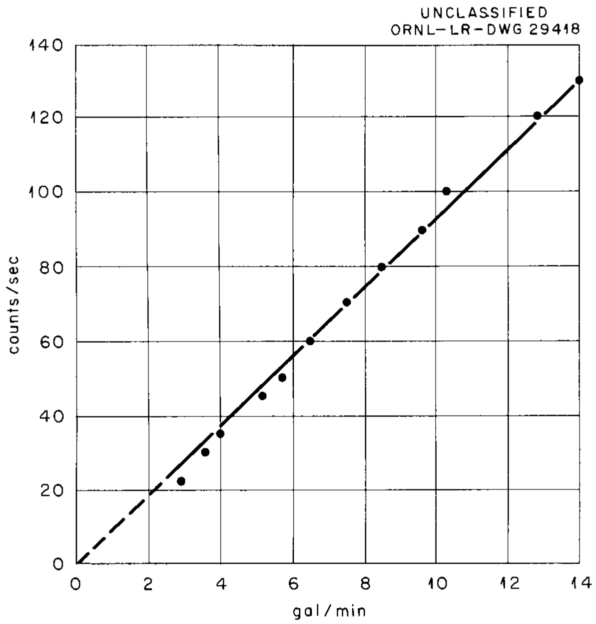

Fig. 96. Turbine-Type Magnetic Flowmeter Calibration Curve (Water).

salts and liquid metals over the intended operating temperature ranges since the viscosity range is approximately 6 centipoises and below.

In order to obtain operating data on the flowmeter, a number of 1-in. units were tested in both fused salt and liquid metal systems. These systems were capable of a maximum flow rate of 5 gpm at temperatures up to 1500°F. The flowmeter to be tested was welded into the system, which contained an orifice as the calibrating standard.

Seven 1-in. flowmeter tests have been attempted with varying degrees of success. Although 7 tests have been run, only 3 complete units have been fabricated. The other tests were made with modified or repaired units, since only one unit was damaged beyond repair during testing. Of the total number of tests, four were made with NaK and three with fused salt. The maximum operating time of any one test was 365 hr with fuel and 143 hr with NaK. Of the total number of units tested, four tests were terminated because of system leaks and three for bearing failures. The bearing failures were apparently a result of oxidation of the titanium carbide which caused the bearings to jam and cease to rotate, with consequent breakage of the bearings due to sudden physical shock.

The extent of oxidation of the bearings was unexpected, and further controlled long-term tests will be required in order to evaluate the bearing material. A later design has incorporated a modified bearing assembly, with larger bearings (Fig. 97), in an attempt to eliminate the breakage problem and to provide better service in case of oxidation. The over-all operating characteristics of the units appear to be satisfactory. The accuracy during tests over the entire operating range was approximately 1% of full scale. With a unit tailored to meet a given system, accuracies better than 1% may possibly be obtained.

In addition to the 1-in. units, two $3\frac{1}{2}$-in. units were fabricated (Fig. 98) and were water-calibrated at flow rates up to 1100 gpm. One of the units was then placed in a NaK pump test loop for testing. The unit, however, failed after a very short period of operation, due to breaking of the bearing pivots while operating at 1200 gpm (Fig. 99).

Upon examination of the unit after its removal from the loop, it was found that both bearing pivots were broken and that a number of turbine blades were missing. It is believed that the bearings broke, allowing the unit to drop down, and while rotating and rubbing against the housing, the blades were eventually broken from the turbine body. This was possible because the loop continued to operate about 60 hr after the initial failure of the unit at flows up to 1600 gpm and at temperatures up to 1600°F. While the initial cause of the breakage cannot be ascertained, it is felt that pump surges in the loop caused large flow excursions which shattered the bearing pivots.

Since the failure of the first large unit under test in NaK, no further tests have been attempted, pending the outcome of test and evaluation of smaller units which are easier to test because the test loop required is much smaller and more easily controlled. It is expected that as soon as the smaller (1-in.) units have been tested and proved satisfactory, a larger unit will again be built and tested.

In summary, it may be stated that the operating principle of the turbine flowmeter appears to be satisfactory for use in fused salt and liquid metal systems at high temperature. The major problems at present appear to be the choice of material and the design of the bearings. In order to solve these problems, further long-term tests will be necessary.

UNCLASSIFIED
PHOTO 40855

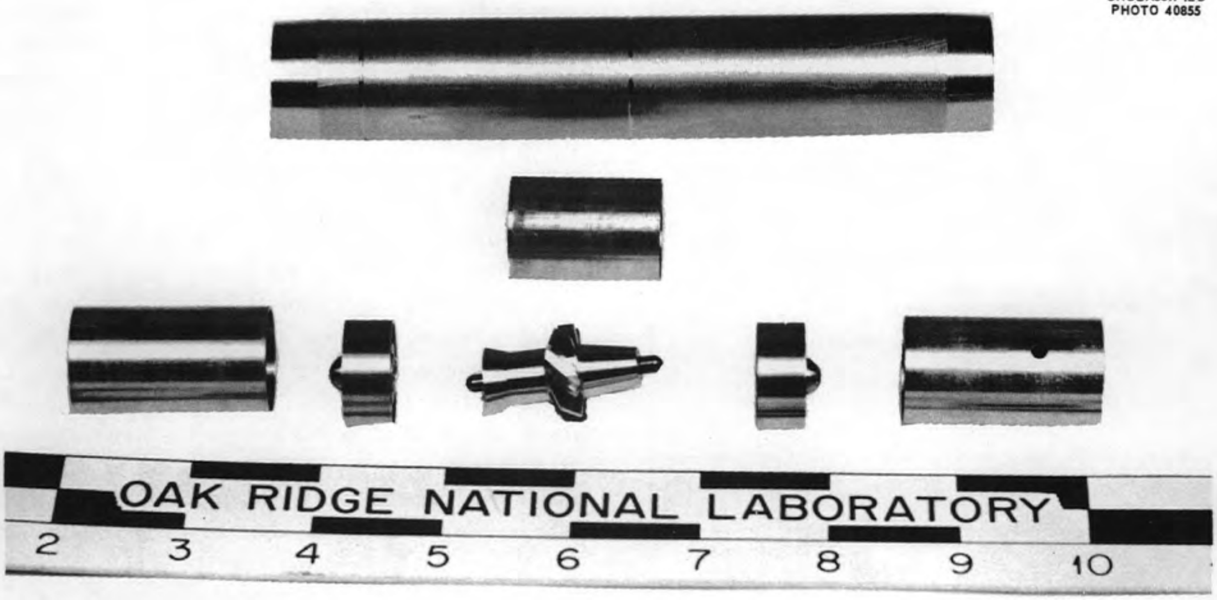

Fig. 97. The 1-in. Turbine-Type Magnetic Flowmeter, Exploded View.

UNCLASSIFIED
PHOTO 27502

Fig. 98. Turbine-Type Magnetic Flowmeter, $3\frac{1}{2}$-in. Model.

UNCLASSIFIED
PHOTO 28283

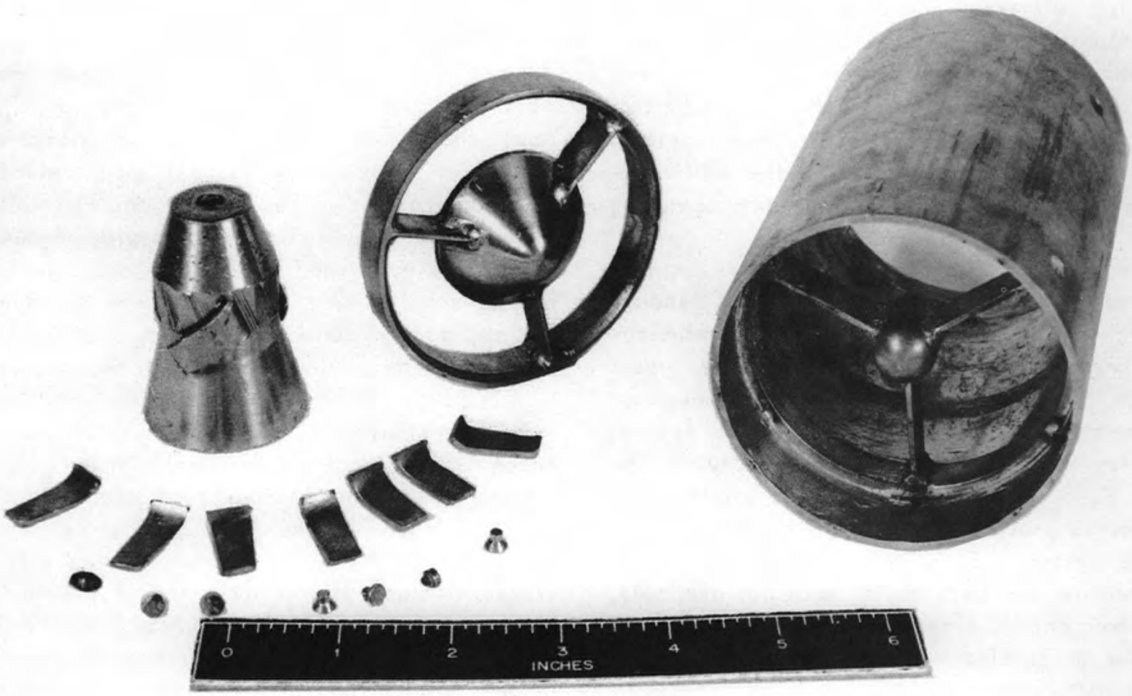

Fig. 99. Damaged Turbine-Type Magnetic Flowmeter, $3\frac{1}{2}$-in. Model, Exploded View.

LIQUID METAL LEVEL MEASUREMENT

G. H. Burger R. E. Pidgeon

Operating criteria for the liquid-metal-level measuring elements included requirements that they operate continuously for 3000 hr at temperatures up to 1500°F at various system pressures and in the presence of high-level radiation. It was also required that they have maximum accuracy and repeatability over the entire operating range and during the entire operating period.

There are generally two types of probes required for level measurement of liquid metals (sodium and NaK) in a reactor system: the continuous and the on-off or fixed-point indicator types. In both types the material of the probes must be compatible with the process fluid for longest possible life and maximum reliability. The units must also be of all-welded construction in order to provide maximum physical reliability for the system. Since units which met all the requirements set forth above were not available, a research and development program was initiated in order to develop and test units which would be satisfactory.

The continuous-level-type system will be considered first. Several different sizes of these units were built with different level ranges from $2\frac{1}{2}$ to 30 in. However, the operating principle and the general design of all units are quite similar. The one exception is in design only and is for a unit which is mounted in a tank bottom instead of in the top, as in the usual case. Figures 100 and 101 show a probe designed for top mounting in NaK pump bowls. This particular unit has a level range of $8\frac{1}{4}$ in. total and $7\frac{1}{4}$ in. linear. This resistance-type transducer consists of Inconel pipe welded in the shape of a J. Two current and two voltage leads, all of Inconel and insulated with magnesium oxide, are positioned inside the pipe. A transformer supplies 3-v 60-cycle power at approxi- 20 amp to the current leads. A sketch of the probe and its equivalent circuit are shown in Fig. 102.

The resistances R_2 and R_3 are the lead resistances of the input current leads, and R_1 is the resistance of the Inconel pipe comprising the sensing leg. As the NaK level rises on the sensing leg, the resistance of the leg will decrease. Since the conductivity of the NaK is high compared with that of the sensing leg, the resistance of the leg, R_1, and therefore the output voltage, is inversely proportional to the NaK level (Fig. 102). The output voltage can vary from 0 to 40 mv and is given by the equation:

$$E_{out} = \frac{3R_1}{R_1 + R_2 + R_3} ,$$

UNCLASSIFIED
PHOTO 28995

Fig. 100. Continuous-Monitor Type of Level Probe for Top-Mounting in NaK Pump Bowls.

UNCLASSIFIED
PHOTO 28994

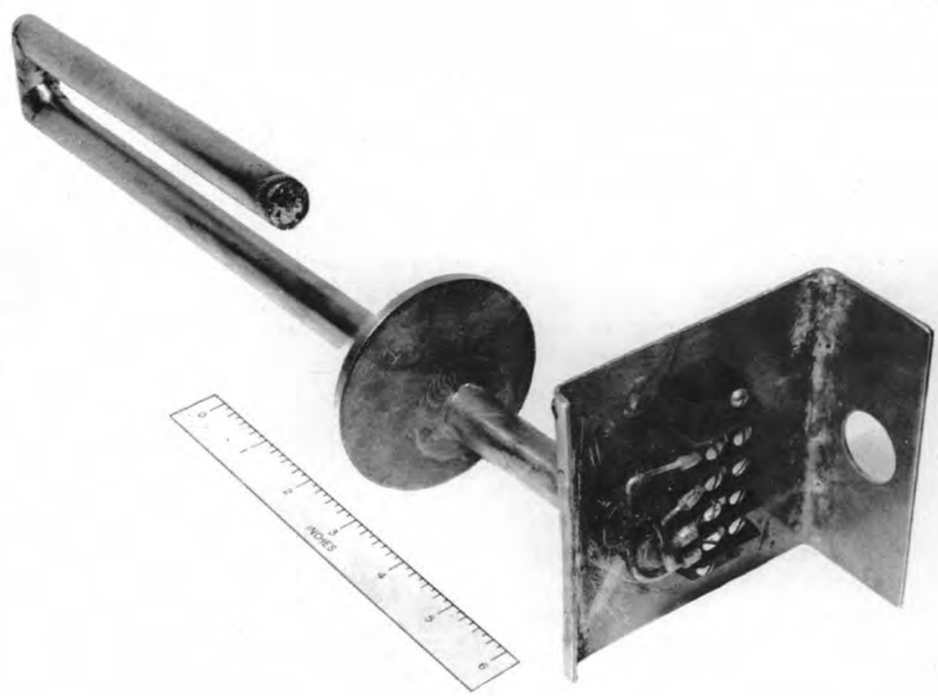

Fig. 101. Top View of Continuous-Monitor Type of Level Probe.

UNCLASSIFIED
ORNL-LR-DWG 29419

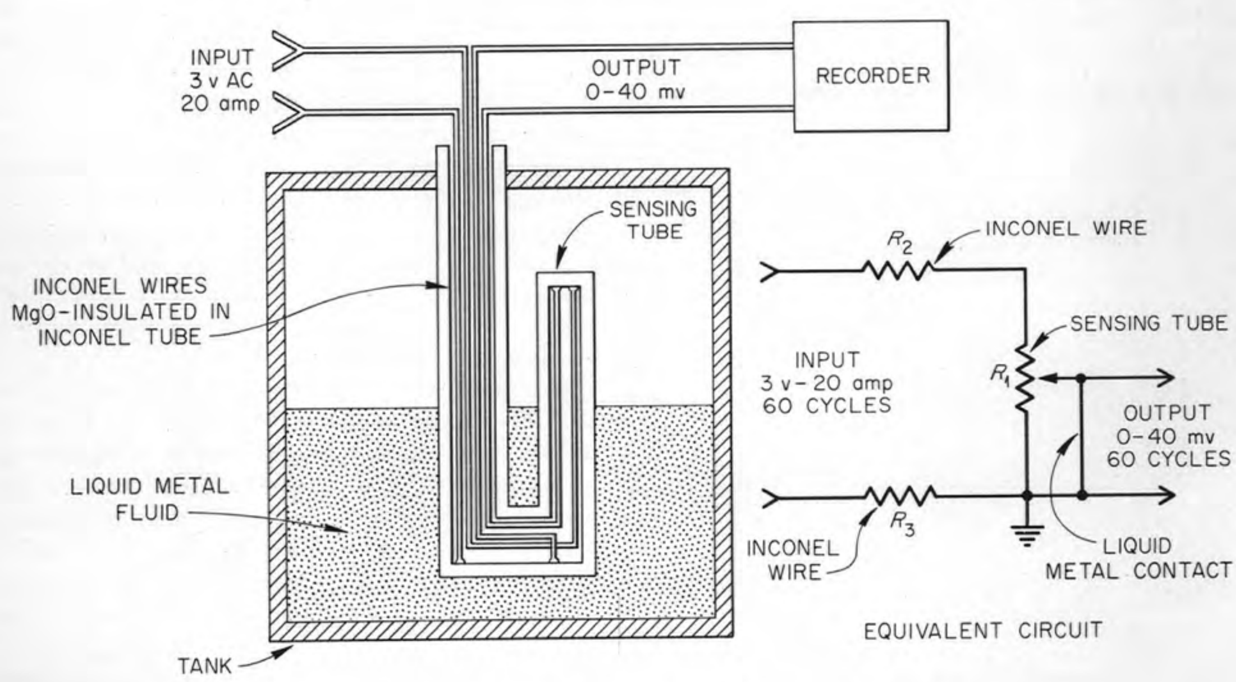

Fig. 102. Operating Principle of Resistance-Type Level Transducer.

which is approximately

$$E_{out} = \frac{3R_1}{R_2 + R_3} ,$$

since $R_1 << R_2 + R_3$.

If the sensing leg and current leads are at the same temperature throughout, and if the temperature coefficients of resistivity of R_1, R_2, and R_3 are the same, the output voltage is independent of the probe temperature. Ideally, when the temperature changes, the numerator and denominator of the equation for the output voltage change by the same factor and the output remains constant. In reality, a small temperature error exists (Fig. 103), because all parts of the resistance probe are not at the same temperature, and the temperature coefficient of resistivity of the Inconel wire and pipe used may not be the same.

A vacuum-tube voltmeter can be used to measure the output voltage. For recording, a Brown strip-chart recorder modified for 60-cycle operation has been quite satisfactory.

In order to supply the required number of level probes for this particular reactor system, two different types and four sizes are required. The total number of all sizes and types required is 75.

In order to test and calibrate the units, test facilities were designed and fabricated. The two facilities completed to date were made in such a manner that the probes could be clamped

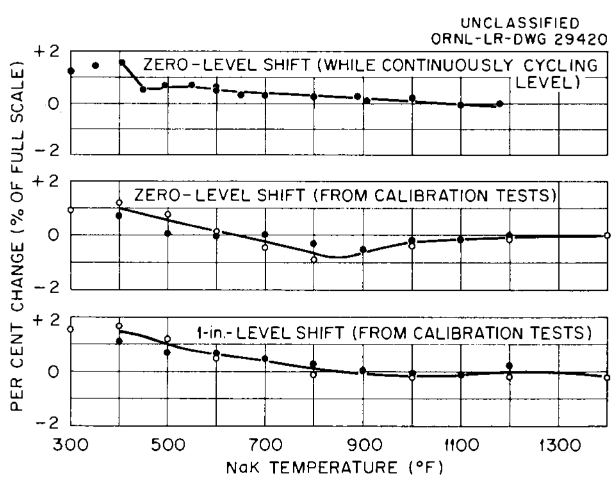

Fig. 103. Graph Showing Temperature Effect on Output Voltage.

into the system and the fluid level and temperature changed as desired (Fig. 104). The systems consist of two pots mounted on a rigid frame which can be rocked or moved by an electric motor. This motion allows the fluid in the pots to be transferred from one to the other at a predetermined rate and temperature. Other facilities have been designed and will be fabricated to test probes of the various types as they are designed and fabricated.

To date, ten of the probes for the NaK pump bowls (Fig. 100) have been tested in the test facilities and six have operated 3000 hr at temperatures up to 1500°F. In addition, three probes have been installed in pump test rigs and operated for long periods of time. There have been some failures of probes, but in all cases the failures were due to poor welds.

The results of the pump-bowl probe tests to date have indicated that the probes have an accuracy of $\frac{1}{16}$ in. or 1% after wetting and calibration and a zero shift of 3% from room temperature to 1400°F (Fig. 105). It is to be noted that the output of the probe is linear except at the extreme ends. The major problem experienced with the probes has been the wetting of the units. This wetting is comparable to tinning a soldering iron and is a function of temperature and time. It affects the output voltage of the unit by causing the sensing leg to have a high electrical resistance in the non-wetted condition. Based on preliminary data to date, it is expected that, in a system which is filled at a temperature of 600°F and above, the wetting problem will be very slight and result in only small errors in output signal. It is contemplated that further tests now in progress will determine the extent of the wetting process to a more exact degree and indicate possible solutions to the problem.

The other type of level probe, mentioned earlier and called the on-off probe, is needed to serve as a level set-point alarm or monitoring device in cases where the continuous-level unit is not needed, such as in fill-and-drain tanks to indicate maximum and minimum fill levels. The probes generally used in the past for this function have been of the "spark plug" type. These units consisted either of regular spark plugs with a long center electrode or plugs of the same general type but of special insulator design. These plugs

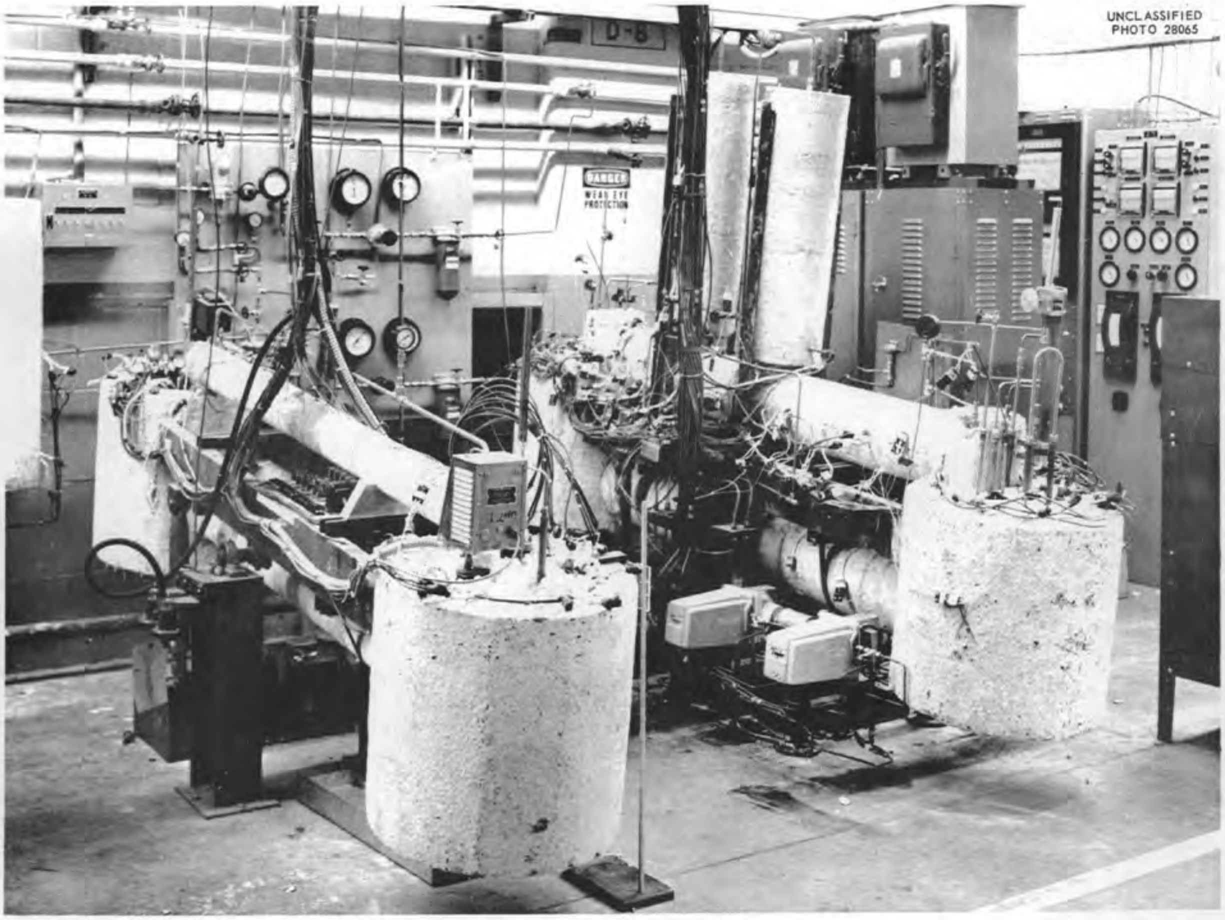

Fig. 104. Test Facility for Liquid-Level Probes.

were used and tested with varying degrees of success. A special Champion probe was tested in one of the level-test rigs. The life of the probe was very short at temperatures above 400°F. Figure 106 shows some of these Champion plugs after 70 hr of NaK service. Other designs and makes of spark plug probes, including a plug with a BeO insulator, have been tested with very little success at temperatures above 400°F. Since the temperature limitation of the spark plug probes could be very serious in come cases (e.g., when used in a radioactive system) a different type of on-off level probe was designed as a replacement. In addition to overcoming the temperature limitations of the spark plug probes, the newly designed on-off probes provide for much greater system safety by being of metal and all-welded construction. This is of particular importance when this type of probe is used in radioactive systems. Figures 107 and 108 show the probe and its operating principle. The probe consists of a thin-walled Inconel tube with a central conductor (an insulated No. 8 AWG copper wire) inside and welded to the probe bottom. A 60-cycle low-voltage high-current signal is applied to the center wire of the probe and to the tank in which the probe is contained. As the liquid metal touches the probe, the probe resistance is decreased, changing the voltage applied to a relay across the probe. This relay is used to activate an appropriate annunciator alarm.

A number of these probes have been built and placed in operating service in test loops and in level test and calibration facilities. The early

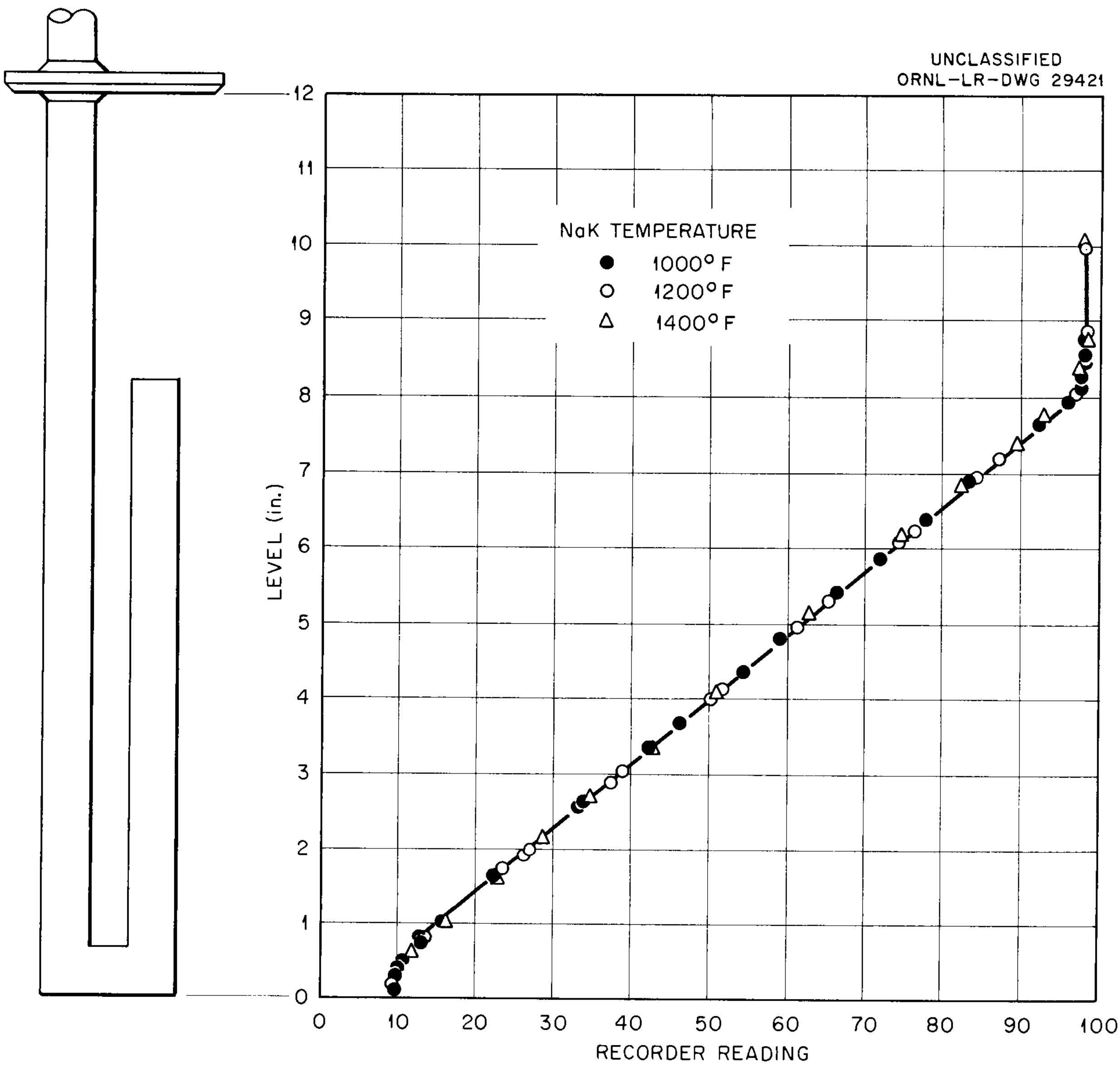

Fig. 105. NaK-Level Calibration Chart for Resistance-Type Level Transducer.

UNCLASSIFIED
PHOTO 27734

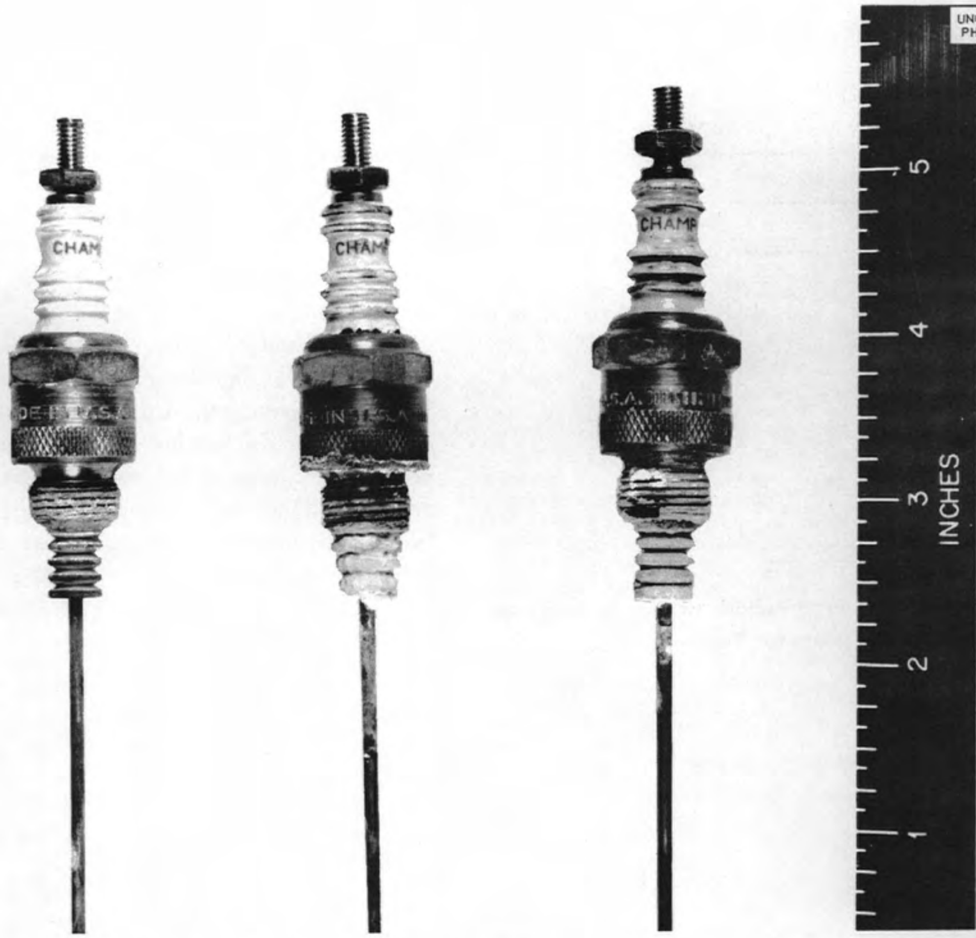

Fig. 106. Spark Plug Electrical Shorting Type of On-Off Probe.

UNCLASSIFIED
PHOTO 27621

Fig. 107. Newly Designed On-Off Probes.

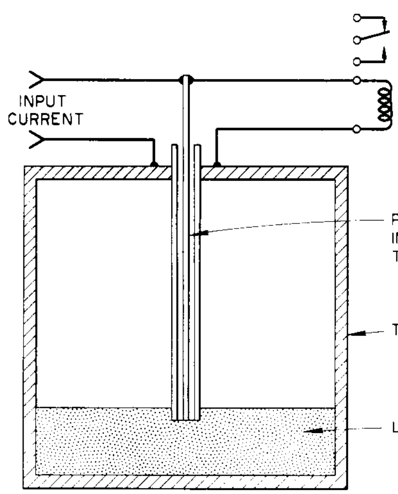

Fig. 108. Operating Principle of Newly Designed On-Off Probe of the Resistance Type.

design of these units was not satisfactory for long operating periods, due to oxidation of the center wire at the weld joint. The probe has been redesigned, using a brazing technique in an attempt to eliminate this problem. At the present, 22 of the earlier-version probes are in service on test rigs, with several more under test. Fabrication of the later version of this probe has begun, and it will be under test in the near future.

As was noted earlier, reliability is of utmost importance for any device used in reactor systems. In order to ensure the maximum possible reliability of all probes installed in a system and also to provide maximum level-measurement accuracy, all probes will be tested and calibrated under simulated operating conditions before final installation. Calibration curves and operating data will be provided for all continuous probes intended for operational service.

THERMOCOUPLE DESIGN AND TESTS

J. T. De Lorenzo

A testing program has been initiated to determine the performance of Inconel-sheathed Chromel-Alumel thermocouples at temperatures ranging from 1100 to 1500°F. The effects of both slow and rapid thermal cycling are being considered. In addition, the integrity of the wires and of the hot-junction closure weld is being examined under conditions of rapid heating and in highly corrosive environments.

A well couple for temperature measurement of high-velocity, high-temperature (1400 gpm, 1100 to 1500°F) liquid metals in Inconel piping has been designed and is undergoing similar testing.

Finally, a thermocouple with No. 20 AWG solid Chromel-Alumel wires has been developed which permits a simple and reliable attachment by Heliarc welding to various Inconel surfaces.

SHEATHED THERMOCOUPLES

The outside diameter of the Inconel sheath is 0.250 in. with a 0.030-in. wall thickness. The sheath contains two pairs of No. 20 AWG Chromel-Alumel thermocouples embedded in hard-packed magnesium oxide. This material was manufactured by the Thermo Electric Co.

Over 5000 hr of drift data has been obtained on samples of this material operating in sodium and fused salt. The test procedure consisted of maintaining the couples at 1500°F, with weekly reductions to 1300 and 1100°F for readings at these temperatures. Nineteen couples were tested in the sodium and sixteen in the fused salt. Three of the latter included units with platinum vs platinum–10% rhodium wires. Figure 109 shows a test sample with its associated connectors and the water-cooled copper chill block which is employed during the welding of the hot junction.

Figures 110 through 112 show typical performances of the Chromel-Alumel couples as they aged in sodium and fused salt. Figure 110 shows a slight upward drift (1 to 3°F total) throughout, which was representative of approximately 47% of the couples tested. Figure 111 shows a slight downward drift (2 to 7°F total) throughout, which was representative of approximately 40% of the

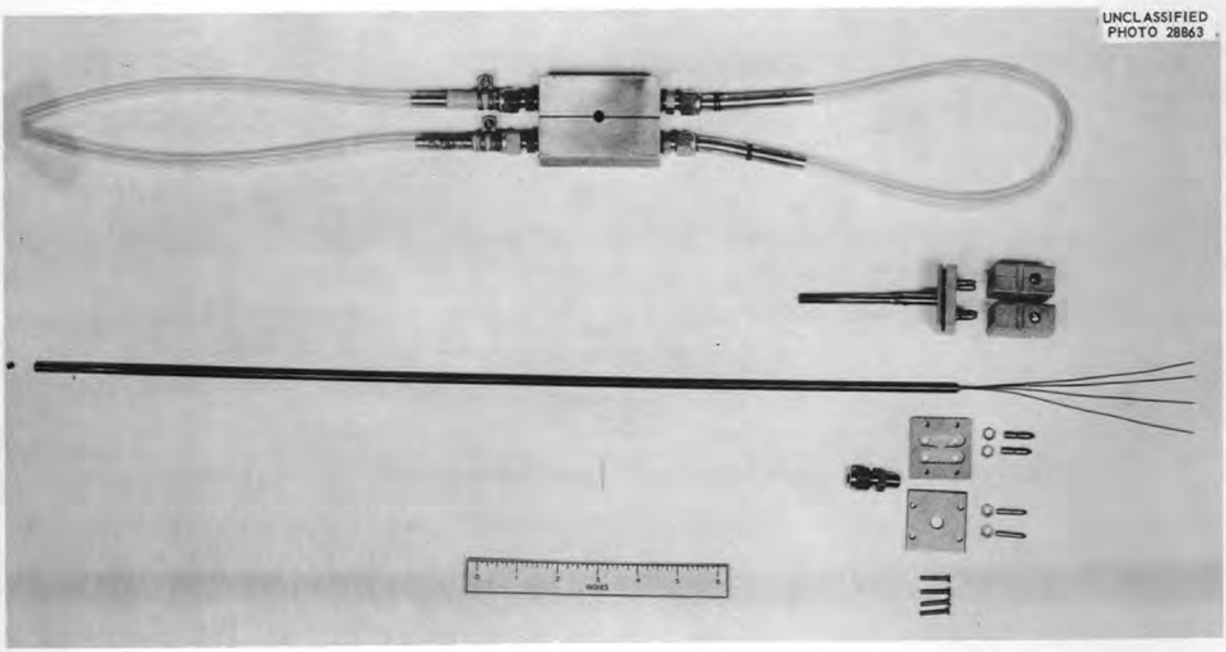

Fig. 109. Thermocouple Test Sample Made of 0.250-in.-OD Inconel-Sheathed Material. Shows assembled and disassembled connectors, water-cooled copper chill-block for junction fabrication, and Inconel filler tip.

UNCLASSIFIED
ORNL-LR-DWG 29423

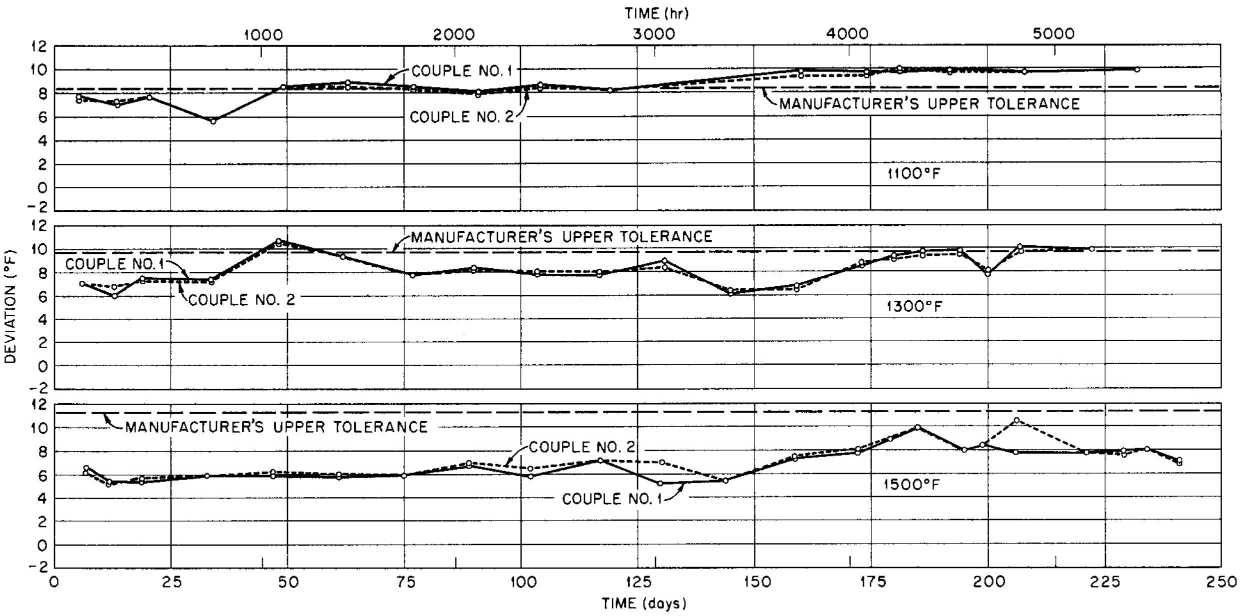

Fig. 110. Typical Drift Curve for 0.250-in.-OD Inconel-Sheathed Chromel-Alumel Thermocouple.

UNCLASSIFIED
ORNL-LR-DWG 29424

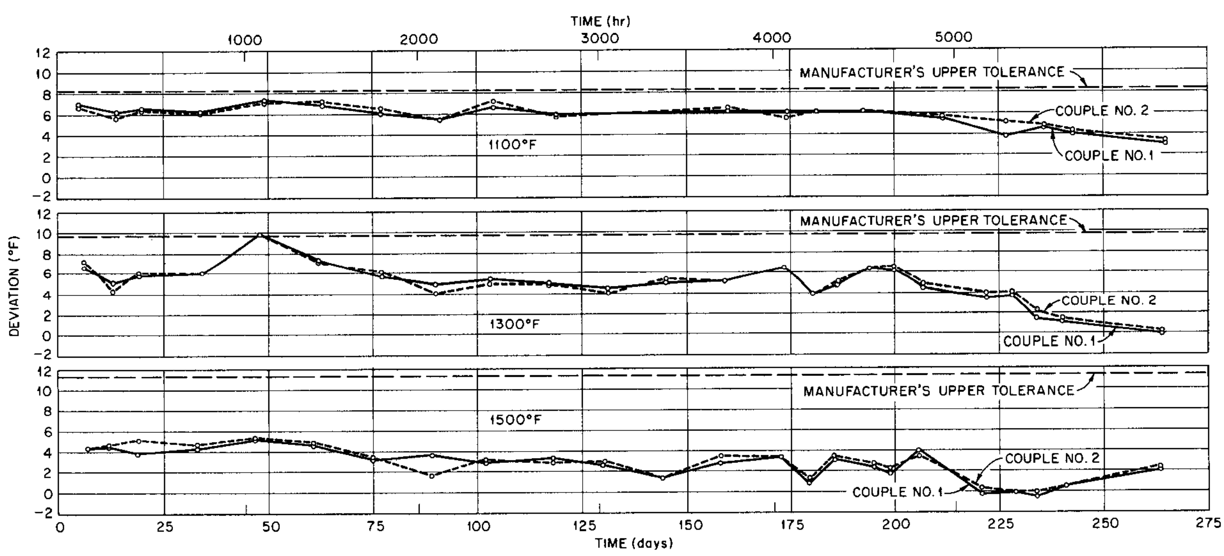

Fig. 111. Typical Drift Curve for 0.250-in.-OD Inconel-Sheathed Chromel-Alumel Thermocouple.

couples tested. Figure 112 shows sharper downward drift (12 to 22°F) which later leveled off, which was representative of about 13% of the data. It should be mentioned that the latest data acquired (after 4000 hr) show a definite reversal of the downward drift for a large percentage of the couples. For comparison, Fig. 113 shows the typical performance of the platinum vs platinum–10% rhodium couples as they aged for over 4000 hr in the fused salt. Figure 114 shows the facility where the drift data were obtained.

Earlier drift data on identical samples of this sheath material operating *continuously* in air at 1800, 1600, and 1300°F revealed an upward drift for *all* couples. It is believed that the cycling of the couples during the tests in sodium and fused salt could have produced "breathing" of the magnesium oxide on the unsealed connector

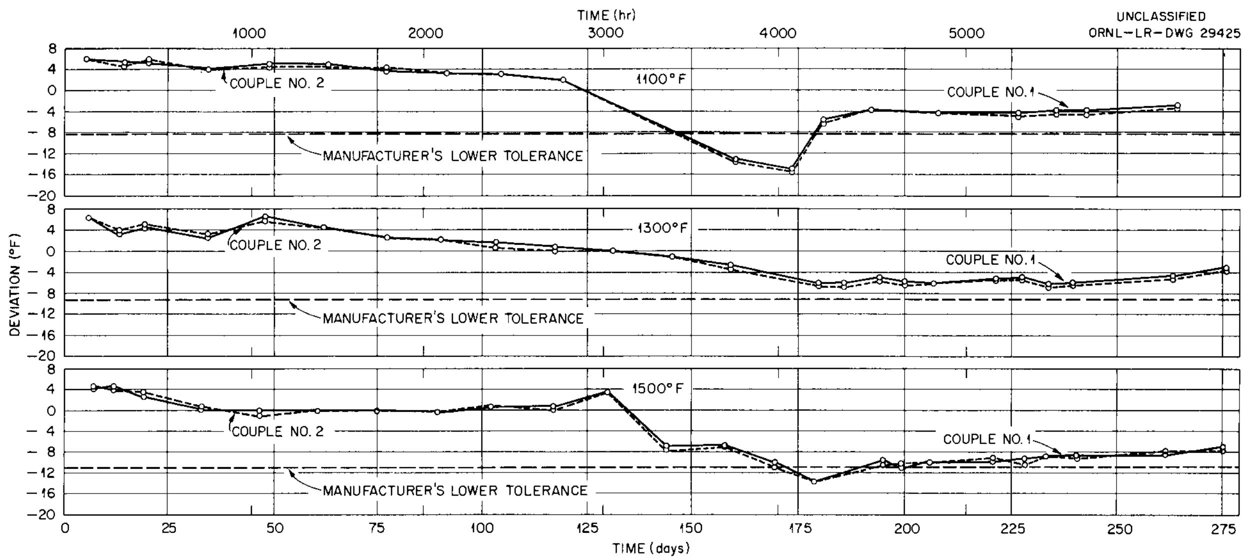

Fig. 112. Typical Drift Curve for 0.250-in.-OD Inconel-Sheathed Chromel-Alumel Thermocouple.

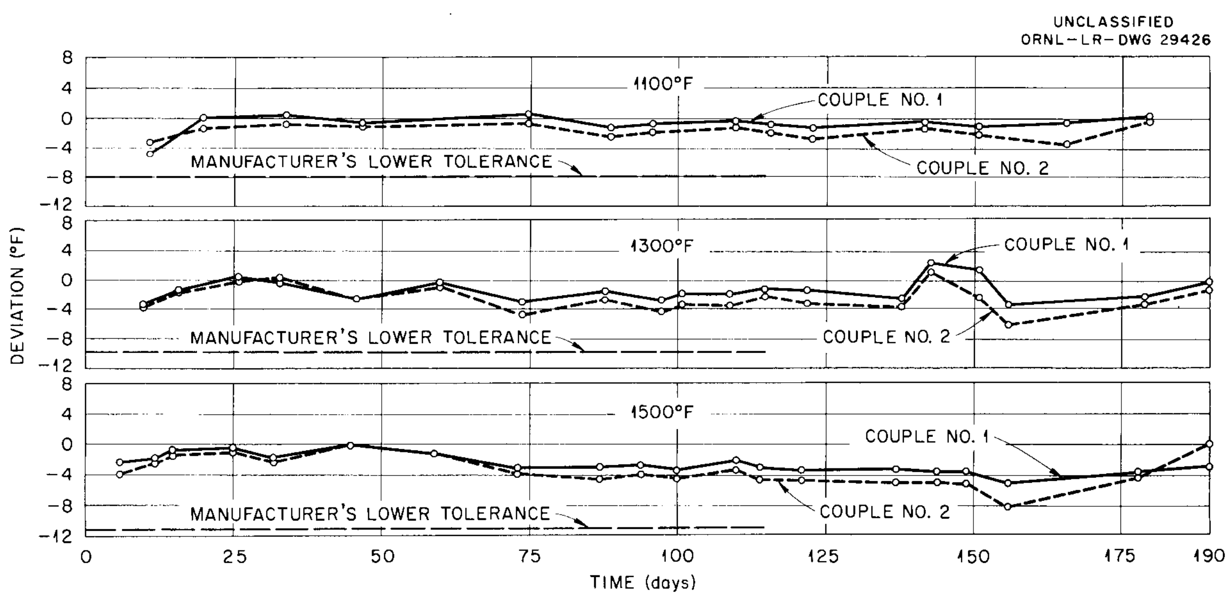

Fig. 113. Typical Drift Curve for 0.250-in.-OD Inconel-Sheathed Pt, Pt–10% Rh Thermocouple.

Fig. 114. Facility for Thermocouple Drift Testing and Calibration. Shows furnace with sheathed couples, five furnace-control cabinets, and operator at calibration console.

end, thereby inducing conditions which might possibly cause downward drifts. Additional drift tests with sealed samples are being proposed to check this.

Figure 115 shows a cross section of the hot-junction end of these sheathed couples. The closure consists of a four-hole Inconel plug which is Heliarc welded to the sheath and wires. A new technique employing a Coast Metals No. 52 brazing scheme is being investigated and appears to be highly desirable for several reasons. Not only will it be considerably less difficult to fabricate, but it offers a minimum void below the tip, along with an accurately positioned thermocouple junction. The test samples for the additional drift tests mentioned above will have the hot junction fabricated with the new brazing scheme.

A 50-kw induction heating unit has been renovated and is being employed to rapidly heat (500°F/sec is possible) samples of thermocouples made from the above-mentioned sheath material. One sample failed after 240 heating cycles between 800 and 1200°F at a heating rate of 100°F per sec. In this failure, both Chromel wires were broken, the Alumel wires remaining intact.

In addition to supplying answers as to the physical soundness of sheathed couples, this induction heating unit provides a simple means to obtain aging data under various degrees of cyclic thermal shock. This induction heating facility is shown in Fig. 116.

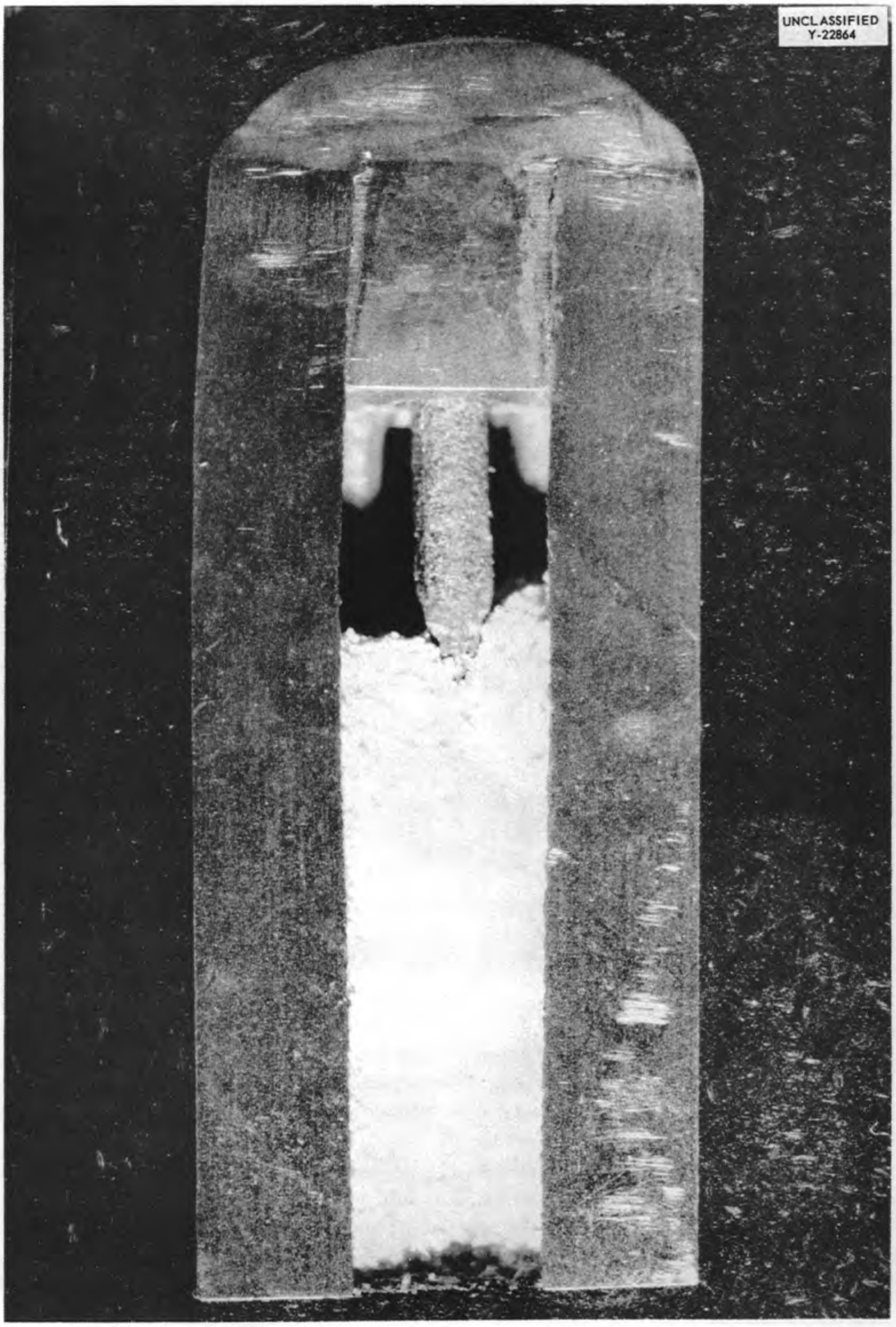

Fig. 115. Cross Section of Heliarc-Welded Junction on Inconel-Sheathed Thermocouple. Shows Inconel filler tip, weld to 0.250-in.-dia × 0.030-in.-wall tubing, No. 20 AWG thermocouple wire, void, and white magnesium oxide insulation.

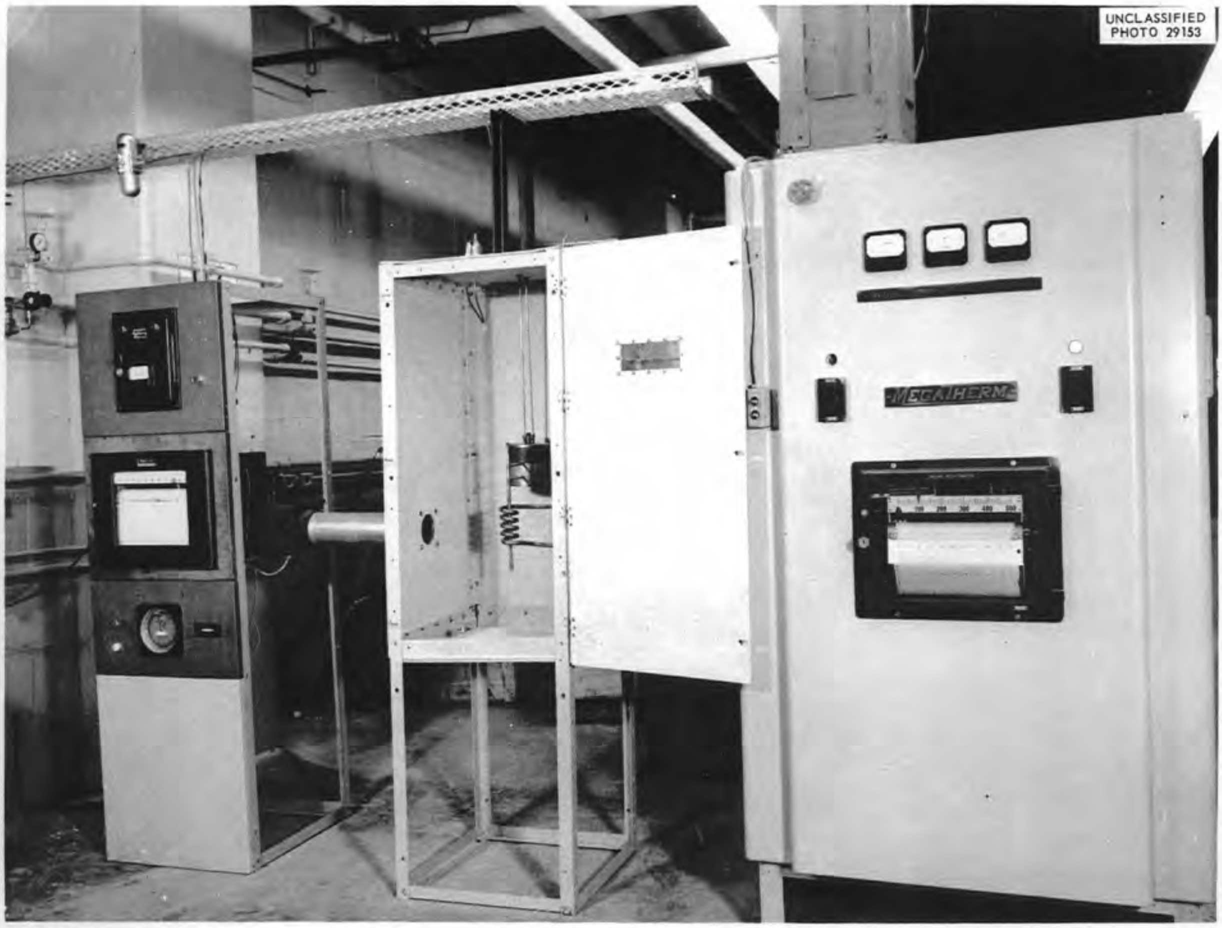

Fig. 116. Induction-Heating Facility for Rapid Heating Tests on Sheathed Thermocouples. Shows control instrument cabinet, test-specimen cabinet with coil, and main control cabinet.

WELL THERMOCOUPLES

The design of a well thermocouple for temperature measurement of high-velocity, high-temperature (1400 gpm, 1100 to 1500°F) liquid metals in Inconel piping has been completed, and several units have been constructed. The thermocouples employed in these units are fabricated from No. 20 AWG solid Chromel-Alumel (± 3/8% accuracy, 530 to 2300°F) wire and are Heliarc welded to the bottom of the well. All ceramic beads contain a minimum of 96% aluminum oxide. Figure 117 shows a typical unit in the assembled and disassembled state, along with jigs required for formation of the junction and attachment by welding to the bottom of the well.

The immersion depth of the well was arbitrarily chosen as one-third of the inside diameter of the pipe line. The material of the well body was selected to be 3/8-in. sched 40 Inconel pipe for pipeline 2½ in. and larger, and 1/4-in. sched 40 Inconel pipe for a 2-in. pipeline. The immersed portion of the body was turned down to a 0.050-in. wall thickness. This well body design was tested for pressure drop on a water loop at velocities up to 1400 gpm. The irrecoverable pressure drop was less than 2.0 psi at 1200 gpm.

The lagging length of the well body was chosen so as not to extend beyond the 4 in. of pipe insulation, in an attempt to minimize heat losses and the selective oxidation effect that is common in long narrow wells at elevated temperatures.

The thickness of the well bottom was determined on the basis of stress analysis at operating pressures and temperatures. A value of 0.109 in. was selected on the basis of this analysis.

UNCLASSIFIED
PHOTO 28859

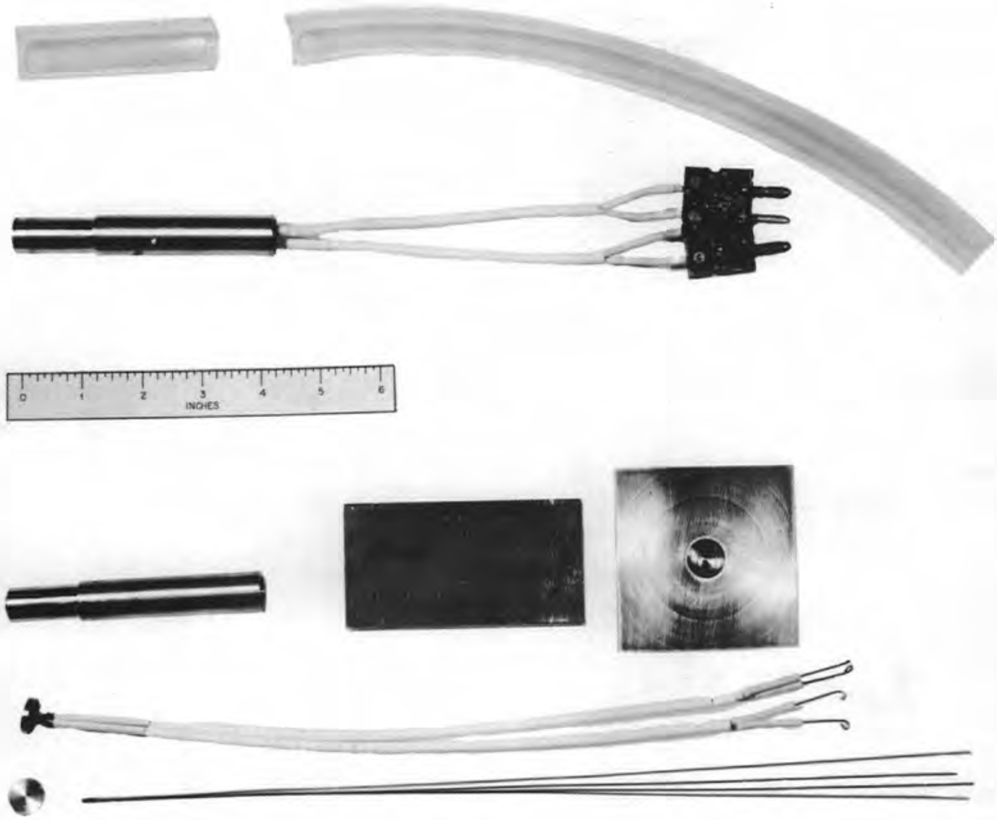

Fig. 117. Well Thermocouple for NaK Piping. Shows assembled and disassembled unit, copper chill block for junction formation, Inconel plate used in attachment of junction to well bottom, and plastic tubing used to protect the unit during handling.

To facilitate the attachment of the couple junction to the well bottom, a technique was developed which permitted the coating of the thermocouple junction with Inconel without any undue burning of the wires. This "wetting" of the junction simplifies the subsequent Heliarc weld to the well bottom. It was discovered that a careful cleaning of any oxide from the wires leads to a more reliable junction. This is shown in Figs. 118*a* and *b*. Here, cross sections of the junction reveal that the carefully cleaned wires were free of chromium oxide deposits at the junction point of the Chromel wire and bead.

Extreme care was taken in the assembly of the well couple. All ceramic beads were carefully washed with distilled water and alcohol and baked. All wires were washed with alcohol. All well body pieces were degreased, washed with alcohol, and baked. All subsequent handling after cleaning was done with clean white gloves.

Each well thermocouple, after its installation, will be provided with a spring-type flexible extension to eliminate any possibility of bending near regions of high temperature gradients.

Drift tests on five sample units operating in NaK have started. The test procedure will be similar to that performed on the sheathed couples.

SURFACE THERMOCOUPLES

The couples for surface attachment to Inconel piping and components will be fabricated in a manner identical with that employed in the well couples. Figure 119 shows such a couple with the copper chill block required for the junction fabrication.

A special procedure has been devised by the Metallurgy Division which permits a reliable and simple method of welding these surface-type couples to the various Inconel surfaces with Heliarc.

Fig. 118*a*. Cross Section of Heliarc-Welded Inconel-Coated Thermocouple Junction of No. 20 AWG Chromel and Alumel Wires. Note chromium oxide deposits in Chromel wire.

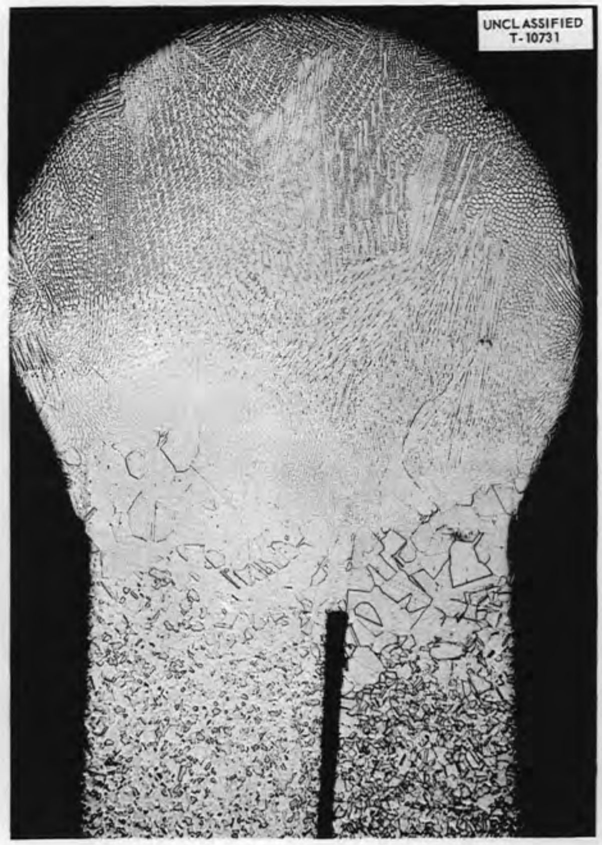

Fig. 118*b*. Cross Section of Heliarc-Welded Inconel-Coated Thermocouple Junction of No. 20 AWG Chromel and Alumel Wires. Wires carefully cleaned before welding. Note absence of chromium oxide deposits.

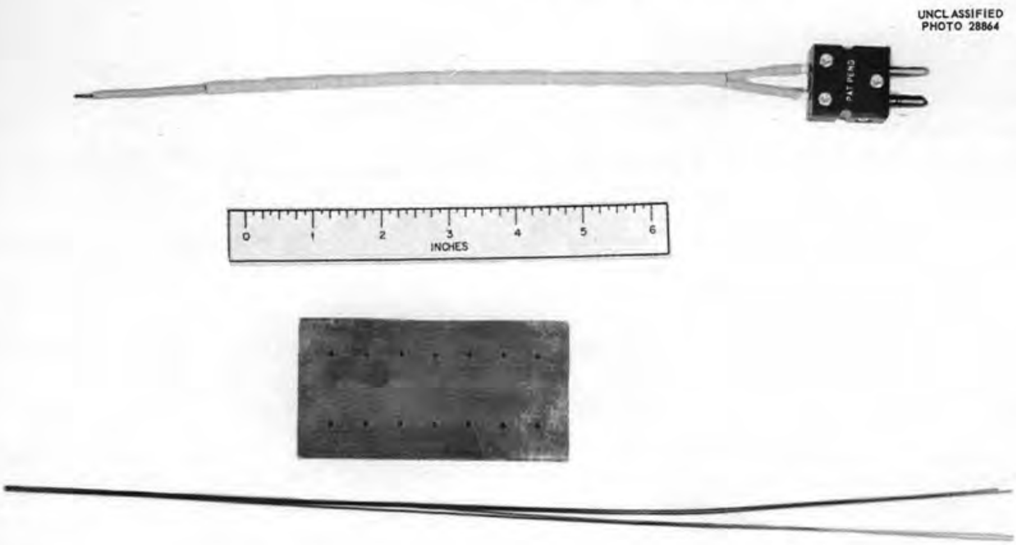

Fig. 119. Thermocouple for Surface Attachment. Shows thermocouple without beads and connector, complete assembly, and copper chill block employed for junction formation.

BUOYANCY-TYPE LIQUID-LEVEL INDICATOR FOR HIGH-TEMPERATURE FLUID

A. L. Southern

This device consists of a gas-filled cylinder extending vertically into the tank in which the level is to be measured. The cylinder is connected by means of a rod to a bellows, then to a transmitter made up of a nozzle and anvil assembly mounted vertically above the cylinder.

The transmitter is forced to buck out the sum of two forces: the force due to the pressure in the tank, and the buoyancy force transmitted to the bellows from the cylinder. The pressure differential between the transmitter output and the pressure in the tank is a measure of the liquid level in the tank.

There are three factors of importance in determining the sensitivity of this device: (1) the diameter of the cylinder, (2) the diameter of the bellows, and (3) the density of the fluid.

From these factors a simple formula for the differential pressure per inch of level change can be stated:

$$\Delta P = \rho \frac{D_c^2}{D_b^2} ,$$

where

- P = pressure in psi,
- ρ = density of fluid at operating temperature in lb/in^3,
- D_c = outside diameter of cylinder,
- D_b = effective diameter of bellows.

Since the differential pressure is proportional to the density of the fluid, the device is somewhat temperature-sensitive. Therefore, a correction curve must be plotted to compensate for this effect.

The sensitivity and calibration of this instrument are not affected by the weight of the cylinder and connecting rod, since the setting of the transmitter is variable and a change in force is being measured. However, this weight should be kept to a minimum to prevent straining the transmitter bellows. Once this weight is established, it becomes one of the criteria for selecting the transmitter bellows.

The unit used in the experiment is shown in Fig. 120. A water-calibration curve is shown in Fig. 121. The accuracy of level indication was ± 2%. Figure 122 shows the level-indicator schematic.

A prototype unit was tested in fused salts for a 2-in. level-change and was found to have a precision of indication to 0.020 in. at 1300°F.

The unit shown in Fig. 120 was successfully operated in NaK at temperatures from room temperature to 1300°F. Figure 123 shows the level as it appears on the recorder for a full-scale range of 6 in. This chart shows how the level was gradually raised, leveled off at 0.84 in., increased to 1.5 in., then dropped to 0.90 in. and then dumped. This was a 14 hr-run.

Some advantages of this unit are: it can become a part of an all-welded system; the zero can be adjusted with the system empty; the range can be changed by simply changing the cylinder length, and therefore the parts stocked could be kept to a minimum.

Some disadvantages of this unit are: it is temperature sensitive; the cylinder must be free to move (this movement is 0.001 in.).

UNCLASSIFIED
ORNL-LR-DWG 29427

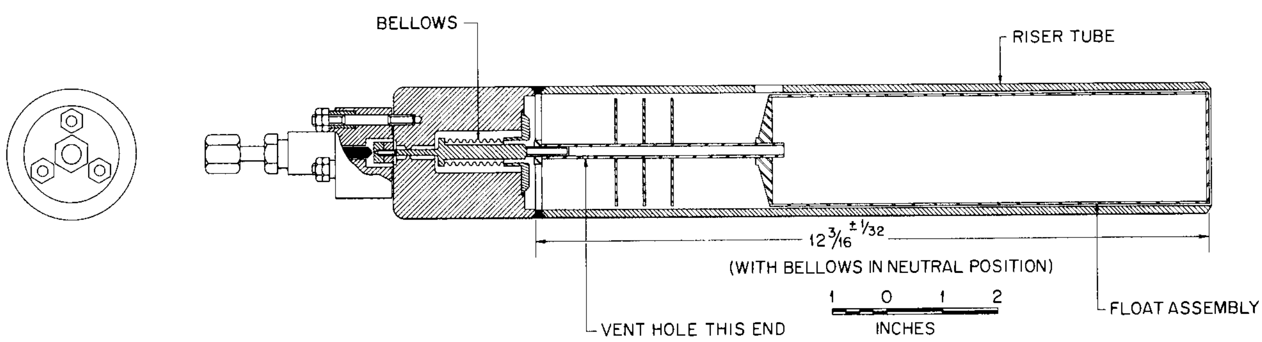

Fig. 120. Buoyancy-Type Liquid-Level Indicator.

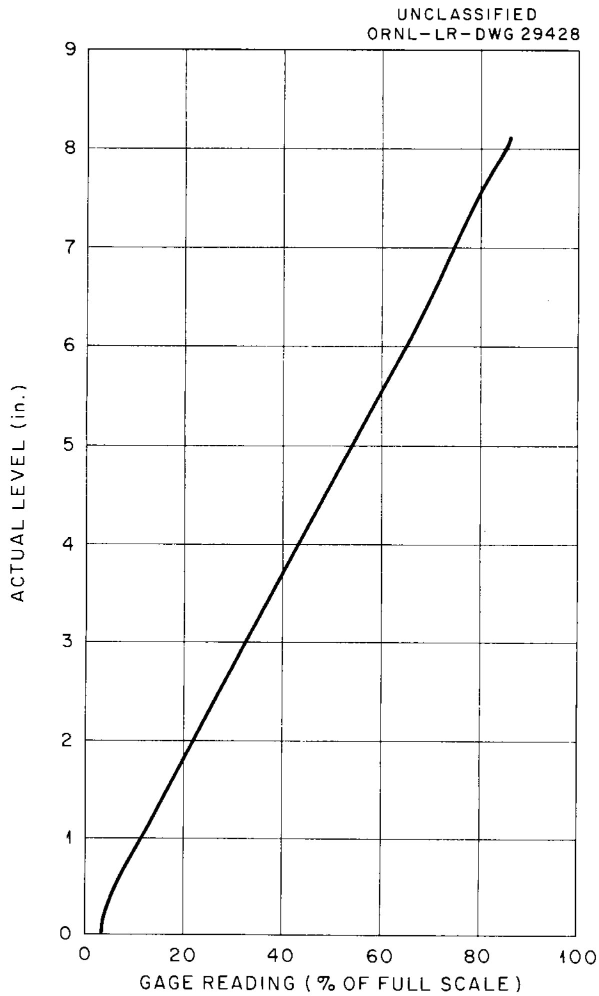

Fig. 121. Curve for Water Calibration of Buoyancy-Type Liquid-Level Indicator.

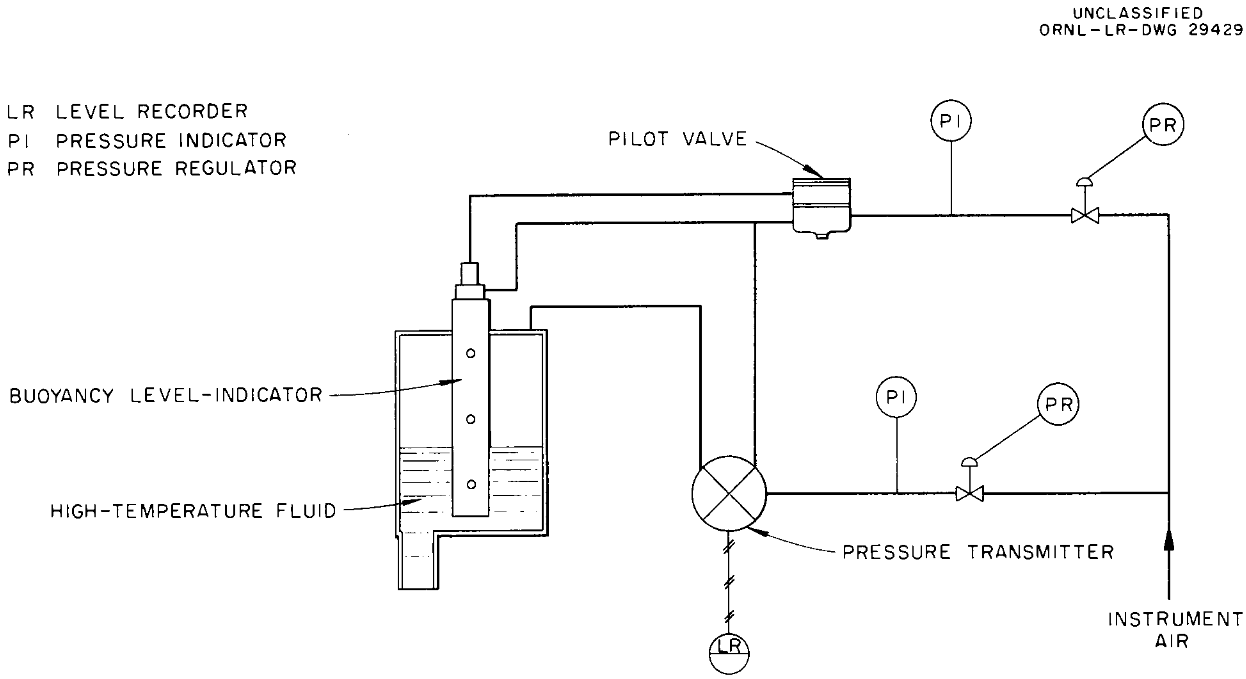

Fig. 122. Schematic of Buoyancy-Type Liquid-Level Indicator.

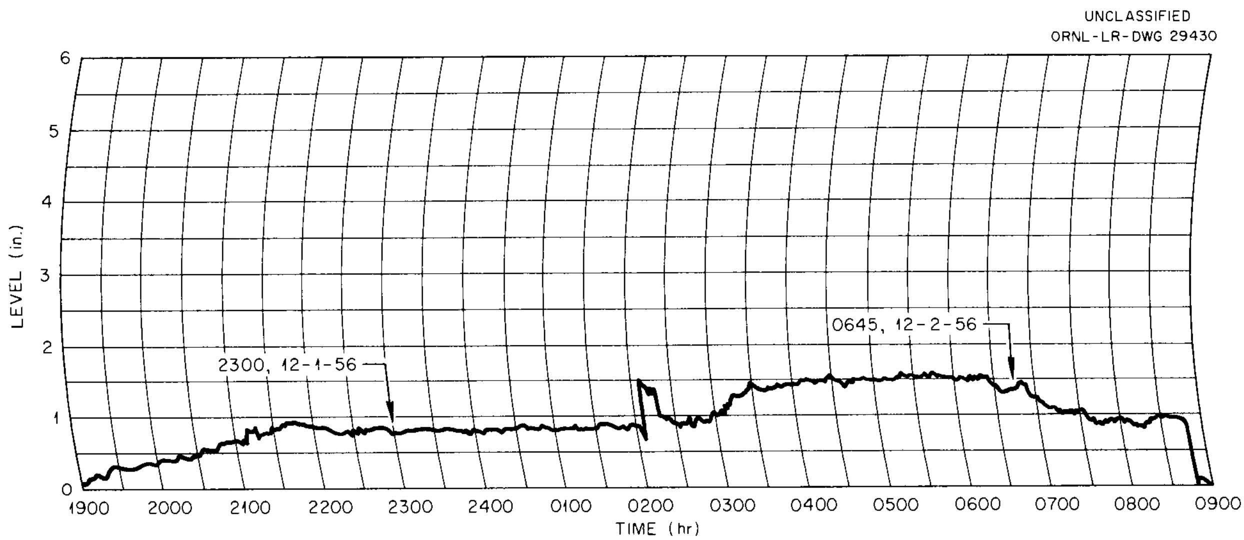

Fig. 123. Typical Level Recording.

HIGH TEMPERATURE FUSED SALT LEVEL DEVICE

R. F. Hyland

A series of tests utilizing the conventional purged-dip-tube technique have demonstrated the feasibility of measuring level in a mixture of fused salts from their melting temperature to 1500°F. Accuracy, reproducibility and precision of measurement are comparable to those obtained in low temperature fluids. Typical data obtained are as follows: accuracy, ± 2% of the total level; reproducibility, ± 1%; sensitivity, 0.03 in. of fluid.

To assure containment of the corrosive, high temperature fluid, the measuring system utilizes an all-welded differential pressure cell as the level sensor.

A test apparatus shown in Fig. 124 employs an all silver-soldered, spectrometer leak tight helium system with moisture trapping and oxygen gettering of the purge gas to preclude contamination of the fluid and subsequent plugging of the dip tubes.

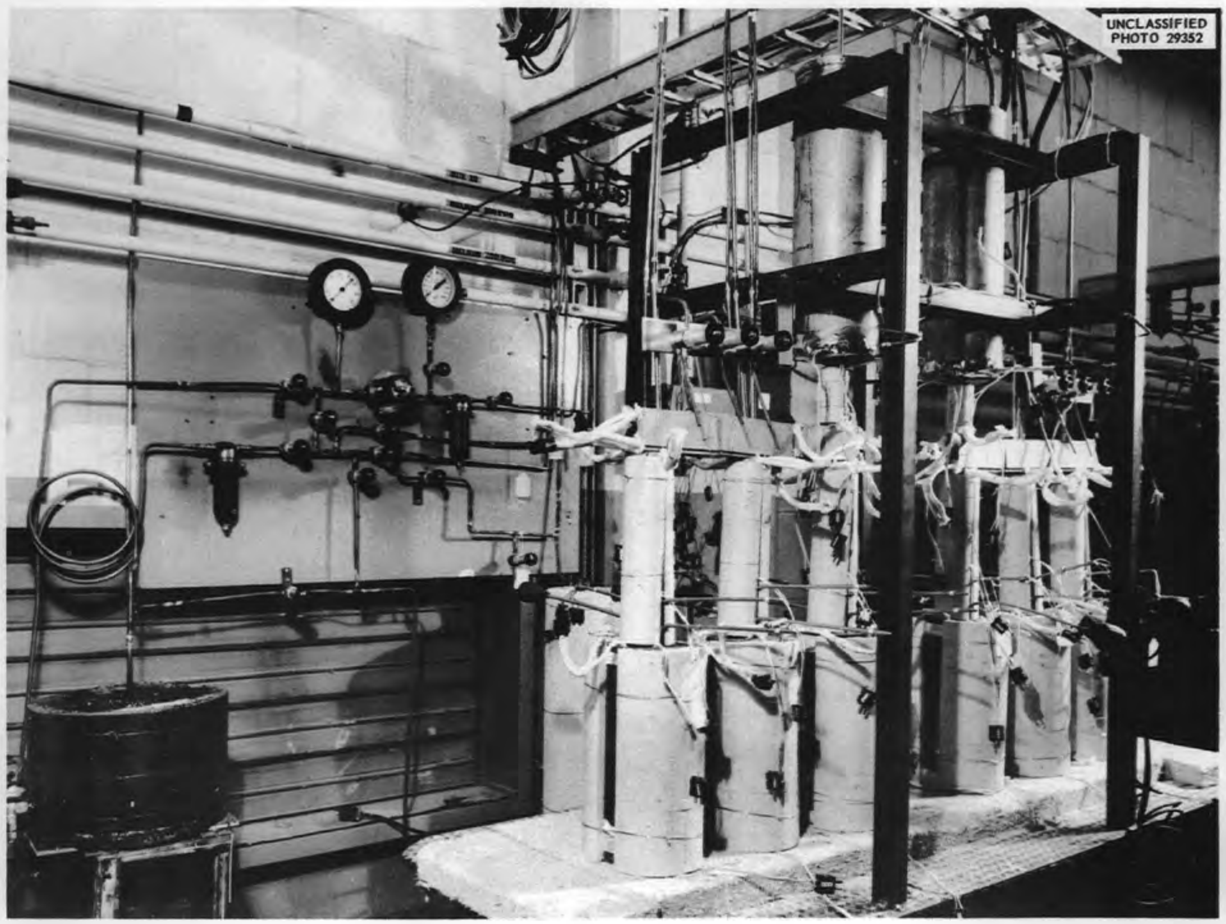

Fig. 124. Apparatus for Testing High Temperature Fused Salt Level Device.

ORNL-2480
Instruments
TID-4500 (13th ed., Rev.)
February 15, 1958

INTERNAL DISTRIBUTION

1. C. E. Center
2. Biology Library
3. Health Physics Library
4-6. Central Research Library
7. Reactor Experimental Engineering Library
8-27. Laboratory Records Department
28. Laboratory Records, ORNL R.C.
29. A. M. Weinberg
30. L. B. Emlet (K-25)
31. J. P. Murray (Y-12)
32. J. A. Swartout
33. E. H. Taylor
34. E. D. Shipley
35. C. S. Harrill
36. M. L. Nelson
37. W. H. Jordan
38. S. C. Lind
39. F. L. Culler
40. A. H. Snell
41. A. Hollaender
42. M. T. Kelley
43. K. Z. Morgan
44. T. A. Lincoln
45. A. S. Householder
46. C. E. Winters
47. H. E. Seagren
48. D. Phillips
49. G. E. Boyd
50. P. R. Bell
51. C. J. Borkowski
52. G. S. Hurst
53. R. S. Livingston
54. E. E. Fairstein
55. C. W. Sheppard
56. W. G. Stone
57. C. P. Keim
58. C. D. Susano
59. P. M. Reyling
60. G. C. Williams
61. M. J. Skinner
62. J. V. Francis
63. R. W. Johnson
64. D. J. Fisher
65. E. G. Struxness
66. J. R. McNally, Jr.
67. J. L. Gabbard
68. R. A. Charpie
69. T. V. Blosser
70. E. L. Olson
71. J. A. Auxier
72. R. K. Abele
73. J. R. Tallackson
74. H. E. Banta
75. E. W. Burdette
76. R. R. Dickison
77. C. A. Mossman
78. D. S. Toomb
79. R. G. Affel
80. H. J. Stripling
81. E. P. Epler
82. F. W. Manning
83. ORNL–Y-12 Technical Library, Document Reference Section

EXTERNAL DISTRIBUTION

84-85. Ohio State University (Professor of Naval Science)
86. R. Hofstadter, Stanford University
87. J. C. Nance, Consolidated-Vultee Aircraft Corporation
88. E. A. Rollor, ANP Project Office, Fort Worth
89. R. N. Keller, University of Colorado
90. Division of Research and Development, AEC, ORO
91-706. Given distribution as shown in TID-4500 (13th. ed., Rev.) under Instruments category (100 copies, OTS)